SCIENCE • TECHNOLOGY • RESEARCH HIGHLIGHTS • VISIONS
Dissertation
107

Synthetic fuels and light olefins from biomass residues, carbon dioxide and electricity

Performance and cost analysis

Ilkka Hannula

VTT

VTT SCIENCE 107

Synthetic fuels and light olefins from biomass residues, carbon dioxide and electricity

Performance and cost analysis

Ilkka Hannula

VTT Technical Research Centre of Finland Ltd

Doctoral dissertation for the degree of Doctor of Science in Technology to be presented with due permission of the Aalto University School of Engineering for public examination and debate in lecture room 216 (K1), at Aalto University (Otaniemi, Finland), on the 16th of October 2015 at 12:00.

ISBN 978-951-38-8342-3 (Soft back ed.)
ISBN 978-951-38-8343-0 (URL: http://www.vttresearch.com/impact/publications)

VTT Science 107

ISSN-L 2242-119X
ISSN 2242-119X (Print)
ISSN 2242-1203 (Online)
http://urn.fi/URN:ISBN:978-951-38-8343-0

JULKAISIJA – UTGIVARE – PUBLISHER

Teknologian tutkimuskeskus VTT Oy
PL 1000 (Tekniikantie 4 A, Espoo)
02044 VTT
Puh. 020 722 111, faksi 020 722 7001

Teknologiska forskningscentralen VTT Ab
PB 1000 (Teknikvägen 4 A, Esbo)
FI-02044 VTT
Tfn +358 20 722 111, telefax +358 20 722 7001

VTT Technical Research Centre of Finland Ltd
P.O. Box 1000 (Tekniikantie 4 A, Espoo)
FI-02044 VTT, Finland
Tel. +358 20 722 111, fax +358 20 722 7001

Juvenes Print, Tampere 2015

Acknowledgements

This thesis work was carried out at VTT Technical Research Centre of Finland Ltd during the years 2009 – 2015. Financial support from Tekes – the Finnish Funding Agency for Innovation, VTT, and sponsor companies of projects UCGFunda, Kaasutusalkoholit, Vetaani and 2G 2020 Biofuels are gratefully acknowledged. Aino ja Kaarlo Tiisalan rahasto and Gasumin kaasurahasto are acknowledged for providing financial support for a 12 month research visit to Princeton University in 2011 and a 6 months writing period in 2014.

I would like to thank my thesis advisors Research Manager Esa Kurkela and Senior Principal Scientist Yrjö Solantausta for their sustained support during the writing of this dissertation. Esa, since hiring me as a diploma thesis worker at VTT, has been generous in sharing his expertise on gasification, and has provided continuous guidance towards problems that are both interesting and relevant. Yrjö's outspoken and practical views on process development and techno-economic assessments have been as valuable as they have been amusing. I would also like to thank my supervising professor Pekka Ahtila for his encouraging comments over the years and for his firm belief that this work will someday be completed.

My special thanks go to Senior Advisor Kai Sipilä for sharing his experiences and insights that have accumulated during decades of work with bioenergy. Dr. Pekka Simell has also been an important mentor and a coworker whose door is never closed, and who always has time to assist with a problem. I would like to thank Dr. Antero Moilanen for our numerous uplifting discussions on thermochemical biomass conversion science, and Dr. Anja Oasmaa for setting such a good example as an actively publishing VTT researcher.

My sincere thanks go to doctors Tom Kreutz, Eric D. Larson and Bob Williams of Princeton University whose sociable nature and openness to information exchange made it possible to learn so much about energy systems analysis during that relatively short period of time.

This thesis would not have been completed without the valuable input from my co-authors Esa Kurkela, Pekka Simell, Vesa Arpiainen, Sanna Tuomi, Matti Nieminen, Ilkka Hiltunen, Noora Kaisalo and Johanna Kihlman. I would also like to thank Antti Arasto, Janne Kärki and Jani Lehto for their sustained support towards my thesis work at VTT.

Finally, I would like to thank my family and friends for taking part in my lifelong quest for higher education and learning. Satu-Marja, thank you for your loving support and for your useful comments and suggestions during manuscript editing. Toivo, watching you grow is an adventure. Let's make it a great one.

Academic dissertation

Supervising professor, Custos

Professor Pekka Ahtila
Aalto University
Espoo, Finland

Thesis advisors

M.Sc. Esa Kurkela
VTT Technical Research Centre of Finland Ltd
Espoo, Finland

Dr. Yrjö Solantausta
VTT Technical Research Centre of Finland Ltd
Espoo, Finland

Preliminary examiners

Dr. Eric D. Larson
Princeton University
Princeton, NJ, USA

Professor Simon Harvey
Chalmers University of Technology
Göteborg, Sweden

Opponents

Dr. Markku Karlsson
VTT Technical Research Centre of Finland Ltd
Espoo, Finland

Professor Simon Harvey
Chalmers University of Technology
Göteborg, Sweden

List of publications

This compilation dissertation is based on the following original research papers, referred to in the text as **Papers I - V**. These publications are reproduced with the kind permission of the publishers.

(I) **Ilkka Hannula**, Esa Kurkela, A semi-empirical model for pressurised air-blown fluidised-bed gasification of biomass, Bioresource Technology, Volume 101, Issue 12, June 2010, Pages 4608-4615.

(II) **Ilkka Hannula**, Esa Kurkela, A parametric modelling study for pressurised steam/O_2-blown fluidised-bed gasification of wood with catalytic reforming, Biomass and Bioenergy, Volume 38, March 2012, Pages 58-67.

(III) Pekka Simell, **Ilkka Hannula**, Sanna Tuomi, Matti Nieminen, Esa Kurkela, Ilkka Hiltunen, Noora Kaisalo, Johanna Kihlman, Clean syngas from biomass - process development and concept assessment, Biomass Conversion and Biorefinery, Volume 4, Issue 4, April 2014, Pages 357-370.

(IV) **Ilkka Hannula**, Co-production of synthetic fuels and district heat from biomass residues, carbon dioxide and electricity: Performance and cost analysis, Biomass and Bioenergy, Volume 74, March 2015, Pages 26-46.

(V) **Ilkka Hannula**, Vesa Arpiainen, Light olefins and transport fuels from biomass residues via synthetic methanol: performance and cost analysis, Biomass Conversion and Biorefinery, Volume 5, Issue 1, March 2015, Pages 63-74.

Author's contributions

In **Paper I**, Ilkka Hannula is the main author. Ilkka Hannula structured and wrote the paper. Esa Kurkela was responsible for all the empirical data and proposed a structure for the gasification model. Ilkka Hannula created the process model with ASPEN Plus and carried out the simulations. The analysis was jointly planned by Esa Kurkela and Ilkka Hannula.

In **Paper II**, Ilkka Hannula is the main author. Ilkka Hannula structured and wrote the paper. Esa Kurkela was responsible for all the empirical data. Ilkka Hannula created the process model with ASPEN Plus and carried out the simulations. The model structure and parametric analysis was jointly planned by Esa Kurkela and Ilkka Hannula.

Paper III was jointly written and structured by the authors. Ilkka Hannula created the process model with ASPEN Plus, carried out the simulations, created a spreadsheet-based cost analysis tool and wrote the concept assessment part of the paper.

In **Paper IV**, Ilkka Hannula is the sole author. Ilkka Hannula structured and wrote the paper, created all plant models, carried out all simulations and was responsible for the techno-economic assessment.

In **Paper V**, Ilkka Hannula is the main author. Ilkka Hannula structured and wrote the paper. Vesa Arpiainen was responsible for gathering background information for modelling, proofreading the text and double-checking the calculations. Ilkka Hannula created the process model with ASPEN Plus and carried out the simulations. The techno-economic analysis was jointly planned by Ilkka Hannula and Vesa Arpiainen.

Contents

"It's been a hard day...night!"
Ringo Starr, 1964

Chapter 1

Introduction

1.1 Background

The concentration of carbon dioxide (CO_2) in the atmosphere has increased from approximately 278 parts per million (ppm) in 1750, the beginning of the Industrial Era, to 400 ppm at the end of 2014. This increase was initially caused by the release of carbon to the atmosphere from deforestation and other human-induced land-use change activities, but from around 1920 until the present, emissions from fossil fuel combustion have become the dominant source of anthropogenic emissions into the atmosphere [1]. Multiple lines of scientific evidence show that these rising levels of CO_2 in the atmosphere are warming the global climate system [2, 3]. In order to keep warming under the 2 °C threshold, agreed on by the world's governments at a 2009 meeting in Copenhagen, the Intergovernmental Panel on Climate Change (IPCC) advises that by 2050 the greenhouse gas emissions must be 40 to 70 percent lower than what they were in 2010 [4].

As transportation causes nearly one quarter of global energy-related CO_2 emissions, it is clear that a widespread decarbonisation of transportation needs to be an integral part of any serious response to global warming [5]. In the transportation sector, emissions can mainly be reduced by improvements in efficiency and change in vehicle fuel. However, many alternative fuel options (e.g. fuel ethanol, biogas and electricity) require modifications to the current vehicle fleet and/or fuel distribution infrastructure, which severely limits near-term potential for emissions cuts from the sector. In addition to transportation, the petrochemical industry is another example of a major carbon emissions source where decarbonisation has proven difficult. This can be explained partly by the limitations in switching to use

electricity in industrial processes. However, through a combination of different technologies, it is possible to produce also petrochemicals (light olefins) from renewable sources. Thus for both of these sectors, a switch to more sustainable fuels and feedstocks is a key to decarbonisation.

Synthetic fuels (synfuels) are substitutes to petroleum fuels that are produced from alternative raw materials by complex chemical processing. Technology for the conversion of fossil feedstocks such as coal or shale to synfuels has existed for almost a century. However, when coal is used as feedstock, the resulting net greenhouse gas (GHG) emissions are about double those from petroleum fuels [6]. It is possible to cut down part of these emissions with capture and storage of the by-product CO_2, but the net GHG emissions would still be reduced only to levels comparable to those from petroleum fuels [7]. Switching partly or completely from fossil feedstocks to renewable plant matter (biomass) is a frequently proposed method for further decarbonisation of synthetic fuel production [8–10]. Unfortunately, all commercial-scale synfuels plants to date have been operated with fossil feedstocks and redesign of some key parts of the process is required to make the switch to biomass possible. Currently, a lot of RD&D work is ongoing to commercialise such technology [11].

Another solution would be to produce synthetic fuels directly from carbon dioxide and renewable electricity with a process referred to here as 'power-to-fuels'. This process begins with splitting water (H_2O) into hydrogen (H_2) and oxygen (O_2) with electricity. The produced hydrogen is then reacted with co-feed CO_2 to form hydrocarbons or alcohols. The hydrogen is thus stored chemically as conventional liquid or gaseous fuel that can be consumed at a chosen time and place within the existing infrastructure. In this sense, the power-to-fuels concept elegantly solves the problems of distribution and storage that normally impede energy concepts based on hydrogen production. However, the present use of CO_2 as a chemical feedstock is limited to only a few industrial processes, although research is ongoing to enable commercial-scale hydrogenation of CO_2 to synthetic fuels [12–15].

The production of renewable synthetic fuels can thus be based on a broad range of technical alternatives. Possible raw materials include biomass residues, carbon dioxide and electricity, or different combinations of these. Different end-product alternatives also exist, ranging from gaseous fuels to alcohols and liquid hydrocarbons. These fuels can be used with a varying degree of ease to decarbonise the transportation sector and some are also suitable as raw materials for the petrochemical industry. In order to successfully develop and commercialise these technologies, accurate estimates of their capital costs and performance are needed. This dissertation reviews technical aspects of selected synthetic fuel production processes and evaluates and compares competing production routes under the same set of technical and economic assumptions. The results can be used to guide future concept

development and to direct experimental research towards key variables that have the highest potential to improve the overall feasibility of the process. In addition, the results can be useful to industry and government in making rational decisions about R&D allocations, commercialisation and required subsidies in order to build this future industry.

1.2 State of the art

A considerable amount of studies that investigate the techno-economics of alternative fuels has been published since the 1973 oil crisis. The early reports were focused mainly on coal utilisation and motivated by price stability and improved energy security [16–18], but the urgency of climate change mitigation has gradually steered interest toward more sustainable processing based on biomass feedstocks or biomass and coal mixes with carbon capture and storage (CCS) [7–9].

Most reports available in the public domain discuss specific case studies of individual biofuels and considerable diversity exists in terms of feedstocks, scale, level of heat integration, use of by-products and technological approaches depending on the geographical location and time of publication. The level of detail and degree of transparency also vary enormously among different reports, thus complicating the effort of producing a comparable assessment on the main findings of decades of research. With these limitations in mind, the following text aims to highlight results from selected recent studies that stand out in their degree of transparency and rigour. To facilitate comparison with petroleum fuels, historical prices of crude oil[1] are shown in Fig. 1.1.

Spath and Dayton [21] reviewed various syngas routes to products and summarised the status of technology. They found that in many cases the production of syngas itself can account even up to 75 % of the total production cost, and to reduce costs, efforts should thus be focused on minimising the cost of clean syngas production. They also noted that, with the exception of mixed alcohols and ethanol, the required downstream syngas conversion technologies have all been demonstrated at commercial scale making biomass conversion to syngas the part that most requires further development. They also noted the significant role that the economies of scale play in lowering the production cost, and that opportunities to co-feed biomass with coal or natural gas might therefore be utilised to introduce renewable fuels into the market place.

Larson et al. [22] assessed large-scale gasification-based systems for producing Fischer-Tropsch fuels, dimethyl ether or hydrogen from switchgrass with

[1] The prices are converted from barrels to GJ assuming 6 GJ/bbl (LHV). The 1955-1983 prices are for Arabian Light and 1983-2015 for Brent.

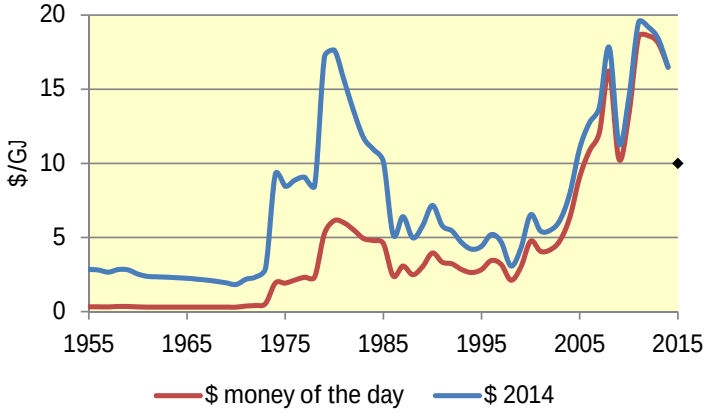

Figure 1.1: Crude oil prices 1955-2014 [19], with 2015 forecast [20].

electricity as a co-product. They too concluded that many of the component technologies of plants that could produce these fuels are commercially established and that no further fundamental research hurdles exist. The study also supported the notion that economic benefits come with increasing plant size. It was noted that because CO_2 needs to be removed from syngas as a requirement of the process design in most cases, the cost of capturing and storing CO_2 from gasification-based synfuel plants would be relatively inexpensive. As a result, with a high enough value of CO_2, the overall economics of fuels production would markedly improve over the non-capture configurations.

Dutta and Phillips [23] studied the production of ethanol from lignocellulosic biomass based on direct oxygen gasification and mixed alcohol synthesis and compared the results with an earlier study [24] of an otherwise identical process but based on indirect steam gasification. They found that direct gasification with oxygen showed higher costs for the production of mixed alcohols in comparison with the indirect gasification-based process. The air separation unit was found to be a major added cost in the direct gasification process, but if an air separation unit would already exist for other purposes, oxygen could be produced at a lower cost using economies of scale. It was also noted that in practise technological maturity and reliability issues impact the selection of gasification techniques for the conversion of biomass to synthetic fuels.

Hamelinck et al. [8] analysed plant configurations capable of producing FT diesel from biomass with a focus either on liquid fuels only, or co-production of liquid fuels and electricity. In the short term the cost of FT diesel from

a moderate scale plant was estimated to be 16 €/GJ but on a longer term, on the assumption of cheaper biomass, larger production scale, technical development and technological learning, the costs could come down to 9 €/GJ. The study found that FT biodiesel seemed to be a 40 - 50% more expensive alternative than biomethanol or biohydrogen, but the advantages of diesel with respect to applicability to the existing infrastructure and vehicle technology was not captured by the analysis. The total capital investment (TCI) of a 400 MW_{th} biomass input plant was estimated to be about 286 M€, which stands at the lower end of estimates usually reported for such a process.

McKeough and Kurkela [9] examined plants producing FT liquids, methanol, methane (SNG) or hydrogen and evaluated the benefits of integration. A production scale of 200 - 400 MW_{th} biomass input was found to be suitable in Finnish conditions as it makes possible the procurement of feedstock at a competitive price, enables feasible integration with pulp and paper mills and because fluidised-bed gasifiers could be realised only in one or two trains on this scale. The production costs were estimated to be 17 €/GJ for FT, 16 €/GJ for methanol and 14 €/GJ for SNG, assuming 5.5 €/GJ for the biomass feedstock.

In contrast to biofuels, the production of olefins from biomass via methanol is a lesser discussed technique in scientific literature. However, Ren and Patel [25] have examined the energy use and CO_2 emissions related to the production of high-value petrochemicals by various routes including a biomass-derived methanol. They found that although the total energy use of coal and biomass-based routes to olefins was about 60 - 150 % higher than that of conventional technologies, the route based on biomass gasification had potential to significantly reduce CO_2 emissions. In another study, Ren et al. [26] studied the economics of 24 different conversion routes to high-value petrochemicals using a wide range of projected energy prices in 2030 - 2050. The study concluded that biomass-based routes counted among the least expensive ways to produce petrochemicals in the future. This somewhat surprising result might be partly explained by the use of fairly optimistic results for biomethanol via gasification by Hamelinck [27].

The production of synfuels directly from CO_2 and electricity has experienced a resurgence of interest as a possible way of producing carbon-neutral synthetic fuels. Graves et al. [28] recently reviewed a variety of possible technological pathways for recycling CO_2 into fuels using renewable or nuclear electricity. They concluded that the dominant costs of the process are the cost of electricity and the electrolyser's capital investment, and that the capital cost is significantly increased when operating intermittently using renewable power sources such as solar and wind. Based on the results, the synthetic fuel price was estimated to become competitive with petroleum-derived gasoline when electricity prices decline below 8 $/GJ from a constant

(ie. not intermittent) source.

The enhancement of synthetic biofuels production with electrolytic hydrogen is a less-studied option, but Mignard and Pritchard [29] have discussed this approach using methanol production as an example. They noted that the integration can contribute to more effective utilisation of biomass, increasing the methanol output up to 130%. They also concluded that co-utilisation of biomass and electricity could become very interesting in the future if competition over land availability with food and feed production starts to limit the contribution of biofuels to a low-carbon economy. Pozzo et al. [30] analysed a yet more advanced concept where dimethyl ether (DME) was produced with biomass gasification and high-temperature co-electrolysis (SOEC). They noted that the specific productivity of DME from biomass could be greatly increased (nearly doubled) by electrolyser enhancement.

Finally, a recent IEA roadmap study [31] found that biofuels can play an important role in reducing CO_2 emissions in the transport sector and that by 2050 biofuels could provide 27 % of total transport fuel consumption while avoiding around 2.1 gigatonnes of CO_2 emissions per year if sustainably produced. Meeting this biofuel demand would require around 65 exajoules of biofuel feedstock, occupying around 100 million hectares of land, which was considered a challenge by the study given the rapidly growing competition for land for food and fibre. The IEA also noted that biofuels are likely to remain slightly more expensive than fossil fuels also in the future.

1.3 Aim and scope of the research

The main objective of this dissertation is to systematically analyse the long-term[2] technical and economic feasibility of selected plant configurations capable of producing synthetic fuels or light olefins from renewable feedstocks. The analysis rests on a detailed investigation into three specific Research Questions:

1. What is the impact of hot-filtration and catalytic reforming on the production of synthetic biofuels?
2. How do synfuels from biomass compare with synfuels from CO_2 and electricity?
3. What is the feasibility of producing light olefins from renewable methanol?

[2] Here 'long-term' refers to a point in time when all plant components have reached commercial maturity. Whether it will take a long time to reach such condition depends upon the rate of deployment of such plants, as technological learning is a function of capacity expansion, not just the passage of time itself [32].

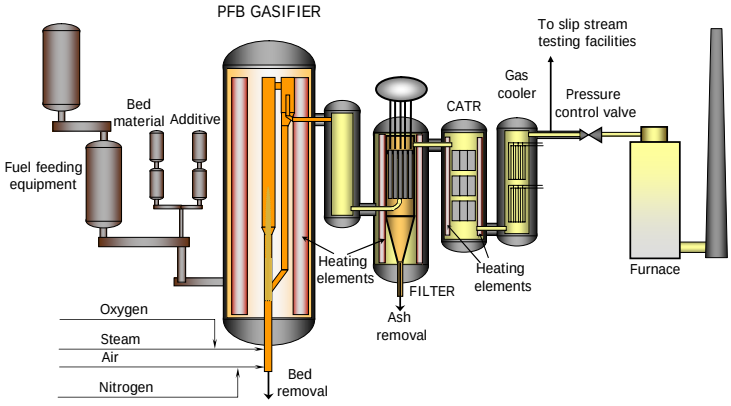

Figure 1.2: The VTT test rig for pressurised fluidised-bed gasification, hot-gas filtration and catalytic reforming.

The biomass conversion technology that was selected as a basis for this work, comprises of a pressurised oxygen gasification in a fluidised-bed reactor, followed by hot-filtration and catalytic reforming of tars and hydrocarbons. This three-piece configuration, called the Ultra-Clean Gas (UCG) process, has been the focus of VTT's biomass gasification R&D since 2006, although the development of pressurised biomass gasification, hot-gas filtration and catalytic tar reforming at VTT can be traced back to the early 90s [33, 34].

At VTT the experimental R&D work with the UCG process has been carried out mainly on a 0.5 MW process development unit (see Figure 1.2), which by 2012 had accumulated circa 4000 operating hours in the pressurised oxygen-blown mode using various wood residues as feedstock [35]. Larger-scale experiments were carried out in parallel by NSE Biofuels, a joint venture between Neste Oil and Stora Enso, in Varkaus, Finland. The Varkaus pilot plant was inaugurated in 2009 and featured a 12 MW gasifier and evaluated all stages of biofuel production, from biomass drying, through gasification, gas cleaning and the testing of Fischer-Tropsch catalysts. The trials carried out at the pilot plant between 2009 and 2011 proved very successful and technically demonstrated the viability of the concept. However, plans for a commercial scale renewable diesel plant were shelved at the time [36].

Writing this dissertation was motivated by the desire to acquire more in-depth understanding of the techno-economics that govern the UCG process. Quantification of the tar clean-up system's improvement potential and its im-

pact on the overall techno-economics of the process was of particular interest, as was the question of how different possible end-fuel alternatives, produced using the UCG process, compare with each other in terms of performance and costs. An emerging alternative for synthetic biofuels, the production of synfuels from carbon dioxide and renewable electricity, is also an interesting concept whose feasibility in comparison to the biomass-based route has not yet, to the understanding of the author, been investigated at the same level of detail as in this dissertation.

The production of renewable chemicals and materials is an active field of research, but mostly focused on biochemical conversion of biomass feedstocks, although a thermal route to chemical-grade raw materials also exists via methanol. Comparing the techno-economics of synthetic light olefins with transportation fuels was a particularly interesting topic that has been examined in this dissertation from a thermochemical perspective.

Although alternative fuels can also be produced from algae or via biochemical conversion, these potential routes were excluded from the scope of this dissertation. Also, all plant configurations examined in this dissertation are based on the conversion of solid biomass in a fluidised-bed reactor thus excluding gasification techniques involving fixed-bed or entrained flow reactors. Additionally, the technology for the clean-up of tars from biomass gasification is based on catalytic reforming of filtered gas in all examined cases and other available methods such as scrubbing with organic liquids were deemed outside the scope of this dissertation. Assessing the life-cycle greenhouse gas emissions of the examined processes was also excluded from the scope of this dissertation.

1.4 Dissertation structure

Paper I discusses modelling of biomass gasification in a pressurised air-blown fluidised-bed reactor. A semi-empirical model is developed based on experimental data using ASPEN Plus® (Aspen) process simulation software. The model is then validated against another set of experimental data by comparing model predictions for product gas composition and carbon conversion with experimental results acquired at the same conditions.

Paper II expands the gasification model originally developed for **Paper I** with catalytic reforming of hydrocarbons and tars. The model is refitted with data from biomass gasification in a pressurised oxygen-blown fluidised-bed reactor. The process is then simulated under different operational parameters and the impact of key parameters to process performance is analysed based on the mass and energy flows produced by the model.

Paper III expands the gasification and reforming model originally devel-

oped for **Paper II** to a full description of a plant capable of producing Fischer-Tropsch liquids from forest residues. Cost analysis is carried out based on a factored approach to produce a preliminary estimate for the required total capital investment (TCI). Based on the simulated mass and energy flows and the estimated TCI, a spreadsheet-based cost model is developed and used to calculate levelised production cost estimates under a set of assumed financial parameters. Mass and energy flows are simulated for different values of key operational parameters, namely filtration temperature and the extent of methane reforming, and their impact on the performance and cost of biofuel production is assessed.

In **Paper IV**, nine distinctive plant designs are created and modelled with Aspen to systematically analyse and compare the production of natural gas (methane), methanol or gasoline from different combinations of biomass, carbon dioxide and electricity. Performance analysis is carried out by comparing the simulated mass and energy flows. The overall economics are evaluated with a spreadsheet-based cost model under alternative feedstock price assumptions. The cost analysis is based on an underlying component-level capital cost estimates generated by a similar type of methodology as used in **Paper III**.

In **Paper V**, a process design for the production of light olefins via renewable methanol is created and simulated with Aspen. The simulated mass and energy flows are used to calculate mass yields for the whole production chain. In addition, a spreadsheet-based cost model is developed to assess the commercial viability of light olefins manufacture from renewable feedstocks.

The Research Questions and the original research papers that comprise this dissertation are connected with each other in the following way: **Paper III** answers Research Question 1, **Paper IV** answers Research Question 2 and **Paper V** answers Research Question 3. **Papers I** and **II** do not address any specific research question posed in this dissertation, but they were instrumental in creating the basis for modelling and analysing complete plants that convert lignocellulosic biomass to synthetic fuels via gasification.

Chapter 2

Technology review

The manufacture of synthetic fuels from biomass requires complex chemical processing that combines elements from power plants, refineries and woodprocessing industry. Most of the components needed to build biomass-to-synfuels plants are already commercially mature, making near-term deployment of such plants possible. However, conversion of solid biomass into clean, nitrogen-free gas, requires some advanced technologies that, although already demonstrated at a pre-commercial scale, are not yet fully commercialised.

A block flow diagram for synthetic biofuels production is illustrated in Fig. 2.1. The front-end process train (blue boxes) combines gasification, hot-gas cleaning and gas conditioning into a process that converts solid biomass into ultra-clean synthesis gas that meets the requirements of a downstream synthesis island (green) consisting of a synthesis loop, product recovery and upgrading sections. Auxiliary equipment (yellow) that support the operation of the plant include a biomass dryer, air separation unit (ASU) and auxiliary boiler. A fully operational plant also features an efficient steam cycle (not shown).

Due to the concise format of research articles, it is not usually possible to discuss features of the technical apparatus or applied design choices at a level that provides the reader with a satisfactory understanding on the object of investigation. Therefore the following text aims to expand and deepen the descriptions available in the papers that comprise this dissertation to provide the reader with a fuller understanding of the technologies behind this work.

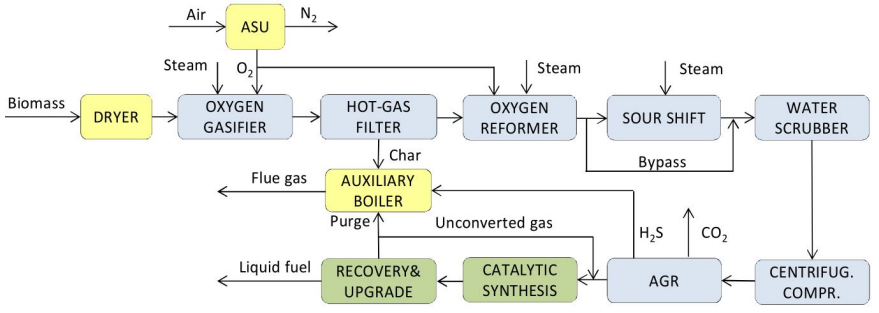

Figure 2.1: Generalised block flow diagram of a stand-alone biomass-to-synfuels plant based on pressurised fluidised-bed gasification with steam and oxygen, hot-gas filtration and catalytic reforming of tars and hydrocarbons.

2.1 Feedstock handling and drying

Feedstock pretreatment is an important part of almost every biomass conversion process. The specific arrangement of a particular pretreatment chain is dependent on the type of feedstock and conversion technology, but usually includes at least transfer, storage, chipping, crushing and drying of feedstock [37]. Operating problems with fuel feeding and handling equipment are the most common denominator for unforeseen shutdowns of biomass conversion processes and reliable solids handling systems are thus essential to successful operation of the plant [38].

2.1.1 Pretreatment

Forest residue chips are consider as feedstock for all examined plant designs. The chips are produced from residue formed during harvesting of industrial wood. It includes needles and has a higher proportion of bark than chips made out of whole trees [39]. The higher heating value (HHV) of the dry matter is 20.67 MJ/kg and the lower heating value (LHV) is 19.34 MJ/kg. The feedstock properties are described in Table 2.1.

Since feed preparation and handling equipment are often expensive and require heat and power to operate, it is preferable to minimise the pretreatment requirement of the conversion process. Fluidised-bed gasifiers are characterised by their wide feedstock base and their ability to convert low-quality feedstocks into synthesis gas. Only minor pretreatment requirements are thus imposed for the considered feedstock. For forest residues this means mainly chipping down to a maximum length of 50 mm, which can take place

Table 2.1: Feedstock properties.

Proximate analysis, wt% d.b.*	
Fixed carbon	25.3
Volatile matter	70.8
Ash	3.9
Ultimate analysis, wt% d.b.	
Ash	3.9
C	53.2
H	5.5
N	0.3
Cl	0
S	0.04
O (difference)	37.06
Other properties	
HHV, MJ/kg	20.67
LHV, MJ/kg	19.34
Bulk density, kg d.b./m3**	293
Sintering temp. of ash, °C	>1000

*wt% d.b. = weight percent dry basis
**1 litre batch, not shaken

either at the harvesting site or alternatively after transportation at the conversion plant.

Forest residues typically have a moisture content of about 50 wt% and a LHV around 8 - 9 MJ/kg. In order to improve the quality of synthesis gas and to increase thermal efficiency of the overall conversion process, chips are dried down to 15 wt% (LHV 16.07 MJ/kg) by utilising low temperature by-product heat sources available from the gasification plant. Drying of biomass to a low moisture contents is problematic and has not been fully optimised for biomass conversion processes [37], although atmospheric band conveyor dryers (belt dryer) can be considered available for reliable execution.

2.1.2 Belt dryer

Belt dryers operate by blowing hot drying medium through a thin layer of feedstock on a permeable belt moving horizontally through the enclosed drying chamber [40]. A belt dryer can be realised based on three different basic designs: i) a single-stage single-pass design, where a continuous single band carries the feedstock through the whole length of the dryer; ii) a multi-stage single-pass design, where a number of belts are arranged in series so that when fuel reaches the end of a belt, it falls onto the beginning of the

next, exposing new feedstock surfaces to drying medium; iii) a multi-stage multi-pass design, where several belts are installed one above the other so that each will discharge its feedstock onto the belt below (see Fig. 2.2). The drying medium is moved through the dryer by a number of fans and can flow either in co- or counter-current with respect to the passage of feedstock [40].

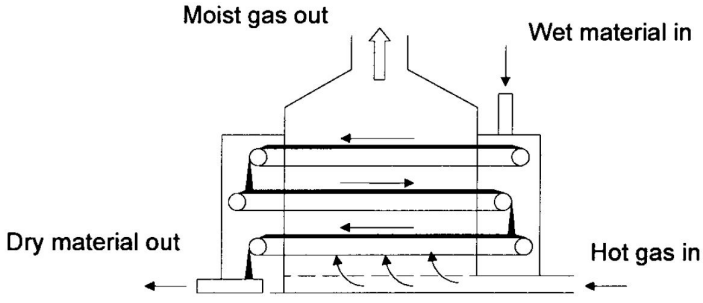

Figure 2.2: An operating principle of a multi-stage multi-pass belt [40].

According to an advertorial brochure [41], belt dryers can be used to dry biomass down to 8 wt% moisture content using various low temperature heat sources. They enable close control of residence time and temperature and due to the relatively thin layer of feedstock on the conveyer belt, a good uniformity of drying is achieved [37]. A single belt dryer is able to evaporate water up to a rate of 20 tonnes per hour and when several dryers are needed, they can be stacked on top of each other to save floor space. Plant configurations examined in this thesis feature belt dryers that operate with hot water (90 °C in, 60 °C out) produced from heat recovered from the first cooling stage of the water scrubber and/or low-pressure steam extracted from the turbine. 20% of the belt dryer's overall heat requirement is satisfied with low (< 60 °C) temperature heat.

The specific energy consumption and evaporation capacity of a dryer depends on the feedstock moisture, inlet and outlet temperature of the drying medium as well as structure and particle size of the feedstock. Based on discussions with industry experts, the specific heat consumption of a belt dryer has been set to 1300 kWh/tH_2O evaporated, and power consumption at 32 kWh/tonne of dry feedstock.

2.1.3 Feeding against pressure

The handling characteristics of biomass are affected by quality, moisture content, particle size and amount of impurities. Pressure is also known to cause changes in the tension and compression strength of the feedstock,

which affects its flow characteristics and thus its behaviour in the feeding equipment [38]. A wide variety of equipment designs for feeding biomass feedstocks into pressurised reactors have been developed since the 1950s, mainly in conjunction with the development of continuous commercial-scale processes in the pulp and paper industries. Some of the designs were adapted from feeders used in pressurised combustion and gasification of coal, although several modifications were required due to biomass' low bulk density and increased resistance to flow. In general, three types of feeding equipment can be considered for feeding dry biomass into high-pressure reactors: rotary valves, lock hoppers and plug feed systems. An ideal biomass pressure feeder would be 1) highly reliable, 2) have low capital, operating and maintenance costs, 3) be suitable for wide range of feedstocks, 4) and have accurate feed control. However, all requirements cannot usually be reached with any single feeder type and compromises must be made.

The suitability of different pressure feeders for biomass applications have been assessed by Rautalin and Wilén [38] and more recently also by Lau et al. [42]. Out of the several types of feeders, the lock hopper-based system is a preferred choice for dry biomass as it has been extensively tested with various biomass feedstocks and is generally considered to be a well-proven system. Lock hopper systems have been used by Lurgi and others for feeding up to 70 tonnes/h of coal at pressures as high as 90 bars [42]. For biomass feedstocks the design has been modified to include a live bottom metering bin, equipped with a multiscrew system for metering the fuel to the injector screw of the pressurised gasifier [38]. Despite these modifications, lock hopper feeding systems offer the advantage of a simple design with few moving parts and the ability to handle a wide variety of biomass fuel types [42].

The operating principle of a lock hopper system is based on a feeding sequence that begins by feeding a batch of fuel via feed hopper into the lock hopper. A valve separating the hoppers is closed and the lock hopper is pressurised with inert gas. After pressure is equalised with a metering bin below, the bottom valve is opened, which causes fuel to flow into the bin by gravity. After the lock hopper has been vacated of fuel, the bottom valve is closed and the hopper is vented to atmospheric pressure. As a final step, the top valve is once again opened to enable feeding. Continuous feeding of biomass into pressure can be achieved by repeating this sequence. If multiple lock hopper systems are operated in parallel, the vent gas of one lock hopper can be used for partial pressurisation of another, thereby reducing the loss of inert gas. The inert gas consumption of a single lock hopper system was reported to be 50 % higher than that for a double system [43].

In a commercial plant, three parallel fuel feeding lines are required to enable continuous gasifier output without interruptions [44]. Common problems related to lock hopper systems include sticking valves, fuel bridging and the

relatively high inert gas consumption per unit of energy fed into the process. However, an ample supply of inert CO_2 and N_2 are available for this from the plant's acid gas removal and air separation units.

2.2 Biomass gasification

Gasification is a thermochemical conversion process that turns carbonaceous feedstocks into a gas mixture rich in carbon monoxide and hydrogen, called product gas or synthesis gas depending on the end-use application. Other major compounds include carbon dioxide, nitrogen, water, methane and a rich spectrum of hydrocarbons and tars. A general objective of gasification is to maximise the yields of light combustible gases and minimise the amounts of condensable hydrocarbons and unreacted char. The exact composition of product gas depends on the type of process feeds, their feed ratios, process parameters and the type of gasification reactor used. In contrast to coal gasification, where char gasification reactions determine the overall yield, in biomass gasification the devolatilisation stage of the feedstock and secondary reactions of primary pyrolysis products play the major role [33]. On a conceptual level, the performance of a gasification process can be measured by calculating its cold gas efficiency (CGE), defined by the following equation:

$$CGE = \frac{(\dot{m} * H)_{\text{syngas}}}{(\dot{m} * H)_{\text{biomass}}}, \tag{2.1}$$

where $\dot{m}$ represents mass flow and H the lower heating value.[1]

Several types of gasification reactors have been developed in the past, but fluidised-bed reactors have been identified as a reliable and practical solution for large-scale gasification of solid lignocellulosic biomass. Autothermal (directly heated) fluidised-bed gasifiers can be realised either as circulating or bubbling bed reactors. Both reactor types are fluidised from the bottom through a distributor plate by air or steam and oxygen while feedstock, bed material and additives are fed from the side to the lower part of the reactor (See Fig. 2.3). Special bed materials can be used to prevent bed agglomeration, otherwise caused by alkali metals of the biomass feedstock [45].

A few important differences exist between these two reactor types. In a bubbling fluidised-bed (BFB) gasifier, biomass is fed directly into the dense bed where it dries and pyrolyses, causing bed material, steam and oxygen to be in contact with the primary pyrolysis products. In a circulating fluidised-bed (CFB) gasifier, biomass is fed above the dense region to an upward flowing

[1] For biomass, values at 50 wt% moisture are used throughout the dissertation.

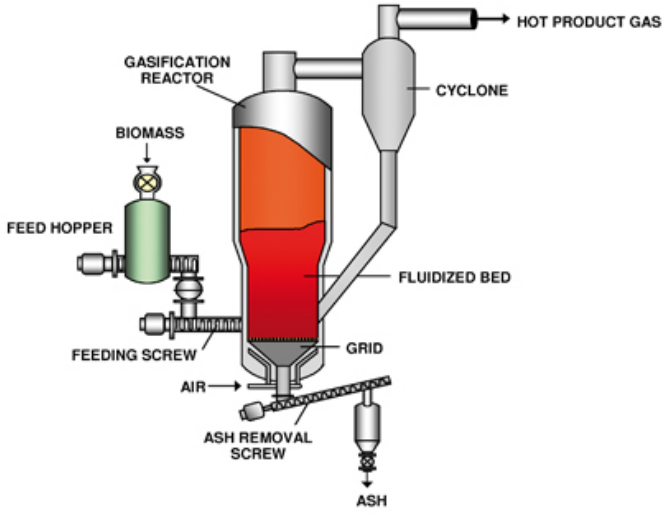

Figure 2.3: A schematic of a bubbling fluidised-bed gasifier developed and offered by ANDRITZ [46].

circulation where drying and pyrolysis take place before fuel particles drop to the dense region at the bottom. At the top of the reactor the circulating bed material and unconverted feedstock are separated from gases by a cyclone and returned back to the bottom via a return pipe. Consequently, bed material, steam and oxygen now primarily meet with residual carbon in the dense bed causing it to be converted not only by (relatively slow) char gasification reactions, but by oxidation as well.

Due to these differences, BFB gasifiers generally produce less tar, but have consequently lower feedstock (carbon) conversion in comparison to CFB gasifiers [35]. Although these factors partly compensate each other, the cold gas efficiency and oxygen consumption are slightly different for a design incorporating a BFB instead of CFB. A further difference between the reactor types is that maximum gasification capacity per reactor is lower for a BFB necessitating multiple trains to achieve large syngas outputs. On the other hand, BFB gasifiers are easier to pressurise in the range of 10-20 bar than CFBs, due to lower fluidisation velocities and easier recycle gas fluidisation arrangement [35]. While CFB and BFB gasifiers exhibit some differences in their performance, as described above, the overall results of this dissertation can be considered valid for a plant using either one of the gasifier types.

The plant configurations created for this work are based on a CFB gasifier fluidised with equal amounts (mass basis) of steam and oxygen and operated

at 4 bar pressure and at 850 °C outlet temperature. At these conditions 98 % carbon conversion for forest residues is assumed. For information on tar loads, see the relevant paper in question.

2.3 Hot filtration

Filters are used to separate particulates from the gasifier effluent to prevent erosion and fouling of downstream units. In addition to particulates removal, filtration has a significant role in controlling the alkali, heavy metal and chloride removal. Chlorine reacts with calcium and alkali metals to form solid chlorides that can be removed by filtration. Although some of the alkali and heavy metals are in vapour phase under typical gasification conditions, they too can be removed if condensed by cooling down the gas before filtration.

The most challenging aspect in the filtration of biomass-derived gas is related to the behaviour of tars. At lower temperatures (~below 350 °C) tars condense in the dust cake, making the dust sticky and causing poor detachment of the cake by reverse-flow pulse cleaning. At higher temperatures (above ~600 °C) tars induce filter blinding by forming a sticky, soot-containing cake on the filter surface which again cannot be fully regenerated by pulse cleaning [47, 48]. The most likely reason for this latter phenomenon is the tendency of tar components to crack, polymerise or condense and form soot on the filter. These soot particles can partially enter the filter pores and block them. The blinding effect has also been found to intensify with low dust content. However, stable filter operation has been obtained at 500 - 600 °C [47] and 550 °C is therefore used as a design temperature in many of the analyses presented in this work.

The impact of filtration temperature on the overall feasiblity of synthetic biofuels production has been acknowledged, and developing solutions that allow stable operation at higher temperatures is a major target for hot-gas cleaning R&D. Simeone et al. [49, 50] have performed filtration tests at around 800 °C in steam-O_2 gasification conditions with different bed material (magnesite, olivine) and biomass feedstock (wood, miscanthus, straw) combinations. These results also confirmed that the selection of bed material/fuel combination plays an important role in filter performance as they influence the gas quality, especially tars, and dust load in the gas as well as the carry-over of bed material to the filter. Filtration development is an ongoing activity, and a lot of experience has been accumulated at VTT in hot-gas filtration of biomass-derived gasification gas with varying tar loads and different filter media such as ceramic and metallic filters [33, 47, 48, 51–56]. There is also ongoing development of catalytically activated filter elements that would be suitable for simultaneous removal of tars and particulates from

biomass-based gasification gas at high temperature [57–68].

2.4 Catalytic reforming

The clean-up of tars from biomass gasification gas has been a topic of numerous R&D projects for decades and has led to two feasible approaches: (1) scrubbing with organic solvents [69, 70] and (2) catalytic reforming [71–76]. Of these, catalytic reforming is particularly suitable for synthesis gas applications because it also handles the non-condensable hydrocarbons and converts organic sulphur species to hydrogen sulphide, a more readily removable form of sulphur for the downstream equipment. The R&D work on catalytic tar reforming started at VTT in the late 1980s and led to the first commercial-scale process designs using catalytic reformers for tar removal in the Skive and Kokemäki CHP plants in the early 2000s [77, 78].

Successful operation of a reformer requires finding the right balance between carbon formation (coking), temperature and reactor design that maximise the conversion of methane. As described in VTT patents [79–81], a working solution has been found to be a staged configuration where the first stage is based on zirconia and the following stages on precious metal and/or nickel catalysts. The zirconia catalysts are first used to selectively oxidise heavy tars and thus decrease the risk for coking in the reformer [82–84]. The precious metal layer then continues to decompose hydrocarbons and together with the zirconia layer enables the use of high temperatures in the final stages where nickel catalyst layers can be used for methane reforming without problems caused by coking or soot.

The plant configurations created for this work are based on the above-described multistage design where the catalytic reformer is operated downstream from filtration at a temperature range of 850-1000 °C as measured at the reformer's exit. The reformer is operated autothermally with oxygen and steam and is assumed to achieve complete conversion of tars and near-complete conversion of light hydrocarbons.

2.5 Syngas conditioning

After reforming, the properties of the gas are comparable to synthesis gas produced by steam reforming of natural gas. As a result, much of the downstream process can readily be adapted from the synthesis gas industry using commercial equipment and process units, which are described in the following paragraphs.

2.5.1 CO shifting and sulphur hydrolysis

During reforming, the H_2/CO ratio of the synthesis gas approaches equilibrium[2] being about 1.4 at the reformer exit. This needs to be adjusted to meet the stoichiometric requirement of the fuel synthesis, where the H_2/CO ratio in the fresh feed needs to be in the range of 1-3 depending on the desired product.

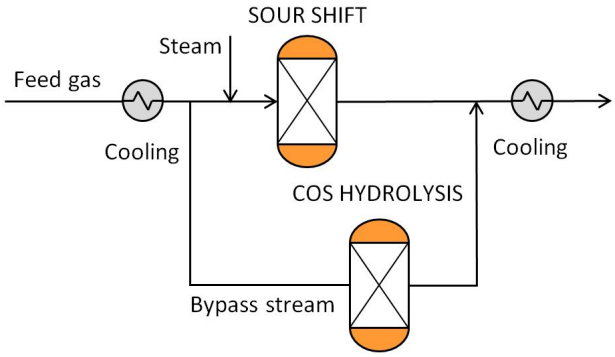

Figure 2.4: Schematic illustration of a CO shift arrangement.

The adjustment can be carried out by catalysing water-gas shift reaction (2.2) further in a reactor filled with sulphur-tolerant cobalt catalyst. To drive the reaction and to suppress catalyst deactivation, steam needs to be added until a minimum steam/CO ratio of 1.8 is achieved at the shift reactor's inlet. In an adiabatic reactor, heat release from the exothermic shift reaction gives rise to an ascending temperature profile along the reactor. To prevent deactivation of the catalyst, the outlet temperature needs to be limited to 404 °C [85]. This can be controlled by adjusting the inlet temperature using a syngas cooler that cools down hot syngas exiting the reformer while recovering sensible heat for steam generation.

$$CO + H_2O = H_2 + CO_2 \quad \Delta H_{298\ \mathrm{K},\ 5\ \mathrm{MPa}} = -49.8\ \mathrm{kJ/mol}, \tag{2.2}$$

In order to avoid an excess amount of CO shift, a portion of the feed gas is bypassed around the reactor (see Fig. 2.4). The amount of bypass is adjusted to achieve a desired H_2/CO ratio after the gas streams are once again combined. In addition to the CO conversion, the sour shift catalysts also convert carbonyl sulphide (COS), hydrogen cyanide (HCN) and other organic sulphur species to hydrogen sulphide (H_2S). To ensure complete hydrolysis of sulphur species, the bypass stream needs to be equipped with a

[2] Caused primarily by additional residence time in elevated temperatures and the fact that nickel and noble metal catalysts also have activity for the water-gas shift reaction.

separate hydrolysis reactor. In the CO shift converter the hydrogenation of COS proceeds in parallel with the water-gas reaction according to equation (2.3), while in the separate reactor the COS hydrolysis follows equation (2.4) [86]. Both reactions approach the equilibrium well with satisfactory space velocities over modern catalysts.

$$H_2 + COS = H_2S + CO \tag{2.3}$$

$$COS + H_2O = H_2S + CO_2 \tag{2.4}$$

2.5.2 Cooling with heat recovery

Several heat exchangers are used in this work to transfer heat between process streams. In the modelling of heat exchangers the heat loss is assumed to be 1 % of heat transferred while pressure drop over the heat exchangers is assumed to be 2 % of the inlet pressure. In addition, 15 °C (gas-liq) and 30 °C (gas-gas) temperature differences are used depending on the process streams.

Heat is recovered from syngas with the following placement of coolers: The first evaporator is placed between the gasifier and the filter where the dust-containing syngas is cooled. The superheater is situated right after the reformer, and is followed by a second evaporator in parallel with the first one. Syngas is then cooled down to 200°C with an economiser. The last cooling step from 200 °C to 40 °C is carried out in a two-stage water scrubber to avoid the risk of residual tar condensation on syngas cooler surfaces. The first scrubber unit recovers heat between 200-60 °C and is used to produce district heat. The second scrubber stage lowers temperature further down to about 30 - 40 °C (depending on the temperature of the cooling water) and the recovered heat is transferred to a nearby lake or sea.[3] Any ammonia contained in the gas will be removed by the scrubber. A portion of scrubber water is continuously sent to an on-site water treatment facility, where it is cleaned and used to produce make-up water for the steam system. Formic acid can occasionally be rationed to the scrubber to control the pH value of the washing solution.

2.5.3 Compression and acid gas removal

Modern synthesis catalysts are very sensitive to impurities and especially all sulphur species must be removed upstream to a single digit ppm_v level to avoid catalyst poisoning and deactivation. In addition to sulphur, an

[3] Or to cooling towers if no natural source of cooling water is available.

upstream removal of CO_2 from syngas will increase productivity of the synthesis. For the removal of these so called 'acid-gases', physical washing processes using organic solvents can be applied. As these processes operate more efficiently at higher pressure, the feed gas stream is normally compressed before treatment to guarantee sufficient removal of CO_2. The molecular mass of the CO_2-rich feed gas is normally high enough to enable the use of relatively inexpensive centrifugal compressors for pressurisation. The absorption capacity of solvents for acid gases also increase as the temperature is lowered. Thus, the removal processes are usually operated at the lowest possible temperature [87]. Minor impurities such as carbonyl sulphide, carbon disulphide and mercaptans are fairly soluble in most organic solvents and are to a large extent removed together with CO_2 and H_2S. The solubilities of hydrocarbons to organic solvents increase with their molecular mass but hydrocarbons above ethane can be to a large extent removed and flashed from the solvent together with acid gases. However, aromatic hydrocarbons are difficult to deal with as they are strongly absorbed by most solvents. They have a tendency to accumulate in the solvent and require a special step to be separated from it [87].

Most organic solvents have much higher solubility for H_2S than for CO_2 and therefore it is possible to carry out a selective removal of hydrogen sulphide to a certain degree by adapting the solvent flow rate to the solubility coefficients of the gas components. Co-removal of CO_2 and sulphur species can be carried out in a single absorber column, while a separate removal of CO_2 and H_2S requires a two-column design where each species is removed in separate columns. Both designs enable virtually any CO_2 removal rate (depending on pressure, column height, solvent flow rate, temperature etc.) while at the same time removing nearly all sulphur species.

The selective removal of sulphur is relevant especially when treating biomass-derived syntheses gases, which are characterised by a high CO_2/H_2S ratio that complicates subsequent treatment of sulphur. By selectively removing first all of the H_2S and only a portion of CO_2, the sulphur stream is more concentrated, and conventional sulphur post-processing becomes possible.

In coal gasification applications the separated H_2S is usually sent to a Claus plant where it is converted to elemental sulphur and sold as a valuable by-product. However, gasification of clean biomass produces too little sulphur for this process to be economically feasible. Therefore, possible options for sulphur processing are conversion to sulphur oxides via combustion or treatment using the Wet Sulphuric Acid (WSA) process.

The basic flow schemes for physical washing processes are simple: For the bulk removal of CO_2 only an absorption stage and solvent regeneration by flashing at successively decreasing pressure levels to atmospheric pressure or vacuum is required. However, this approach is applicable only if H_2S

is present at very low concentrations. Where H_2S is present in significant amounts, thermal regeneration is usually necessary to reach stringent H_2S purity requirements [87, 88].

Following the physical removal process, catalytic absorbents – called guard beds – are generally used to protect the downstream synthesis catalysts from poisoning by removing the residual amounts of sulphur from the feed gas. The catalytic sorbents are usually single-use fixed-bed solid catalysts that react with H_2S to remove it from the gas stream. A common absorbent is zinc oxide that is capable of bringing the sulphur concentration down to a level around 0.005 ppm_v [89]. It reacts with hydrogen sulphide according to the following reaction:

$$ZnO + H_2S = ZnS + H_2O. \tag{2.5}$$

The zinc sorbent can not be regenerated and must therefore be landfilled after use. As a result, this option quickly becomes uneconomical due to the cost of zinc as the amount of sulphur species rise to the two digits ppm_v level. As a practical requirement, sulphur concentration in the guard bed feed gas should be low enough to avoid changing of the beds outside scheduled turnarounds.

2.6 Synthesis gas conversion

A synthesis island is a combination of process equipment that convert synthesis gas to desired products at an elevated pressure and temperature in the presence of a catalyst. The system can be divided into synthesis loop, product recovery and upgrading steps. In the synthesis loop, carbon monoxide and hydrogen are converted into the desired product(s) by catalysing the wanted and suppressing the unwanted reactions. The amount of synthesis gas that can be converted to product(s) in a single pass of gas through the reactor depends on the composition of the fresh feed, selection of catalyst and design and size of the reactor. Recycling of unconverted synthesis gas back to the upstream process makes it possible to convert a larger fraction of biomass energy to synthetic fuel. Although the recycle design enables high overall conversion, it increases gas flows within the recycle, necessitates a feed/effluent heat exchanger and requires a recirculator (compressor) to counter pressure losses in the loop.

Gases such as methane, argon and nitrogen are considered inerts in the synthesis loop and their build-up needs to be controlled by continuously purging part of the recycle flow. The concentration of these inerts should be minimised already in the upstream process as higher amounts of inerts lead

to increased purge gas volumes in the synthesis loop thus having an adverse effect on the economics.

The catalytic reactions are associated with a substantial release of heat as by-product. Typical liquid fuel syntheses operate in the range of 200-300 °C[4], and the released reaction heat can thus be recovered by raising saturated steam in the range of 15-85 bar.

The focus in syntheses designs for this dissertation has been on minimising specific synthesis gas consumption in the conversion loop as it is expect to provide favourable economics due to reduced feedstock costs together with investment savings in the upstream process due to lower gas volumes. This objective is achieved by maximising synthesis gas efficiency η_{sg}

$$\eta_{sg} = 1 - \frac{(CO + H_2)_{\text{in purge}}}{(CO + H_2)_{\text{in fresh feed}}}, \tag{2.6}$$

where CO and H_2 refer to the molar flows of these components in the gas. In most cases the bulk of the formed product is recoverable from the reactor effluent (at synthesis pressure) simply by condensation with cooling water at 20-45 °C. The design of an upgrading area is highly dependent on the product being produced and ranges from a simple distillation approach to a full-blown refinery employing hydrocrackers and treaters. These issues are discussed further in the appropriate sections.

2.7 Synthesis of methane

Conversion of carbon oxides and hydrogen to methane over catalysts based on nickel and other metals (Ru, Rh, Pt, Fe and Co) was first discovered in 1902 by Sabatier and Senderens [90]. The process of methanation can be described with the water-gas shift (2.2) and the following reactions:

$$CO + 3H_2 = CH_4 + H_2O \quad \Delta H = -206 \text{ kJ/mol}, \tag{2.7}$$

$$CO_2 + 4H_2 = CH_4 + 2H_2O \quad \Delta H = -165 \text{ kJ/mol}. \tag{2.8}$$

As both reactions are exothermic and accompanied by a net decrease in molar volume, the equilibrium is favoured by high pressure and low temperature. Although many metals are suitable for catalysing these reactions, all commercially available modern catalyst systems are based on nickel due to its favourable combination of selectivity, activity and price [91]. Technology

[4] High temperature methanation being a notable departure from this.

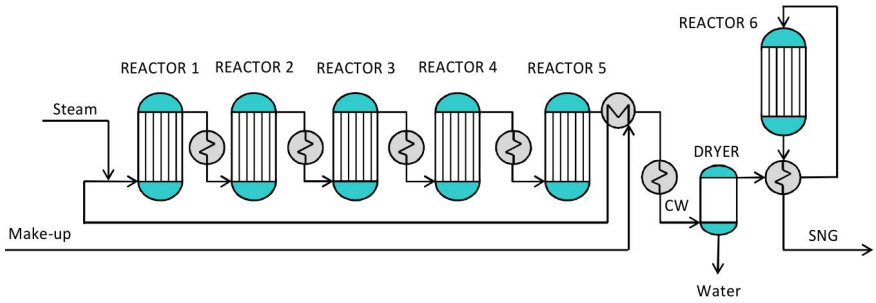

Figure 2.5: Simplified layout of the high-temperature methanation design.

for the production of synthetic methane (also called Synthetic Natural Gas, SNG) from lignite and coal was intensively studied through the 1960s and 1970s in the United States, Germany and Great Britain. This development resulted in a few pilot and demonstration plants, but only one commercial-scale installation: the Great Plains Synfuels Plant commissioned in 1984 (North Dakota, USA) [92]. Recently, a plant producing methane from solid biomass feedstocks was inaugurated in Gothenburg, Sweden. The official start-up of this 20 MW_{th} facility was in October 2013 and once fully operational, it will be the world's first plant that produces biomethane via gasification. The biomethane will be injected to the Sweden's natural gas grid and will be used for vehicle fuel, feedstock for process industry and fuel for CHP or heat production [93].

2.7.1 Synthesis design

Controlling the release of heat during methanation is a major concern for an SNG process design. Efficient heat management is required to minimise catalyst deactivation by thermal stress and maximise methane yield by avoiding equilibrium limitations. In practise, two main reactor concepts have proven suitable for reliable execution of catalytic methanation: (1) fluidised-bed reactors and (2) series of adiabatic fixed-bed reactors using either intermediate cooling or gas recycle, although only the latter has been utilised for industrial operation [94].

The simulation model developed for this dissertation is based on the fixed-bed concept and inspired by the high temperature methanation process 'TREMP', developed and offered by Haldor Topsøe [95]. A simplified layout of the high-temperature methanation design is given in Fig. 2.5. It features six adiabatic fixed-bed reactors connected in series and equipped with intercoolers. The pressure at the inlet of the first reactor is 15 bar. The

inlet syngas ('make-up' in the figure) is mixed with steam and preheated to 300 °C. The amount of steam addition is chosen to limit temperature increase in the first reactor to 700 °C.[5] Due to the high temperature window in the first reactor, special catalysts are needed that combine good low-temperature activity with high-temperature stability [94]. The hot effluent exiting from the first four reactors is cooled to 300 °C before entering the next reactor in the series. Effluent from the fifth reactor is cooled down to condense and separate the by-product water before being fed to the last reactor. Overall conversion of syngas to methane is >99.5 % and the effluent exits the system at 11 bar pressure. Equilibrium conversions in the reactors are calculated with Aspen using the Soave-Redlich-Kwong (SRK) equation of state model. The recovered heat is used to produce high-pressure superheated steam for the plant's steam cycle.

2.7.2 Product recovery and upgrade design

When the synthesis product is liquid, it can be conveniently recovered from unconverted gases of the reactor's effluent by means of condensation. However, in methanation the main product is gaseous and such separation is not possible. Therefore, to achieve high-methane-content SNG product, the amount of inert gases (nitrogen, argon, etc.) needs to be minimised along the production chain. The quality of the SNG product can be estimated by calculating its Wobbe index, I_W, defined as

$$I_W = \frac{\Delta H_v}{\sqrt{\rho/\rho_0}}, \tag{2.9}$$

where ΔH_v is the higher heating value of the SNG product, ρ the density of SNG under standard conditions (STP) and ρ_0 the density of dry air at STP. The I_W is a measure of the interchangeability of different fuel gases[6] and when equal Wobbe indices are reached, distribution of SNG within the natural gas infrastructure can be executed without problems to end-users. Typical I_W values for natural gas range from 45.7 to 54.7 MJ/Nm^3 [96]. For countries where natural gas has high energy content, some propane addition might be needed to reach the required Wobbe index for the product.[7]

The produced SNG also needs to be pressurised to enable distribution within the existing natural gas infrastructure. As the required level of compression

[5] An alternative design would employ a recycle around the first reactor to limit temperature rise. This design does not require steam, but calls for a compressor and electricity to run it.

[6] When two fuels have identical Wobbe indices they will release the same amount of energy during combustion at a given pressure.

[7] For example, Sweden is supplied with Danish natural gas that is characterized by a high methane content. Therefore, propane needs to be added to biomethane to match the Wobbe index of the natural gas [96].

differs among countries and applications, compression of the SNG product to any specific pressure is not considered in the analysis presented in this dissertation. However, it is acknowledged that in vehicle use gas tanks are usually designed to operate up to 200 bar pressure, a fairly uniform standard.

2.8 Synthesis of Fischer-Tropsch liquids

Conversion of synthesis gas to aliphatic hydrocarbons over metal catalysts was first discovered in the early 1920's by Franz Fischer and Hans Tropsch at the Kaiser-Wilhelm-Institut für Kohlenforschung in Mülheim, Germany. Fischer and Tropsch showed that hydrogenation of CO over iron, cobalt and nickel catalysts at 180-250 °C and atmospheric pressure result in a product mixture of linear hydrocarbons [97, 98]. The Fischer-Tropsch process is based on the following reaction [99]

$$CO + 2H_2 \rightarrow (CH_2) + H_2O \quad \Delta H = -165 \text{ kJ/mol}, \tag{2.10}$$

where (CH_2) represents a product that consists mainly of paraffinic hydrocarbons of variable chain length. This raw product from the FT synthesis, called syncrude, is recovered from the reactor effluent and refined to produce marketable hydrocarbon liquids such as high cetane diesel or aviation fuel. The FT process can also be used to produce gasoline, but the overall complexity of this application makes it less attractive than the diesel fuel option, where high linearity and low aromatic content of the syncrude are desirable features during refining [100]. The characteristics of the FT synthesis product depends on the catalyst, process conditions and reactor design, ranging from methane to high-molecular-mass paraffins and olefins [101]. A small amount of low-molecular-mass oxygenates such as alcohols and organic acids are also formed [102].

The product distribution obeys a relationship called the ASF-distribution (Anderson-Schulz-Flory), which can be described fairly accurately by a simple statistical model that predicts a linear relation between the logarithm of the molar amount of a paraffin and its carbon number with a single parameter named α [103, 104]. According to Anderson [105], the mathematic expression can be written as:

$$C_n = (1 - \alpha) \times \alpha^{n-1}, \tag{2.11}$$

where C_n is the mole fraction of a hydrocarbon with chain length n and chain growth probability α independent of n. The α determines the total carbon number distribution of FT products and its range depends on the reaction conditions and catalyst type.

Table 2.2: Comparison of product distributions after the FT synthesis and after the hydrocracker as a function of the chain growth probability α [106].

	ASF-distribution of Fischer-Tropsch products			Calculated distributions in the two-stage process	
Growth change	Product wt-%			Product wt-%	
α	<C10	C10-C20	>C20	<C10	C10-C20
0.80	62.4	31.8	5.8	63.6	36.4
0.85	45.6	38.9	15.5	48.7	51.3
0.90	26.4	37.1	36.5	33.7	66.3
0.95	8.6	19.8	71.7	22.9	77.1
0.98	1.6	4.9	93.5	20.3	79.1
0.99	0.4	1.4	98.2	20	80

The theoretical implication of the ASF-distribution is that only methane can be produced with 100% selectivity, while all other products are produced with relatively low selectivity. In addition to light gases, the only product fraction that can be produced with high selectivity is heavy paraffin wax. For this reason FT syntheses are normally designed to produce a long-chained hydrocarbon wax [106]. Out of the most common catalyst metals for Fischer-Tropsch (Fe, Co, Ni and Ru), only iron and cobalt are available today for industrial application [107]. In contrast to cobalt, alkalised iron FT catalysts exhibit water-gas shift activity, making it suitable for the conversion of CO-rich synthesis gases like those derived from coal, whereas cobalt is suitable for hydrogen-rich gases like those derived from steam reforming of natural gas.

Most of the produced hydrocarbons can be recovered from the reactor effluent by means of condensation with cooling water at 45 °C and at synthesis pressure. Although a recovery of C_1-C_4 hydrocarbons would improve the overall carbon efficiency of the process, it would require cryogenic separation that comes with cost and extra complexity [101].

As Fischer-Tropsch reaction does not allow selective production of materials of narrow carbon number range, the raw syncrude needs to be upgraded by hydrocracking to form desired products. Table 2.2 lists product distributions from direct FT syncrude to final product for different values of α. It illustrates how the "two-step" process can be elegantly tuned to first minimise the formation of undesired light products (using high alpha) and then to produce three narrow-carbon-number range fractions (C_{10-11}, C_{14-16} and C_{16-17}) by selectively hydrocracking the heaviest compounds [106]. The FT wax hydrocracking differs from crude oil hydrocracking in a number of ways [108, 109]. First of all, it can be performed at milder conditions and it consumes much less hydrogen due to the low heteroatom and aromatics content

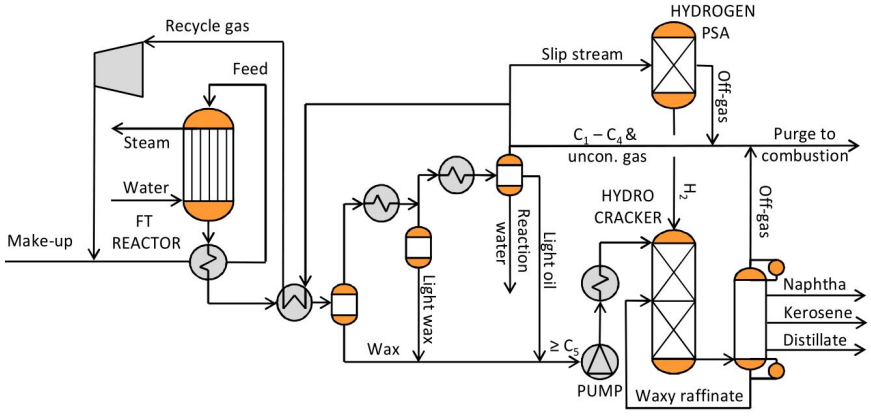

Figure 2.6: Simplified layout of the FT synthesis, product recovery and refinery section. As the upgrading area operates at higher pressure than the FT reactor, waxes and light oils need to be pumped before being fed to the hydrocracker.

of the FT syncrude [101]. In addition, unsulfided noble metal catalysts based on $Pt/SiO_2 - Al_2O_3$ can be used to achieve high selectivity and conversion to distillate, as syncrude is essentially sulphur-free [101].

2.8.1 Synthesis design

The simulation model developed for this dissertation combines the chain-length-independent FT reaction with the chain-length-dependent cracking process to produce paraffinic distillate range products. In the effort to minimise the capital footprint of the plant, a partial refining approach was chosen where only transportable fuel-related products are produced on site instead of complete refining to final products. A simplified layout of the design is shown in Fig. 2.6.

Synthesis gas is converted to paraffinic wax using cobalt-based catalysts in a boiling-water reactor. The reactor is operated at 200 °C and 30 bar and simulated with Aspen using the Soave-Redlich-Kwong (SRK) equation of state model. The reactor has 80 % per pass CO conversion and recirculation is applied to achieve 94 % overall conversion. In recycle conditions the α value is 0.90 and selectivity to C_{5+} is 92 % [110]. The pressure drop over the reactor is set to 5 bar. Input H_2O, CO_2, N_2 as well as unreformed methane, ethane and longer hydrocarbons are considered inert.

2.8.2 Product recovery and upgrade design

The C_5 and heavier oil fractions are recovered while lighter products (C_1-C_4) together with unconverted syngas are recycled back to the synthesis reactor. A small amount of the recycle flow is continuously purged to prevent accumulation of inerts and sent for combustion. The $\geq C_5$ oil fraction and wax are hydrocracked to fuel-related products and the aqueous product (reaction water) is treated as waste water. The refinery section for the highly paraffinic product-slate can be made extremely simple as the aim is not to produce final on-specification diesel fuel, but distillate blendstock that can be produced by the mild trickle-flow hydrocracking process [106].

In the simulated design, the hydrocracking process is operated at 325 °C and 40 bar [106] and > 360 °C boiling material (waxy raffinate) is recycled to extinction in the hydrocracker. The mass ratio of required hydrogen to hydrocracker feed is set to 1 % and gas make from the process to 2 % [101]. Depending on the hydrocracking severity, yield ratios of naphtha, kerosene and gas oil can be varied from 15-25-60 (gas oil mode) to 25-50-25 (kerosene mode) [103]. It is assumed that the recovery of waste heat provides the needed utilities for the upgrading, leading to zero net parasitic utilities demand for the area.

2.9 Synthesis of methanol

The production of methanol (MeOH) from synthesis gas was first described by Patart [111] and soon after produced by BASF chemists in Leuna, Germany in 1923 [112]. This became possible through the development of sulphur- and chlorine-resistant zinc oxide ($ZnO-Cr_2O_3$) catalyst that benefitted from the engineering knowhow acquired from the prior development of ammonia synthesis technology [113]. The main shortcoming of this process was the low activity of the catalyst, which required the use of relatively high reaction temperatures in the range of 300-400 °C. As a result, a high (about 350 bar) pressure was also needed to reach reasonable equilibrium conversions [114]. Despite the drawbacks, high pressure methanol synthesis was the principal industrial production route of methanol for 40 years. In the 1960s workers at ICI pioneered an improved process using more active and highly selective copper oxide catalyst, which became a practical option through the advent of virtually sulphur-free ($H_2S < 0.1$ ppm) synthesis gas produced by natural gas steam reformers. This low-pressure methanol synthesis, operated at 250-280 °C and 60-80 bar has since become the exclusive production process for industrial-scale methanol with the largest plants having a capacity of more than 5000 metric tons per day (MTPD) [115, 116].

All commercially available modern methanol catalysts are based on *Cu-*

$ZnO\text{-}Al_2O_3$ or Cr_2O_3 with different additives and promoters. These catalysts allow the production of methanol at over 99.9% selectivity with higher alcohols, ethers, esters, hydrocarbons and ketones as primary by-products. In addition to the water-gas shift reaction (2.2), methanol synthesis can be described with the following reactions [117]

$$CO + 2H_2 = CH_3OH \ \Delta H_{25^\circ\mathrm{C}} = -90.9 \text{ kJ/mol}, \tag{2.12}$$

$$CO_2 + 3H_2 = CH_3OH + H_2O \ \Delta H_{25^\circ\mathrm{C}} = -50.1 \text{ kJ/mol}. \tag{2.13}$$

The kinetics and mechanisms of methanol synthesis have been discussed since the beginning of methanol research. An enduring question has been whether the formation of methanol proceeds primarily via CO or CO_2 hydrogenation; some authors have reported a sharp maximum of the reaction rate for CO_2 contents in the range of 2-5%, while others have reported a constant increase with increasing CO_2 content [116]. According to Hansen [118], there is an array of evidence favouring the CO_2 route to methanol and only a few proponents still believe that methanol is formed from CO in any substantial quantities, at least with industrial catalysts and conditions.

As both methanol reactions are exothermic and accompanied by a net decrease in molar volume, the equilibrium is favoured by high pressure and low temperature. However, the copper-based catalyst is not active at temperatures much lower than 220 °C and a compromise between reaction kinetics and equilibrium considerations is required [117]. Methanol synthesis is characterised by the ratio (H_2 - CO_2)/(CO + CO_2), where H_2, CO and CO_2 represent their respective concentrations in the fresh feed that is continuously fed to the synthesis loop. This ratio, often referred to as the module M, should equal 2.03 for an ideal composition of fresh feed to synthesis [119]. Typical inerts in the MeOH synthesis are methane, argon and nitrogen [119].

2.9.1 Synthesis design

Several different basic designs for methanol converters have been proposed since the start of production on an industrial scale in the 1960s [116]. Design of the methanol loop in this dissertation is based on a quasi-isothermal tubular reactor where synthesis gas flows axially through the tubes filled with catalysts and surrounded by boiling water. The reaction heat is continuously removed from the reactor to maintain essentially isothermal conditions at 250 °C and 80 bar by controlling the pressure of the steam drum. The reaction temperature needs to be kept low to ensure favourable equilibrium conditions and to prevent loss of catalyst activity caused by sintering of the copper crystallites.

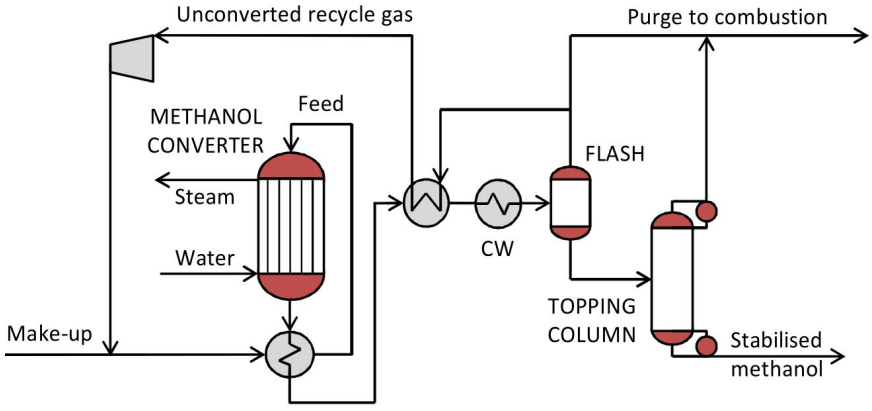

Figure 2.7: Simplified layout of the low-pressure methanol synthesis loop, product recovery and 'low-grade' distillation section.

Boiling-water reactors are easy to control and they approach the optimum reaction rate trajectory well. However, the design itself is complicated and the maximum single line capacity is constrained to about 1800 metric tonnes per day, due to the tube sheet that restrains reactor diameter to around 6 m [118]. The equilibrium conversions in the methanol converter is calculated with Aspen Plus using the Soave-Redlich-Kwong (SRK) equation of state model, which has been found to give better agreement with experimental findings than the Peng-Robinson equation of state, the virial equation, the Redlich-Kwong equation or Lewis and Randall's rule [118].

A simplified layout of the methanol loop design is given in Fig. 2.7. The compressed fresh feed ('make-up') is first mixed with unconverted recycle gas and preheated in a feed/effluent heat exchanger before feeding to the methanol converter. As the per-pass conversion of reactants to methanol is limited by equilibrium, a substantial amount of unconverted gas still exists at the reactor outlet and needs to be recycled back to the reactor to boost overall conversion. The pressure drop across the methanol loop is set to 5 bar.

2.9.2 Product recovery and upgrade design

After the reactor, effluent is cooled against the feed stream in a feed/effluent heat exchanger followed by further cooling with water to separate raw methanol product from unconverted gases by means of condensation. The unconverted gases are recompressed and recycled back to the reactor while the condensed crude methanol is sent to further purification.

The raw methanol contains also water that was formed as a by-product of CO_2 conversion. For carbon-rich syngas, the desired M can be achieved with minimal CO_2 content in the fresh feed, leading to limited by-product water formation and thus reducing the amount of energy needed for distillation.

Two generally accepted product quality standards exist for methanol: fuel-grade and chemical-grade; designated according to the use for which they are destined. The requirements for fuel-grade[8] methanol are less stringent than those for chemical-grade methanol. In cases where even lower qualities can be tolerated, like subsequent conversion to gasoline or olefins, individual specifications can be agreed between the user and producer [113]. Higher purities can be achieved simply by adding more distillation columns, which contributes to additional capital and energy costs. For example, energy consumption for the production of fuel-grade methanol is only one third of that needed for chemical-grade methanol [113].

For the purpose of this analysis, a one column separation design was adopted where light ends (ethers, ketones and aldehydes) and any dissolved gases like hydrogen, carbon oxides, methane and nitrogen are removed from the overhead of an atmospheric column having 80 trays. The bottom product, called stabilised methanol, has a methanol content of 98.5 vol%, the balance being essentially water, and is stored in offsite tanks.

The column is simulated with Aspen Plus using the Non-Random Two-Liquid (NRTL) activity coefficient model [120]. For this 'low-grade' design, the recovery of waste heat provides the needed utilities for the upgrading, leading to zero net parasitic utilities demand for the area.

2.10 Synthesis of gasoline

The most significant development in synthetic fuels technology since the discovery of the Fischer-Tropsch process has been the development of methanol-to-gasoline (MTG) synthesis by Mobil in the 1970's [121–123]. Both processes enable the production of liquid hydrocarbons from carbonaceous feedstocks that can be used as drop-in replacements for conventional petroleum fuels. However, in contrast to the FT process that produces an array of hydrocarbons at a wide carbon number range, gasoline synthesis is very selective, producing primarily finished gasoline blendstock and a by-product stream that resembles liquefied petroleum gas (LPG).

The production of synthetic gasoline is a two-step process that involves 1)

[8] The main criteria for fuel-grade methanol are that it doesn't contain any dissolved gases or low-boiling substances (such as dimethyl ether) and that the water content is below 500 wt-ppm [113].

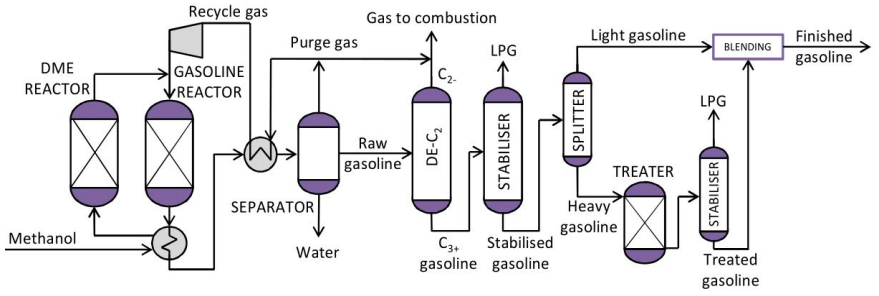

Figure 2.8: Simplified layout of the two-step gasoline synthesis, product recovery and distillation section, adapted from [129].

production of oxygenates from synthesis gas and 2) subsequent conversion of oxygenates to higher hydrocarbons boiling in the gasoline range [124]. These processes may be carried out as separate steps using methanol as the intermediate oxygenate, or in integrated fashion by producing a methanol/dimethyl ether mixture directly from syngas that is conveyed in its entirety to a downstream gasoline converter [125]. A simplified layout of the design adopted for this dissertation is shown in Fig. 2.8.

The conversion of methanol to gasoline proceeds essentially according to the reaction

$$CH_3OH \rightarrow (CH_2) + H_2O, \tag{2.14}$$

while dimethyl ether is converted according to

$$CH_3OCH_3 \rightarrow (CH_2)_2 + H_2O. \tag{2.15}$$

In these reaction equations, (CH_2) represents the paraffinic and aromatic hydrocarbons that are produced in the gasoline synthesis step [126]. A more detailed discussion on the reaction mechanisms is available in Ref. [122]. The conversion of oxygenates into C_2-C_{10} hydrocarbons is catalysed by zeolites such as ZSM-5 that have a silica to alumina mole ratio of at least 12 and a pore size defined by 10 membered rings. The manufacture of these zeolites is well known and commercial catalysts are available [127]. A unique characteristic of the gasoline product is the abrupt termination in carbon number at around C_{10} due to the shape-selective nature of the zeolite catalyst. As a result, the composition and properties of the C_{5+} fraction are those of a typical high-quality aromatic gasoline, boiling in the 120-200 °C range [123, 128].

One disadvantage of synthetic gasoline is its relatively high (3-6 wt%) durene content in comparison to conventional (0.2-0.3 wt%) gasoline. Although durene has a good octane number and it boils within the gasoline boiling range, it has a high melting point (79 °C) which is known to cause carburettor "icing" if the gasoline durene concentration is too high. To eliminate this problem, the content of durene should be reduced to under 2 wt% [130].

In addition to ExxonMobil, Haldor Topsøe has developed a gasoline process called Topsøe Integrated Gasoline Synthesis (TIGAS). The key distinction from ExxonMobil's MTG technology is that in TIGAS the synthesis gas is converted directly to a mixture of DME and methanol, followed by conversion to gasoline in a downstream reactor thus making upstream production and intermediate storage of methanol unnecessary [131].

2.10.1 Synthesis design

The synthesis design is based on the conventional two-step gasoline process, where methanol is produced first and then stored until subsequent conversion to gasoline that might or might not take place at the same site as the manufacture of methanol. In the design, methanol is first pumped to 22.7 bar and then vaporised and superheated to 297 °C in heat exchange with the hot reactor effluent. The methanol is then fed to an adiabatic fixed-bed dehydration (DME) reactor where it is converted to an equilibrium mixture of methanol, DME and water. The effluent exits the reactor at 409 °C and 21.7 bar and is admixed with recycle gas and fed to a second reactor where it is converted to gasoline [123]. A large recycle stream is needed to limit the outlet temperature of the adiabatic gasoline reactor to 400 °C. We assume the molar recycle to fresh feed ratio to be 7.5:1 [129]. To control the build-up of inerts in the synthesis loop some gas needs to be purged from the recycle flow, which is then transferred to combustion. The equilibrium conversion of methanol to DME and water is simulated with Aspen Plus using the Soave-Redlich-Kwong (SRK) equation of state model [132].

Due to the proprietary nature of the process, very little information has been published about the performance of the MTG reactor, thus complicating the process simulation effort. However, a RYield block was chosen to simulate gasoline synthesis using the product yield structure of the MTG's gasoline reactor (See Table 2.3) as reported by Larson et al. [133] based on the work of Barker et al. [134] and Schreiner [135].

Table 2.3: MTG yield structure for a fixed-bed reactor given per kg of pure methanol input to a DME reactor [133].

Component name	**Formula**	**Molar mass**	**kmol/kgMeOH**
Hydrogen	H_2	2.02	0.00001049
Water	H_2O	18.02	0.03137749
Carbon monoxide	CO	28.01	0.00000446
Carbon dioxide	CO_2	44.01	0.00001390
Methane	CH_4	16.04	0.00019586
Ethene	C_2H_4	28.05	0.00000473
Ethane	C_2H_6	30.07	0.00005067
Propene	C_3H_6	42.08	0.00002055
Propane	C_3H_8	44.10	0.00042752
1-Butene	C_4H_8	56.11	0.00008593
n-Butane	C_4H_{10}	58.12	0.00019381
i-Butane	C_4H_{10}	58.12	0.00062811
Cyclopentane	C_5H_{10}	70.13	0.00001514
1-Pentene	C_5H_{10}	70.13	0.00014015
N-pentane	C_5H_{12}	72.15	0.00008633
I-pentane	C_5H_{12}	72.15	0.00075797
Gasoline*	C_7H_{16}	100.2	0.00283472

*Gasoline is assumed to be represented as n-heptane (C_7H_{16})

2.10.2 Product recovery and upgrade design

The gasoline reactor effluent is condensed and separated into water, raw gasoline, purge and recycle gas streams. The water phase contains about 0.1-0.2 wt% oxygenates (alcohols, ketones and acids) that can be treated with conventional biological means to yield an acceptable effluent for discharge [124]. The condensed raw gasoline is sent to a product recovery section where it is fractionated by distillation. The liquid hydrocarbons are first transferred to a de-ethaniser where C_{2-} fraction is separated from the overhead and the bottoms are passed to a stabiliser where a stream of LPG is produced overhead. The stabilised gasoline is sent to a gasoline splitter where it is separated into light and heavy gasoline streams. The heavy gasoline stream undergoes durene treatment (HGT) that includes: isomerisation, disproportionation, transalkylation, ring saturation and dealkylation/cracking reactions. Yield loss of C_{5+} due to the treatment is minimal as only 10 - 15 % of the gasoline needs to be processed [124, 130]. After HGT the treated heavy gasoline is blended with light gasoline and C_4's to produce finished gasoline containing less than 2 wt% durene [124, 130].

The required hydrogen for the durene treatment can be separated from synthesis gas via pressure swing adsorption. However, Larson et al. [133] have estimated that the hydrogen requirement of durene treatment is only 0.2 to 0.6 kg of hydrogen per tonne of total gasoline produced. Due to this

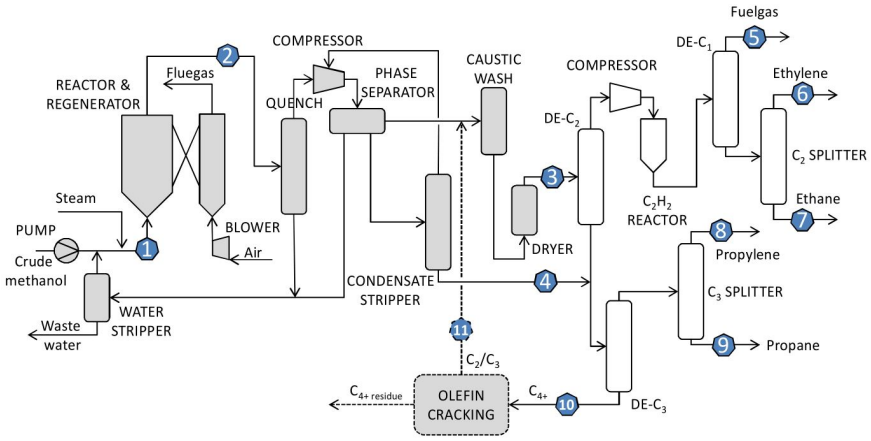

Figure 2.9: Simplified layout of a methanol to olefins plant.

minuscule consumption, this step was not included in the simulation. In addition, it is assumed that the recovery of waste heat provides the needed utilities for the upgrading, leading to zero net parasitic utilities demand for the area.

2.11 Synthesis of olefins

Mobil (now ExxonMobil) discovered a zeolite-based ZSM-5 catalyst in the early 1970s that was capable of converting methanol to gasoline and olefins. This led to the development of methanol to olefins technology (MTO) in the mid-1980s as a spin-off to a methanol to gasoline process demonstrated at that time in New Zealand. Later in the 1980s scientists at Union Carbide developed SAPO-34 (Silicoalumino-Phosphates) catalysts with high selectivity for the MTO reaction [136]. The MTO development was transferred from Union Carbide to UOP in 1988 but went largely unused until the mid-1990s when UOP teamed up with Norsk Hydro to build a pilot plant in Norway. A successful 100 bbl/d demonstration plant was later operated in Germany with U.S. and German government support [123]. Since then, Lurgi has developed its own version of the process, called methanol to propylene (MTP). The Chinese have also been active in this field and the Dalian Institute of Chemical Physics has recently developed a similar process called DMTO [137].

Major differences between MTP and MTO technology are that the MTP process uses a ZSM-5 catalysts in a fixed-bed reactor to produce preferentially

propylene, whereas the MTO technology is based on a MTO-100 catalyst (a modified SAPO-34 catalyst) in a fluidised-bed reactor producing both ethylene and propylene with an adjustable product ratio. The analysis presented in this dissertation is based on UOP/Hydro's MTO technology.

2.11.1 Synthesis design

A simplified block diagram in Fig. 2.9 illustrates a possible design for a stand-alone MTO process. The fluidised-bed reactor/regenerator system converts feed methanol into a mixture of olefins, which is then fractionated to yield polymer-grade light olefins as major products. The feed methanol is first compressed to 3 bar, preheated and vaporised in heat exchange with reactor effluent and then mixed with recycled methanol from the downstream process. The methanol stream is mixed with steam to increase olefin selectivity and decrease catalyst deactivation in the reactor. The combined stream of methanol and water is superheated to 310 °C and fed to a fast fluidised MTO reactor operating at 400-450 °C and 3 bar. At the presence of a proprietary MTO-100 catalyst a nearly complete (99.8 %) conversion of methanol is achieved with ~80% carbon selectivity to ethylene and propylene (see Table 2.4). Coke will gradually build-up on the catalyst surface and to maintain activity, a portion of the catalyst is continuously sent to a combustor (operating at 600 °C) where the coke is burned off with air before returning the regenerated catalyst to the MTO reactor. The mass ratio between ethylene and propylene in the effluent (stream 2 in Fig. 2.9) can be varied from 0.75 to 1.5 by adjusting the operating severity. Higher temperature will lead to more ethylene being produced [138], although the highest overall yield to light olefins (ethylene plus propylene) is achieved with about equal amounts of both [139].

2.11.2 Product recovery and fractionation

The reactor effluent is cooled down to 240 °C in a feed/effluent heat exchanger and then further to condense the water and unconverted methanol by a scrubber (labelled quench in the flowsheet). The recovered methanol is recycled back to the reactor. The bottom stream of the stripper contains most of the water contained in the MTO reactor's effluent and is sent to waste water treatment after exchanging heat with the reactor feed preheater. The gaseous effluent is compressed to 25 bar and flashed at 33 °C in a phase separator to produce a vapour stream and a condensate stream with two liquid phases. The aqueous phase is separated from the condensate and sent to the stripper while the organic layer is stripped in a separate column and the produced organic concentrate is sent to a downstream depropaniser (labelled De-C_3).

Acid gases from the phase separator's vapour stream are removed by caustic wash. The treated acid-free effluent is then cooled to 22 °C, dried with a molecular sieve, cooled further to 10 °C and sent to a de-ethaniser (De-C_2) where a majority of ethylene is recovered overhead and most of the propylene from the bottom (condenser temperature -25 °C, reboiler 66 °C). The overhead vapour is compressed to 33 bar and sent through an acetylene converter (C_2H_2 reactor) where the small amount of acetylene produced in the MTO reactor is hydrogenated to ethane over a palladium-based catalyst. The treated effluent is then chilled to -20 °C and fed to a demethaniser (De-C_1) that produces methane-rich fuel gas overhead (5) and a mixture of C_2 hydrocarbons from the bottom. Very low temperatures (-90 °C in the condenser) are needed to carry out this separation. The fuel gas is routed through a Pressure Swing Adsorption unit that recovers 86 % of the hydrogen contained in the stream. After hydrogen recovery the rest of the gas is directed to combustion. The C_2 stream from the bottom is directed to a C_2-splitter column that produces a polymer-grade ethylene stream overhead (6) and an ethane-rich (about 70 mol%) by-product stream from the bottom (7). The bottom stream from the de-ethaniser (De-C_2) is mixed with the bottoms from the organic layer stripper (condensate stripper) and sent to a depropaniser (De-C_3). The overhead stream goes to a large C_3-splitter producing polymer-grade propylene (8) overhead and a propane-rich (around 60 mol%) by-product (9) from the bottom. The De-C_3 bottoms (stream 10) consists of heavy hydrocarbons characterised as a C_{4+} stream.

Table 2.4: Mass yield structures used for the simulation of the MTO and Olefin Cracking Process [136, 138, 140].

Component	**MTO**	**OCP**
H2	0.0648	
CO	0.0128	
CO_2	0.0519	
CH_4	1.0486	2
C_2H_4	16.7210	19
C_2H_6	0.3581	2
C_3H_6	16.7208	71
C_3H_8	0.2245	4
C_4H_8	5.1564	2
C_4H_{10}	0.0389	
C_5H_{10}	2.1076	
Coke	1.3255	
H_2O	56.1692	
SUM	100.0000	100

2.11.3 Olefin cracking process

Two different MTO plant designs are examined in this dissertation. They differ from each other in the way the by-product C_{4+} stream is processed. In the 'base case MTO' design, the C_{4+} by-product is sent to an alkylation unit, where 1-butene and 2-butene react with isobutane to form valuable high-octane alkylates used as gasoline additives. In the 'Advanced MTO' design the C_{4+} stream is sent to an Olefin Cracking Process (OCP) where it is converted to higher-value propylene and ethylene.

The Advanced MTO process can reach close to 90 % overall carbon selectivity to ethylene and propylene from methanol, a marked improvement from the 80 % of the base case MTO. While the propylene to ethylene (P/E) ratio of conventional MTO is about 1, for OCP the P/E ratio is 3.5-4.0. The P/E of the combined MTO + OCP process can thus range from 1.3 to 2.1 [136, 141, 142]. The integration of MTO with OCP is fairly straightforward, because the recovery section of the MTO unit remains unchanged, needing only to be resized to accommodate the added circulation to and from the olefin cracking process [143].

The olefin cracking process was developed by Total Petrochemicals and comprises a selective hydrogenation reactor, olefin cracking reactor and two fractionating columns (depropaniser and debutaniser). In the selective hydrogenation reactor, diolefins and acetylenes present in the feed are converted to mono-olefins to prevent their conversion to coke and further to methane later in the process. The selective hydrogenation is performed at relatively mild conditions (30-200 °C, 4.5-22 bar) in liquid phase using a cylindrical fixed bed reactor with an alumina catalyst [144].

In the olefin cracking reactor heavy C_{4+} olefins are cracked down to light olefins in the C_2 to C_3 range under gaseous phase conditions and in the presence of an olefin cracking catalyst [144]. The reactor is operated at 500-600 °C and 1-5 bar [136]. For the assumed mass yield structure of the olefin cracker process, see Table 2.4.

The light olefin product stream is recovered from overhead of the depropaniser fractionating column. The debutaniser fractionating column is used to collect and redirect a portion of the depropaniser bottoms stream for process recycle and also to remove process purge comprising C_4 and heavier hydrocarbons to avoid the build-up of paraffinic compounds. The depropaniser and debutaniser columns operate at 8 to 21 bar [144].

2.12 Auxiliary boiler

Synthesis plants consume varying amounts of electricity depending on the pressure levels of process equipment (compression work) and overall plant design. In the studied thermochemical configurations electricity is produced with a turbine connected to the steam system. Roughly half of the electricity consumption can be generated using steam recovered from syngas cooling. The rest needs to be satisfied with the combination of steam generated by combustion of by-products and purchases from the electricity grid.

Some carbon is always left unconverted in the gasifier and some syngas is left unconverted in the synthesis loop. The filter ash stream of a 100 MW_{th} gasifier having a carbon conversion of 98% corresponds to an energy flow of about 2 MW_{th}. This energy can be recovered by combustion of the filter ash (containing about 50/50 carbon/ash) in a suitable boiler. The amount of energy contained in the purge gas varies considerably depending on the type and configuration of the synthesis. If the unconverted gas is separated from the synthesis effluent and recycled back to the reactor inlet, only small amount of gas is eventually left unconverted. Such small purges could be combusted in a boiler together with filter ash, or separately in a gas engine to achieve higher power production efficiency. A further option for larger purge gas streams would be combustion in a gas turbine integrated with the plant steam system.

The saturated steam raised in the synthesis reactor carries substantial amount of enthalpy but little exergy due to its low temperature that limits the amount of work that can be recovered from it. Its value could be greatly increased by superheating in an auxiliary boiler before injection to turbine, or alternatively it could be used directly as process steam via a pressure let down. An auxiliary boiler also increases the flexibility of plant operation by its ability to produce steam independently from the gasification plant, a convenient attribute during start-ups, process failures, et cetera.

All thermochemical and hybrid plant configurations considered in this dissertation feature a bubbling fluidised-bed combustor producing 93.5 bar superheated steam at 500 °C operated with lambda 1.2 and modelled in Aspen as RStoic. The pressure drop over the reactor is set to 0.1 bar, and heat is recovered from flue gas cooling to generate steam and to preheat the combustion air to 250 °C. The outlet temperature of flue gas is 150 °C.

2.13 Steam system

All thermochemical and hybrid plant configurations examined in this dissertation feature a back-pressure steam turbine design that co-generates electricity, process steam and district heat (DH). All plant configurations are

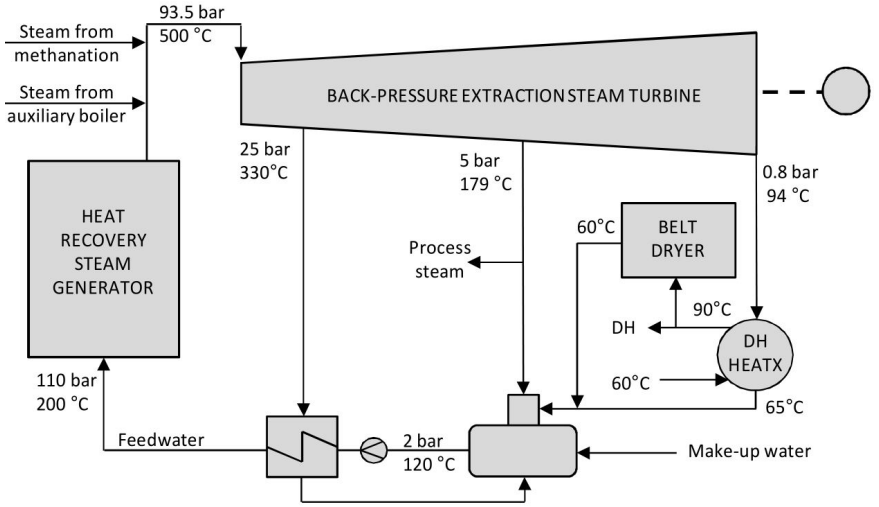

Figure 2.10: Simplified layout of the steam cycle design.

designed self-sufficient in terms of steam, while electricity is balanced with grid purchases and surplus heat is sold to a nearby district heating network. A simplified layout of the steam cycle is illustrated in Fig. 2.10.

The effluent from the syngas water scrubber is sent to an on-site water treatment process where it is purified and used to produce make-up water for the steam cycle. The make-up is fed to the feedwater tank operating at 2 bar and 120 °C and heated with deaeration (process) steam. From the tank the feed water is distributed to the auxiliary boiler, the gasification plant and the synthesis island. To avoid possible residual tar condensation on the cooler surfaces, feed water entering the syngas cooling system is preheated to 200 °C with extraction steam from the turbine.

Steam is generated at several locations in the overall process. The majority is raised by recovering heat from syngas cooling. Additional steam is produced by combusting unconverted carbon from the gasifier (filter dust) and unconverted syngas from the synthesis (if available) in an auxiliary boiler. The live steam parameters are 93.5 bar[9] and 500 °C, which are typical values for a small-scale biomass power plant [145].

In plant designs that feature synthetic natural gas production, the synthesis exotherm is utilised to produce superheated steam that can be used in the turbine as additional live steam. In plant designs that feature methanol production, the synthesis exotherm is utilised to produce saturated steam at

[9] After 17.5 bar pressure drop mostly caused by superheaters.

43 MPa and 255 °C that is used to satisfy part of the plant's process steam consumption.

The steam turbine size is approximately 20 MW_e in the studied configurations. Such small turbine is physically limited to a maximum of 4 extraction holes that needs to be considered when designing the steam system [146]. The turbine is modelled as isentropic using the ASME 1967 steam table correlations with following specifications: isentropic efficiency 78 %, generator efficiency 97 % and mechanical efficiency 98 %. The first steam extraction point from the turbine is fixed at 25 bar and 330 °C and used to preheat feedwater to 200 °C. The second extraction point is fixed at 5 bar[10] and 179 °C and used to supply steam for the gasifier, reformer, deaerator and AGR solvent regeneration. The rest of the steam is extracted at the turbine's back-pressure (0.8 bar), condensed and used to produce hot water at 90 °C. The hot water provides heat for drying the wet biomass feed and the rest is sold to a nearby district heating grid.

In practise the size and duration of district heat demand sets limits for the heat integration possibilities at the plant site. Some guidelines for sizing are discussed later in section 3.3, but in this dissertation it is assumed that the produced district heat can be always fully utilised when the gasification plant is running.

2.14 Air separation unit

When gasification and reforming are based on partial oxidation, pure oxygen is required for the generation of nitrogen-free synthesis gas. Although the investment cost of oxygen production is substantial, it is considered to be offset by the reduced costs of the smaller equipment and more efficient recycle configuration around the synthesis made possible by the absence of nitrogen in the syngas. A variety of processes exist for the separation of oxygen and nitrogen from air (e.g. adsorption processes, polymeric membranes or ion transportation membranes), but for the production of large quantities (>20 tons per day) of oxygen and nitrogen at high recoveries and purities, the conventional multi-column cryogenic distillation process still remains as the most cost-effective option [147].

In the cryogenic air separation unit, air is first pressurised and then purified from CO_2 and moisture by a molecular sieve unit. The clean compressed air is then precooled against cold product streams, followed by further cooling down to liquefaction temperature by the Joule-Thompson effect. The liquefied air is then separated to its main components in a distillation tower operating between the boiling points of nitrogen and oxygen (-196 °C to -183 °C). Because the boiling point of argon is very similar to that of oxygen,

[10] 1 bar higher than gasification pressure to allow pressure drop for the inlet valves.

the purity of the oxygen product from a double column unit is limited to around 96 %. However, when higher purity oxygen is required, argon can be removed by adding a third distillation column that yields a pure argon product [148]. ASU design adopted for this dissertation features a stand-alone cryogenic air separation unit producing 99.5 mol% oxygen at a 1.05 bar delivery pressure.

Cryogenic air separation is an energy-intensive process that requires a substantial amount of power to operate. According to [147] a plant producing 890 tons of oxygen per day at 500 psig (35.5 bar) using a full pumped liquid oxygen cycle consumes about 12.5 MW of electric power. Based on an Aspen simulation, compression of oxygen from 1.05 to 35.5 bar[11] consumes 3.76 MW_e. Subtracting this from 12.5 gives 8.7 MW, which yields a specific power consumption of 260 kWh/tonO_2 for an ASU delivering oxygen at 1.05 bar pressure.

2.15 Electrolysis of water

Hydrogen can be produced by passing an electric current through two electrodes immersed in water. In the process, water molecules are split to produce oxygen and hydrogen according to the following overall reaction:

$$2H_2O(l) \rightarrow 2H_2(g) + O_2(g). \tag{2.16}$$

Presently the production of hydrogen via electrolysis is mainly limited to small or special applications, while larger quantities are produced by steam reforming of natural gas or other fossil fuels. The most established and commercially available technology is based on alkaline electrolysers, while proton exchange membrane (PEM) electrolysis and solid oxide electrolysis cells (SOEC) are examples of more advanced and emerging systems [149]. SOEC electrolysers are the most efficient but the least developed. PEM electrolysers are more efficient than alkaline and do not have issues with corrosion or seals as do the SOEC systems, but cost more than alkaline systems. Alkaline electrolysers have the lowest efficiency, but are the most developed and lowest in capital cost [150].

In this dissertation, electrolytic hydrogen is produced via low temperature alkaline water electrolysis.[12] The system is composed of electrodes, a microporous separator, an aqueous solution of water and 25-30 wt% of potassium hydroxide (KOH) as an electrolyte [151]. The liquid electrolyte is not consumed in the reaction, but must be replenished over time to cover losses

[11] Assuming centrifugal compressor having a polytropic efficiency of 87 %, driver efficiency of 92 % and 5 stages with intercooling to 35 °C.

[12] Norsk Hydro's Atmospheric Type No. 5040 (5150 Amp DC).

that occur during hydrogen recovery. Water is decomposed into hydrogen and OH^- in the cathode. The OH^- travels through the electrolytic material to the anode where O_2 is formed, while hydrogen is left in the alkaline solution and separated by a gas/liquid separator unit outside the electrolyser cell. Nickel with a catalytic coating, such as platinum, is the most common cathode material, while for the anode nickel or copper metals coated with metal oxides, such as manganese, tungsten or ruthenium are used [150].

Commercial systems are typically run with current densities in the range of 100 - 300 mA/cm^2. The product hydrogen and oxygen can be assumed to be of 100 % purity due to the very low concentration of contaminants [152]. The system efficiency of an alkaline electrolyser, defined as hydrogen output (LHV) divided by electrical energy consumed by the electrolysis system, is set to 62 % (74 % HHV) [152].

2.16 Carbon dioxide capture

Carbon dioxide is available at almost inexhaustible quantities in the atmosphere where it can be captured either directly with an industrial process or indirectly via plant matter [153]. Capturing carbon dioxide from air is fairly easy in a chemical sense, but as atmospheric CO_2 is very dilute (0.04 %), the development of a practical system for capturing commercially significant quantities has proved challenging [154].

In a direct air capture (DAC) plant diluted CO_2 is dissolved into a solution or solid sorbent from which a concentrated stream of CO_2 is produced in the regeneration phase. Currently proposed systems are often based on NaOH sorbent followed by regeneration with chemical caustic recovery [155]. The long-term cost estimates[13] for such direct air capture systems are about 115 €/tCO_2 ± 40 €/tCO_2 [153, 155]. Despite the high costs, it deserves to be noted that DAC has the unique ability to provide abatement across all economic sectors at a fixed marginal cost [153]. In other words, the cost of DAC represents the upper limit for any conceivable CO_2 abatement strategy.

A third possible source for carbon dioxide, in addition to direct and indirect capture from air, is to utilise exhaust CO_2 from industrial plants [156]. Today, carbon dioxide is routinely separated at some large industrial plants and also at several small power plants. The capture costs are estimated to be around 40 €/tCO_2 [157, 158] for new supercritial pulverised coal boilers and around 50 €/tCO_2 for new natural gas combined cycle plants [158] both employing an amine-based system for post-combustion CO_2 capture, excluding the cost of transport and storage.[14] However, it is acknowledged that

[13] Based on US$150/$tCO_2$ ± $50/$tCO_2$.
[14] Based on US$50/$tCO_2$ and US$60/$tCO_2$, respectively.

new or improved methods of CO_2 capture have the potential to significantly reduce the cost of capture and the required energy use [159].

2.17 Carbon dioxide hydrogenation

Carbon dioxide can be used as a C_1 building block for making organic chemicals, materials and fuels [160]. However, it is considered a less favourable feedstock for fuels production than carbon monoxide due to more intensive use of resources (energy, H_2, more reaction steps, etc.) [161]. Presently, the use of CO_2 as a chemical feedstock is limited to few industrial processes such as urea synthesis and its derivatives, salicylic acid and carbonates [161].

Production of methane from CO_2 via Sabatier reaction (2.8) is a well-known route that can be realised using existing methanation catalysts. In addition, catalysts allowing direct hydrogenation of CO_2 to methanol via reaction (2.13) have been developed, and pilot-scale plants based on this technology demonstrated [162–166]. However, the conversion of pure CO_2 into methanol is challenging due to difficulties associated with the chemical activation of CO_2 and commercial catalyst systems used for this task have low catalytic activity and greatly reduced yield [29, 167, 168]. In addition, almost one third of the input H_2 is consumed to produce by-product water.

Despite these challenges, plant configurations developed for this dissertation assume that catalyst systems for CO_2-based methanol production are available and operate close to equilibrium conversion with the same catalyst productivity than commercial alternatives using carbon monoxide as the main feed. This approach is motivated by recent breakthroughs in catalyst development suggesting that the activity of a catalyst in transformation of CO_2 to methanol can be greatly improved [169].

Chapter 3

Materials and methods

This chapter discusses and summarises process design parameter assumptions used for the the mass & energy simulations. Parameters and methods used in estimating the overnight capital costs and carrying out the economic assessments are also presented. A brief outline on the biomass gasification model as well as selected production route options and their characteristics is also provided. In case of discrepancies among parameters used in **Papers I - V**, values from **Paper IV** are reported.

3.1 Performance analysis

Process modelling was used as a tool for carrying out the performance analyses reported in this dissertation. Models were created using ASPEN Plus® (Aspen) process simulation software. Mass and energy flows were simulated and used to analyse the performance characteristics of selected plant designs. A semi-empirical approach was chosen for the modelling of fluidised-bed gasification and catalytic reforming. This was made possible by access to an extensive amount of operational data from VTT's past experimental campaigns with biomass gasification and reforming of tar-containing gases. Based on this data, empirical correlations were created for carbon conversion and formation of hydrocarbons and tars during gasification and conversion of said hydrocarbons and tars during reforming. The correlations were then used to adjust equilibrium calculations to achieve better match with experimental data as discussed in **Papers I** and **II**. The accuracy of the models were evaluated by validating model predictions against other sets of experimental data. For gasification, a fairly good agreement between experimental data and model predictions was achieved for the main gas components. The

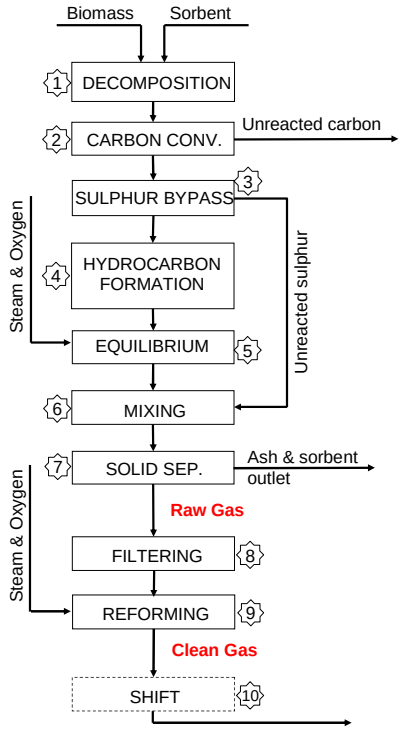

Figure 3.1: A schematic illustration of the biomass gasifier, hot-filtration and catalytic reformer model.

average relative error for components H_2, CO, CO_2, and CH_4 was found to be 14 %, while the magnitude of error in the used experimental data was estimated to be around 5 %. Accuracy of the reformer model was not evaluated in the papers due to the lack of public data at the time.

The schematic structure of the model is illustrated in Figure 3.1. The core blocks of the model are equilibrium (RGibbs) blocks 5 and 9, used to convert feeds to equilibrium products based on the minimisation of Gibbs free energy. Almost all other blocks in the model are used for simulating phenomena that are observed not to comply with chemical equilibrium. The gasifier simulation begins (block 1) with the decomposition of the biomass to elemental gases, carbon and ash, based on the ultimate analysis of the feedstock. In blocks 2 and 3 the carbon conversion and sulphur removal are modelled by extracting fixed amounts of elemental carbon and sulphur to an outlet stream[1] and to bypass, respectively. The formation of tars is sim-

[1] When simulating complete synfuel plants the unconverted carbon is combusted in an auxiliary boiler.

ulated in block 4 and they are handled as inerts in the block 5, where rest of the feeds are converted to equilibrium products. The streams are then mixed together in block 6 and feedstock ash is separated to an outlet stream in block 7. The outlet stream of block 7, labelled 'Raw gas', is considered as the gasifier's end product. The gas is then cooled down to simulate filtration, followed by a reformer block (9) where Raw gas, steam and oxygen are converted to equilibrium products. To match the conversion of methane and higher hydrocarbons in the reformer with experimental data, appropriate fractions of hydrocarbons are handled as inerts in the block. The outlet stream from block 9, labelled 'Clean gas', is considered as the reformer's end product. For more detailed discussion on the gasifier and reformer models please refer to **Papers I** and **II**.

Table 3.1: Summary of process design parameters.

Item	**Design parameters**	**Notes**
Air separation unit	Oxygen delivered from ASU at 1.05 bar pressure. Oxygen product (mol-%): O_2 = 99.5 %, N_2 = 0.5 %, Ar = 0 %. Power consumption 263 kWh/tonO_2.	a
Feedstock preparation and handling	Feeding screw power consumption 7 kJ/kg biomass. Lock-hopper inert gas consumption: 0.07642 Nm^3/kg biomass for a double lock-hopper system that uses purge gas from LH to partly pressurise another LH. For a single lock-hopper system inert gas consumption 50 % higher.	b
Atmospheric band conveyor dryer	Biomass moisture: inlet 50 wt-%, outlet 15 wt-%, hot water: T_{in}=90 °C, T_{out}=60 °C, steam: 0.8 bar & 94 °C, heat consumption: 1300 kWh/tonH_2O_{evap}, power consumption: 32 kWh/ton_{drybio}	c
Pressurised circulating fluidised-bed steam/O_2 gasifier	Heat loss = 1 % of biomass LHV. Δp = -0.2 bar. Carbon conversion: 98 %. Modelled in two steps with RStoic and RGibbs using Redlich-Kwong-Soave equation of state with Boston-Mathias modification (RKS-BM). Hydrocarbon formation (kmol/kg of fuel volatiles): CH_4 = 6.7826, C_2H_4 = 0.4743, C_2H_6 = 0.2265, C_6H_6 = 0.2764. Tars modelled as naphthalene: $C_{10}H_8$ = 0.0671, All fuel nitrogen converted to NH_3. All other components assumed to be in simultaneous phase and chemical equilibrium.	d, e

Table 3.1 – continued from previous page

Item	Design parameters	Notes
Ceramic hot-gas filter	Δp = -0.2 bar. Inlet temperature 550 °C.	e
Catalytic autothermal partial oxidation reformer	Modelled as RGibbs using Redlich-Kwong-Soave equation of state with Boston-Mathias modification (RKS-BM). Phase and chemical equilibrium conversion for C_{2+} and tar. Ammonia conversion restricted to 50 %. Outlet temperature and CH_4 conversion: 957 °C & 95 % or 850 °C & 35 % depending on the case investigated. Δp = -0.2 bar	d, e
Sour shift	T_{out} = 404 °C, steam/CO = 1.8 mol/mol, Δp = -0.2 bar. Modelled as REquil using Redlich-Kwong-Soave equation of state with Boston-Mathias modification (RKS-BM). Equilibrium reactions: CO + H_2O = CO_2 + H_2, T_{appr} = 10 K. COS + H_2O = CO_2 + H_2S, T_{appr} = 0 K. HCN + H_2O = CO + NH_3, T_{appr} = 10 K.	f, e
Scrubber	Scrubbing liquid: water. T_{inlet} 200 °C. Two-step cooling: T^1_{out}= 60 °C, T^2_{out}= 30 °C. Complete ammonia removal. Modelled as Flash using Soave-Redlich-Kwong (SRK) equation of state model.	e
Rectisol acid gas removal	100 % H_2S capture, for CO_2 capture level see case designs. Utilities: Electricity (other than for refrigeration) = 1900 kJ/kmol(CO_2+H_2S); Refrigeration 3 x duty needed to cause -12 K temperature change in the syngas; 5 bar steam = 6.97 kg/kmol (H_2S+CO_2).	g
High temperature methanation	Six adiabatic fixed-bed reactors connected in series and equipped with intercoolers. Pressure at system inlet = 15 bar, pressure at system outlet 11 bar. T_{input} to reactors 300 °C. T_{output} from the first reactor restricted to 700 °C with steam dilution. Gas dried before feeding to last reactor. Syngas conversion to methane >99.5 %. Equilibrium reactions: CO + $3H_2$ = CH_4 + H_2O, $T_{appr.}$ = 20 K; CO_2 + $4H_2$ = CH_4 + $2H_2O$, $T_{appr.}$ = 20 K. Reactors modelled as REquils using Soave-Redlich-Kwong (SRK) equation of state model.	e
Low-temperature Fischer-Tropsch synthesis	$T_{reaction}$ = 200 °C, $P_{fresh\ feed}$ = 30 bar, Δp =-5 bar, Boiling-water reactor using cobalt catalysts modelled with REquil using Redlich-Kwong-Soave equation of state with Boston-Mathias modification (RKS-BM). 80 % per-pass CO conversion with recirculation to achieve 94 % overall conversion. 0.90 α value and 92 % C_5+ selectivity. Input H_2O, CO_2, N_2 as well as unreformed methane, ethane and longer hydrocarbons considered inert. Hydrocracker operated at 325 °C and 40 bar. Mass fraction of required hydrogen to hydrocracker feed = 1 %, gas make from the process = 2 %, Depending on the hydrocracking severity, yield ratios of naphtha, kerosene and gas oil can be varied from 15:25:60 (gas oil mode) to 25:50:25 (kerosene mode)	e

Table 3.1 – continued from previous page

Item	Design parameters	Notes
Low-pressure methanol synthesis	$T_{reaction}$= 260 °C, $P_{fresh\ feed}$= 80 bar, Δp =-5 bar, Boiling-water reactor modelled with REquil with Soave-Redlich-Kwong equation of state (SRK). Equilibrium reactions: CO + $2H_2$ = CH_4O, $T_{appr.}$ = 10 K; CO_2 + $3H_2$ = CH_4O + H_2O, $T_{appr.}$ = 10 K.	e
Methanol to Gasoline	DME reactor: T_{in}= 297 °C, T_{out}=407 °C, P_{in}= 23 bar, Δp =-1 bar, Boiling-water reactor modelled with REquil using Soave-Redlich-Kwong equation of state (SRK). Equilibrium reaction: $2CH_4O$ = C_2H_6O + H_2O, T_{appr} = 30 K. Gasoline reactor: $T_{reactor}$= 400 °C, P_{in}= 22 bar, Δp =-1 bar, Modelled as REquil using Soave-Redlich-Kwong equation of state (SRK). Relative mass yields from 1 tonne of raw product in the refining area are 880 kg of gasoline blendstock, 100 kg of LPG and 20 kg of purge gas.	h
Methanol to Olefins	Water content in methanol feed: 29 vol-%. Feed mixture compressed to 3 bar and superheated to 310 °C. Fast-fluidised MTO reactor operated at 410 °C & 3 bar and modelled with RYield using Peng-Robinson equation of state (PENG-ROB). Regenerator operated with air at 600 °C and modelled with RStoic using Peng-Robinson equation of state (PENG-ROB). 99.8 % overall methanol conversion with 80 % carbon selectivity to light olefins. Propylene to ethylene mass ratio = 1.	e
Olefin cracking process	Propylene to ethylene mass ratio = 4. Mass yield structure: CH_4 = 2 %, C_2H_4 = 19 %, C_2H_6 = 2 %, C_3H_6 = 71 %, C_3H_8 = 4 %, C_4H_8 = 2 %. Modelled with RYield using Peng-Robinson equation of state (PENG-ROB).	e
Alkaline electrolysis	H_2 and O_2 purity 100 %. Both delivered at atmosperic pressure and 25 °C, Electrolyser system efficiency = 62 % (LHV).	e, i
Auxiliary boiler	Modelled as RStoic, Δp = - 0.1 bar, Lambda = 1.20, Air preheat to 250 °C with flue gas	e
Heat exchangers	Δp/p = 2 %; ΔT_{min} = 15°C (gas-liq), 30 °C (gas-gas). Heat loss = 1 % of heat transferred.	g
Heat recovery & Steam system	Flue gas T_{out}=150 °C, feed water pressure 110 bar, steam drum blowdowns: 2 % of inlet flow, Deaerator T_{out} = 120 °C.	e
Steam turbine	Inlet steam parameters: 93.5 bar, 500 °C; Extraction steam parameters: HP = 25 bar, 330 °C; LP = 5 bar, 179 °C; $\eta_{isentropic}$ = 0.78, $\eta_{generator}$=0.97 , $\eta_{mechanical}$=0.98.	c, e, j
Compressors	Stage pressure ratio <2, $\eta_{polytropic}$= 0.85, η_{driver}= 0.92, $\eta_{mechanical}$= 0.98.	k
Multistage compressors (>4.5 kg/s)	Stage pressure ratio <2, $\eta_{polytropic}$= 0.87, η_{driver}= 0.92, $\eta_{mechanical}$= 0.98, $T_{intercooler}$= 35 °C, $\Delta p/p_{intercooler}$= 1 %.	l

Table 3.1 – concluded from previous page

Item	Design parameters	Notes
Multistage compressors (<4.5 kg/s)	Stage pressure ratio <2, $\eta_{\text{polytropic}}$= 0.85, η_{driver}= 0.90, $\eta_{\text{mechanical}}$= 0.98, $T_{\text{intercooler}}$= 35 °C, $\Delta p/p_{\text{intercooler}}$= 1 %.	l
Pumps	$\eta_{\text{hydraulic}}$= 0.75, η_{driver} = 0.90.	k

a - Taken from Smith et al. [147].
b - Taken from Swanson et al. [43]. The original value in the reference was given for bagasse (160 kg/m^3), which is here fitted for forest residues (293 kg/m^3) assuming that LH is filled with feedstock up to 90 %.
c - Based on personal communication with Andras Horvath, Carbona-Andritz, May 15$^{\text{th}}$ 2012.
d - Modelling principles taken from Refs. [170] and [171].
e - Operating parameters chosen by the author.
f - Outlet temperature and steam/CO ratio based on personal communication with Wolfgang Kaltner, Süd-Chemie AG, July 9$^{\text{th}}$, 2012.
g - Taken from Liu et al. [172].
h - Taken from Larson et al. [133]. For MTG reactor yield structure, see section 2.10.
i - System efficiency calculated based on information taken from Ivy [152].
j - Based on personal communication with Reijo Kallio, ÅF-Consult, October 2012.
k - Taken from Chiesa et al. [173].
l - Taken from Glassman [174].

The gasification and reforming model was significantly expanded in **Papers III-V** to enable the simulation of entire plants capable of producing synthetic fuels or light olefins from biomass residues or carbon dioxide and electricity. Design parameters for the modelling of equipment downstream from the reformer was gathered from publicly available data and discussions with various relevant experts. A summary of modelling parameters is given in Table 3.1. In addition to comparing different mass and energy flows, some helpful metrics were also calculated to assist the investigation. These included overall thermal efficiency to synfuel

$$\eta_{synfuel} = \frac{(\dot{m} * H)_{\text{synfuel}}}{(\dot{m} * H)_{\text{biomass}}}, \tag{3.1}$$

where $\dot{m}$ represents mass flow and H the lower heating value; and efficiency to district heat

$$\eta_{dh} = \frac{Q_{\text{dh out}} - Q_{\text{dh to drying}}}{(\dot{m} * H)_{\text{biomass}}}, \tag{3.2}$$

where Q denotes the released heat flow. In addition input/output balances for steam and electricity were calculated and analysed. All the examined plant configurations were designed self-sufficient in terms of heat and steam, but electricity was balanced with the electric grid. In all calculations lower heating value for biomass at 50 wt% moisture is used.

3.2 Cost analysis

There is some deviation in the way costs are handled in **Papers III - V**. However, the general methodology, which draws inspiration from Refs. [7, 175, 176], has been consistently applied throughout the work and is briefly explained below. For a detailed discussion on how costs are exactly handled in each case, the reader is advised to refer to the original research paper in question.

Table 3.2: Reference equipment costs database with cost factors employed in estimating Total Plant Costs.

CC	CSP	S_0	UEC	IC	C_0	IDC	PC	k	Notes
Civil works	Feed, MW_{th}	300			12.8	10 %	30 %	0.85	a
ASU incl. compr.	Oxygen, t/h	76.6			36.8	10 %	10 %	0.50	b
Feedstock handling	Feed, MW_{th}	157			5.3	10 %	10 %	0.31	c
Belt dryer	Water evap, kg/s	0.342			1.9	10 %	10 %	0.28	d
Pressurised fluid-bed gasifier	Dry biom, kg/s	17.8	25.1	50 %	37.7	15 %	30 %	0.75	a
Ceramic hot-gas filter	Syngas, kmol/s	1.466	5.9	15 %	6.8	15 %	30 %	0.67	a
Catalytic reformer	Syngas, kmol/s	2.037	14.5	50 %	21.8	15 %	30 %	0.67	a
WGS stage	Gasif. feed, MW_{th}	1377			12.6	15 %	30 %	0.67	e
Scrubber	Syngas, kmol/s	1.446			5.2	15 %	30 %	0.67	a
Syngas compr.	Compr. work, MW_e	10			5.0	15 %	30 %	0.67	f
CO_2 compr.	Compr. work, MW_e	10			5.0	15 %	30 %	0.67	f
O_2 compr.	Compr. work, MW_e	10			5.7	15 %	30 %	0.67	f
H_2 compr.	Compr. work, MW_e	10			5.7	15 %	30 %	0.67	g
AGR incidentals compr.	Compr. work, MW_e	10			5.0	15 %	30 %	0.67	f

Table 3.2 – concluded from previous page

CC	CSP	S_0	UEC	IC	C_0	IDC	PC	k	Notes
AGR	kNm3/hr (NTP)	200	49.3	15 %	56.7	15 %	30 %	0.63	h
Alkaline electrol.	Power, MW_e	223.5			121.9	15 %	10 %	0.93	i
HRSG	Heat transf, MW_{th}	43.6	5.2	15 %	6.0	15 %	30 %	0.80	b
Aux. boiler & fluegas treatm.	Feed, MW_{th}	5.9	5.1	15 %	5.9	10 %	10 %	0.65	j, k
Steam turbine unit	Power, MW_e	15.2	6.8	15 %	7.8	10 %	10 %	0.85	j, l
CHP equipment	Power, MW_e	15.2	4.1	15 %	4.7	10 %	10 %	0.85	j, m
Other steam cycle equipment	Power, MW_e	15.2	6.3	15 %	7.3	10 %	10 %	0.85	j, n
Guard beds	Syngas, MW_{th}	260	5.2	15 %	6.0	10 %	10 %	0.85	o
MeOH loop	MeOH, MW_{th}	210	28.3	15 %	32.5	10 %	10 %	0.67	o
Methanol distill. (min)	MeOH, MW_{th}	210	4.2	15 %	4.8	10 %	10 %	0.88	o, p
Methanol distill. (chem-grade)	MeOH, MW_{th}	210	12.6	15 %	14.5	10 %	10 %	0.88	o, p
Methanation equipment	Methane, MW_{th}	210	28.3	15 %	32.5	15 %	30 %	0.67	q
MTG DME reactor	Gasoline, bbl/day	16 667			45.3	15 %	30 %	0.67	r
MTG gasoline reactor	Gasoline, bbl/day	16 667			101.2	15 %	30 %	0.67	r
MTG gasoline finisher	Gasoline, bbl/day	5 556			8.2	15 %	30 %	0.67	r

Note: C_0 is the cost of an installed reference equipment of size S_0 in 2010 euros and k is the cost scaling factor. UEC stands for uninstalled equipment cost, IC for installation costs, IDC for indirect costs and PC for project contingency.
a - Author's estimate.
b - Taken from Larson et al. [22].
c - Costs taken from Ref. [44]. Scaling exponent calculated from two different size handling systems using feedstock energy flow as scaling parameter.
d - Reference capacity and costs taken from Ref. [44]. Scaling exponent calculated based on information on two different size dryers using water removal rate as scaling

parameter. Drying capacity is increased by extending the dryer, which results in unusually low scaling factor (middle parts are fairly affordable in comparison to the ends of the dryer).
e - Extracted from Kreutz et al. [176]. This cost is for two-stage equipment that includes balance of plant (15 %) and indirect costs (15 %). It is assumed that a single-stage adiabatic sour shift reactor is 40 % of the cost of a two-stage system (see Ref. [172]). Balance of plant and indirect costs have been removed.
f - Taken from Kreutz et al. [176].
g - It is likely that a H_2 compressor is more expensive than an O_2 compressor of similar size (electricity usage), but in the lack of reliable cost data an equal cost is assumed.
h - This cost is for a Rectisol system that separates CO_2 and H_2S into separate streams (separate column for each compound). Taken from Liu et al. [172].
i - Cost is for an alkaline electrolysis installation containing 96 individual NorskHydro's No. 5040 atmospheric electrolysers each having a capacity of 2.3 MW. Cost taken and scaling exponent fitted with data from Floch et al. [177].
j - Costs based on Thermoflow PEACE equipment cost estimator and discussions with experts at ÅF-Consult.
k - Includes boiler and related systems such as air preheaters, fans, ducts, stack, fabric filter et cetera.
l - Includes turbine, generator and electrification related to the delivery.
m - Includes items such as a water cooled condenser, district heaters, deaerator et cetera.
n - Includes items such as tanks, pumps, fans, makeup water system, fuel & ash handling systems et cetera.
o - Taken from Ref. [178], originally based on a quotation from Haldor Topsøe in September 2003. Recalculated.
p - Cost (down) scaling factor from Wan [138].
q - Methanation system is assumed to have the same cost as a methanol loop (i.e. distillation equipment excluded) with equal fuel output.
r - Taken from Larson et al. [133]. Approximately one third of the raw gasoline from MTG reactors is processed through a finisher.

3.2.1 Plants producing synthetic fuels

Capital cost estimates were used as basis for evaluating the prospective economics of synthetic fuel production. These estimates were based on a self-consistent set of component-level capital cost data assembled using literature sources, vendor quotes and discussions with industry experts. When data for a given piece of equipment was unattainable, the costs were estimated based on similar equipment and engineering judgement. A summary of the equipment cost database used in **Papers III - V** is given in Table 3.2.[2] All equipment costs have been escalated to correspond with 2010 euros using *Chemical Engineering* magazine's Plant Cost Index[3] to account for inflation. Individual cost scaling exponents (k) have been used to scale the reference capital costs (C_o) to a capacity that corresponds with simulation results (S)

[2] In case of deviations between cost data used in **Papers III - V**, values from **Paper IV** are used.
[3] For more information, see: www.che.com/pci.

using the following relation:

$$C = C_0 \times \left(\frac{S}{S_0}\right)^k, \tag{3.3}$$

where S_0 is the scale of reference equipment and C the cost of equipment at the size suggested by the simulation.

Total plant cost (TPC) is defined as the "overnight" capital investment required to construct a plant and includes all main equipment (with initial catalyst loadings) plus installation (labour), indirect costs (engineering and fees), project contingency and (in some instances) unscheduled equipment. These cost items are reported as fractions from the (installed) equipment costs. The total capital investment (TCI) is then obtained by adding interest during construction to TPC. The estimates are assumed to carry an accuracy of -15%/+30%, which is typical for studies based on prefeasibility level factored approach [175].

The levelised cost of fuel (LCOF) production is evaluated according to the following equation:

$$LCOF(€/GJ) = \frac{F + E + C + O - R}{P}, \tag{3.4}$$

where

- F is the annual cost of feedstock (biomass residues and carbon dioxide),
- E is the annual cost of electricity,
- C is the annualised capital charge, including return on equity and interest on debt,
- O is the annual operating and maintenance costs, and
- R is the annual revenue from selling by-products (district heat, steam, electrolytic oxygen, purge gas and LPG).[4]

The sum of these annual costs (€/a) is divided by P, which is the annual output of fuel (GJ/a) from the plants. When defined in this way, the LCOF (€/t) indicates the product sale price needed to break-even under the technical and economic parameters assumed.

[4] Steam, purge gas and LPG are sold only from the MTG plant, oxygen is sold only from plants that feature electrolysis.

3.2.2 Plants producing light olefins

As for synfuel plants, analysing the cost of light olefins was also underpinned by capital cost estimates. However, the economics were evaluated in terms of maximum methanol purchase price (MMPP), which was calculated according to the following equation:

$$MMPP(€/t) = \frac{P + U + C + O}{M}, \tag{3.5}$$

where

- P is the annual revenue from selling the hydrocarbon and olefin products,
- U is the annual cost of utilities (net electricity, high- and low-pressure steam),
- C is annualised capital charge, including return on equity and interest on debt, and
- O is the annual operating and maintenance costs.

Incomes are considered positive and expenses negative costs. The sum of these annual costs (€/a) is divided by M, which is the annual methanol input (t/a) to the MTO process. Defined in this way, the MMPP (€/t) indicates the maximum price that can be paid from the MTO's feedstock to break-even under the technical and economic parameters assumed.

3.2.3 Assessing the costs of innovative technologies

The cost estimation methodology applied in this dissertation is based on the assumption of mature technology (also known as the N^{th} plant assumption). The author acknowledges that the use of 'unproven technologies' in plant designs is highly likely to cause increased capital costs and decreased plant performance. In fact, conventional estimating techniques, like the one used in this work, have been found out to routinely understate the costs of innovative technologies [179]. Thus, it is almost certain that the first commercial scale installations of these plants will be more expensive than estimated in this dissertation, although the probable level of misestimation is difficult to assess in advance. In any case, one of the main aims of this dissertation has been to evaluate and understand the *long-term* commercial viability of the examined plant designs, i.e. when all plant components have already reached commercial maturity and the employed methodology is considered well suited for this. It is further emphasised that even though methods suitable for the analysis of first-of-a-kind plant costs have been proposed, perhaps the most famous being that based on empirical formulae developed

by RAND Corporation [179], carrying out such analysis was excluded from the scope of this dissertation.

3.3 Scale of production

The overall costs of synthetic fuel production are subject to economies of scale, which creates an incentive to build large conversion plants. However, due to limitations in the availability of biomass feedstock, biofuel plants are confined to a much smaller scale than modern synfuel plants based on coal, shale or natural gas conversion. For example, the largest pulp and paper mills in Europe process annually about one million tons of dry biomass that relates to about 600 MW of constant energy flow,[5] which in this dissertation is considered as a practical cap on the size of biomass conversion plants.

Another possible way of estimating a proper scale for a biomass conversion plant would be to consider maximal by-product utilisation. In northern Europe, a typical annual heat demand for district heating networks, situated at or close to wooded territories, range from 450 to 1700 GWh/a with peak loads between 150 to 650 MW.[6] However, a better indicator for scale would be the minimum continuous load (summer load), which ranges from 50 to 150 MW [180].

In observance of these realities, the fuel output of the examined plants was set between 150 - 200 MW, which was considered large enough of a range to attain some economies of scale, while at the same time keeping feedstock requirements under practical limits and ensuring that by-product heat can be utilised to full extent.

3.4 Plant configurations

Several different types of plant configurations are examined in this dissertation. In general, all configurations can be divided into one of three groups depending on whether synfuels are produced from:

- biomass residues via gasification (thermochemical);
- carbon dioxide and electricity via electrolysis of water (electrochemical); or

[5] Assuming 8000 annual operating hours and 8.6 MJ/kg lower heating value for forest residues at 50 wt% moisture.

[6] The data is based on municipal DH networks situated in eastern Finland sampled from Ref. [180].

- biomass residues and electricity via gasification and electrolysis of water (hybrid).

In addition to different feedstocks, several end-product alternatives are also evaluated, including methane, methanol, gasoline, light olefins (MTO) and Fischer-Tropsch liquids. As gasoline and olefins are both produced from methanol via a separate post-processing step, they share upstream settings with the corresponding methanol plants. The basic features of the alternative production 'pathways' are discussed briefly in the following paragraphs.

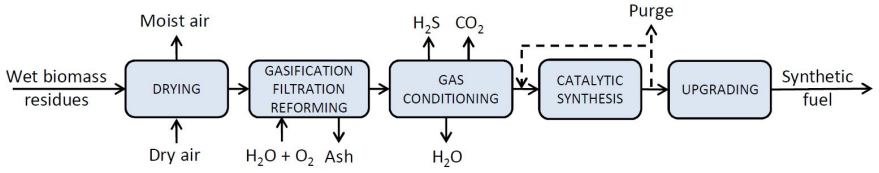

Figure 3.2: Simplified block flow diagram of the thermochemical route. Biomass residues are received at 50 wt-% moisture. Recycle is not used in configurations producing methane.

3.4.1 Thermochemical pathway

Production of synthetic fuels from carbonaceous feedstocks is a century-old and well-established technique. Unfortunately, all commercial scale synfuels plants to date have been operated with fossil feedstocks and redesign of some key parts of the process is required to make the switch to biomass possible (Fig. 3.2). Currently, a lot of RD&D work is ongoing to commercialise such technology [11]. Some of the past attempts to produce synthetic fuels from biomass-derived synthesis gas have ended in difficulties [181, 182], although technical hurdles have since been overcome and synthetic biofuels technology can currently be considered successfully demonstrated at pre-commercial scale [36, 183, 184]. Nonetheless, commercial applications are still lacking. The slow commercialisation pace is often attributed to the technology's high specific investment cost, financing gaps on the path from the pre-revenue stage to commercial operations and uncertainty about the stability of carbon policies and lack of knowhow in sourcing and processing lignocellulosic biomass.

3.4.2 Electrochemical pathway

The concept of producing synthetic fuels from carbon dioxide via the electrochemical pathway (Fig. 3.3) was first proposed in the late 1970s and studied

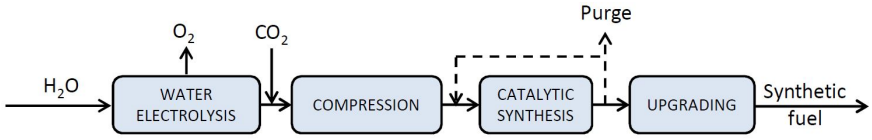

Figure 3.3: Simplified block flow diagram of the electrochemical route. CO_2 is used as the sole source of carbon for the synthesis.

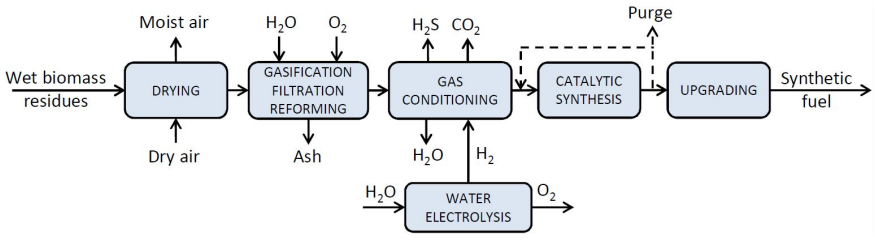

Figure 3.4: Simplified block flow diagram of the hybrid route. Biomass residues are received at 50 wt-% moisture. Hydrogen is fed before compression and CO is used as the source of carbon for the synthesis. Recycle is not used in configurations producing methane.

further in the early 80s [156, 185–187]. The early concepts were based on nuclear energy sources and low temperature electrolysis, while more recently the focus has turned to solar and wind using high temperature electrolysis for hydrogen production [28]. The renewed interest in the topic has been fuelled by the improved availability and economics of electricity produced from renewable sources, especially from wind and solar. Synfuels are not currently produced commercially from CO_2 as the main feed, although research is also ongoing to make it possible [161, 167, 188].

3.4.3 Hybrid pathway

Hydrogen and carbon needs to be fed to the synthesis in the correct proportions to achieve maximal conversion to fuels. Their ratios can be controlled upstream with a reactor that catalyses the water-gas shift reaction (2.2). Another possibility for adjusting the syngas stoichiometry would be to remove the shift reactor completely and directly import the required amount of hydrogen from external sources [29, 189, 190]. This approach would also allow more of the syngas CO to be converted into fuel, as losses incurred during the WGS reaction could be avoided. However, such an arrangement requires constant external hydrogen input leaving little space for flexibility.

The third group of production pathways examined in this dissertation is based on a combination of the above-described approaches into a one hybrid

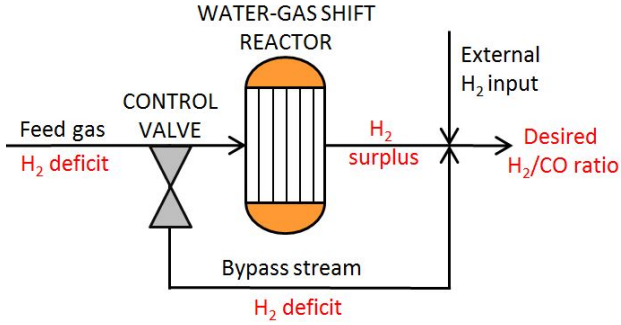

Figure 3.5: Schematic illustration of a configuration suitable for regulating the syngas stoichiometry with a combination of water-gas shift and external hydrogen input.

system that features both a grid-connected electrolyser and a WGS step (see Figs. 3.4 and 3.5). With such a hybrid approach, time-variable control over the amount of external hydrogen addition becomes possible. The improved flexibility allows the operation of the electrolyser only during times of excess supply of renewable electricity, making it possible to participate in levelling the peaks of time-variable renewable energy production. In principle, no additional technical barriers should be introduced as a result of the hybrid approach, making it possible to deploy such configurations in tandem with synthetic biofuels technology.

Chapter 4

Results

This chapter discusses three Research Questions originally outlined in section 1.4 of this dissertation. All results are derived from the original research papers comprising this compilation.

4.1 Impact of hot-gas cleaning on feasibility

The production of clean synthesis gas from biomass is the key enabling technology for synthetic biofuels manufacture and there is a clear need for better understanding of the techno-economics behind hot-gas cleaning in synthetic biofuel applications. The technology is currently approaching commercial maturity and is likely to experience further development and optimisation in the coming years. It is therefore of interest to estimate how much this prospective development can be expected to improve the overall efficiency and costs of the process. The results discussed in this section answer Research Question 1 and were originally published in **Paper III**.

4.1.1 Performance results

Mass and energy balances were simulated with Aspen for a plant that produces 337 metric tonnes (110 kton/a) of Fischer-Tropsch liquids per day. From the 300 MW biomass input, 157 MW of FT liquids is produced together with 79 MW of district heat. Thus, the thermal efficiency from wet biomass is 52.4 % to FT liquids and 78.8 % to FT liquids and saleable heat. As previously discussed, process efficiency and economics both benefit from the increase of filtration temperature until the outlet temperature

of the gasifier is achieved. The overall impact can be divided into several causes: when inlet temperature to the reformer (i.e. filtration temperature) increases,

- less combustion is needed for heat generation in the reformer and thus more gas is conserved for conversion to liquids;
- less oxygen and steam need to be produced for the reformer and
- smaller heat exchanger between the gasifier and the filter unit is needed.

On the other hand, as temperature difference between the gasifier and filter decreases, less heat is recovered for steam generation. In the special case where the gasifier's outlet temperature equals filtration temperature, no heat exchanger for cooling the gas is any longer needed. This leads to increased simplicity, ease of operation and reduced need for capital.

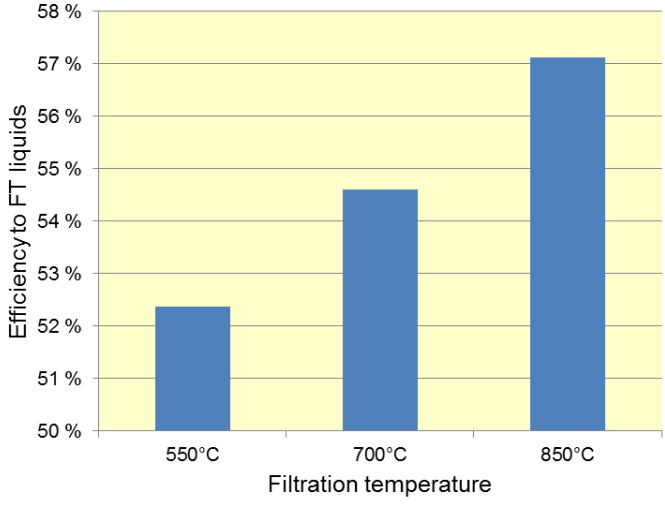

Figure 4.1: Overall thermal efficiency from wet biomass to FT liquids at three different filtration temperatures.

The combined impact of these effects on overall efficiency was investigated by simulating the plant at three filtration temperatures (550, 700 and 850 °C) while keeping all other parameters unchanged. Based on the results shown in Fig. 4.1, the overall thermal efficiencies to FT liquids are 52.4 % for 550 °C, 54.6 % for 700 °C and 57.1 % for 850 °C filtration temperature. Thus, the potential improvement in the overall efficiency from biomass to FT liquids is 4.7 percentage points if filtration temperature can be successfully elevated in the future from the current 550 °C to the level of 850 °C.

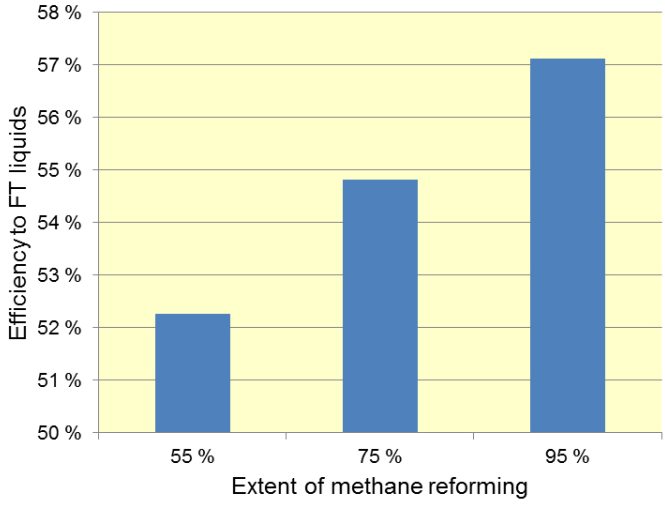

Figure 4.2: Overall thermal efficiency from wet biomass to FT liquids at three different methane conversion levels.

The amount of chemical energy in the form of methane in synthesis gas is not available for conversion by FT synthesis[1]. By catalytically reforming syngas methane to (mainly) CO and H_2, it is possible to convert part of this unavailable energy into usable feedstock for downstream synthesis. Although reforming effectively increases the amount of CO and H_2, there are also opposing effects. Because methane reforming is an endothermic reaction, maintaining constant temperature inside the reformer requires heat generation by partially combusting the gas with oxygen. Higher methane conversion thus requires more heat generation via combustion leading to increased oxygen and steam consumption. The combined impact of these effects on the overall efficiency was investigated by simulating the plant at three different methane conversions (55, 75 or 95 %), at 850 °C filtration temperature, while keeping all other parameters unchanged. Based on the results shown in Fig. 4.2, the overall thermal efficiencies to FT liquids are 52.3 % for 55 % conversion, 54.8 % for 75 % conversion and 57.1 % for 95 % conversion. Thus, a 10 % increase in the methane reforming extent leads to a 1.2 percentage point improvement in overall efficiency.

[1] Methane is an undesired component for all syntheses with the exception of SNG production where methane is actually the desired end-product and minimum conversion of methane in the reformer should be achieved instead.

Table 4.1: Cost parameters assumed for the biomass-to-FTL plant.

Annuity factor (10 %, 20 a)	0.12
Annual O&M cost factor	0.04*
Forest residues, €/GJ	4.7
District heat, €/GJ	8.3
Electricity, €/GJ	13.9

*Fraction of Total Capital Investment

4.1.2 Cost results

Based on an underlying component-level capital cost estimates the total plant cost (TPC) was estimated to be 346 M€ giving, after adding interest during construction, total capital investment (TCI) of 370 M€. Using cost parameters reported in Table 4.1, the levelised production cost of FT liquids for a plant operating at 550 °C filtration temperature and 95 %, methane reforming extent was calculated to be 19.0 €/GJ (68.3 €/MWh).

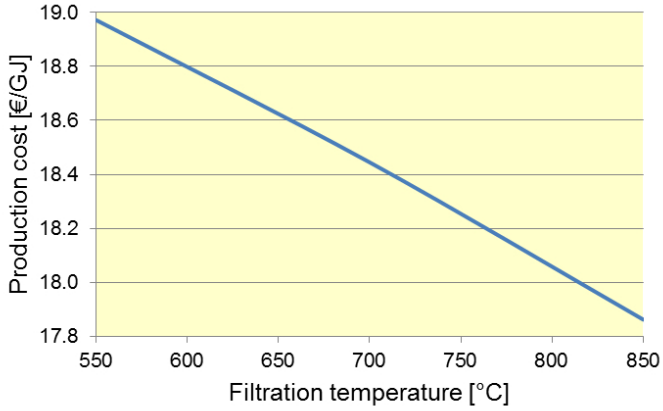

Figure 4.3: Impact of filtration temperature on the levelised cost of FT liquids from biomass.

The impact of filtration temperature on the production cost of FT liquids, at 95 % methane reforming extent, is shown in Fig. 4.3. At 550 °C filtration, the production cost is 19.0 €/GJ but it decreases steadily as temperature rises reaching 17.9 €/GJ at 850 °C. Thus, the potential reduction in production cost is 1.1 €/GJ if filtration temperature can be successfully elevated in the future from the current 550 °C level to the target 850 °C. The impact of methane reforming on the production cost of FT liquids, at 850 °C filtration temperature, is presented in Fig. 4.4. At 55 % methane conver-

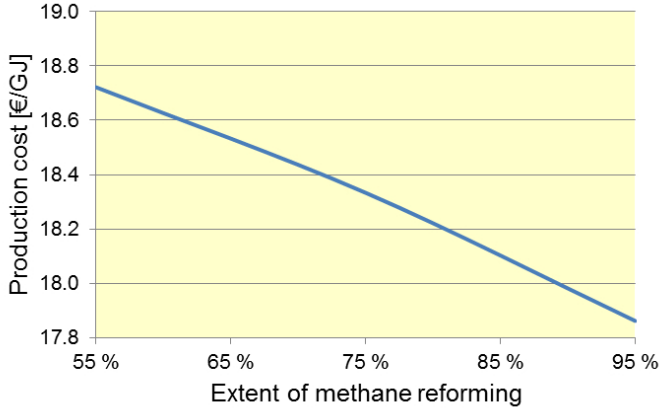

Figure 4.4: Impact of methane reforming extent on the levelised cost of FT liquids from biomass.

sion, the production cost is 18.7 €/GJ but it decreases steadily as methane conversion rises reaching 17.9 €/GJ at 95 %. Thus, a 10 % increase in the methane reforming extent leads to a 0.22 €/GJ reduction in the production cost.

4.2 Impact of feedstock on feasibility

Once clean synthesis gas is produced from biomass, several end-product options become available. These include FT liquids, methanol, gasoline and methane among others. Comparing efficiencies and costs of these options with each other is an important part of this dissertation. The production of synthetic fuels directly from carbon dioxide and electrolytic hydrogen (ie. without biomass) has recently garnered a lot of attention in Europe as a potential source of low-carbon fuels in the future. Such expectations have been underpinned by claims of low-cost hydrogen (electricity) becoming widely available in the future, possibly fuelled by periods of negative price electricity currently experienced in Germany, a side effect of the country's ambitious *energiewende* policies. There is thus a clear need for detailed techno-economic analysis on the relative pros and cons of different combinations to assess whether power-to-fuels concepts can live up to these expectations. The results discussed in this section answer Research Question 2 and were originally published in **Paper IV**.

4.2.1 Performance results

To more closely examine the research question, mass and energy flows were simulated with Aspen for 9 individual plant configurations summarised and named in Table 4.2. Based on the results, shown in Table 4.3, 66.7 MW of natural gas or 60.0 MW of methanol can be produced from 100 MW of wet biomass with thermochemical plant configurations. Producing the same amount of fuels at an electrochemical plant requires 129.6 MW of electricity and 3.6 kg/s of CO_2 (natural gas plants), or 116.1 MW of electricity and 4.36 kg/s of CO_2 (methanol plants). When syngas production is boosted with the maximum amount[2] of electrolytic hydrogen (hybrid configurations) the output of synthetic natural gas increases by 50 % to 100.3 MW and methanol output by 31 % to 78.3 MW. The greater increase in natural gas production is due to the larger hydrogen requirement in relation to methanol production.

Table 4.2: Summary of the considered plant configurations. The plants are identified by a sequence of two letters: the first letter identifies the production route and the second letter the main product.

	Thermochemical	**Hybrid**	**Electrochemical**
Natural gas	TN	HN	EN
Methanol	TM	HM	EM
Gasoline	TG	HG	EG

The net electricity output is negative for all examined plant configurations. For the electrochemical and hybrid plants, electricity consumption of the alkaline electrolysis clearly dominates electricity balance, leading to deeply negative net outputs. As already noticed, more electricity (i.e. hydrogen) is required to produce synthetic natural gas than methanol. However, the difference in net electricity requirement between methanol and natural gas production is smaller for the electrochemical than for hybrid configurations. This can be explained by the increased role of compression work in electrochemical plants (feed gases starting at atmospheric pressure, while a gasifier operates at 4 bara) that level down differences in electricity consumption caused by fuel production stoichiometry.[3]

In addition to synfuel, most plant designs co-produce district heat (DH) at 90 °C. The district heat outputs for methanol plants are 12.3 MW (TM) or 16.6 MW (HM) depending on the configuration. With natural gas configurations some district heat can also be produced from the methanation area in addition to steam cycle. The combined district heat output from such plants is 10.5 MW (TN), 21.3 MW (HN) or 12.1 MW (EN) depending

[2] Complete bypass of water-gas shift reactors.
[3] Methanol production requires less hydrogen than methanation but takes place at much higher pressure.

Table 4.3: Process simulation results on a lower heating value basis.

Configuration		**TN**	**TM**	**HN**	**HM**	**EN**	**EM**
Carbonaceous feeds							
Biomass (50 wt-%)	MW	100	100	100	100		
Biomass (15 wt-%)	MW	112	112	112	112		
Biomass, dry	kg/s	5.9	5.9	5.9	5.9		
Feestock CO_2	kg/s					3.6	4.36
Oxygen balance							
Consumption, t/d		*280*	*324*	*280*	*324*		
Gasifier O_2 input	kg/s	2.3	2.3	2.3	2.3		
Reformer O_2 input	kg/s	0.9	1.4	0.9	1.4		
ASU output, t/d		*280*	*324*	*280*	*324*		
Electricity balance							
Consumption, MW		*-9.1*	*-12.4*	*-10.3*	*-13.9*	*-4.8*	*-7.3*
Oxygen production	MW	-3.1	-3.6	-3.1	-3.6		
Oxygen compression	MW	-0.6	-0.7	-0.6	-0.7		
Feed screw & LH	MW	-0.2	-0.2	-0.2	-0.2		
Feed drying	MW	-0.7	-0.7	-0.7	-0.7		
Syngas compression	MW	-3.0	-5.2	-2.5	-5.1		
Acid gas removal	MW	-1.0	-0.9	-0.8	-0.8		
Electrol. H_2 compr.	MW			-1.9	-1.6	-3.7	-5.4
CO_2 compression	MW					-0.9	-1.6
Synthesis	MW	0.0	-0.3	0.0	-0.4		
All blowers & pumps	MW	-0.2	-0.3	-0.2	-0.3		
Miscellaneous	MW	-0.4	-0.6	-0.4	-0.6	-0.2	-0.3
Turbine output, MW		*7.7*	*8.3*	*8.4*	*8.6*		
Steam balance							
Consumption, kg/s		*7.2*	*8.0*	*6.7*	*7.6*		
Gasifier	kg/s	2.4	2.4	2.4	2.4		
Reformer	kg/s	0.9	1.4	0.9	1.4		
AGR solvent regen.	kg/s	1.2	1.1	0.9	0.9		
Deaerator	kg/s	1.2	1.4	1.1	1.3		
Economiser	kg/s	1.5	1.7	1.4	1.7		
Gross output, kg/s		*12.5*	*16.1*	*13.3*	*17.0*		
By-products							
Char							
Heating value	MJ/kg	7.0	7.0	7.0	7.0		
Energy	MW	2.1	2.1	2.1	2.1		
Purge gas							
Heating value	MJ/kg		11.5		13.0		14.5
Energy	MW		4.9		6.1		3.7
Alkaline electrolysis							
Electricity input	MW			65.8	35.4	129.6	116.1
Hydrogen output	kg/s			0.34	0.18	0.67	0.60
Oxygen output	kg/s			2.70	1.45	5.32	4.76
Energy outputs							
Methanol	MW		60.0		78.3		60
SNG (methane)	MW	66.7		100.3		66.7	
Net electricity output	MW_e	-1.4	-4.0	-67.7	-40.7	-134.4	-123.4
DH (steam cycle)	MW	3.1	12.3	8.0	16.6		
DH (synthesis)	MW	7.4		13.3		12.1	

Table 4.4: Simulation results for upgrading the methanol to synthetic gasoline using the MTG process.

		TG	**HG**	**EG**
Gasoline synthesis part				
Methanol input	MW	60.0	78.3	60.0
Inlet pressure to synthesis	MPa	2.3	2.3	2.3
Outlet pressure from synthesis	MPa	1.7	1.7	1.7
DME reactor inlet temp.	°C	297	297	297
DME reactor outlet temp.	°C	407	407	407
Once-through MeOH conversion	%	82	82	82
MTG reactor outlet temp.	°C	400	400	400
Recycle/MeOH	mol/mol, wet	7.5	7.5	7.5
Purge gas energy flow	MW	3.0	3.9	3.0
Total MeOH conversion	%	100	100	100
Gasoline (LHV)	MJ/kg	44.7	44.7	44.7
LPG (LHV)	MJ/kg	45.9	45.9	45.9
Net electricity output	MW	-0.2	-0.2	-0.2
Net steam output	kg/s	2.2	2.8	2.2
Overall MTG plant				
Gasoline energy	MW	51.8	67.6	51.8
LPG energy	MW	6.1	7.9	6.1
Net electricity output	MW	-4.2	-40.9	-123.6
District heat (from steam cycle)	MW	12.3	16.6	
Net steam output	MW	2.2	2.8	2.2

on the configuration. As the production of methanol from CO_2 propagates along reaction 2.13, a large amount of byproduct water needs to be separated from raw methanol by distillation. This increases the required reboiler duty considerably in comparison to biomass-derived methanol configuration, leading to zero district heat being produced from the electrochemical methanol plant.

The gasifier's oxygen consumption is constant for all configurations, but the amount of oxygen required for reforming depends on the targeted methane conversion. For purely thermochemical plants, the combined oxygen requirement is 3.2 kg/s (natural gas) or 3.7 kg/s (methanol). Oxygen is also produced as a co-product with hydrogen in configurations that feature alkaline electrolysis. For hybrid configurations, byproduct oxygen from the electrolysis could not however replace the need for a dedicated air separation unit as the maximum net oxygen output would be -2.3 kg/s (HM) or -0.5 kg/s (HN). For electrochemical plants, where oxygen is not consumed by the process, the net oxygen output is 4.8 kg/s (EM) and 5.3 kg/s (EN).

The production of gasoline is treated as a post-processing step that may or may not take place at the same site as methanol production. The results of the methanol-to-gasoline process are summarised in Table 4.4. 60.0 MW of methanol was produced by the thermochemical and electrochemical con-

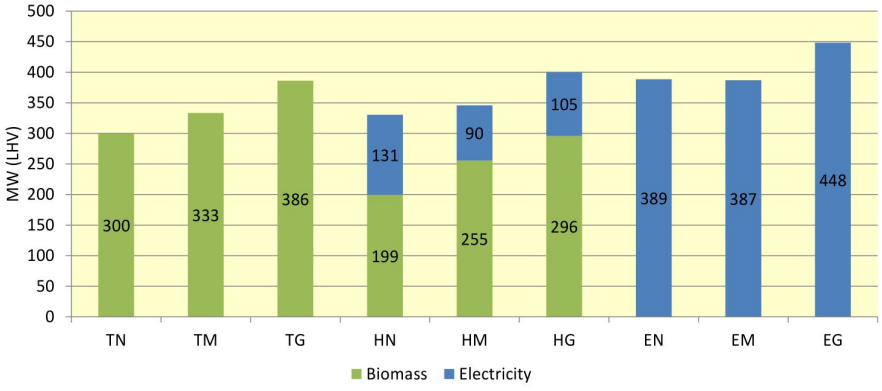

Figure 4.5: Feedstock requirements for all examined plant configurations producing 200 MW (LHV) of fuel. The numbers include only that part of electricity that is used for hydrogen production.

figurations, which can be converted to 51.8 MW of gasoline and 6.1 MW of LPG via the MTG process. From the 78.3 MW of methanol produced by the hybrid process, 67.6 MW of gasoline and 7.9 MW of LPG can be produced. Some high-pressure saturated steam is also generated from the gasoline reaction's exotherm, which can be sold as process steam or utilised as an admission steam if a steam cycle is available nearby.

Fig. 4.5 illustrates energy input breakdowns for each of the examined plant configurations. In the figure, the fuel outputs are rescaled to 200 MW (LHV) for all plants. For the thermochemical configurations, the following amounts of wet biomass are required to produce 200 MW of synthetic fuel: 300 MW (TN), 333 MW (TM) or 386 MW (TG). A notable drop in biomass requirement is achieved with hybrid configurations where biomass is partly replaced with electricity used in the alkaline electrolyser to produce hydrogen. The feedstock requirements are: 199 and 131 MW (biomass and electricity) for natural gas, 255 and 90 MW for methanol, 296 and 105 MW for gasoline production. Due to differences in reaction stoichiometry, less electricity is needed for configurations that produce methanol than synthetic natural gas. For pure electrochemical designs, where biomass is fully replaced with electricity and carbon dioxide, 200 MW of synthetic fuel can be produced from: 389 MW (EN), 387 MW (EM) or 448 MW (EG) of electricity and: 10.8 kg/s (EN), 14.5 kg/s (EM) or 16.8 kg/s (EG) of carbon dioxide.

4.2.2 Cost results

The TCIs (total capital investments) range from 363 to 611 M€ among the cases analysed. The gasoline configurations (TG, HG and EG) are the most capital intensive as they include all the components of a methanol plant[4] plus equipment required for the conversion of methanol to gasoline. For all end-products, thermochemical configurations have the highest and electrochemical the lowest TCIs. The TCIs for hybrid plants are slightly lower than those for corresponding thermochemical plants. Differences in TCIs are smaller among plants producing natural gas (TN, HN and EN) than plants that produce other fuels. This can be explained by the higher hydrogen requirement in comparison to methanol production (3 moles instead of 2 in CO hydrogenation and 4 moles instead of 3 in CO_2 hydrogenation) that increases the size and cost of alkaline electrolysis and H_2 compression systems in synthetic natural gas configurations.

Table 4.5: Financial parameters employed in the cost analysis.

Financial parameters	
Annuity factor (10 %, 20 a)	0.12
Annual O&M cost factor	0.04*
Annual operating hours	8000
Interest during construction	5%*
Investment support, M€	0
Values of inputs/outputs	
Biomass residue chips, €/GJ	5
District heat, €/GJ	8
Fuel gas, €/GJ	10
LPG, €/GJ	12
Electricity, €/GJ	14
Water, €/t	0
Oxygen, €/t	27
Steam, €/t	30
Carbon dioxide, €/t	40

*Fraction of Total Capital Investment

The levelised cost of fuel (LCOF) production has been calculated under the assumed technical and economic parameters (See Table 4.5). The contribution of different cost categories to the total LCOFs are shown in Table 4.6. Among the cases analysed, the LCOFs range from 18 to 48 €/GJ (64 - 173 €/MWh). For thermochemical configurations (TM, TN, TG) the capital charges and cost of biomass feedstock make about an equal contribution to the LCOF, whereas for hybrid plants (HM, HN, HG) the main contributions

[4] With the exception of methanol distillation, that is cheaper for gasoline configurations, because water does not have to be completely removed from the MTG unit's feed.

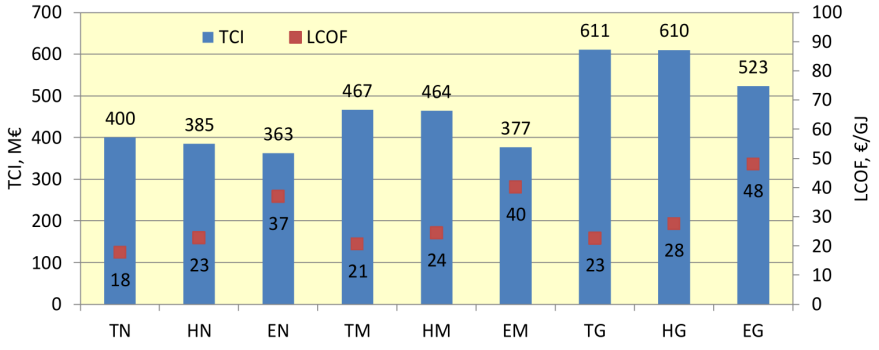

Figure 4.6: Summary of total capital investments (TCIs) and fuel production costs (LCOFs) for plants producing 200 MW (LHV) of fuel.

come from capital charges, biomass feedstock and electricity. Electricity clearly dominates the production costs in the electrochemical cases and revenue received from selling by-products is small in comparison to the main cost items for all cases analysed. For each product, thermochemical plants have the lowest and electrochemical plants the highest LCOFs with hybrid configurations placing in between the two. For a given route, natural gas (SNG) is the cheapest and gasoline the most expensive to produce. It is interesting to note that for a given product, the configuration requiring the highest investment has the lowest production cost and vice versa. This can be explained by the relative affordability of biomass residues in comparison to electricity under the assumptions used in the analysis. The main results have been visualised in Fig. 4.6 that summarises TCIs and LCOFs for all the examined plant configurations.

Table 4.6: Breakdown of levelised cost of fuel (LCOF) under economic assumptions summarised in Table 4.5. All costs in €/GJ unless otherwise noted.

Configuration	**TN**	**HN**	**EN**	**TM**	**HM**	**EM**	**TG**	**HG**	**EG**
Biomass	7.5	5.0		8.3	6.4		9.7	7.4	
CO_2			2.2			2.9			3.4
Electricity	0.3	9.4	28.2	0.9	7.3	28.8	1.1	8.5	33.4
District heat	-1.3	-1.7	-1.5	-1.6	-1.7		-1.9	-2.0	
Steam							-1.3	-1.2	-1.3
Oxygen		-0.7	-2.2		-0.5	-2.1			
Fuel gas							-0.6	-0.6	-0.6
LPG							-1.4	-1.4	-1.4
O&M	2.8	2.7	2.5	3.2	3.2	2.6	4.2	4.2	3.6
Capital charges	8.3	8.0	7.6	9.7	9.7	7.9	12.7	12.7	10.9
LCOF, €/GJ	17.7	22.7	36.8	20.6	24.4	40.0	22.6	27.6	48.0
LCOF, €/MWh	63.6	81.7	132.6	74.1	87.7	144.1	81.3	99.4	173.0

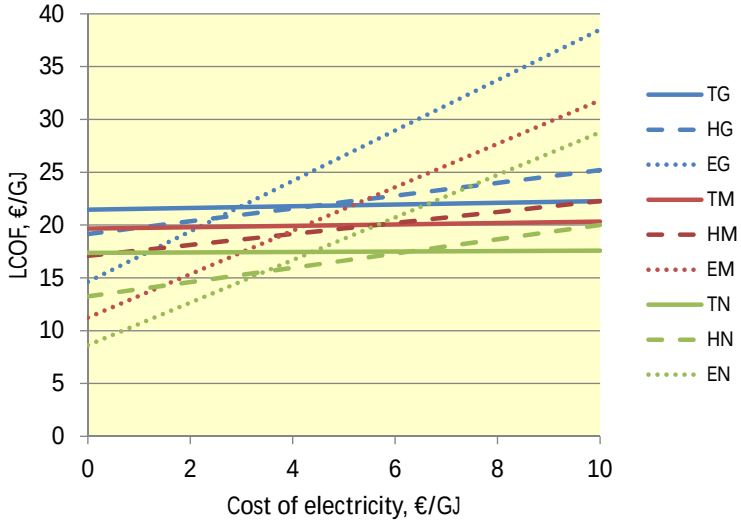

Figure 4.7: Levelised cost of fuel production (LCOF) for the examined plant configurations as a function of the electricity price.

Cost implications of alternative feedstock prices are then investigated. Fig. 4.7 shows production costs for all examined plant configurations as a function of electricity price while keeping the cost of biomass and feedstock carbon dioxide constant at 5 €/GJ (18 €/MWh) and 40 €/t, respectively. All gasoline (MTG) plants are indicated with blue, methanol plants with red and natural gas (SNG) plants with green lines. In addition, the lines are continuous for thermochemical plants, dashed for hybrid plants and dotted for electrochemical plants. As expected, the LCOFs for the thermochemical plants are only slightly sensitive to changes in the cost of electricity due to their low net electricity consumption. When the price of electricity changes by 1 €/GJ, it causes a change in the LCOF that is, on average, 0.6 €/GJ for hybrid and 2.2 €/GJ for electrochemical plants. In addition, it can be seen that the costs for hybrid plants are lower in comparison to corresponding thermochemical plants producing the same fuel when the price of electricity is below 6 €/GJ (22 €/MWh). For electrochemical configurations this price threshold is 4 €/GJ (14 €/MWh). It should be noted that these required threshold values are markedly lower than the current EU27 average prices, 16 - 20 €/GJ (58 - 72 €/MWh), paid by the chemical industry.[5]

A similar analysis is performed as a function of feedstock carbon dioxide price while keeping the cost of biomass and electricity constant at 5 and

[5] Average prices for chlorine and ammonia sectors taken from Ref. [191], based on data from the Centre for European Policy Studies.

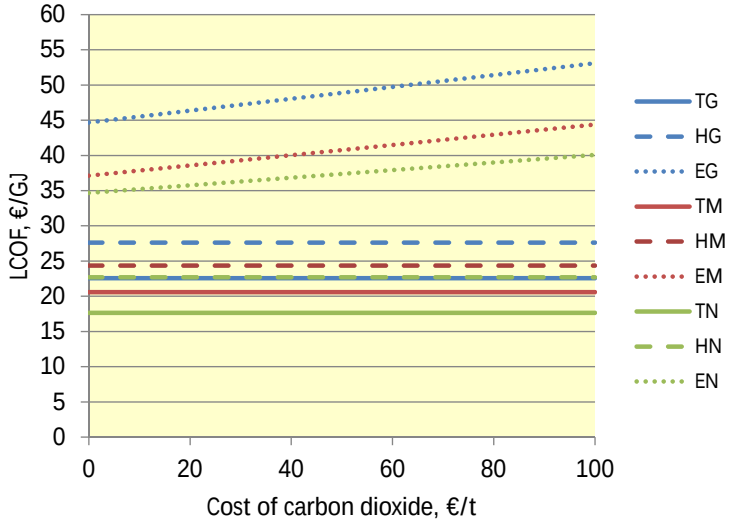

Figure 4.8: Levelised cost of fuel production (LCOF) for the examined plant configurations as a function of the carbon dioxide price.

14 €/GJ, respectively. The results are illustrated in Fig. 4.8. The costs of thermochemical and hybrid plants remain unchanged (because external CO_2 feed is not used), but for electrochemical plants, every 10 €/t change in the price of CO_2 causes, on average, a 0.7 €/GJ change in the LCOF. Somewhat surprisingly, even zero cost carbon dioxide would not be enough to make electrochemical plants more feasible in comparison to thermochemical configurations.

Cost implications of alternative biomass feedstock price are also investigated in Fig. 4.9, while keeping the cost of electricity and carbon dioxide constant at 14 €/GJ (50 €/MWh) and 40 €/t, respectively. The LCOFs of electrochemical plants are naturally not sensitive to changes in the cost of biomass feedstock. Hybrid and thermochemical plants are almost equally sensitive, although the slopes for thermochemical plants are steeper. When the price of biomass feedstock changes by 1 €/GJ, it causes a change in the LCOF that is, on average, 1.7 €/GJ for thermochemical and 1.3 €/GJ for hybrid plants. According to the results, purely thermochemical plants have lower production costs than corresponding hybrid plants producing the same fuel when the price of biomass stays under 14 €/GJ (50 €/MWh). For purely electrochemical configurations this threshold biomass feedstock price is about 17 €/GJ (61 €/MWh).

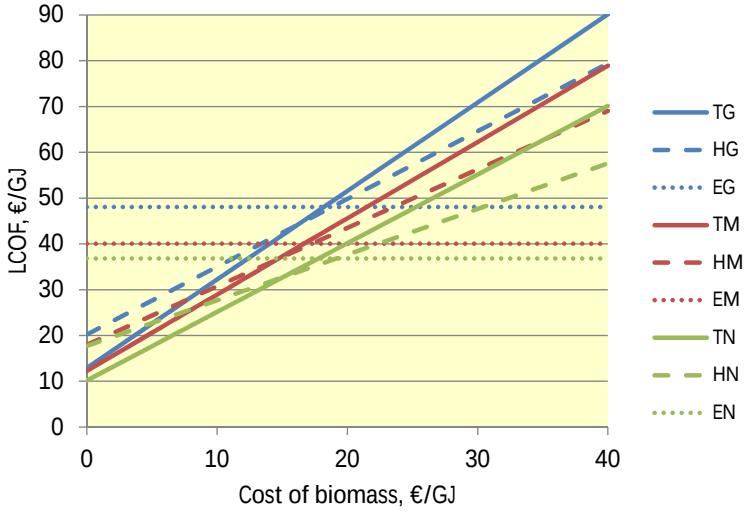

Figure 4.9: Levelised cost of fuel production (LCOF) for the examined plant configurations as a function of the biomass price.

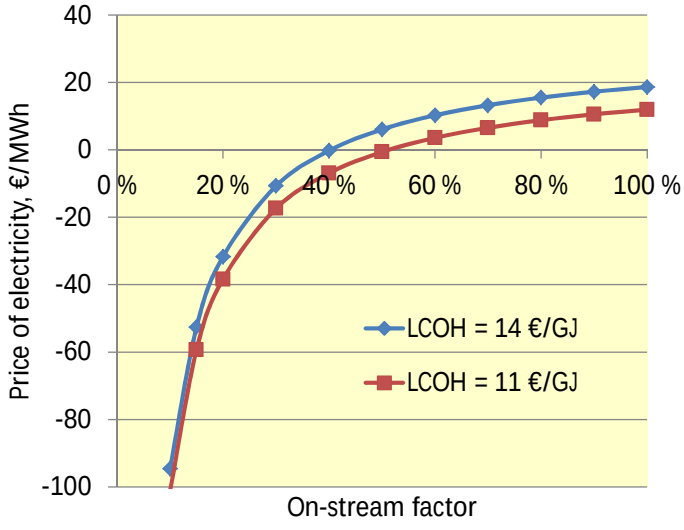

Figure 4.10: Electricity prices for an alkaline electrolysis system having a levelised cost of hydrogen (LCOH) of 14 or 11 €/GJ as a function of the on-stream factor.

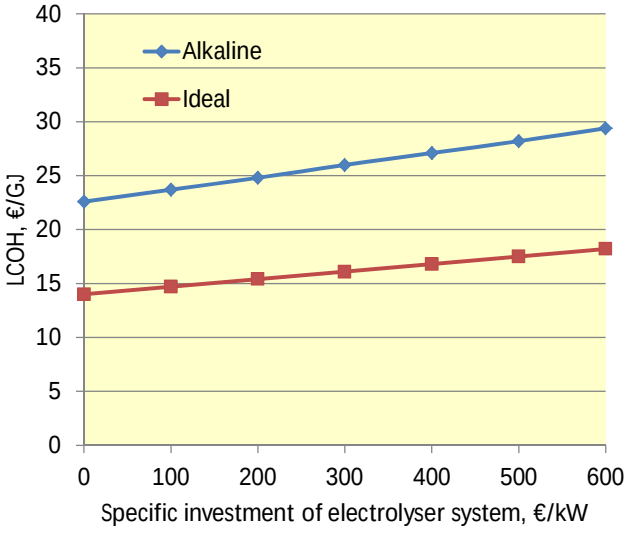

Figure 4.11: Levelised cost of hydrogen production (LCOF) for alkaline (system efficiency 62 % (LHV)) and ideal (100 %) electrolyser systems as a function of specific investment cost.

4.2.3 Preconditions for electrolytic hydrogen

The threshold electricity price that makes hybrid configurations more feasible than thermochemical plants was found to be 6 €/GJ. For purely electrochemical plants this value was found to be about 4 €/GJ. Using these electricity prices, the corresponding production cost for hydrogen is calculated to be 14 €/GJ for hybrid plants and 11 €/GJ for electrochemical plants. Therefore, when hydrogen is produced at a lower cost than these values, hybrid and electrochemical configurations become more feasible in comparison to thermochemical plants.

If the desire is to run the electrolysis only during times of excess renewable electricity, the impact of intermittent production on the levelised cost of hydrogen (LCOH) calls for additional analysis. This is carried out by calculating those electricity prices that maintain these threshold hydrogen prices (LCOH 14 and 11 €/GJ) at different annual operating hours, indicated by an on-stream factor (100 % on-stream factor = 8766 h/a).

The results are illustrated in Fig. 4.10. It can be seen how the LCOHs gradually become more and more sensitive to the price of electricity as the on-stream factor becomes smaller. For both threshold values, there is a point on the axis where the average price of electrolyser feedstock (electricity) must go negative in order to maintain the fixed LCOHs as the annual operating

hours continue to decrease: for the hybrid processes this happens at 40 % (3530 h/a) and for electrochemical plants at 51 % (4490 h/a). For on-stream factors smaller than 20 %, the LCOHs become highly sensitive to the price of electricity. For example, if the electrolyser would operate only 10 % of the year (877 h) the average price of electricity would need to be -91 €/MWh and -97 €/MWh to keep LCOHs at 14 €/GJ and 11 €/GJ, respectively.

Lastly, the impact of the electrolyser's investment cost is analysed. Fig. 4.11 shows LCOHs as a function of the specific investment cost while keeping the price of electricity and annual operating hours constant at 14 €/GJ and 8000 hours, respectively.[6] The results are calculated for an alkaline electrolyser having a system efficiency of 62 % (LHV) and also for a 100 % efficient 'ideal' electrolyser.

When the specific investment cost changes by 100 €/, it causes a change in the LCOH that is 1.1 €/GJ for an alkaline electrolyser and 0.7 €/GJ for an 'ideal' electrolyser. Surprisingly, the target hydrogen prices (14 and 11 €/GJ) can not be reached even with a 100 % efficient electrolyser system, running 8000 hours annually and having zero investment cost.

4.3 Light olefins via synthetic methanol

As outlined in the beginning of this dissertation, cutting down industrial emissions has proven to be an especially challenging task partly due to limitations in the electrification potential of industrial processes. Thus, switching to more sustainable feedstocks is a key to the decarbonisation of this sector, together with carbon capture and storage where applicable. Once technology for the production of renewable synfuels in large quantities becomes fully commercialised, it opens up a possibility to produce, not only fuels, but also light olefins that are main components of the petrochemical industry. Technology for the production of olefins from methanol is already commercial with several plants currently being built and operated in China for the production of olefins from coal [192]. It is therefore of interest to investigate the techno-economics of producing renewable olefins and to compare it against the production of synthetic transportation fuels. The results discussed in this section answer Research Question 3 and were originally published in **Paper V**.

[6] The value of by-product oxygen is not considered as it was already included when the target LCOH values were calculated.

4.3.1 Performance results

Mass and energy balances were simulated with Aspen for two different plant configurations, both producing light olefins from synthetic methanol. The plants are integrated with an existing steam cracking plant and used to fractionate the raw MTO effluent. Ethylene and propylene (ethene and propene) are the main products, both fractionated to ≥ 99.5 % purity. The main by-product from the process is a C_{4+} fraction while other by-products include ethane-rich (~70 mol-%) stream, propane-rich (~60 mol-%) stream and methane-rich (~60 mol-%) stream.

Table 4.7 summarises the main simulation results for the methanol to olefins process. In the MTO design the C_{4+} stream is sent to alkylation, while in the Advanced MTO design it is sent to the Olefin Cracking Process and the C_1-C_3 fraction of the OCP effluent (see Table 2.4 and Fig. 2.9) is recycled back to the MTO process. In the MTO design, equal amounts of propylene and ethylene are produced on mass basis, while in the Advanced MTO design the simulated P/E ratio is 1.2.

The overall mass yield from dry biomass to methanol is 0.5108 kg/kg and from dry biomass to light olefins 0.169 kg/kg and 0.203 kg/kg for the MTO and Advanced MTO, respectively. The two plant designs also consume a different amount of utilities. In both cases the largest consumer of electricity is MTO effluent's compression that requires 106 kJ of electricity for every kilogram of methanol fed into the process. Refrigeration is the second largest at 62 kJ/kg_{MeOH} with the Advanced MTO design requiring an additional 7 kJ/kg_{MeOH} to offset the increased cooling duties caused by fractionation of additional light olefins from the olefin cracker.

Steam is both produced and consumed in the MTO process. In the conversion area, heat is recovered both from the exothermic MTO reaction and from the regenerator's flue gas to produce 0.33 kg/kg_{MeOH} of high-pressure superheated (125 bar, 520 °C) steam, while 0.32 kg/kg_{MeOH} of saturated low-pressure (15 bar, 198 °C) steam is used to vaporise water prior to mixing with the methanol feed. In the separation area, 0.17 kg/kg_{MeOH} of low-pressure steam is required to heat the reboilers of the MTO and 0.24 kg/kg_{MeOH} of the Advanced MTO configuration. When combined, these amount to 0.49 and 0.56 kg/kg_{MeOH} low-pressure steam requirement for the MTO and Advanced MTO designs, respectively.

4.3.2 Cost results

A fully functional MTO process requires all the main equipment illustrated in Fig. 2.9 plus equipment to provide utilities like steam and refrigeration. However, major savings in capital investment could possibly be attained by coupling the MTO process with an existing steam cracking plant so that the

Table 4.7: Key simulation results for MTO and Advanced MTO (MTO + OCP) plants. Yields refer to final yields after separation and recycling.

Products, kg/kg$_{MeOH}$	**MTO**	**MTO+OCP**
Ethylene	0.1659	0.1798
Propylene	0.1655	0.2173
C_{4+}	0.0737	0.0015
H_2	0.0006	0.0006
Fuelgas*	0.0114	0.0080
Ethane-rich	0.0049	0.0067
Propane-rich	0.0025	0.0054
Utilities	**MTO**	**MTO+OCP**
Work, kJ/kg$_{MeOH}$		
Air blower (MTO)	-35	-35
Compression (MTO)	-106	-106
Compression (OCP)		-33
Cryogenic work (MTO)	-62	-69
Steam, kg/kg$_{MeOH}$		
HP steam (MTO)	0.33	0.33
LP steam (MTO)	-0.49	-0.56
Overall yields, kg/kg		
Ethylene/biomass (dry)	0.0847	0.0918
Light olefins/biomass (dry)	0.1693	0.2028

*After H_2 separation by PSA and combustion in OCP

MTO process could benefit from the steam cracker's fractionation capacity and utility equipment. In this case the required investment would be limited only to the methanol conversion section, i.e. the grey shaded boxes shown in Fig. 2.9. Such an 'Integrated MTO' design would produce two intermediate streams: a C_1-C_3 and a C_{4+} stream (indicated with numbers 3 and 4 in Fig. 2.9) that would be integrated into external units for further processing. In the studied plant configurations, the C_1-C_3 stream is routed to the fractionation part of the steam cracking plant and the C_{4+} stream either to alkylation or olefin cracking depending on the examined case.

To make sure that there is enough capacity available at the steam cracking plant for the fractionation of the MTO's C_1-C_3 stream, it is assumed that a steam cracking oven of comparable size is taken off-line before start-up of the MTO process. Due to differences in yield structures between steam cracking and MTO, equal amounts of produced ethylene is not an ideal indicator for quantifying equal capacities. For this reason, it was decided to compare capacities based on equal amount of light olefins (ethylene + propylene) produced. A 0.57 light olefin mass yield was assumed for naphtha steam cracking and 0.33 for MTO. Based on these assumptions, 1.73 kg of methanol is required to replace 1 kg of naphtha to produce a commensurate

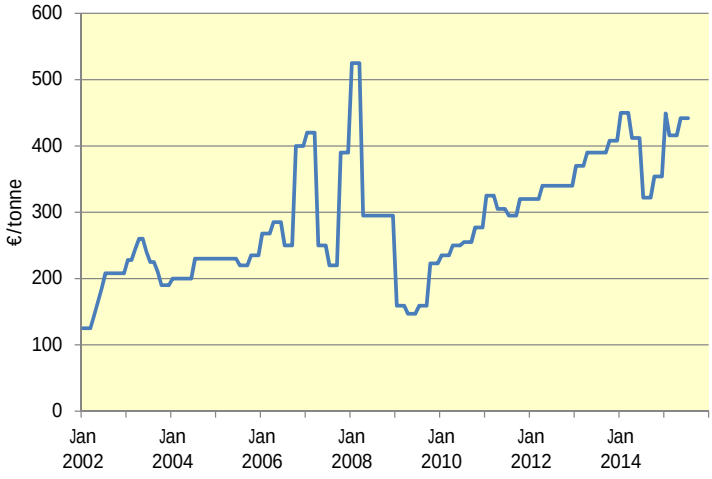

Figure 4.12: Methanex European Posted Contract Price 2002-2015 for methanol.

amount of light olefins.

Based on discussions with industry experts, a modern naphtha cracking oven with a feed input of 50 t/h was assumed to have total capital investment in 2014 (TCI) of 45 M€. It was further assumed that an MTO conversion section of a commensurate size (86 t/h MeOH) requires double the TCI at 90 M€[7]. It was estimated that the TCI of an MTO conversion section using 30 t/h of methanol is 37 M€. Based on simulation results the C_{4+} by-product flow from a 30 t/h methanol MTO plant is 2.2 t/h. It was assumed that the cost of an MTO conversion section and an Olefin Cracking Process of comparable size (as measured in terms of feed input) are equal and thus the TCI of such an OCP was estimated to be 4 M€.

It was also assumed that process energy demand in naphtha steam cracking is met by combustion of by-products, together with heat recovery from flue gases and waste heat [193]. In addition, all the required steam was assumed to be generated within the process by quenching the hot gas mixture from the cracker furnace with transfer line exchangers, leading to zero net steam import or export. As a result, it was expected that the replacement of an naphtha oven with an MTO reactor would not cause any major changes in the heat and steam balance of the entire steam cracking plant.

[7] These higher costs are due to the more expensive double fluidised-bed reactor/regenerator system, reactor internals, catalyst and combustion air blower.

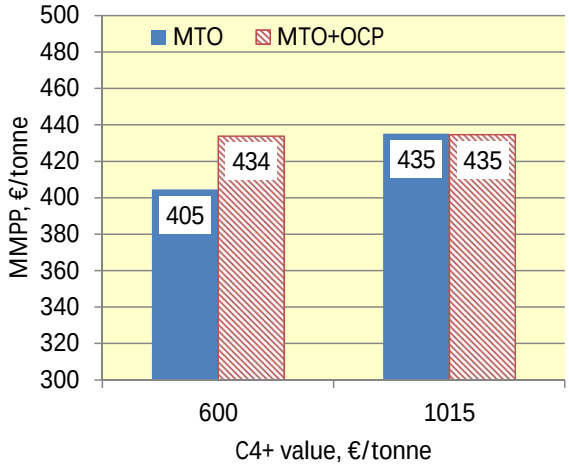

Figure 4.13: Maximum methanol purchase price calculated with two different values for the C_{4+}: 600 €/t (when end-product conventional motor fuel), and 1015 €/t (when end-product biofuel).

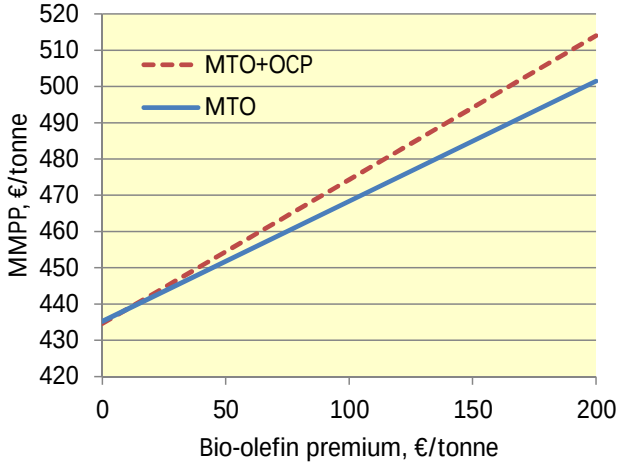

Figure 4.14: Maximum methanol purchase price calculated as a function of bio-olefin premium.

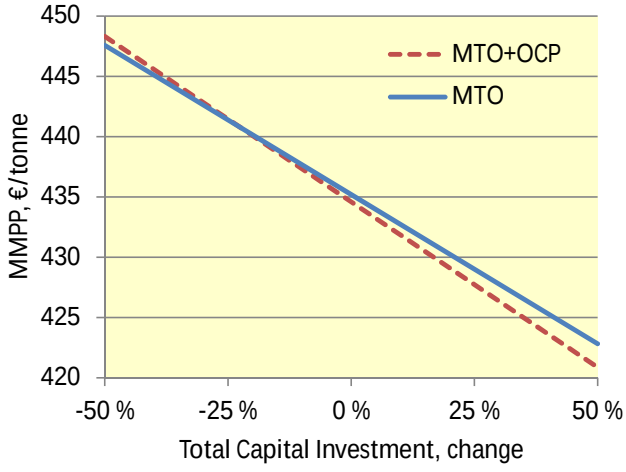

Figure 4.15: Maximum methanol purchase price calculated as a function of change in Total Capital Investment.

The prospective economics of methanol to olefins were evaluated in the form of a sensitivity analysis. In contrast to other cost results presented in this dissertation, the economics were calculated 'backwards' using Maximum Methanol Purchase Price (MMPP) as the economic indicator. To facilitate comparison with historical prices of fossil-derived methanol, the Methanex European Posted Contract Price 2002-2015 is shown in Fig. 4.12.

Fig. 4.13 illustrates the impact of C_{4+}'s value on the maximum methanol purchase price. In alkylation the C_{4+} stream is converted to premium gasoline blending stock. When bio-methanol is used as feedstock for the MTO, blending stock produced from the C_{4+} becomes a biofuel component. Various mandates and obligations are already in place in the biofuels market, making it possible to charge price premiums. Conventional petroleum-derived motor fuel was priced at 750 €/t (before taxes at the refinery gate) and biofuel at 1269 €/t (gasoline eq.), the FOB price for Brazilian T2 ethanol in Rotterdam on June 2013 [194].

According to the results, if the seller is unable to charge a price premium on the by-product alkylate, the maximum methanol purchase price is 405 and 434 €/t for the MTO and Advanced MTO designs, respectively. However, when mandates are in place, MMPP for the MTO design rises to 434 €/t and becomes on a par with Advanced MTO. This happens because only a very small amount of C_{4+} is produced in the Advanced MTO design (most of it is cracked to light olefins in OCP), making its economics non-sensitive to the value of alkylate.

Fig. 4.14 illustrates the impact of the bio-olefin premium on the maximum methanol purchase price. If the olefin seller is unable to charge any premium from bio-olefins relative to the prevailing market price (ethylene 1100 €/t and propylene 1200 €/t), the MMPP is 435 €/t for both MTO and Advanced MTO. However, if a bio-olefin premium exists, then every 100 €/t (9 %) increase in the price of light olefins will lead, on average, to a 36 €/t increase in the MMPP. For example, at a 200 €/t premium the MMPP is 501 €/t and 514 €/t for base case MTO and Advanced MTO, respectively. The Advanced MTO design is more sensitive to the olefin value because of the increased output caused by the OCP.

The impact of a change in the total capital investment (TCI) on the MMPP was also examined in Fig. 4.15. If the TCI would be 50 % less than in the estimate, then the MMPP would increase, on average, by 13 €/t to 448 €/t for the MTO and Advanced MTO. A 50 % increase in the TCI would have a similar size impact on the other direction, lowering the MMPP to 423 for MTO and 421 €/t for Advanced MTO. The Advanced MTO design is slightly more sensitive to changes in TCI due to the higher absolute investment caused by the addition of the Olefin Cracking Process.

Chapter 5

Discussion

Analysing the long-term technical and economic feasibility of selected plant configurations capable of producing synthetic fuels or light olefins from renewable feedstocks has been a major theme in this dissertation. The choice of feedstock, conversion route and end-product were all found to have significant impact on the efficiency and cost of synfuels production. According to **Paper IV**, the costs are:

- 18 €/GJ (methane), 21 €/GJ (methanol) and 23 €/GJ (gasoline) for purely thermochemical plants;
- 23 €/GJ (methane), 24 €/GJ (methanol) and 28 €/GJ (gasoline) for hybrid plants;
- 37 €/GJ (methane), 40 €/GJ (methanol) and 48 €/GJ (gasoline) for electrochemical plants.

Thus for all the examined configurations, methane (ie. synthetic natural gas) was found to be the lowest-cost fuel to produce, followed by methanol and then by gasoline. This ranking is also supported by previous biofuels research (e.g. Hamelinck et al. [8], McKeough and Kurkela [9], Spath and Dayton [21]). However, it deserves to be noted that although methane was identified as the lowest-cost fuel to produce on a per-GJ basis, neither the added costs of compression and delivery to refuelling stations, nor the added cost of a methane-using vehicle were included in the analysis.

For a given end-product, the lowest costs were associated with thermochemical production from forest residues, while the highest costs were associated with electrochemical production from carbon dioxide and electricity. The hybrid plants were found capable of producing fuels at a lower cost than purely electrochemical plants, but not lower than purely thermochemical

plants. The results cover a wide range of production costs from 18 €/GJ to 48 €/GJ. For synthetic gasoline, the corresponding break-even oil prices are \$124/bbl via thermochemical, \$154/bbl via hybrid and \$274/bbl via electrochemical production route.[1] These prices can be compared with the IEA's recent oil price scenarios[2] shown in Table 5.1 [195]. When contrasted with these forecasts, only gasoline produced via thermochemical process seems to have the potential to become competitive with petroleum fuels under certain future scenarios, while gasoline produced via the hybrid or electrochemical route doesn't break even under any of the presented price predictions.

Table 5.1: IEA WEO oil price forecasts (\$/bbl) by scenario in real terms (2012 prices).

Year	Current Policies	New Policies	450
2020	120	113	110
2025	127	116	107
2030	136	121	104
2035	145	128	100

In addition to being a feedstock for gasoline manufacture, methanol could be used as a transportation fuel either directly or as a blending component [196]. Indeed, the use of methanol as a motor fuel option has been a recurring theme in the history of alternative fuels, especially in the 1970s and 1980s [197]. Currently in Europe no more than 3 vol-% of methanol is allowed[3] to be blended in gasoline, but for example in China methanol is used today in various blends ranging from 5 % methanol in gasoline (M5) to 100 % methanol (M100). Higher blends like M85 can be used only in special Flexible Fuel Vehicles (FFVs) where the fuel system materials have been adapted to methanol [197]. The manufacture of a FFV vehicle is not much more expensive than a normal gasoline vehicle, but in Europe their supply has been diminishing due to the new Euro 6 exhaust standards that require emission certification at low temperatures (-7 °C) also for alcohol fuels.

As already discussed in section 3.2, the presented analysis is expected to contain uncertainties, which are addressed in this dissertation by carrying out sensitivity studies. For concept-stage feasibility assessments, like those presented in **Papers III - V**, the accuracy is expected to be around -15%/+30%

[1] Assuming \$14/bbl refining margin, 6 GJ/bbl and 1.0 €/\$ exchange rate.
[2] It should be noted that these forecasts were released before the 60 per cent fall in oil prices between June 2014 and January 2015.
[3] See Fuel Quality Directive (2009/30/EC) and CEN standard (EN 228).

[175]. However, a recent report, after reviewing a number of complex and large energy projects, ended up recommending much higher contingency factors than conventionally used. For example, a contingency factor as high as 55 % was recommended for a concept-stage N^{th} plant cost estimate [198]. Still, the strength of the methodology applied in this dissertation lies not in the accuracy of *absolute* costs, but rather in that it enables the estimation of cost *differences* among alternative process configurations with a reasonably high degree of confidence.

The production of clean synthesis gas from biomass is the key enabling technology for synthetic biofuels manufacture. The improvement potential of the tar clean-up system and its impact on the overall techno-economics of the UCG-based process was studied in **Paper III**, using Fischer-Tropsch plant configuration as an example. The findings show that the potential improvement in the overall efficiency from biomass-to-FT liquids is 4.7 percentage points if filtration temperature can be successfully elevated from the current ~550 °C to the target level of 850 °C. The resulting reduction in the cost of synfuel was found to be 1.1 €/GJ. The results further showed that a 10 % increase in the methane reforming extent leads to a 1.2 percentage point improvement in overall efficiency causing a 0.22 €/GJ reduction in the cost of synfuel.

One important objective of this dissertation was to investigate the techno-economics of producing synthetic fuels from carbon dioxide and electricity via water electrolysis. Such 'electrofuels' could be used to radically increase the amount of renewable fuels that can be produced globally by relying on biomass alone. However, despite the promising potential, the techno-economic analysis showed that electrofuels seem to be characterised by high costs under a wide range of practical economic assumptions. For example, it was shown that in order to become competitive with biomass-derived synfuels, the annual average cost of feedstock electricity should remain below 4 €/GJ for a continuously (8000 h/a) operated process. With fewer operational hours, the need for even lower cost electricity becomes pressing, requiring negative price with less than ~4500 annual operating hours. The competitiveness of electrofuels was shown to be relatively insensitive to the cost of the CO_2 feedstock. Somewhat surprisingly, not even a zero-cost CO_2 feedstock nor zero-cost electrolyser would make electrofuels competitive with synthetic biofuels under present-day financial assumptions. The notion of the importance of long-term low electricity costs to the feasibility of electrofuels is also supported by previous research (e.g. Graves et al. [28]).

An interesting aspect of the electrochemical route is the possibility to integrate it with biomass gasification. In comparison with purely electrochemical configurations, the key benefit from such integration is the possibility to use CO as the source of carbon for the synthesis instead of CO_2, leading to more efficient fuel production. The level of integration can vary within a

wide range, but complete hydrogenation of syngas CO was set as the upper limit for configurations examined in this dissertation. With such enhancement, it was shown to be possible to increase the output of methanol and gasoline by 31 % and methane by 50 %, a finding that is also supported by previous research (e.g. Mignard and Pritchard [29]). However, if the syngas CO_2 would also be used as feedstock, the output could be increased even further as about half of the biomass carbon is normally rejected from the process in the form of CO_2 [199]. The separated stream of CO_2 could be hydrogenated to methane or methanol in a separate synthesis island, or alternatively the CO_2 would be allowed to enter the main synthesis with carbon monoxide and an adequate amount of hydrogen (the base from biomass gasification and the balance from an external source) [200]. As a result, such electrolyser-enhanced biofuels could potentially reshape the discussion over biomass availability, as more than twice the amount of fuel could be produced from a given amount of biomass when the process is fully augmented by an external hydrogen supply [30].

The techno-economics of light olefins production was assessed in **Paper V**. The motivation behind the production of materials lies in the higher value of chemicals over fuels. However, many high-value chemicals have very small demand making it difficult to achieve notable reductions in global emissions by decarbonising their production. In this respect, light olefins are interesting commodities as they combine relatively high value with considerable global demand: in 2011 the global end use markets were 127 million tonnes for ethylene and 79 million tonnes for propylene [201]. Technically the production of light olefins from alternative feedstocks is very similar to gasoline, as both are produced by upgrading methanol. According to simulation results, a metric tonne of dry biomass can be converted via gasification to 511 kg of methanol and further to 169-203 kg of light olefins depending on the MTO configuration. Significant integration opportunities were also identified between MTO and existing steam cracking technology. The economic analysis further showed that at current ethylene and propylene prices bio-olefins break even with fossil alternatives if renewable methanol can be procured at less than ~430 €/tonne. An interesting observation was that differences in economic performance between biofuel and olefin plants became negligible when taking into account current price premiums enjoyed by biofuels but not by bio-olefins. In other words, process economics made possible by current low-carbon policies and mandates in the biofuels market can be achieved at the petrochemical side based on market prices alone, without the 'green premiums'.

Like gasoline, olefins can also be produced via electrochemical route using methanol as an intermediate. Combining findings from **Paper IV** and **Paper V**, it can be shown that producing one metric tonne of light electro-olefins would require 3641 - 4367 kilograms of CO_2 and 724 - 869 kilograms of hydrogen. For the electrolyser-enhanced hybrid route the consumption

of resources is 3775 - 4528 kilograms of biomass and 115 - 138 kilograms of hydrogen.

The findings of this dissertation support the general perception that renewable alternative fuels are more expensive than fossil fuels under present-day financial assumptions. Therefore, to meet the vision of CO_2-neutral transportation, sustained policy measures are needed to help overcome the gap between established (fossil) and emerging (renewable) energy technologies until a self-sustaining growth path for biofuels is reached. Such measures should include continued investment in research and development but most importantly a strategic deployment programme that aims to accelerate the pace of improvement through market experience.

Bibliography

[1] C. Le Quéré, R. J. Andres, T. Boden, T. Conway, R. A. Houghton, J. I. House, G. Marland, G. P. Peters, G. R. van der Werf, A. Ahlström, R. M. Andrew, L. Bopp, J. G. Canadell, P. Ciais, S. C. Doney, C. Enright, P. Friedlingstein, C. Huntingford, A. K. Jain, C. Jourdain, E. Kato, R. F. Keeling, K. Klein Goldewijk, S. Levis, P. Levy, M. Lomas, B. Poulter, M. R. Raupach, J. Schwinger, S. Sitch, B. D. Stocker, N. Viovy, S. Zaehle, N. Zeng, The global carbon budget 1959-2011, Earth System Science Data 5 (1) (2013) 165–185. doi:10.5194/essd-5-165-2013.

[2] D. Hartmann, A. K. Tank, M. Rusticucci, L. Alexander, S. Brönnimann, Y. Charabi, F. Dentener, E. Dlugokencky, D. Easterling, A. Kaplan, B. Soden, P. Thorne, M. Wild, P. Zhai, Observations: Atmosphere and surface, in: T. Stocker, D. Qin, G.-K. Plattner, M. Tignor, S. Allen, J. Boschung, A. Nauels, Y. Xia, V. Bex, P. Midgley (Eds.), Climate Change 2013: The Physical Science Basis. Contribution of Working Group I to the Fifth Assessment Report of the Intergovernmental Panel on Climate Change, Cambridge University Press, Cambridge, United Kingdom and New York, NY, USA, 2013.

[3] IPCC, Climate Change 2007: Synthesis Report. Contribution of Working Groups I, II and III to the Fourth Assessment Report of the Intergovernmental Panel on Climate Change, IPCC, Geneva, Switzerland, 2007, p. 104.

[4] IPCC, Summary for policymakers, in: O. Edenhofer, R. Pichs-Madruga, Y. Sokona, E. Farahani, S. Kadner, K. Seyboth, A. Adler, I. Baum, S. Brunner, P. Eickemeier, B. Kriemann, J. Savolainen, S. Schlömer, C. von Stechow, T. Zwickel, J. Minx (Eds.), Climate Change 2014: Mitigation of Climate Change. Contribution of Working Group III to the Fifth Assessment Report of the Intergovernmental

Panel on Climate Change, Cambridge University Press, Cambridge, United Kingdom and New York, NY, USA, 2014.

[5] IEA, Transport, energy and CO_2: Moving toward sustainability, International Energy Agency (2009).
URL http://bit.ly/1CAFZQG

[6] T. Kreutz, E. Larson, R. Williams, G. Liu, Fischer-Tropsch fuels from coal and biomass, in: Proceedings of the 25th Annual International Pittsburgh Coal Conference, Pittsburgh, PA, USA, 2008.

[7] G. Liu, E. D. Larson, R. H. Williams, T. G. Kreutz, X. Guo, Making Fischer-Tropsch fuels and electricity from coal and biomass: Performance and cost analysis, Energy & Fuels 25 (1). doi:10.1021/ef101184e.

[8] C. N. Hamelinck, A. P. Faaij, H. den Uil, H. Boerrigter, Production of FT transportation fuels from biomass; technical options, process analysis and optimisation, and development potential, Energy 29 (11) (2004) 1743 – 1771. doi:10.1016/j.energy.2004.01.002.

[9] P. McKeough, E. Kurkela, Process evaluations and design studies in the UCG project 2004-2007, VTT Research Notes 2434, Technical Research Centre of Finland, VTT (2008).

[10] L. Van Bibber, E. Shuster, J. Haslbeck, M. Rutkowski, S. Olsen, S. Kramer, Baseline technical and economic assessment of a commercial scale Fischer-Tropsch liquids facility, Tech. Rep. DOE/NETL-2007/1260, National Energy Technology Laboratory (2007).

[11] I. Landälv, Demonstration plants for advanced biofuels production based on thermochemical pathways - status and reflections, in: Proceedings of the 21st European Biomass Conference and Exhibition, Copenhagen, Denmark, 2013.

[12] Audi unveils e-gas project, Green Car Congress, May 13, 2011.
URL http://bit.ly/1qHXLke

[13] Sunfire acquiring staxera to support development of technology to generate synthetic fuels from renewable energy sources, water and CO_2, Green Car Congress, May 23, 2011.
URL http://bit.ly/1BBqPj9

[14] Audi in new e-fuels project: synthetic diesel from water, air-captured CO_2 and green electricity; "Blue Crude", Green Car Congress, Nov 14, 2014.
URL http://bit.ly/1LukKGW

[15] Hydrogenics to supply 1 MW electrolyzer to project converting CO_2

to methanol; power-to-gas, Green Car Congress, Jan 26, 2015.
URL http://bit.ly/1CZa90a

[16] L. R. Cohen, R. G. Noll, Synthetic fuels from coal, in: The Technology Pork Barrel, The Brookings Institution, Washington, DC, 1991, Ch. 10.

[17] J. M. Deutch, R. K. Lester, Synthetic fuels, in: Making Technology Work - Applications in Energy and the Environment, Massachusetts Institute of Technology, Cambridge MA, 2005, Ch. 12.

[18] L. Anadon, G. Nemet, B. Schock, The US Synthetic Fuels Corporation: Policy consistency, flexibility, and the long-term consequences of perceived failures. Historical case studies of energy technology innovation, in: The Global Energy Assessment, Cambridge University Press: Cambridge, UK, 2012, Ch. 24.

[19] BP Statistical Review of World Energy June 2015, BP, http://www.bp.com/statisticalreview, 2015.

[20] Short-Term Energy Outlook, U.S. Energy Information Administration, July 2015.

[21] P. Spath, D. Dayton, Preliminary screening — technical and economic assessment of synthesis gas to fuels and chemicals with emphasis on the potential for biomass-derived syngas, Tech. Rep. NREL/TP-510-34929, National Renewable Energy Laboratory (2003).

[22] E. D. Larson, H. Jin, F. E. Celik, Large-scale gasification-based coproduction of fuels and electricity from switchgrass, Biofuels, Bioproducts and Biorefining 3 (2) (2009) 174–194. doi:10.1002/bbb.137.
URL 10.1002/bbb.137

[23] A. Dutta, S. Phillips, Thermochemical ethanol via direct gasification and mixed alcohol synthesis of lignocellulosic biomass, Tech. Rep. NREL/TP-510-45913, National Renewable Energy Laboratory (2009).

[24] S. Phillips, A. Aden, J. Jechura, D. Dayton, T. Eggeman, Thermochemical ethanol via indirect gasification and mixed alcohol synthesis of lignocellulosic biomass, Tech. Rep. NREL/TP-510-41168, National Renewable Energy Laboratory (2007).

[25] T. Ren, M. K. Patel, Basic petrochemicals from natural gas, coal and biomass: Energy use and CO_2 emissions, Resources, Conservation and Recycling 53 (9) (2009) 513 – 528. doi:10.1016/j.resconrec.2009.04.005.

[26] T. Ren, B. Daniels, M. K. Patel, K. Blok, Petrochemicals from oil, natural gas, coal and biomass: Production costs in 2030 - 2050,

Resources, Conservation and Recycling 53 (12) (2009) 653 – 663. doi:10.1016/j.resconrec.2009.04.016.

[27] C. Hamelinck, Outlook for advanced biofuels, Ph.D. thesis, Utrecht University, The Netherlands (2004).

[28] C. Graves, S. D. Ebbesen, M. Mogensen, K. S. Lackner, Sustainable hydrocarbon fuels by recycling CO_2 and H_2O with renewable or nuclear energy, Renewable and Sustainable Energy Reviews 15 (1) (2011) 1 – 23. doi:10.1016/j.rser.2010.07.014.

[29] D. Mignard, C. Pritchard, On the use of electrolytic hydrogen from variable renewable energies for the enhanced conversion of biomass to fuels, Chemical Engineering Research and Design 86 (5) (2008) 473 – 487. doi:10.1016/j.cherd.2007.12.008.

[30] M. Pozzo, A. Lanzini, M. Santarelli, Enhanced biomass-to-liquid BTL conversion process through high temperature co-electrolysis in a solid oxide electrolysis cell SOEC, Fuel 145 (0) (2015) 39 – 49. doi:10.1016/j.fuel.2014.12.066.

[31] IEA, Technology Roadmap - Biofuels for Transport, International Energy Agency (2011).
URL http://bit.ly/1MqB4Kd

[32] K. Neuhoff, Large scale deployment of renewables for electricity generation, Cambridge working papers in economics CWPE 0460, University of Cambridge (2006).

[33] E. Kurkela, Formation and removal of biomass-derived contaminants in fluidized-bed gasification processes, VTT Publications Vol.287, Technical Research Centre of Finland, VTT (1996).

[34] P. Simell, Catalytic hot gas cleaning of gasification gas, Ph.D. thesis, Helsinki University of Technology, TKK (1997).

[35] E. Kurkela, M. Kurkela, I. Hiltunen, The effects of wood particle size and different process variables on the performance of steam-oxygen blown circulating fluidized-bed gasifier, Environmental Progress & Sustainable Energy 33 (3) (2014) 681–687. doi:10.1002/ep.12003.

[36] Neste Oil, Stora Enso shelve plans for renewable diesel plant, Biomass magazine, August 22, 2012.
URL http://bit.ly/1mUBfPz

[37] L. Fagernäs, J. Brammer, C. Wilen, M. Lauer, F. Verhoeff, Drying of biomass for second generation synfuel production, Biomass and Bioenergy 34 (9) (2010) 1267–1277.

[38] A. Rautalin, C. Wilén, Feeding biomass into pressure and related safety engineering, Research notes 1428, VTT, Laboratory of Fuel and Pro-

cess Technology (1992).
URL http://bit.ly/1KkimVQ

[39] C. Wilen, A. Moilanen, E. Kurkela, Biomass feedstock analyses, VTT Publications 282, Technical Research Centre of Finland, VTT (1996).

[40] J. Brammer, A. Bridgwater, Drying technologies for an integrated gasification bio-energy plant, Renewable and Sustainable Energy Reviews 3 (4) (1999) 243 – 289.

[41] Metso brochure on KUVO belt dryer, Accessed July 8, 2013. [link].
URL http://bit.ly/10IwPme

[42] F. Lau, D. Bowen, R. Dihu, S. Doong, E. Hughes, R. Remick, R. Slimane, S. Turn, R. Zabransky, Techno-economic analysis of hydrogen production by gasification of biomass: Appendix B - Identification / Evaluation of solids handling systems, Final technical report under DOE contract number: DE-FC36-01GO11089, Gas Technology Institute (2002).

[43] M. Swanson, M. Musich, D. Schmidt, J. Schultz, Feed system innovation for gasification of locally economical alternative fuels (FIGLEAF) Final report, Tech. rep., U.S. Department of Energy (2002).

[44] BiGPower deliverable 71: Finnish case study report, Project co-funded by the European Commission within the Sixth Framework Programme project no. 019761, Carbona, Inc. (2009).

[45] E. Kurkela, A. Moilanen, K. Kangasmaa, Gasification of biomass in a fluidised bed containing anti-agglomerating bed material, patent WO 00/011115 (2003).

[46] Bubbling fluidized bed gasification, ANDRITZ, Accessed Sept, 2015.
URL http://bit.ly/1EPeDh0

[47] E. Kurkela, P. Ståhlberg, J. Laatikainen, Pressurized fluidized-bed gasification experiments with wood, peat and coal at VTT [Espoo, Finland] in 1991-1992, Part 1: Test facilities and gasification experiments with sawdust, VTT Publications 161, Technical Research Centre of Finland, VTT (1993).

[48] E. Kurkela, P. Ståhlberg, J. Laatikainen, P. Simell, Development of simplified IGCC-processes for biofuels: Supporting gasification research at VTT, Bioresource Technology 46 (1-2) (1993) 37–47, Power Production from Biomass.

[49] E. Simeone, M. Nacken, W. Haag, S. Heidenreich, W. de Jong, Filtration performance at high temperatures and analysis of ceramic filter elements during biomass gasification, Biomass and Bioenergy 35,

Supplement 1 (0) (2011) S87 – S104, CHRISGAS. doi:10.1016/j.biombioe.2011.04.036.

[50] E. Simeone, M. Siedlecki, M. Nacken, S. Heidenreich, W. de Jong, High temperature gas filtration with ceramic candles and ashes characterisation during steam-oxygen blown gasification of biomass, Fuel 108 (0) (2013) 99 – 111. doi:10.1016/j.fuel.2011.10.030.

[51] E. Kurkela, P. Ståhlberg, J. Laatikainen, M. Nieminen, Removal of particulates and alkali-metals from the product gas of a pressurized fluid-bed gasifier, Proc. Int. Filtration & Separation Conf. Filtech Europa 1991, Karlsruhe, Germany (1991).

[52] M. Nieminen, E. Kurkela, Filtration of biomass and waste-derived gasification product gas, in: A. Bridgwater, D. Boocock (Eds.), Science in Thermal and Chemical Biomass Conversion, CPL Press, 2006, pp. 788–798.

[53] M. Nieminen, K. Kangasmaa, E. Kurkela, P. Ståhlberg, Durability of metal filters in low sulphur gasification gas, in: 3rd Symposium and Exhibition Gas Cleaning at High Temperatures, Karlsruhe, Germany, 1996, pp. 120–131.

[54] M. Nieminen, P. Simell, J. Leppälahti, P. Ståhlberg, E. Kurkela, High temperature cleaning of biomass-derived fuel gas, in: Proceedings of the 9th European Bioenergy Conference, Copenhagen, Denmark, 1996, pp. 1080–1086.

[55] T. Eriksson, J. Isaksson, P. Ståhlberg, E. Kurkela, V. Helanti, Durability of ceramic filters in hot gas filtration, Bioresource Technology 46 (1–2) (1993) 103 – 112, Power Production from Biomass. doi:10.1016/0960-8524(93)90060-O.

[56] E. Kurkela, P. Ståhlberg, J. Laatikainen, Pressurized fluidized-bed gasification experiments with wood, peat and coal at VTT in 1991-1994, Part 2: Experiences from peat and coal gasification and hot gas filtration, VTT Publications 249, Technical Research Centre of Finland (1995).

[57] L. Ma, H. Verelst, G. Baron, Integrated high temperature gas cleaning: Tar removal in biomass gasification with a catalytic filter, Catalysis Today 105 (3–4) (2005) 729 – 734, 2nd International Conference on Structured Catalysts and Reactors. doi:10.1016/j.cattod.2005.06.022.

[58] M. Nacken, L. Ma, S. Heidenreich, G. V. Baron, Performance of a catalytically activated ceramic hot gas filter for catalytic tar removal from biomass gasification gas, Applied Catalysis B: Environmental 88 (3–4) (2009) 292 – 298. doi:10.1016/j.apcatb.2008.11.011.

[59] M. Nacken, L. Ma, S. Heidenreich, F. Verpoort, G. V. Baron, Development of a catalytic ceramic foam for efficient tar reforming of a catalytic filter for hot gas cleaning of biomass-derived syngas, Applied Catalysis B: Environmental 125 (0) (2012) 111 – 119. doi:10.1016/j.apcatb.2012.05.027.

[60] M. Nacken, L. Ma, S. Heidenreich, G. V. Baron, Catalytic activity in naphthalene reforming of two types of catalytic filters for hot gas cleaning of biomass-derived syngas, Industrial & Engineering Chemistry Research 49 (12) (2010) 5536–5542. doi:10.1021/ie901428b.

[61] M. Nacken, L. Ma, K. Engelen, S. Heidenreich, G. V. Baron, Development of a tar reforming catalyst for integration in a ceramic filter element and use in hot gas cleaning, Industrial & Engineering Chemistry Research 46 (7) (2007) 1945–1951. doi:10.1021/ie060887t.

[62] E. Simeone, E. Holsken, M. Nacken, Study of the behaviour of a catalytic ceramic candle filter in a lab-scale unit at high temperatures, International Journal of Chemical Reactor Engineering 8 (2010) 1–19.

[63] K. Engelen, Y. Zhang, G. Baron, Development of a catalytic candle filter for one-step tar and particle removal in biomass gasification gas, International Journal of Chemical Reactor Engineeringdoi:10.2202/1542-6580.1062.

[64] L. Ma, G. V. Baron, Mixed zirconia-alumina supports for Ni/MgO based catalytic filters for biomass fuel gas cleaning, Powder Technology 180 (1-2) (2008) 21 – 29, papers presented at the 6th International Symposium on Gas Cleaning at High Temperature, Osaka, Japan 20-22 October 2005. doi:10.1016/j.powtec.2007.02.035.

[65] D. J. Draelants, H. Zhao, G. V. Baron, Preparation of catalytic filters by the urea method and its application for benzene cracking in H_2S-containing biomass gasification gas, Industrial & Engineering Chemistry Research 40 (15) (2001) 3309–3316. doi:10.1021/ie0009785.

[66] Y. Zhang, D. J. Draelants, K. Engelen, G. V. Baron, Development of nickel-activated catalytic filters for tar removal in H_2S-containing biomass gasification gas, Journal of Chemical Technology & Biotechnology 78 (2-3) (2003) 265–268. doi:10.1002/jctb.767.

[67] H. Zhao, D. J. Draelants, G. V. Baron, Performance of a nickel-activated candle filter for naphthalene cracking in synthetic biomass gasification gas, Industrial & Engineering Chemistry Research 39 (9) (2000) 3195–3201. doi:10.1021/ie000213x.

[68] K. Engelen, Y. Zhang, D. J. Draelants, G. V. Baron, A novel catalytic filter for tar removal from biomass gasification gas: Improvement of the catalytic activity in presence of H_2S, Chemical Engineering Science

58 (3–6) (2003) 665 – 670, 17th International Symposium of Chemical Reaction Engineering. doi:10.1016/S0009-2509(02)00593-6.

[69] F. Kirnbauer, V. Wilk, H. Hofbauer, Performance improvement of dual fluidized bed gasifiers by temperature reduction: The behavior of tar species in the product gas, Fuel 108 (0) (2013) 534 – 542. doi:10.1016/j.fuel.2012.11.065.

[70] L. Rabou, R. Zwart, B. Vreugdenhil, L. Bos, Tar in biomass producer gas, the Energy Research Centre of the Netherlands (ECN) experience: An enduring challenge, Energy & Fuels 23 (12) (2009) 6189–6198. doi:10.1021/ef9007032.

[71] Z. Abu El-Rub, E. A. Bramer, G. Brem, Review of catalysts for tar elimination in biomass gasification processes, Industrial & Engineering Chemistry Research 43 (22) (2004) 6911–6919. doi:10.1021/ie0498403.

[72] S. Anis, Z. Zainal, Tar reduction in biomass producer gas via mechanical, catalytic and thermal methods: A review, Renewable and Sustainable Energy Reviews 15 (5) (2011) 2355 – 2377. doi:10.1016/j.rser.2011.02.018.

[73] D. Dayton, A review of the literature on catalytic biomass tar destruction, milestone completion report NREL/TP-510-32815, National Renewable Energy Laboratory (2002).

[74] Y. Shen, K. Yoshikawa, Recent progresses in catalytic tar elimination during biomass gasification or pyrolysis - A review, Renewable and Sustainable Energy Reviews 21 (0) (2013) 371 – 392. doi:10.1016/j.rser.2012.12.062.

[75] C. C. Xu, J. Donald, E. Byambajav, Y. Ohtsuka, Recent advances in catalysts for hot-gas removal of tar and NH_3 from biomass gasification, Fuel 89 (8) (2010) 1784 – 1795. doi:10.1016/j.fuel.2010.02.014.

[76] M. M. Yung, W. S. Jablonski, K. A. Magrini-Bair, Review of catalytic conditioning of biomass-derived syngas, Energy & Fuels 23 (4) (2009) 1874–1887. doi:10.1021/ef800830n.

[77] Gasification of biomass is a success, Tech. rep., AAEN A/S, retrieved Dec 7th 2014 (2011).
URL http://bit.ly/1BqIAkm

[78] I. Hannula, K. Lappi, P. Simell, E. Kurkela, P. Luoma, I. Haavisto, High efficiency biomass to power - operation experiences and economical aspects of the novel gasification process, in: 5th European Biomass Conference and Exhibition, from Research to Market Deployment, Berlin, 2007.

[79] S. Toppinen, I. Eilos, P. Simell, E. Kurkela, I. Hiltunen, Method of reforming gasification gas, Patent application US 2013/0058855 A1 (2012).

[80] P. Simell, E. Kurkela, Multiple stage method of reforming a gas containing tarry impurities employing a zirconium-based catalyst, Granted patent US 8100995 B2 (2012).

[81] P. Simell, E. Kurkela, Method for the purification of gasification gas, Granted patent US7455705 B2 (2008).

[82] S. J. Juutilainen, P. A. Simell, A. O. I. Krause, Zirconia: Selective oxidation catalyst for removal of tar and ammonia from biomass gasification gas, Applied Catalysis B: Environmental 62 (1–2) (2006) 86 – 92. doi:10.1016/j.apcatb.2005.05.009.

[83] H. Rönkkönen, E. Rikkinen, J. Linnekoski, P. Simell, M. Reinikainen, O. Krause, Effect of gasification gas components on naphthalene decomposition over ZrO_2, Catalysis Today 147, Supplement (0) (2009) S230 – S236, 3rd International Conference on Structured Catalysts and Reactors, ICOSCAR-3, Ischia, Italy, 27-30 September 2009. doi:10.1016/j.cattod.2009.07.044.

[84] H. Rönkkönen, P. Simell, M. Reinikainen, O. Krause, The effect of sulfur on ZrO_2-based biomass gasification gas clean-up catalysts, Topics in Catalysis 52 (8) (2009) 1070–1078. doi:10.1007/s11244-009-9255-8.

[85] W. Kaltner, Clariant/Süd-Chemie AG, Personal communication (July 2012).

[86] E. Supp, How to produce methanol from coal, Springer-Verlag, Berlin, Heidelberg, 1990.

[87] A. Kohl, R. Nielsen, Gas Purification (5th Edition), Elsevier, 1997.

[88] H. Weiss, Rectisol wash for purification of partial oxidation gases, Gas Sep Pur 2 (4) (1988) 171–176.

[89] Feed purification catalysts, Brochure, Haldor Topsøe A/S (2013). URL http://bit.ly/17MQUqF

[90] P. Sabatier, J. Senderens, Nouvelles syntheses du methane, Acad Sci 314 (1902) 514–6.

[91] J. Kopyscinski, T. J. Schildhauer, S. M. Biollaz, Production of synthetic natural gas (SNG) from coal and dry biomass - A technology review from 1950 to 2009, Fuel 89 (8) (2010) 1763 – 1783.

[92] Practical experience gained during the first twenty years of operation of

the great plains gasification plant and implications for future project, Tech. rep., U.S. Department of Energy (2006).

[93] M. Hedenskog, Gasification of forest residues - IRL in a large demonstration scale, Presentation at IEA biomass gasification workshop in Karlsruhe, Göteborg Energi (2014).
URL http://bit.ly/1OmgA4p

[94] T. Nguyen, L. Wissing, M. Skjøth-Rasmussen, High temperature methanation: Catalyst considerations, Catalysis Today 215 (0) (2013) 233 – 238, Catalysis and synthetic fuels: state of the art and outlook. doi:10.1016/j.cattod.2013.03.035.

[95] From solid fuels to substitute natural gas (SNG) using TREMP, Tech. rep., Haldor Topsøe (2009).

[96] P. Huguen, G. Le Saux, Perspectives for a European standard on biomethane: a Biogasmax proposal, Project supported by the European Commission under RTD contract: 019795 (2010).
URL http://biogasmax.eu/

[97] F. Fischer, H. Tropsch, Uber die herstellung synthetischer olgemische(synthol) durch aufbau aus kohlenoxyd und wasserstoff, Brennst. Chem. 4 (1923) 276–285.

[98] F. Fischer, H. Tropsch, German patent 484337 (1925).

[99] S. Sie, R. Krishna, Fundamentals and selection of advanced Fischer-Tropsch reactors, Applied Catalysis A: General 186 (1–2) (1999) 55–70. doi:10.1016/S0926-860X(99)00164-7.

[100] M. Dry, The Fischer-Tropsch process: 1950-2000, Catalysis Today 71 (3-4) (2002) 227–241, Fischer-Tropsch synthesis on the eve of the XXI Century. doi:10.1016/s0920-5861(01)00453-9.

[101] A. de Klerk, Fischer-Tropsch refining, Wiley-VCH, 2011.

[102] Fischer-Tropsch (ft) synthesis, in: NETL website, Accessed July 9, 2013.
URL 1.usa.gov/12j99WK

[103] S. Sie, M. Senden, H. V. Wechem, Conversion of natural gas to transportation fuels via the shell middle distillate synthesis process (smds), Catalysis Today 8 (3) (1991) 371–394. doi:10.1016/0920-5861(91)80058-H.

[104] R. Anderson, Kinetics and reaction mechanism of the Fischer-Tropsch synthesis, in: Catalysis, ed. P.H. Emmett, 2nd edn., Vol. IV, Reinhold, 1961.

[105] R. Anderson, Catalysts for the Fischer-Tropsch synthesis, vol. 4, Van Nostrand Reinhold, New York, 1956.

[106] J. Eilers, S. Posthuma, S. Sie, The shell middle distillate synthesis process (smds), Catalysis Letters 7 (1-4) (1990) 253–269. doi:10.1007/BF00764507.

[107] H. Schulz, Short history and present trends of Fischer-Tropsch synthesis, Applied Catalysis A: General 186 (1-2) (1999) 3–12. doi:10.1016/S0926-860X(99)00160-X.

[108] R. Sullivan, J. Scott, The development of hydrocracking, in: Heterogeneous Catalysis, 1983, Ch. 25, pp. 293–313. doi:10.1021/bk-1983-0222.ch024.

[109] I. Kobolakis, B. W. Wojciechowski, The catalytic cracking of a Fischer-Tropsch synthesis product, The Canadian Journal of Chemical Engineering 63 (2) (1985) 269–277. doi:10.1002/cjce.5450630212.

[110] N. Hargreaves, velocys, Inc., Personal communication (Feb 2013).

[111] M. Patart, French patent 540 343 (1921).

[112] P. Tijm, F. Waller, D. Brown, Methanol technology developments for the new millennium, Applied Catalysis A: General 221 (1-2) (2001) 275–282, Hoelderich Special Issue. doi:10.1016/S0926-860X(01)00805-5.

[113] M. Appl, Ammonia, Methanol, Hydrogen, Carbon Monoxide - Modern Production Technologies, Nitrogen, 1997.

[114] K. Mansfield, ICI experience in methanol, Nitrogen 221 (27).

[115] J.-P. Lange, Methanol synthesis: a short review of technology improvements, Catalysis Today 64 (1-2) (2001) 3–8.

[116] J. Ott, V. Gronemann, F. Pontzen, E. Fiedler, G. Grossmann, D. Kersebohm, G. Weiss, C. Witte, Methanol, in: Ullmann's Encyclopedia of Industrial Chemistry, Wiley-VCH Verlag GmbH & Co, 2012.

[117] Converter options for methanol synthesis, Nitrogen 210 (1994) 36–44.

[118] J. B. Hansen, P. E. Hojlund Nielsen, Methanol synthesis, in: Handbook of Heterogeneous Catalysis, Wiley-VCH Verlag GmbH & Co. KGaA, 2008. doi:10.1002/9783527610044.hetcat0148.

[119] R. Katofsky, The production of fluid fuels from biomass, CEES Rpt 279, Center for Energy and Environmental Studies, Princeton University (1993).

[120] H. Renon, J. M. Prausnitz, Local compositions in thermodynamic excess functions for liquid mixtures, AIChE Journal 14 (1) (1968) 135–144.

[121] C. D. Chang, A. J. Silvestri, The conversion of methanol and other O-compounds to hydrocarbons over zeolite catalysts, Journal of Catalysis 47 (2) (1977) 249–259.

[122] C. Chang, Hydrocarbons from methanol, Catal.Rev. 25 (1) (1983) 1–118.

[123] Wiley Critical Content - Petroleum Technology, Vol.1-2, John Wiley & Sons, 2007.

[124] S. Yurchak, Development of Mobil's fixed-bed methanol-to-gasoline (MTG) process, Stud.Surf.Sci.Catal. 36 (1988) 251–272.

[125] P. Nielsen, F. Joensen, J. Hansen, E. Sø rensen, J. Madsen, R. Mabrouk, Process for the preparation of hydrocarbons from oxygenates, Patent US 8067474 B2, Haldor Topsøe A/S (2011).

[126] E. Jorn, J. Rostrup-Nielsen, Process for the preparation of hydrocarbons, Patent US 4481305, Haldor Topsøe A/S (1984).

[127] F. Joensen, B. Voss, N. Schiø dt, Process to conversion of oxygenates to gasoline, patent US 8202413 B2, Haldor Topsøe A/S (2012).

[128] F. Joensen, B. Voss, J. Nerlov, Process for converting difficulty convertible oxygenates to gasoline, U.S. patent, Haldor Topsøe A/S (2010).

[129] A. Kam, M. Schreiner, S. Yurchak, Mobil methanol-to-gasoline process, in: Handbook of Synfuels Technology, R.A. Meyers (ed.), McGraw-Hill, 1984.

[130] J. Penick, W. Lee, J. Maziuk, Development of the methanol-to-gasoline process, in: Chemical Reaction Engineering - Plenary Lectures, ACS Symposium Series, Vol. 226, 1983, Ch. 3, pp. 19–48.

[131] J. Topp-Jø rgensen, Topsøe integrated gasoline synthesis - the tigas process, Stud.Surf.Sci.Catal. 36 (1988) 293–305.

[132] G. Soave, Equilibrium constants from a modified Redlich-Kwong equation of state, Chemical Engineering Science 27 (6) (1972) 1197 – 1203.

[133] E. Larson, R. Williams, T. Kreutz, I. Hannula, A. Lanzini, G. Liu, Energy, environmental, and economic analyses of design concepts for the co-production of fuels and chemicals with electricity via co-gasification of coal and biomass, Final report under contract DEFE0005373 to the National Energy Technology Laboratory, US Department of Energy, Princeton University (2012).

[134] E. Barker, J. Begovich, J. Clinton, P. Johnson, Aspen modeling of the tri-state indirect liquefaction process, contract no. W-7405-eng-6, Oak Ridge National Laboratory (1983).

[135] M. Schreiner, Research guidance studies to assess gasoline from coal by methanol-to-gasoline and sasol-type Fischer-Tropsch technologies, Final report to doe under contract no. ef-77-c-01-2447 (1978).

[136] B. Glover, Light olefin technologies, journées Annuelles du Pétrole (2007).

[137] ChemSystems, ethylene PERP 08/09-5, Report Abstract (2009). [link]. URL http://bit.ly/17gcREt

[138] V. Wan, Methanol to olefins, Report no. 261, SRI Consulting (2007).

[139] R. Meyers (Ed.), Handbook of Petroleum Refining Processes (3rd edition), The McGraw-Hill, New York, 2003.

[140] K. Kuechler, J. Lattner, Process for converting oxygenates to olefins with direct product quenching for heat recovery, U.S. patent 6121504, Exxon Chemical Patents Inc (2000).

[141] P. Barger, UOP Advanced MTO Technology - Integration of Methanol-to-Olefins and Olefin Cracking Processes, synFuel2012 Symposium (2012).

[142] R. Kempf, Advances in commercialization of the UOP advanced MTO technology, 2011 Middle East Chemical Week Conference (2011).

[143] J. Q. Chen, A. Bozzano, B. Glover, T. Fuglerud, S. Kvisle, Recent advancements in ethylene and propylene production using the UOP/Hydro MTO process, Catalysis Today 106 (1-4) (2005) 103 – 107, international Conference on Gas-Fuel 05.

[144] D. G. Stewart, J. E. Zimmermann, A. P. Furfaro, B. V. Vora, Apparatus and process for light olefin recovery, U.S. patent 7268265 B1, UOP LLC (2007).

[145] A. Horvath, Carbona/Andritz, Personal communication (2012).

[146] R. Kallio, ÅF-consult, Personal communication (October 2012).

[147] A. Smith, J. Klosek, A review of air separation technologies and their integration with energy conversion processes, Fuel Processing Technology 70 (2) (2001) 115–134. doi:10.1016/S0378-3820(01)00131-X.

[148] S. Rackley, Carbon Capture and Storage, Elsevier, 2010.

[149] L. Bertuccioli, A. Chan, D. Hart, F. Lehner, B. Madden, E. Standen, Study on development of water electrolysis in the EU, Fuel cells and hydrogen joint undertaking (2014).

[150] J. Holladay, J. Hu, D. King, Y. Wang, An overview of hydrogen production technologies, Catalysis Today 139 (4) (2009) 244 – 260, Hydrogen Production - Selected papers from the Hydrogen Production Symposium at the American Chemical Society 234th National Meeting & Exposition, August 19-23, 2007, Boston, MA, USA. doi:10.1016/j.cattod.2008.08.039.

[151] J. Turner, G. Sverdrup, M. K. Mann, P.-C. Maness, B. Kroposki, M. Ghirardi, R. J. Evans, D. Blake, Renewable hydrogen production, International Journal of Energy Research 32 (5) (2008) 379–407. doi:10.1002/er.1372.

[152] J. Ivy, Summary of electrolytic hydrogen production - Milestone completion report, Tech. Rep. NREL/MP-560-36734, National Renewable Energy Laboratory (2004).

[153] D. Keith, M. Ha-Duong, J. Stolaroff, Climate strategy with CO_2 capture from the air, Climatic Change 74 (1-3) (2006) 17–45. doi:10.1007/s10584-005-9026-x.

[154] F. Martin, W. Kubic, Green freedom - A concept for producing carbon-neutral synthetic fuels and chemicals, Overview, Los Alamos National Laboratory (2007).

[155] F. S. Zeman, D. W. Keith, Carbon neutral hydrocarbons, Philosophical Transactions of the Royal Society A: Mathematical, Physical and Engineering Sciences 366 (1882) (2008) 3901–3918.

[156] M. Corbett, S. Salina, Production of synthetic hydrocarbons from air, water and low cost electrical power, U.S. patent 4282187, Grumman Aerospace Corporation (1981).

[157] M. R. Hamilton, H. J. Herzog, J. E. Parsons, Cost and U.S. public policy for new coal power plants with carbon capture and sequestration, Energy Procedia 1 (1) (2009) 4487 – 4494, Proceedings of the 9th International Conference on Greenhouse Gas Control Technologies (GHGT-9), 16–20 November 2008, Washington DC, USA. doi:10.1016/j.egypro.2009.02.266.

[158] E. S. Rubin, C. Chen, A. B. Rao, Cost and performance of fossil fuel power plants with CO_2 capture and storage, Energy Policy 35 (9) (2007) 4444 – 4454. doi:10.1016/j.enpol.2007.03.009.

[159] B. Metz, O. Davidson, H. de Coninck, M. Loos, L. Meyer (Eds.), IPCC Special Report on Carbon Dioxide Capture and Storage. Prepared by Working Group III of the Intergovernmental Panel on Climate Change, Cambridge University Press, Cambridge, United Kingdom and New York, NY, USA, 2005.

[160] C. Song, Global challenges and strategies for control, conversion and

utilization of CO_2 for sustainable development involving energy, catalysis, adsorption and chemical processing, Catalysis Today 115 (1-4) (2006) 2–32.

[161] S. Saeidi, N. A. S. Amin, M. R. Rahimpour, Hydrogenation of CO_2 to value-added products - A review and potential future developments, Journal of CO_2 Utilization 5 (0) (2014) 66 – 81. doi:10.1016/j.jcou.2013.12.005.

[162] T. Inui, T. Takeguchi, Effective conversion of carbon dioxide and hydrogen to hydrocarbons, Catalysis Today 10 (1) (1991) 95 – 106. doi:10.1016/0920-5861(91)80077-M.

[163] T. Inui, K. Kitagawa, T. Takeguchi, T. Hagiwara, Y. Makino, Hydrogenation of carbon dioxide to C_1-C_7 hydrocarbons via methanol on composite catalysts, Applied Catalysis A: General 94 (1) (1993) 31 – 44. doi:10.1016/0926-860X(93)80043-P.

[164] M. Sahibzada, D. Chadwick, I. Metcalfe, Hydrogenation of carbon dioxide to methanol over palladium-promoted $Cu/ZnO/A1_2O_3$ catalysts, Catalysis Today 29 (1–4) (1996) 367 – 372, second Japan-EC Joint Workshop on the Frontiers of Catalytic Science and Technology for Energy, Environment and Risk Prevention. doi:10.1016/0920-5861(95)00306-1.

[165] K. Ushikoshi, K. Moria, T. Watanabe, M. Takeuchi, M. Saito, A 50 kg/day class test plant for methanol synthesis from CO_2 and H_2, in: T. Inui, M. Anpo, K. Izui, S. Yanagida, T. Yamaguchi (Eds.), Advances in Chemical Conversions for Mitigating Carbon Dioxide Proceedings of the Fourth International Conference on Carbon Dioxide Utilization, Vol. 114 of Studies in Surface Science and Catalysis, Elsevier, 1998, pp. 357 – 362. doi:10.1016/S0167-2991(98)80770-2.

[166] M. Saito, R&D activities in Japan on methanol synthesis from CO_2 and H_2, Catalysis Surveys from Japan 2 (2) (1998) 175–184.

[167] T. Inui, Highly effective conversion of carbon dioxide to valuable compounds on composite catalysts, Catalysis Today 29 (1–4) (1996) 329 – 337, Second Japan-EC Joint Workshop on the Frontiers of Catalytic Science and Technology for Energy, Environment and Risk Prevention. doi:10.1016/0920-5861(95)00300-2.

[168] Y. Amenomiya, Methanol synthesis from CO_2 + H_2 II. Copper-based binary and ternary catalysts, Applied Catalysis 30 (1) (1987) 57 – 68. doi:10.1016/S0166-9834(00)81011-8.

[169] J. Graciani, K. Mudiyanselage, F. Xu, A. E. Baber, J. Evans, S. D. Senanayake, D. J. Stacchiola, P. Liu, J. Hrbek, J. F. Sanz, J. A. Rodriguez, Highly active copper-ceria and copper-ceria-titania catalysts

for methanol synthesis from CO_2, Science 345 (6196) (2014) 546–550. doi:10.1126/science.1253057.

[170] I. Hannula, E. Kurkela, A semi-empirical model for pressurised air-blown fluidised-bed gasification of biomass, Bioresource Technology 101 (12).

[171] I. Hannula, E. Kurkela, A parametric modelling study for pressurised steam/O_2-blown fluidised-bed gasification of wood with catalytic reforming, Biomass and Bioenergy 38 (0) (2012) 58–67, Overcoming Barriers to Bioenergy: Outcomes of the Bioenergy Network of Excellence 2003-2009. doi:10.1016/j.biombioe.2011.02.045.

[172] G. Liu, E. D. Larson, R. H. Williams, T. G. Kreutz, X. Guo, Supporting information for making Fischer-Tropsch fuels and electricity from coal and biomass: Performance and cost analysis, Energy & Fuels 25 (1). doi:10.1021/ef101184e.

[173] P. Chiesa, S. Consonni, T. Kreutz, R. Williams, Co-production of hydrogen, electricity and CO_2 from coal with commercially ready technology. Part A: Performance and emissions, International Journal of Hydrogen Energy 30 (7) (2005) 747–767. doi:10.1016/j.ijhydene.2004.08.002.

[174] A. Glassman, Users manual for updated computer code for axial-flow compressor conceptual design, Tech. rep., University of Toledo, Toledo, Ohio (1992).

[175] J. Black, Cost and performance baseline for fossil energy plants volume 1: Bituminous coal and natural gas to electricity, Revision 2a, September 2013 DOE/NETL-2010/1397, U.S. National Energy Technology Laboratory (2007).

[176] T. Kreutz, R. Williams, S. Consonni, P. Chiesa, Co-production of hydrogen, electricity and CO_2 from coal with commercially ready technology. Part B: Economic analysis, International Journal of Hydrogen Energy 30 (7) (2005) 769 – 784. doi:10.1016/j.ijhydene.2004.08.001.

[177] P. Floch, S. Gabriel, C. Mansilla, F. Werkoff, On the production of hydrogen via alkaline electrolysis during off-peak periods, International Journal of Hydrogen Energy 32 (18) (2007) 4641 – 4647. doi:10.1016/j.ijhydene.2007.07.033.

[178] T. Ekbom, M. Lindblom, N. Berglin, P. Ahlvik, Technical and commercial feasibility study of black liquor gasification with methanol/DME production as motor fuels for automotive uses - BLGMF, Tech. Rep. Contract No. 4.1030/Z/01-087/2001, Nykomb Synergetics (2003).

[179] E. Merrow, K. Phillips, C. Myers, Understanding cost growth and

performance shortfalls in pioneer process plants, Tech. Rep. RAND/R-2569-DOE, RAND Corporation, Santa Monica, USA (1981).

[180] Kaukolämpötilasto, Statistics in Finnish, Energiateollisuus (2012).
URL http://bit.ly/1qjFidl

[181] German biofuel firm Choren declares insolvency, Reuters, July 8, 2011.
URL http://bit.ly/1nZYaus

[182] Range Fuels cellulosic ethanol plant fails, U.S. pulls plug, Bloomberg, December 3, 2011.
URL bloom.bg/1lp8eJB

[183] Report from the bio-DME plant in Piteå, ChemrecNews, May, 2012.
URL http://bit.ly/1u9aIlN

[184] Haldor Topsøe and partners produce biobased gasoline, Biomass magazine, June 26, 2013.
URL http://bit.ly/1mUBv0U

[185] M. Steinberg, Electrolytic synthesis of methanol from CO_2, U.S. patent 3959094, United States Energy Research and Development Administration (1976).

[186] J. Lewis, A. Martin, Method for obtaining carbon dioxide from the atmosphere and for production of fuels, U.S. patent 4140602, Texas Gas Transmission Corporation (1979).

[187] M. Steinberg, Synthetic carbonaceous fuels and feedstocks, U.S. patent 4197421, United States Energy Research and Development Administration (1980).

[188] R. Kieffer, M. Fujiwara, L. Udron, Y. Souma, Hydrogenation of CO and CO_2 toward methanol, alcohols and hydrocarbons on promoted copper-rare earth oxides catalysts, Catalysis Today 36 (1) (1997) 15 – 24, copper, Silver and Gold in Catalysis. doi:10.1016/S0920-5861(96)00191-5.

[189] N. Ouellette, H.-H. Rogner, D. Scott, Hydrogen from remote excess hydroelectricity. part ii: Hydrogen peroxide or biomethanol, International Journal of Hydrogen Energy 20 (11) (1995) 873 – 880. doi:10.1016/0360-3199(95)00018-9.

[190] P. G. Cifre, O. Badr, Renewable hydrogen utilisation for the production of methanol, Energy Conversion and Management 48 (2) (2007) 519 – 527. doi:10.1016/j.enconman.2006.06.011.

[191] Energy prices and costs report, European Commission staff working document (2014). [link].
URL http://bit.ly/1tANeta

[192] ICIS, China develops coal-to-olefins projects, which could lead to ethylene self-sufficiency (2012).
URL http://bit.ly/MgIGE6

[193] T. Ren, M. Patel, K. Blok, Olefins from conventional and heavy feedstocks: Energy use in steam cracking and alternative processes, Energy 31 (4) (2006) 425 – 451.

[194] Platts, Biofuelscan 2 (137).

[195] IEA, "Scope and methodology", in World Energy Outlook 2013, IEA/OECD, Paris, 2013. doi:10.1787/weo-2013-en.

[196] J. Ott, V. Gronemann, F. Pontzen, E. Fiedler, G. Grossmann, D. Kersebohm, G. Weiss, C. Witte, Methanol, in: Ullmann's Encyclopedia of Industrial Chemistry, Wiley-VCH Verlag GmbH & Co, 2012.

[197] P. Biedermann, T. Grube, B. Hoehlein, Methanol as an energy carrier, Schriften des Forschungszentrums Julich 55 (2003).

[198] C. Greig, A. Garnett, J. Oesch, S. Smart, Guidelines for scoping and estimating early mover ccs projects, Milestone 5, final report, The University of Queensland (2014).

[199] I. Hannula, E. Kurkela, Liquid transportation fuels via large-scale fluidised-bed gasification of lignocellulosic biomass, VTT Technology 91, Technical Research Centre of Finland (2013).

[200] I. Hannula, Doubling of synthetic biofuel production via hydrogen from renewable energy sources, A seminar presentation at Chalmers in Sweden, VTT (2014).
URL http://bit.ly/1xOAyla

[201] B. Hyde, Light olefins market review, Foro Pemex Petroquimica (2012).

Paper I

Ilkka Hannula, Esa Kurkela

A semi-empirical model for pressurised air-blown fluidised-bed gasification of biomass

Bioresource Technology, 2010
Volume 101, Issue 12, Pages 4608-4615.

Bioresource Technology 101 (2010) 4608–4615

Contents lists available at ScienceDirect

Bioresource Technology

journal homepage: www.elsevier.com/locate/biortech

A semi-empirical model for pressurised air-blown fluidised-bed gasification of biomass

Ilkka Hannula *, Esa Kurkela

Technical Research Centre of Finland, P.O. Box 1000, FI-02044 VTT, Finland

ARTICLE INFO

Article history:
Received 28 September 2009
Received in revised form 18 January 2010
Accepted 19 January 2010
Available online 11 February 2010

Keywords:
Gasification
Biomass
Fluidised-bed
Model
Aspen Plus

ABSTRACT

A process model for pressurised fluidised-bed gasification of biomass was developed using Aspen Plus simulation software. Eight main blocks were used to model the fluidised-bed gasifier, complemented with FORTRAN subroutines nested in the programme to simulate hydrocarbon and NH_3 formation as well as carbon conversion. The model was validated with experimental data derived from a PDU-scale test rig operated with various types of biomass. The model was shown to be suitable for simulating the gasification of pine sawdust, pine and eucalyptus chips as well as forest residues, but not for pine bark or wheat straw.

1. Introduction

1.1. Biomass gasification

Global climate change together with increasing energy prices and depleting fossil resources have provoked major interest towards renewable forms of energy and resources. Gasification of biomass offers an efficient way to utilise renewable carbonaceous feedstocks and has significant commercial and environmental potential in the production of green chemicals, synthetic fuels and electricity.

Gasification produces a gas mixture rich in carbon monoxide and hydrogen. Other major compounds include carbon dioxide, nitrogen, water, methane and a rich spectrum of hydrocarbons. A general objective of gasification is to try to maximise the yields of gaseous products and minimise the amounts of condensable hydrocarbons and unreacted char. Exact composition of product gas depends on the type of process feeds, their feed ratios, process parameters and the type of gasification reactor used.

In contrast to coal gasification, where char gasification reactions contribute most to the overall yield, in biomass gasification the devolatilisation stage and the secondary reactions of primary pyrolysis product play the major role (Kurkela, 1996).

1.2. Modelling of biomass gasification

The objective of process modelling is to construct a mathematical description of a process that can be used to predict reactor temperature and outlet concentrations from inlet flows and operating conditions. A model that fits well to the experimental data can help to reveal major trends in a multivariable system and be a great comfort when an engineer is faced with scaling-up a reactor to produce the full-scale design (Rose, 1982). A suitable model also permits more efficient control of the reactor and offers a safe way to simulate reactor behaviour in continuous and transient conditions (Buekens and Schouters, 1984).

Mathematical models of fluidised-bed gasifiers are usually based either on kinetic rates or thermodynamic equilibrium.

Models based on rates attempt to predict product gas concentrations by combining a hydrodynamic model of the fluidised-bed with appropriate kinetic schemes for the heterogeneous and homogeneous processes occurring inside the gasifier (Gururajan et al., 1992). However, as a large number of dynamic parameters involved in fluidised-bed gasification are presently unknown and very difficult to measure, estimation of product gas composition through kinetic models often becomes exceedingly difficult (Kovacik et al., 1990).

A model can also be constructed by applying the principles of chemical equilibrium. In this approach, the complex kinetics can be disregarded by assuming that gasification reactions occur fast enough for them to reach equilibrium. However, it has been widely reported that for fluidised-bed gasifiers, product gas compositions

* Corresponding author. Tel.: +358 20 722 6370; fax: +358 20 722 7048.
E-mail address: ilkka.hannula@vtt.fi (I. Hannula).

0960-8524/$ - see front matter © 2010 Elsevier Ltd. All rights reserved.
doi:10.1016/j.biortech.2010.01.072

are not in equilibrium, possibly due to the slow kinetics involved (Schuster et al., 2001). Kilpinen et al. (1991) has shown that for CO, CO_2, H_2, and H_2O the equilibrium seems to be established under certain assumptions, whereas the amounts of solid carbon, methane, HCN and NH_3 are underpredicted. In this work, experimental data is used to take account of these above mentioned conversions, which would otherwise be estimated wrong by equilibrium approach.

Despite their limitations, equilibrium models have been widely published in the literature. Gururajan et al. (1992) have critically examined several simulation models proposed for fluidised-bed gasification of coal. The work done in fluidised-bed gasification of biomass has been more limited and described in some detail by Schuster et al. (2001).

De Kam et al. (2009) have recently modelled gasification with an Aspen Plus RGibbs reactor by separately specifying a set of reactions with temperature approach to equilibrium, and by fixing the production of certain species based on the amount of fuel being used. However, data about validation results was not reported.

Doherty et al. (2009) divided the gasifier into six separate blocks to cater for drying, pyrolysis, partial oxidation and gasification reactions. The outcomes of these processes were then fed to equilibrium reactor where final composition of the syngas was formed under restricted conditions. The final block was used to separate and recycle solids entrained in the gas, thus simulating a CFB cyclone. The validation of the model was performed for three test runs and the results were reported to be in good agreement with experimental data, with the exception of overpredicted methane. Heavier hydrocarbons were not considered in the model.

The approach of Nikoo and Mahinpey (2008) was to divide the gasifier to decomposition of the feed, volatile reactions, char gasification and gas–solid separation. In addition, the effect of hydrodynamic parameters and reaction kinetics of biomass gasification in fluidised-beds were simulated with FORTRAN codes. This slightly more complex approach did not seem to result in much improved predictions, probably due to the inaccurate methane estimations and the absence of higher hydrocarbons in the model.

2. Methods

2.1. Experimental work

In this work, a model for pressurised air-blown fluidised-bed gasifier using biomass as a feedstock is developed using Aspen Plus simulation software.

The model is fitted with experimental data originally derived from fluidised-bed air gasification studies with pine sawdust in 1991–1992. The testing was conducted in a VTT's PDU-scale test rig as a part of the National Combustion Programme LIEKKI, and was aimed to support the development of simplified integrated gasification combined-cycle process. The results of these sawdust gasification experiments are published and summarised by Kurkela et al. (1993). A brief description of the process and the gasification experiments used to fit the parameters of the model is given in the following paragraphs.

2.2. Description of the experimental equipment and arrangement

The heart of the pressurised fluidised-bed gasification test rig is a refractory-lined reactor with a bed diameter of 15 cm and freeboard diameter of 25 cm. The height from the air distributor to the gas outlet pipe is 4.2 m. Typical gas-phase residence times range from 5 to 8 s depending on the fluidising velocity.

Primary air and a small amount of steam are introduced into the reactor through a multiorifice plate distributor. Two different distributor plates can be used depending on the required range of fluidising air flow rate. The first plate is a 10 mm thick slightly conical plate with 21 mm holes and an open area of 0.62% of the reactor cross-sectional area. The other air distributor is a 10 mm thick horizontal plate with 2 mm holes and a total open area of 1.7% of the reactor area. Bottom ash is removed through a 38 mm (id) pipe located in the centre of the distributor plate.

Secondary air can be introduced above the fluidised-bed through two pipes which both have eight air nozzles. The heights from the air distributor to the secondary air injection ports are

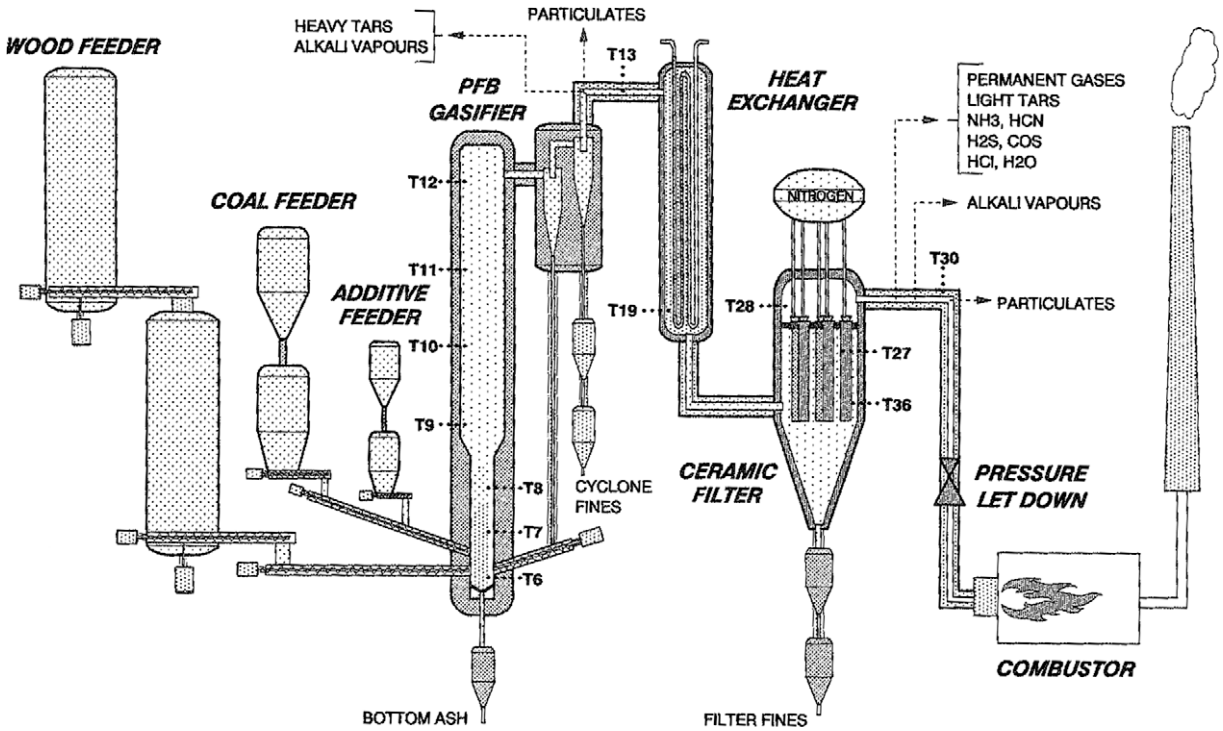

Fig. 1. Schematic diagram of the pressurised fluidised-bed gasification test rig (Kurkela et al., 1993).

1.5 and 1.9 m. The locations of the measuring and sampling points are shown in Fig. 1. The test facility is equipped with a wide variety of process measurements, which are collected to a data logger and processed by a microcomputer. The product gas outlet temperature used in the model was measured with thermocouple t_{13} also visible in Fig. 1.

2.3. Description of the data used in parameter fitting

The data used to fit the parameters of the gasification model is described briefly in this paragraph. Most of the data is from two 1-week test runs, dedicated to sawdust gasification.

The measurements with pure saw dust were carried out in 10 different operating variable sets. The length of different set points varied from 2 to 9 h. During the set point periods the feed rates of fuel, air and steam were kept as constant as possible. At some set points, however, changes in fuel quality had to be compensated for by small (±5%) changes in feed rate. All process data were recorded by a computer at 3–5 min intervals, and all discharged cyclone and filter fines as well as bottom ashes were collected, weighed and samples at the set points. The fuel was also weighed and sampled before charging it into the feeding system.

After the test run a material balance was calculated for each of the set points, based on the average values of the data. Hydrogen and nitrogen balances were used to calculate the water vapour content of gas and raw gas flow rate, which are difficult to measure with the same accuracy as the other measurements. The closure of carbon and oxygen balances (out/in) at qualified set points were within 5%, but the ash balance was worse, since the ash content of sawdust was very low and part of the fine filter dust was lost in the depressurisation of the dust removal hopper of the ceramic filter unit.

A summary of the key operational parameters at different set points is shown in Table 1. Set points 1–7 were run with sawdust A (SD A) while sawdust B (SD B) was used at set points 8–10. The ultimate and proximate analyses of the feedstock are presented in Table 2.

The main variable in the tests was gasification temperature, controlled by changes in air-to-fuel ratio.

2.4. The utilisation of experimental data in the model

The limitations of equilibrium approach, as summarised in Section 1.2, were dealt in this work by fitting a selection of parameters to experimental data. The intention was to construct a simple and generic model for gasification of biomass that could be fitted to match a specific gasification reactor using easily measurable empiric correlations. For this reason the incorporation of such parameters as feedstock particle size and reactor geometry were decided to be ignored, as their inclusion would lead to a need of a more complex model, still not necessarily able to generate more accurate predictions. The selection of the approach stemmed from the lack of complete understanding about the kinetic and hydrodynamic phenomena pertaining to fluidised-bed gasification of biomass as discussed in Section 1.2.

Table 2
Proximate and ultimate analyses of the feedstock used in model fitting (Kurkela et al., 1993).

	Sawdust A	Sawdust B
Proximate analysis (wt.%) d.b.:		
Volatile matter	83.0	82.8–83.1
Fixed carbon	16.7–16.8	16.8–17.0
Ash	0.20–0.34	0.08–0.23
Ultimate analysis (wt.%) d.b.:		
C	50.2–50.4	51.0–51.4
H	6.00–6.10	5.99–6.20
N	0.08–0.11	0.08–0.09
S	n.d.	<0.01
O	43.2–43.5	42.1–42.8
Ash	0.20–0.34	0.08–0.23
Moisture content (wt.%)	4.0–11.3	6.4–15.5
LHV (dry) (MJ/kg)	n.d.	19.03–19.07

Although the experimental data used in this work has been published already a while ago, to our knowledge, it has not yet been used for validation of a gasification model based on thermodynamical equilibrium approach. However, a model for bubbling fluidised-bed, incorporating bed and freeboard hydrodynamics, fuel drying, devolatilisation and chemical reaction kinetics has been published by Hamel and Krumm (2001) and validated with the same data from Kurkela et al. (1993) with seemingly good, although narrowly reported results. The aim of this work was to develop a considerably simpler model, with the ability to yield equally good results.

2.5. Process scheme

Eight main blocks were used to model the fluidised-bed gasifier, complemented with FORTRAN subroutines nested in the programme to simulate carbon conversion, as well as NH_3 and hydrocarbon formation. All calculation blocks were thermally integrated in order to represent a single gasification reactor.

The core of the model is the equilibrium reactor block (RGibbs), where major part of the feed is converted to gasification products according to equilibrium approach. Almost all the other blocks included in the model are used to cater for the non-equilibrium behaviour perceived in real life gasifiers. These phenomena consist of incomplete carbon conversion as well as formation of hydrocarbons and nitrogen species. The division of the model to separate blocks could also have been executed differently, as the model examples of Section 1.2 imply. However, it was considered more rational to handle each non-equilibrium phenomenon in a separate block, rather than treating them in a one RGibbs block by restricting the equilibrium of the reactor.

The main structure of the model is illustrated schematically in Fig. 2. As a first step of the simulation, biomass is decomposed to

Table 1
Key parameters related to the experimental data used in model fitting.

Set point	1	2	3	4	5	6	7	8	9	10
Feed stock	SDA	SDA	SDA	SDA	SDA	SDA	SDA	SDB	SDB	SDB
Fuel moisture (wt.%)	11.3	5.8	10.4	4.0	4.0	4.0	4.0	6.7	15.3	6.9
Pressure (bar)	4	4	4	4	4	4	4	5	5	5
Air ratio	0.28	0.39	0.43	0.32	0.30	0.34	0.31	0.31	0.39	0.39
Gasifier outlet temperature (°C)	882	856	955	901	881	941	893	868	919	864
Steam-to-fuel ratio (kg/kg-daf)	0.08	0.28	0.23	0.17	0.16	0.17	0.16	0.15	0.20	0.18
Nitrogen to steam ratio (kg/kg)	0.60	0.45	1.05	0.95	0.90	0.80	0.70	0.85	1.25	0.85

daf = dry, ash free.

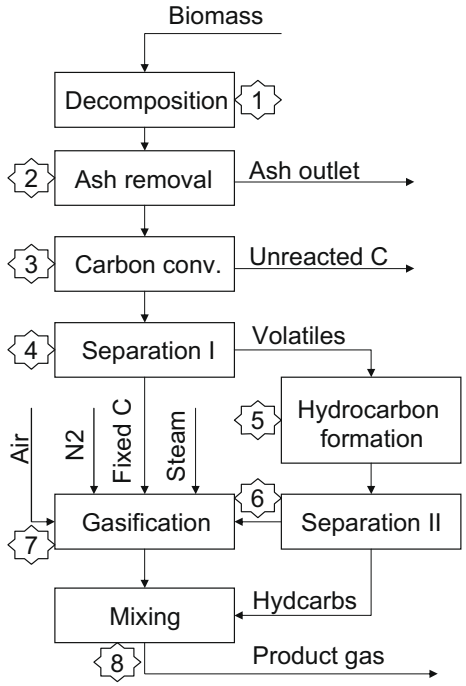

Fig. 2. A schematic illustration of the gasification model.

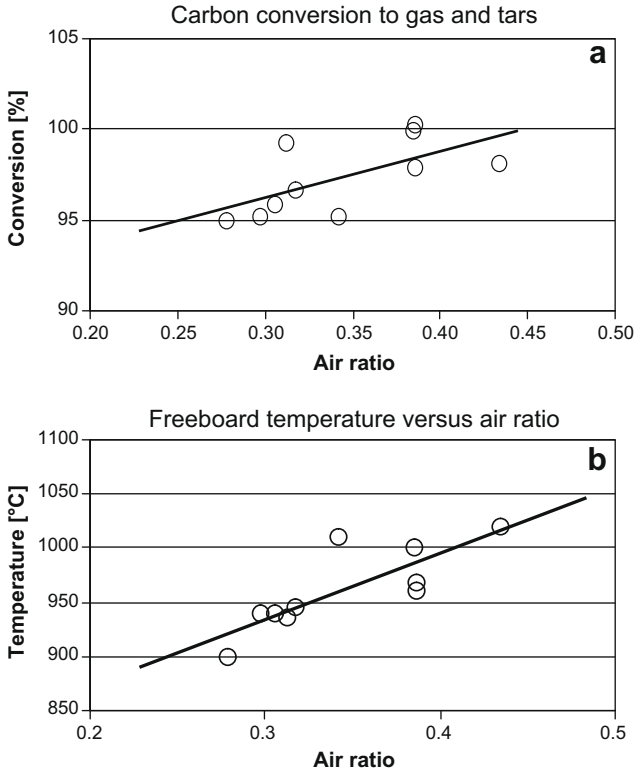

Fig. 3. (a and b) Perceived correlations of freeboard temperature and carbon conversion as a function of air ratio (Kurkela et al., 1993).

hydrogen, oxygen, nitrogen, carbon, sulphur and ash, based on the ultimate analysis of the feedstock. Then all of the ash is separated to the ash outlet, followed by the modelling of carbon conversion by extracting a certain amount of elemental carbon to an outlet stream. As the hydrocarbons are largely formed from the volatile components of the biomass, the feed is first divided into two separate streams of volatiles and fixed carbon. The volatiles are then led to a simulation block where parts of the stream are converted into hydrocarbons according to experimental data. The stream of fixed carbon is mixed with air, steam and unreacted volatiles and converted to gasification products according to thermodynamic equilibrium. As the last step of the simulation, hydrocarbons and gasification products are mixed together to form the final product. More detailed description of the main unit operations of the simulation is given in the following paragraphs.

2.5.1. Biomass decomposition

A yield reactor (Ryield) was used to simulate the decomposition of the feed. In block number 1, biomass was converted to hydrogen, oxygen, nitrogen, carbon, sulphur and ash by specifying the yield composition based on ultimate analysis of the feedstock.

2.5.2. Ash removal

In the block number 2, ash removal was simulated with component separator by removing all the feedstock ash to the ash outlet.

2.5.3. Carbon conversion

According to equilibrium, all of the feedstock's carbon should exist in gas-phase under typical gasification conditions. However, a significant amount of carbon is usually found from the bottom and fly ash of an air-blown fluidised-bed reactor. To overcome this discrepancy, a FORTRAN equation was created to represent observed correlation between carbon conversion and gasification air ratio (see Fig. 3a). The correlation (see Table 3) was nested in block number 3 and used to calculate the amount of elemental carbon that has to be extracted from the feed to simulate the incomplete conversion. The air ratio (E) and carbon conversion (η_C) were defined, respectively, as

$$E = \frac{m_O/m_B}{m_{St.O}/m_B}, \quad (1)$$

where m_O is the weight of used oxygen, m_B – weight of biomass, $m_{St.O}$ – weight of stoichiometric oxygen.

$$\eta_C = \frac{C_{gas} + C_{tar}}{C_{fuel}}, \quad (2)$$

where C_{gas} is the carbon output in dry gas (g/s), C_{tar} – carbon output in tar (g/s), C_{fuel} – carbon input in fuel (g/s).

2.5.4. Separation I

In block number 4, the feed was separated to streams of fixed carbon and volatiles according to proximate feedstock analysis. In reality the yields of char and volatiles depend also from particle size, heating rate and other parameters. However, these factors were not considered in the model.

2.5.5. Hydrocarbon formation

As already mentioned, the equilibrium approach also underpredicts the amounts of hydrocarbon and nitrogen components. To

Table 3
Empirical correlations used in the model to simulate carbon, hydrocarbon and NH_3 conversions.

Carbon conversion	$25.7 \times E + 88.5$
NH_3 conversion	$0.819–1.154 \times E$
Hydrocarbon conversions	
CH_4	$0.5166–0.8621 \times E$
C_2H_2	0.0046
C_2H_4	$0.138–0.311 \times E$
C_2H_6	$0.02–0.038 \times E$

E = air ratio.

tackle this shortage in the approach, a FORTRAN subroutine was nested in block 5 (Rstoic) to calculate the conversions based on experimental data illustrated in Fig. 4a–d. CH_4, C_2H_2, C_2H_4, C_2H_6 and NH_3 were chosen to be included in the model as they represent the most voluminous hydrocarbon and nitrogen compounds in biomass-derived product gas. These experimentally observed correlations (see Table 3) were used in the model to calculate the fractional conversion of elemental carbon in the stream 'Volatiles' separately for each component.

All the curves were drawn as a function of air ratio, as Kurkela et al. (1993) have shown that it correlates well with the average freeboard temperature of a fluidised-bed gasifier (see Fig. 3b) and as according to Bruinsma and Moulijn (1988) as well as Simell et al. (1992) the total concentration of tar from fluidised-bed gasifier depends mainly on gasification temperature and the type of feedstock.

2.5.6. Separation II

In the block number 6, the hydrocarbons were separated from the stream to a bypass using an Aspen Plus component separator and the remainder of the stream was directed into the gasification block. This was necessary to prevent the NH_3 and hydrocarbons from decomposing in block 7.

2.5.7. Gasification

In the block 7, a Gibbs reactor (Rgibbs) was used to mix the feed with streams of air, steam, purge nitrogen and remaining volatiles from block 5, and to convert them to equilibrium products. Nitrogen was added to simulate purge nitrogen, originally used in the test rig to seal off leakages and to keep the measurement equipment operational.

2.5.8. Mixing

In the block number 8, a stream mixer was used to connect the bypass stream with products from block 7.

2.5.9. Heat integration

All the heat streams related to endo- and exothermic reactions taking place in the process were connected together and summed up by a calculator block (not shown in Fig. 2) representing the heat loss from the system to the surroundings.

2.6. Model description

SOLIDS and RK-SOAVE were chosen as base and property methods in Aspen Plus, based on the instructions of Aspen Plus User guide and VTT's in-house experiences about gasification modelling.

The following substances were considered as main components in the product gas: CO, H_2, CO_2, N_2, H_2O, CH_4, C_2H_2, C_2H_4, C_2H_6, NH_3 and O_2.

When gasifier temperature was fixed as an input, energy balance was used to calculate the heat loss and when heat loss was assumed, energy balance was used to predict the gasification temperature.

Inlet temperatures for steam, air and nitrogen were set to 200 °C and for biomass to 30 °C.

3. Results and discussion

3.1. Validation of the model

The data used for validation of the model is based on pressurised fluidised-bed air gasification of pine sawdust, pine bark, forest residues, wheat straw, and eucalyptus (see Table 4 for feedstock analyses). The reactor used in the studies was the PDU-scale gasification test rig presented in Section 2.2.

The results of these studies are published in detail by Kurkela et al. (1995). For validation purposes, six different operating variable sets, called set points, were chosen from five test campaigns conducted in 1993–94 as a part of the APAS Clean Coal Technology Programme.

First the values of biomass feed, air ratio, steam-to-fuel ratio, outlet temperature of the gasifier and process pressure were set in the model to correspond with the values of validation data as listed in Table 5. The model predictions for the product gas composition and carbon conversion were then compared with experimentally acquired values at the same set point conditions and are illustrated in Fig. 5a–d.

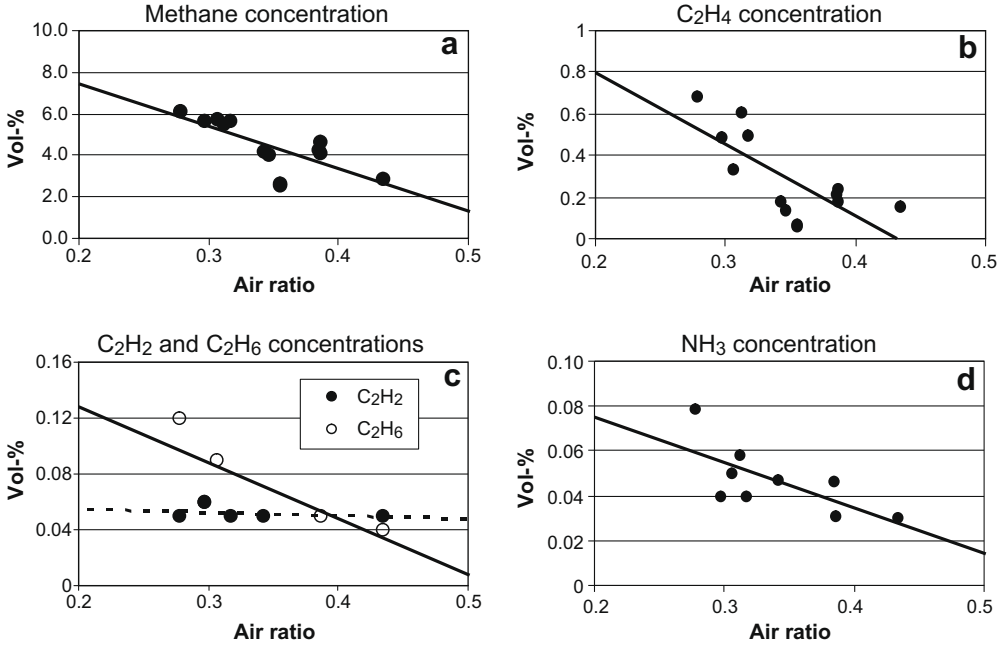

Fig. 4. (a–d) Hydrocarbon and NH_3 conversions as a function of the air ratio (Kurkela et al., 1993).

Table 4
Proximate and ultimate analyses of the feedstock used in the model validation (Kurkela et al., 1995).

	Pine sawdust	Pine chips	Forest residues	Pine bark	Eucalyptus chips	Wheat straw
Proximate analysis (wt.%) d.b.:						
Fixed carbon	16.8	18	21.2	26.7	18.8	18.2
Volatile matter	83.1	81.5	76.7	71.8	80.4	75.8
Ash	0.08	0.43	2.1	1.6	0.8	6.1
Ultimate analysis (wt.%) d.b.:						
C	51	50.5	52.3	53.9	51.2	46.1
H	6	6.1	6	5.8	6	5.6
N	0.08	0.17	0.56	0.35	0.17	0.52
S	0	0.03	0.04	0.03	0.02	0.08
O	42.8	42.8	39	38.4	41.8	41.6
Ash	0.08	0.43	2.1	1.6	0.8	6.1
Moisture content (wt.%)	6.1–16	6.3–6.7	9.2–12	5.6–6.7	4.3	6.1

Table 5
Process parameters related to the set points in the validation data.

Set point	1	2	3	4	5	6
Feedstock	Pine sawdust	Pine chips	Forest residues	Pine bark	Eucalyptus chips	Wheat straw
Pressure (bar)	5	5	5	5	5	5
Air-to-fuel ratio (kg/kg-daf)	2.33	1.65	1.97	2.27	1.90	1.37
Gasifier outlet temperature (°C)	930	905	890	980	935	835
Steam-to-fuel ratio (kg/kg-daf)	0.20	0.09	0.14	0.12	0.14	0.31

daf = dry, ash free.

The predicted and measured concentrations of the main components are summarised in Fig. 5e and f with lines demonstrating +10% and −10% deviations between the values.

Judging from the results, a fairly good agreement between experimental data and model predictions has been achieved for the main gas components. The average relative error for components H_2, CO, CO_2, and CH_4 was 14%, while the magnitude of experimental error in the data is expected to be around 5%.

Fig. 6 illustrates model estimations for carbon conversion along with the experimentally acquired results. It can be noticed, that although the model is able to produce relatively good product

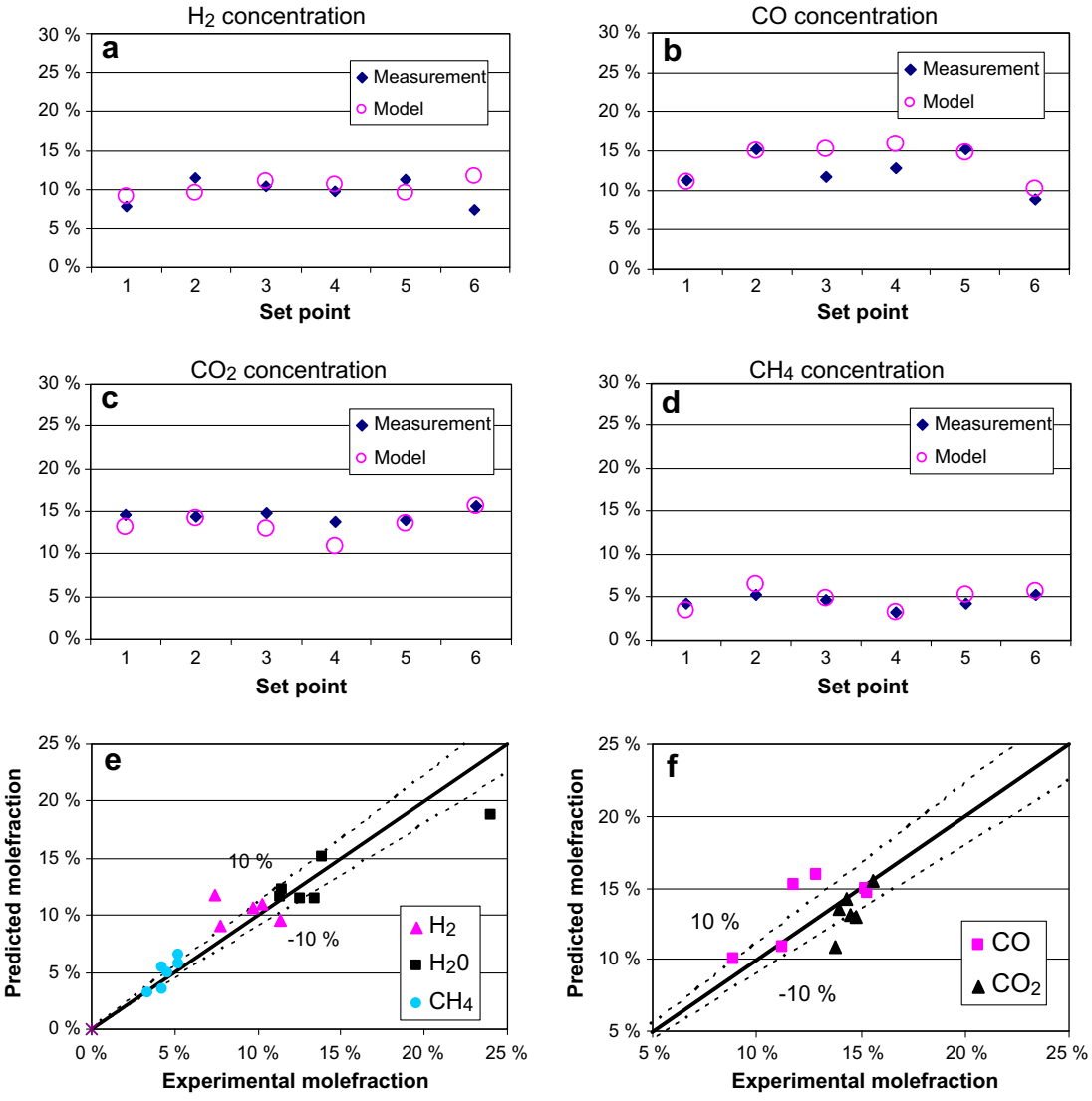

Fig. 5. (a–f) Comparison of measured values with values predicted by the model for CO, H_2, CO_2 and CH_4 concentrations in wet gas.

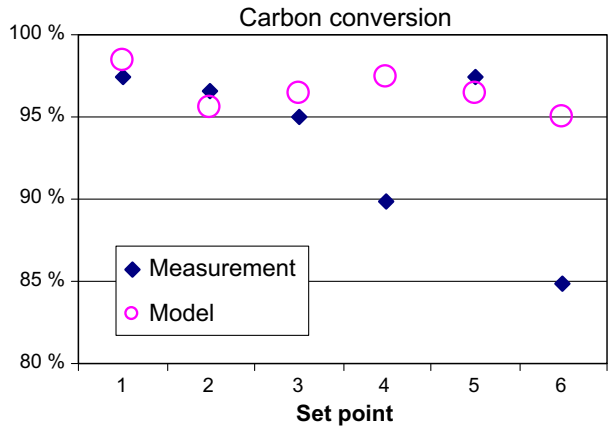

Fig. 6. Comparison of measured values with values predicted by the model for carbon conversion.

gas composition estimates for all set points, it manages to predict carbon conversion well for only four fuel types out of six used in the validation. Possible reasons for this outcome are discussed in Section 3.2.

3.2. The range of validity

A semi-empirical model can be considered valid only within the range of the data that was used to fit the model parameters. To assess this range of validity, the limiting values of the experimental data that was used in the parameter fitting, are listed in Table 6. A good prediction capability can be expected only within these values.

The gasifier type should also be considered when estimating the suitability of this model for process simulation purposes. It is emphasised that only gasifiers that share a similar type of geometry with the PDU-gasifier described in Section 2.2 should be simulated with this model.

The carbon conversion of a gasifier is known to be closely related with the gasification rate of the fuel, i.e., its reactivity. The set point 4 was run with pine bark and set point 6 with wheat straw. The poor prediction capability of the model with these fuels seems to suggest that the reactivities of pine bark and wheat straw differ much from the reactivity of pine sawdust, used in the parameter fitting. For the same reason, the reactivities of pine sawdust, pine chips, forest residues and eucalyptus chips could be expected to be quite similar to each other.

There are some experimental results that seem to support this argument. For example Moilanen and Kurkela (1995) have studied carbon conversions for different types of fuels in a fluidised-bed gasifier and have found great differences in their gasification behaviour. Especially bark and straw were found difficult to be completely gasified.

Moilanen (2006) measured the instantaneous reaction rate of several fuels at 95% fuel conversion and with 1 bar steam and found the reaction rates to be 25%/min for pine sawdust and 30%/min for forest residue (pine), whereas the rates were 17%/min for wheat straw and 13%/min for pine bark. These numbers seem to imply that the differences in the accuracy of the model predictions can be explained, to some extent, by differences in reaction rates between the fuel types.

Thus, it can be concluded that the gasification model presented here, should not be used for fuels whose gasification reactivity differs greatly from the reactivity of pine sawdust.

Table 6
Assessment of the model's validity range.

Type of feedstock	Sawdust
Feedstock moisture content (wt.%)	4.0–15.3
Gasification temperature (°C)	856–955
Steam-to-fuel ratio (kg/kg)	0.08–0.28
Air ratio	0.28–0.39

3.3. Future work

The estimation of gasification behaviour requires detailed knowledge about the fuel structure and ash chemistry. Moilanen and Saviharju (1997) has speculated that the differences in the gasification behaviour of different fuels are due to the behaviour of the ash-forming substances in gasification. Therefore, in order to improve the prediction capability of the present model, information about the fuel characteristics should be incorporated in the carbon conversion predictor. This task will be one of the goals in the future work aiming to improve this model.

4. Conclusions

Experimental data from a PDU-scale reactor was used to fit and validate a semi-empirical model for the gasification of biomass. The model seems to be suitable for simulating gasification of pine sawdust, pine and eucalyptus wood chips as well as forest residues, but is not suitable for pine bark or wheat straw. The model is capable of predicting the concentrations of main product gas components with an average relative error of 14%. The greatest weakness of the model pertains to the prediction capability of carbon conversion when using fuels whose gasification reactivity differs greatly from the reactivity of pine sawdust.

Acknowledgements

The work presented in this paper is a part of the research project "Fundamental studies of synthesis gas production based on fluidised-bed gasification of biomass", UCGFunda. It is funded by the Finnish Funding Agency for Technology and Innovation (Tekes) and Technical Research Centre of Finland (VTT).

References

Bruinsma, O.S.L., Moulijn, J.A., 1988. The pyrolytic formation of polycyclic aromatic hydrocarbons from benzene, toluene, ethylbenzene, styrene, phenylacetylene and n-decane in relation to fossil fuels utilization. Fuel Processing Technology 18 (3), 213–236.

Buekens, A.G., Schouters, J.G., 1984. Mathematical modelling in gasification. In: Bridgewater, A.V. (Ed.), Thermochemical Processing of Biomass. Butterworths, London, UK, pp. 177–199.

De Kam, M.J., Vance Morey, R., Tiffany, D.G., 2009. Biomass integrated gasification combined cycle for heat and power at ethanol plants. Energy Conversion and Management 50 (7), 1682–1690.

Doherty, W., Reynolds, A., Kennedy, D., 2009. The effect of air preheating in a biomass CFB gasifier using ASPEN Plus simulation. Biomass and Bioenergy 33 (9), 1158–1167.

Gururajan, V.S., Agarwal, P.K., Agnew, J.B., 1992. Mathematical modelling of fluidized bed coal gasifiers. Chemical Engineering Research and Design 70, 211–238.

Hamel, S., Krumm, W., 2001. Mathematical modelling and simulation of bubbling fluidised bed gasifiers. Powder Technology 120 (1–2), 105–112.

Kilpinen, P., Hupa, M., Leppälahti, J., 1991. Nitrogen chemistry at gasification – a thermodynamic analysis. Report 91-14. Combustion Chemistry Research Group, Abo Academi University, Finland.

Kovacik, G., Oguztöreli, M., Chambers, A., Özüm, B., 1990. Equilibrium calculations in coal gasification. International Journal of Hydrogen Energy 15 (2), 125–131.

Kurkela, E., 1996. Formation and Removal of Biomass-derived Contaminants in Fluidized-bed Gasification Processes. VTT Publications No. 287, pp. X-47.

Kurkela, E., Stahlberg, P., Laatikainen, J., 1993. Pressurized Fluidized-Bed Gasification Experiments with Wood, Peat, and Coal at VTT [Espoo, Finland] in 1991–1992, 1: Test Facilities and Gasification Experiments with Sawdust. VTT Publications No. 161. VTT, Espoo, Finland.

Kurkela, E., Laatikainen, J., Ståhlberg, P., 1995. Cogasification of biomass and coal. In: Bemtgen, J.M., Hein, K.R.G., Minchener, A.J. (Eds.), Co-Gasification of Coal/Biomass and Coal/Waste Mixtures, Volume III: FINAL REPORTS, EC-Research Project: APAS-Contract COAL-CT92-0001, University of Stuttgart, Stuttgart.

Moilanen, A., 2006. Thermogravimetric Characterisations of Biomass and Waste for Gasification Processes. Espoo, VTT. 103 p. + app. 97 p. VTT Publications; 607ISBN 951-38-6846-X; 951-38-6847-8.

Moilanen, A., Kurkela, E., 1995. Gasification Reactivities of Solid Biomass Fuels. Preprints of Papers Presented at the 210th ACS National Meeting, Chicago, vol. 40, No. 3, p. 688.

Moilanen, A., Saviharju, K., 1997. Gasification reactivities of biomass fuels in pressurised conditions and product gas mixtures. In: Bridgwater, A.V., Boocock, D.G.B. (Eds.), Developments in Thermochemical Biomass Conversion, vol. 2. Blackie Academic and Professional, London, pp. 828–837.

Nikoo, M.B., Mahinpey, N., 2008. Simulation of biomass gasification in fluidized bed reactor using ASPEN PLUS. Biomass and Bioenergy 32 (12), 1245–1254.

Rose, L.M., 1982. Chemical Reactor Design in Practice. VTT, Espoo.

Schuster, G., Löffler, G., Weigl, K., Hofbauer, H., 2001. Biomass steam gasification – an extensive parametric modeling study. Bioresource Technology 77 (1), 71–79.

Simell, P.A., Leppaelahti, J.K., Bredenberg, J.B., 1992. Catalytic purification of tarry fuel gas with carbonate rocks and ferrous materials. Fuel 71 (2), 211–218.

Paper II

Ilkka Hannula, Esa Kurkela

A parametric modelling study for pressurised steam/O2-blown fluidised-bed gasification of wood with catalytic reforming

Biomass and Bioenergy, 2012
Volume 38, Pages 58-67.

Available at www.sciencedirect.com

ScienceDirect

http://www.elsevier.com/locate/biombioe

A parametric modelling study for pressurised steam/O_2-blown fluidised-bed gasification of wood with catalytic reforming

*Ilkka Hannula**, *Esa Kurkela*

Technical Research Centre of Finland, P.O. Box 1000, FI-02044 VTT, Finland

ARTICLE INFO

Article history:
Received 27 August 2010
Received in revised form
16 February 2011
Accepted 22 February 2011
Available online 12 May 2011

Keywords:
Gasification
Model
Biomass
Oxygen
Catalytic reforming

ABSTRACT

A model for pressurised steam/O_2-blown fluidised-bed gasification of biomass with catalytic reforming of hydrocarbons and tars was developed using Aspen Plus simulation software. Seven main blocks were used to model the fluidised-bed gasifier and two for the catalytic reformer. Modelling blocks were complemented with FORTRAN subroutines to simulate the observed non-equilibrium behaviour of the process. The model was fitted with experimental data derived from a 0.5 MW scale test rig operated with crushed wood pellets and forest residues and was shown to be capable of predicting product gas composition from gasification of clean wood. A parametric analysis indicated that a significant improvement in the syngas efficiency could be achieved by rising the filtration temperature and reformer conversions. Other improvement possibilities include fuel drying and lower reforming temperature.

1. Introduction

1.1. Biomass gasification

Increasing energy prices, depleting fossil resources and growing awareness about human-induced environmental issues have provoked major interest towards renewable sources of energy. Gasification of biomass enables the advanced utilisation of these resources and has significant commercial and environmental potential in the production of green chemicals, synthetic fuels and electricity.

Gasification is a thermochemical conversion process that turns carbonaceus feedstocks into a gas mixture rich in carbon monoxide and hydrogen, called product gas or synthesis gas. Other major compounds include carbon dioxide, nitrogen, water, methane and a rich spectrum of hydrocarbons. A general objective of gasification is to maximise the yields of gaseous products and minimise the amounts of condensable hydrocarbons and unreacted char. The exact composition of product gas depends on the type of process feeds, their feed ratios, process parameters and the type of gasification reactor used.

In contrast to coal gasification, where char gasification reactions determine the overall yield, in biomass gasification the devolatilisation stage and secondary reactions of primary pyrolysis products play the major role [1].

1.2. Steam/O_2-blown fluidised-bed gasification

The main factors that influence the heating value of product gas are the selection of the heat transportation method and oxygen-carrier medium. Low heating value gas is produced

* *Corresponding author.*
E-mail address: ilkka.hannula@vtt.fi (I. Hannula).
0961-9534/$ – see front matter © 2011 Elsevier Ltd. All rights reserved.
doi:10.1016/j.biombioe.2011.02.045

with autothermal reactors using air as the oxidising agent, whereas medium heating value gas can be generated with indirectly heated reactors or by using oxygen instead of air in an autothermal reactor.

According to Ref. [2] synthesis gas produced by oxygen gasification and reforming is suitable for all known end uses, whereas synthesis gas produced by air gasification is best suited for power applications and for syntheses that exclude recycling loops, namely hydrogen production with pressure swing adsorption (PSA) separation and once-through Fischer-Tropsch synthesis. Once-through processes also exist for methanol (CH_3OH) and synthetic natural gas (SNG), but they can not be considered promising when using air as an oxidant.

1.3. *Modelling of fluidised-bed gasification of biomass*

The objective of process modelling is to construct a mathematical description of a process that can be used to predict reactor temperature and outlet concentrations from inlet flows and operating conditions. A model that fits well to the experimental data can help to reveal major trends in a multivariable system and be a great comfort when an engineer is faced with scaling-up a reactor to produce the full-scale design [3]. A suitable model also permits more efficient control of the reactor and offers a safe way to simulate reactor behaviour in continuous and transient conditions [4].

Numerous mathematical models for fluidised-bed gasification of biomass have been developed and reported in the literature. Many of the models are based on theories about fluidisation hydrodynamics, coupled with kinetic schemes for the heterogeneous and homogeneous processes occurring inside the gasifier [5]. These can include such fuel-related phenomena as drying, volatilisation, partial combustion with O_2, char gasification with H_2O and CO_2 as well as secondary reactions of condensable hydrocarbons. Taking all these phenomena into account requires the utilisation of numerous empirical correlations and hypotheses about chemical and physical phenomena occurring in different phases (bubble and emulsion) of the fluidised-bed, adding to the mathematical complexity of the model [6]. A large number of these dynamic parameters are also unknown and very difficult to measure, which makes product gas composition estimates often exceedingly difficult for kinetic models [7].

Another group of gasification models is based on the idea of chemical equilibrium. In this approach, the complex kinetics can be disregarded by assuming that gasification reactions occur fast enough for them to reach equilibrium at the reactor outlet. However, equilibrium models fail to predict some of the most important characteristics of fluidised-bed gasification. These include kinetically and hydrodynamically controlled phenomena such as unconverted solid carbon and the formation of gaseous hydrocarbons [6,8,9]. To eliminate these problems, equilibrium models are usually adjusted using empirical parameters or correlations to match measured data from the gasification reactors.

Despite their limitations, equilibrium models have been widely published in the literature. A number of simulation models have been proposed for gasification of coal, while the work done for gasification of biomass has been more limited [5,9]. Especially models for steam/O_2-blown fluidised-bed gasification of biomass with reforming of tars are not abundant among scientific literature. However, very similar features pertain to both air and steam/O_2-blown fluidised-bed gasification of biomass and reviewing the recent development in the field of air gasification modelling can thus be considered justified.

It has been recently suggested in Ref. [10] that a gasifier could be modelled by dividing it into separate blocks, which enable the modelling of drying, pyrolysis, partial oxidation and gasification reactions. The final composition of the syngas is formed in a Gibbs reactor under restricted conditions and additional block is used to separate solids entrained in the gas. The validation of this model was performed for three test runs and the results were reported to be in good agreement with experimental data, with the exception of overpredicted methane. Any heavier hydrocarbons were not considered in the model.

The approach of Ref. [11] was to divide the gasifier into four distinctive parts, namely decomposition of the feed, volatile reactions, char gasification and gas solid separation. In addition, the effects of hydrodynamic parameters and reaction kinetics pertaining to biomass gasification in fluidised-beds were simulated with FORTRAN codes. This slightly more complex approach did not seem to result in much improved predictions, probably due to the absence of higher hydrocarbons and tars in the model.

In several modelling studies, the formation of higher hydrocarbons and tars is often completely neglected. This exclusion is usually defended by pointing out to the very low concentrations of tars in the product gas, suggesting that even if tars are a factor to consider in the plant operation, they do not play an important role in the modelling of biomass gasification.

This assumption seems to be in contrast with the experiences accumulated during our modelling work. It is true that the volume concentrations of tar and higher hydrocarbons are very low in comparison with the main gas components like H_2, CO, CO_2, H_2O and even CH_4, but this should not lead to a conclusion that the modelling of tars is purposeless. The tar components generally have very high molar masses in comparison to the main gas components, which greatly increases their importance. It seems that without the inclusion of tar and hydrocarbon formation in a biomass gasification model, an accurate prediction of product gas composition is not likely to succeed.

1.4. *Experimental work*

In this work, an equilibrium model for pressurised steam/O_2-blown fluidised-bed gasification of biomass with catalytic reforming is developed using Aspen Plus simulation software. The model is fitted with experimental data from gasification tests using crushed wood pellets and forest residues. The tests were conducted with a 0.5 MW scale process development unit (PDU) in a project titled “Development of Ultra-Clean Gas Technologies for Biomass Gasification”. The project was aimed for the development of innovative biomass gasification and gas cleaning technologies for the production of ultra-clean synthesis gas. It was carried out from 2004 to 2007 and co-ordinated by the Technical Research Centre of Finland

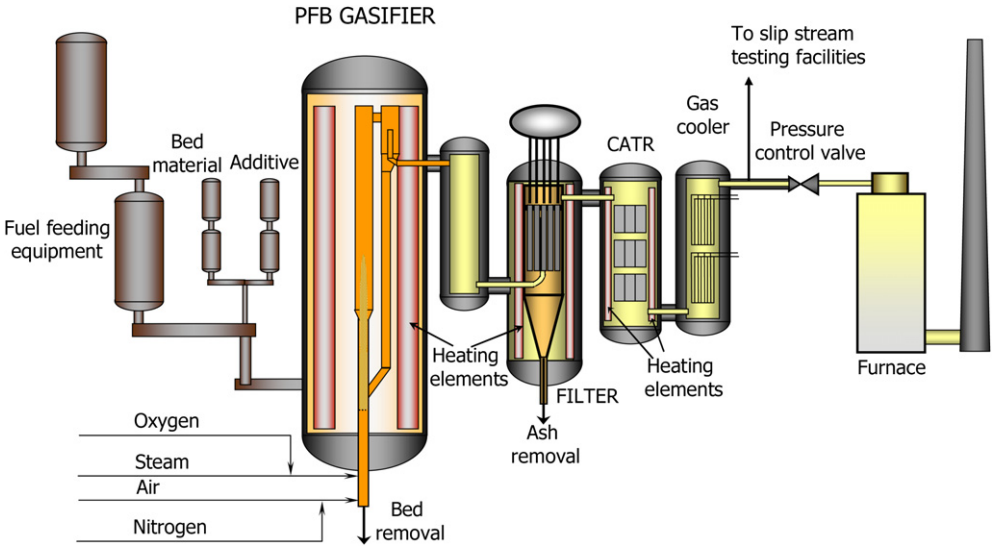

Fig. 1 – The pressurised fluidised-bed gasification test rig.

(VTT). The results of these gasification experiments are published and summarised in Ref. [2]. A brief description of the process and the gasification experiments are also given in the following paragraphs.

1.5. *Description of the experimental equipment and arrangement*

A 0.5 MW test rig, located at VTT, was taken into operation at the end of 2006. The heart of the gasification test rig is a fluidised-bed reactor, mounted inside of an electrically heated oven to compensate heat losses. The oven is thermally insulated and placed inside of a pressure vessel that contains a gasifier, a cyclone separator and a return leg. The vessel is approximately 11 m high with a diameter of 1.6 m.

The product gas flows from the gasifier's outlet to another pressure vessel that reserves space for a pre-reformer and contains a gas cooler and a hot-gas filter. The actual reformer is situated downstream from the filtration unit and is constructed in a way that allows modifications in the inner vessel for the study of different kinds of catalysts. After the reformer, product gas is cooled, depressurised and eventually destroyed in a small boiler.

It is possible to separate small sidestreams from the process for various additional research purposes. The test rig is also equipped with a wide variety of process measurements, all collected to a data logger and processed by a microcomputer. An illustration of the test rig is presented in Fig. 1.

2. Materials and methods

2.1. *Description of the gasification experiments*

The data that was used to fit the model parameters consists of 5 individual operating variable sets, each referring to a specific array of process conditions. During the set point periods, feed rates of fuel, oxygen and steam were kept as constant as possible. Measurement lengths lasted several hours for each set point, while process data was recorded at few minutes intervals. Discharged cyclone and filter fines as well as bottom ashes were collected, weighed and sampled at the set points. Carbon conversion η_C was calculated based on these measurements according to the following equation:

$$\eta_C = 1 - \frac{C_{ash}}{C_{fuel}}, \quad (1)$$

where C_{ash} represents elemental carbon in the ash and C_{fuel} elemental carbon in the fuel.

After a test run, material balances for individual set points were calculated based on the average values of the data. Hydrogen and carbon balances were used to calculate water vapour content and raw gas flow rate, as they are difficult to measure with the same accuracy as the other parameters.

A summary of the key operational parameters at different set points is shown in Table 1. Set points 1, 2, 3 and 5 were run with crushed wood pellets while forest residues were used at set point 4. Ultimate and proximate analyses of the feedstocks are presented in Table 2. The wood pellets were made from dry sawmill residues originating from pine wood (*Pinus sylvestris*). The forest residues (i.e. logging residues) were from eastern Finland from Norway spruce (*Picea abies*) dominated forests. Forest residues were branches and tops of trees from final cutting area. The residues were collected in summer 2006, dried in a storage dryer to circa 10% moisture using warm air at 30 °C and crushed to below 10 mm screen. Then the feedstock was packed in 1 m^3 air tight super bags.

Wood pellets were crushed to make particle size closer to that of realistic wood fuels. Crushed peat pellets were also used as fuel during some of the experiments. This data, however, is not included in this work. Sand and limestone were fed into the gasifier along with the feedstock in order to maintain a stable bed.

The composition of the product gas was measured before the filter and after the reformer with continuous gas analysers and gas chromatographs. Product gas compositions related to

Table 1 – Process parameters related to set point conditions.

Set point	1	2	3	4	5
Feedstock	Wood chips	Wood chips	Wood chips	Forest residues	Wood chips
Fuel moisture, wt%	6.9	6.9	6.9	10.4	7.4
Pressure, MPa	0.25	0.25	0.25	0.25	0.25
Oxygen to fuel ratio, kg kg^{-1}	0.31	0.37	0.42	0.37	0.46
Steam to fuel ratio, kg kg^{-1}	0.50	0.54	0.54	0.54	0.75
Gasifier freeboard temp, °C	823	838	886	830	868
Reformer outlet temp, °C	856	864	867	866	870
Carbon conversion, %	98.86	99.39	99.80	98.72	97.13

For the oxygen to fuel ratio and steam to fuel ratio the fuel is considered as dry and ash free.

each set point are presented in Table 3. The high amounts of nitrogen in the gas can be explained by nitrogen purges that were used in the fuel feeding system and measurement lead-ins to seal off leakages and to keep the equipment operational. However, the effect of these nitrogen purges to product gas composition can be ignored and removed computationally if wanted, as the dilution effect of the purges is much smaller in commercial-scale gasifiers than in a PDU-scale test rig.

2.2. *Utilisation of experimental data in the model*

The limitations of equilibrium models, as discussed in Section 1.3, were dealt with by fitting selected parameters to experimental data. The intention was to first construct a simple and generic model for gasification of biomass that could then be fitted to match a more specific gasifier and fuel type, using easily measurable empirical correlations.

For this reason the incorporation of such parameters as feedstock particle size and reactor geometry were decided to be ignored, although their effects are indirectly embedded in the empiric correlations. Also, the inclusion of these parameters into the model's generic framework would have required much more complex model, still not necessarily able to generate more accurate predictions.

2.3. *Model description*

The core blocks of the model are the equilibrium blocks 5 and 9 (RGibbs), where major parts of feeds are converted to equilibrium products, based on the minimisation of Gibbs-free energy. Almost all the other blocks of the model are used to simulate phenomena that are observed not to comply with the rules of chemical equilibrium. The division of the model to separate blocks could have been conducted in many ways.

Table 2 – Proximate and ultimate analyses of the feedstock. For the calculation of the higher heating value (HHV) see Section 2.5.2.

Set point	1,2,3	4	5
Fuel type	Wood chips	Forest residues	Wood chips
Proximate analysis, wt% d.b.:			
Fixed carbon	16.5	20.6	16.7
Volatile matter	83.3	76.8	82.9
Ash	0.2	2.6	0.4
Ultimate analysis, wt% d.b.:			
C	50.7	51.3	51.1
H	6.2	6.1	6.1
N	0.1	0.5	0.1
CI	0	0	0
S	0.01	0.05	0.01
O	42.8	39.5	42.3
Ash	0.2	2.6	0.4
Moisture content, wt-%	6.9	10.4	7.4
HHV	20.58	20.96	20.64

wt% d.b. = weight percent dry basis.

Table 3 – Product gas compositions after the gasifier (Raw Gas) and after the reformer (Clean Gas) at the set points.

Wet gas composition, vol-%

Set point	1	2	3	4	5
Raw gas					
CO	0.13	0.12	0.12	0.11	0.09
CO_2	0.19	0.20	0.20	0.20	0.18
H_2	0.15	0.14	0.14	0.15	0.13
N_2	0.10	0.09	0.10	0.10	0.13
CH_4	0.05	0.05	0.05	0.05	0.04
C_2H_2	0.0004	0.0004	0.0004	0.0004	0.0003
C_2H_4	0.0146	0.0130	0.0131	0.0140	0.0094
C_2H_6	0.0033	0.0024	0.0025	0.0031	0.0018
C_3-C_5	0.0003	0.0002	0.0002	0.0003	0.0001
NH_3	0	0.0004	0	0	0.0004
H_2O	0.36	0.38	0.37	0.37	0.42
Total	1.00	1.00	1.00	1.00	1.00
Clean gas					
CO	0.11	0.09	0.09	0.10	0.08
CO_2	0.16	0.17	0.16	0.17	0.14
H_2	0.18	0.16	0.16	0.17	0.15
N_2	0.09	0.11	0.13	0.09	0.12
CH_4	0.01	0.01	0.01	0.01	0.01
C_2H_2	0.00003	0.00002	0	0.00004	0
C_2H_4	0.0010	0.0007	0.0005	0.0008	0.0006
C_2H_6	0.00017	0.00010	0.00005	0.00012	0.00005
C_3-C_5	0	0	0	0	0
NH_3	0.0003	0.0003	0	0	0.0002
H_2O	0.45	0.47	0.45	0.46	0.50
Total	1.00	1.00	1.00	1.00	1.00

However, it was considered rational to handle most of the non-equilibrium phenomena in separate blocks, rather than treating them all at once in a single equilibrium block with various restrictions.

The schematic structure of the model is illustrated in Fig. 2. The simulation begins with the decomposition of the biomass to elemental gases, carbon and ash, based on the ultimate analysis of the feedstock. In the next two blocks the approach to equilibrium sulphur removal and carbon conversion are modelled by extracting fixed amounts of sulphur and elemental carbon to a bypass and to an outlet stream, respectively. The formation of tars is simulated next and they are handled as inerts in the following block, where other parts of the feeds are converted to equilibrium products. This is followed by mixing of streams and a separation of the feedstock ash to an outlet stream. The outlet stream of block 7 is the end product of the gasifier, and is labelled as 'Raw gas'.

The Raw gas is then cooled down to simulate the filtration of the gas, followed by a reformer modelling block. For the purposes of the sensitivity study, an additional block 10 was added to adjust the H_2/CO ratio of the gas to a desired value. More detailed descriptions of the model blocks are given in the following paragraphs.

2.3.1. *Biomass decomposition*

A yield reactor (Ryield) is used to simulate the decomposition of the feed. In the first block, biomass is converted to hydrogen, oxygen, nitrogen, carbon, sulphur and ash based on the ultimate analysis of the feedstock.

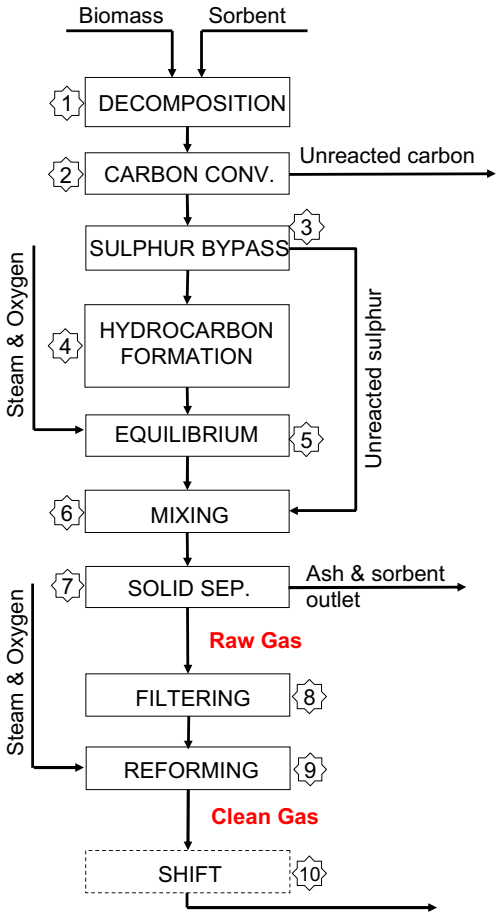

Fig. 2 – A schematic illustration of the model.

2.3.2. *Carbon conversion*

According to equilibrium calculations, feedstock's carbon should convert completely to products under typical gasification conditions in a fluidised-bed. However, a significant amount of carbon is usually found from the reactor's ash streams. Carbon conversion has thus a major effect to the gasifier's efficiency and high conversion levels are therefore desired.

Carbon conversion is adjusted in the model to match with experimental data by conveying part of the feed carbon to an outlet stream. The calculation is based on the observed correlation between carbon conversion and gasification temperature (see Table 4) and nested in block 2 (Sep) as a FORTRAN subroutine.

2.4. *Sulphur capture with calcium-based sorbents in reducing conditions*

In gasification processes the removal of sulphur is usually carried out in two steps. The bulk of the sulphur can be removed by feeding calcium-based sorbents in the gasifier at temperatures from 700 °C to 1100 °C. Additional step is however needed later in the process to remove sulphur completely, since in gasification conditions the calcium-based capture is thermodynamically limited.

According to [12] the principal sulphur capture reactions in the reducing (gasification) atmosphere are:

$$CaO(s) + H_2S(g) = CaS(s) + H_2O(g) \quad (2)$$

$$CaCO_3(s) + H_2S(g) = CaS(s) + H_2O(g) + CO_2(g) \quad (3)$$

$$CaO(s) + COS(g) = CaS(s) + CO_2(g) \quad (4)$$

Table 4 – Conversion correlations used to model the non-equilibrium phenomena.

Conversions related to gasification	
Carbon	0.0155 * G + 86.068 %
CH_4	−0.003 * G + 7.074 mol kg^{-1}
C_2H_2	−0.00004 * G + 0.06454 mol kg^{-1}
C_2H_4	−0.002 * G + 2.987 mol kg^{-1}
C_2H_6	−0.001 * G + 1.196 mol kg^{-1}
C_3H_8	−0.000155 * G + 0.150921 mol kg^{-1}
C_6H_6	0.27 mol kg^{-1}
$C_{10}H_8$	0.3 mol kg^{-1}
NH_3	0.04154 mol kg^{-1}
Conversions related to reforming	
CH_4	0.2247 * R - 127.36 %
C_2H_2	0.8439 * R - 634.66 %
C_2H_4	0.3818 * R - 237.31 %
C_2H_6	0.2753 * R - 143.5 %
C_3H_3	100 %
C_6H_6	0.1875 * R - 76.532 %
$C_{10}H_3$	94.6 %
NH_3	1.0679 * R - 899.25 %

G = Gasifier freeboard temperature [°C].
R = Reformer outlet temperature [°C].

It can be observed, that the gaseous products (H_2O and CO_2) of sulphur capture in gasification conditions are also major compounds in the product gas. Thus the overall efficiency of sulphur capture is not controlled by pressure and temperature alone (as is the case with combustion), but also by the product gas composition [12].

The approach to equilibrium sulphur removal is modelled first in block 3 and the actual equilibrium removal in block 5. Fig. 3 illustrates the experimental correlation between approach to equilibrium sulphur removal and Ca/S molar ratio. The data is based on a pressurised fluidised-bed gasification tests with Finnish peat and German brown coal published in Ref. [12]. It can be observed that sulphur capture is strongly affected by the Ca/S ratio in the reactor. The higher the ratio, the better the approach to equilibrium sulphur removal has been obtained. This observed correlation can be represented with the following equation:

$$A_{eq} = 0.213R + 0.029, \quad (5)$$

where A_{eq} is the approach to equilibrium and R the molar ratio of Ca/S. In the block 3 (Sep) a $1 - A_{eq}$ share of the fuel sulphur is conveyed to a bypass stream, representing the amount of sulphur that does not take part to the equilibrium sulphur removal.

The sulphur removal feature of the model does not rise into a relevant role in this work, as the concentration levels of sulphur in the gas are already below the equilibrium concentrations that limit the removal potential. This is due to the very low levels of sulphur in the fuels (see Table 2). However, this feature becomes important when modelling fuels with higher amounts of sulphur, such as peat.

2.4.1. *Hydrocarbon, tar and NH_3 formation*

According to [13], hydrocarbons formed in a fluidised-bed gasification of biomass are mainly a product of secondary reactions of condensable hydrocarbons (usually referred to tars), formed in the primary pyrolysis stage. These secondary reactions can take place both homogeneously in the gas phase and heterogeneously on the surfaces of char, gasifier bed material, fuel particles and on reactor walls.

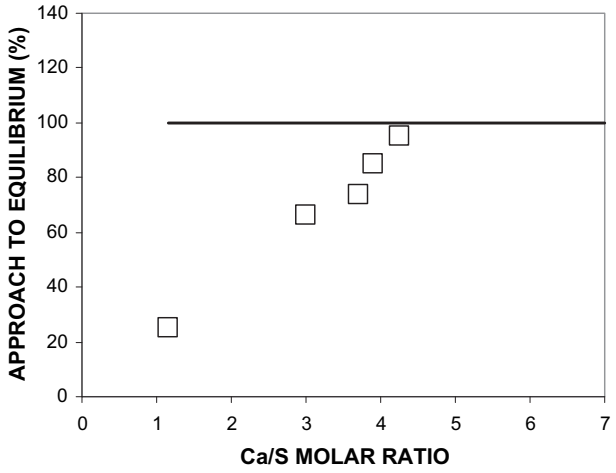

Fig. 3 – Approach to equilibrium sulphur removal as a function of Ca/S molar ratio [12].

The formation of tars and nitrogen species are underpredicted by equilibrium models. The model was thus adjusted to better match with these observations by calculating the correct conversions to tars and hydrocarbons in block 4 (RStoic) from the experimental data. The hydrocarbons were modelled as CH_4, C_2H_2, C_2H_4, C_2H_6, C_3H_8, and C_6H_6, the nitrogen species as NH_3 and tars as $C_{10}H_8$. The formation equations for these compounds were formed as a function of the gasifier's freeboard temperature, as it is known to have a strong correlation with the total tar concentration in fluidised-bed gasification of biomass [14–16]. The equations are presented in Table 4 and used to calculate the molar extent of each compound that is formed from the feed in block 4.

2.4.2. *Equilibrium phenomena*

In block 5, a Gibbs reactor (RGibbs) is used to mix the feed with oxygen and steam and to convert these into equilibrium products. The hydrocarbons, tars and NH_3 are handled as inerts to prevent their decomposition.

2.4.3. *Mixing*

In block 6, a stream mixer is used to connect the bypass stream with products from the equilibrium block.

2.4.4. *Separation of solids*

As the last step of the gasifier model, ash removal is simulated in block 7 (Sep) by directing the feedstock ash to an outlet stream. The product stream of block 7 is the model's estimation of the product gas composition coming out of the fluidised-bed gasifier at given conditions and is labelled as 'Raw gas'.

2.4.5. *Filtration*

Before product gas can be fed into the reformer, its dust load has to be lowered to an allowable level. Barrier filters are normally used for this as the purity requirements can not be met with cyclone separators alone. The filtration step is modelled with a cooler block that lowers the temperature of the raw gas to a level acceptable for the barrier filters to operate without problems. There is no need to simulate any actual dust removal as the formation of fly ash is not modelled in the gasification part.

2.5. *Catalytic reforming of hydrocarbons*

According to [17] the stoichiometry of a steam reforming system can be described with three individual reactions: the steam reforming reaction (6), the water gas shift reaction (7) and the methanation reaction (8), represented by the following equations:

$$C_nH_m + nH_2O \rightarrow nCO + \left(n + \frac{m}{2}\right)H_2 \left(-\Delta H^0_{298} < 0\right), \quad (6)$$

$$CO + H_2O = CO_2 + H_2 \left(-\Delta H^0_{298} = 41.2 \text{ kJ mol}^{-1}\right), \quad (7)$$

$$CO + 3H_2 = CH_4 + H_2O \left(-\Delta H^0_{298} = 206.2 \text{ kJ mol}^{-1}\right). \quad (8)$$

Although reaction (6) is endothermic, the overall heat of the reactions can be positive, zero or negative, depending on the

process conditions. For most processes that involve the production of synthesis gas, low methane content is desired at the reformer outlet. Achieving this requires the use of high steam to carbon ratios and high catalyst exit temperatures, leading to an endothermic overall reaction [17].

To drive this endothermic overall reaction, enough heat has to be supplied into the reformer. This can be achieved by using either tubular or autothermal reformer design [18]. In a tubular reformer the catalysts are loaded into a number of tubes and placed inside of a furnace, whereas in an autothermal reformer the reaction heat is generated by internal combustion with oxygen. The latter design is usually considered more suitable for gasification processes where partial oxidation is already used in the gasifier.

In the model, a Gibbs reactor (RGibbs) is used to convert streams of Raw gas, steam and oxygen to equilibrium products. However, according to experimental data, complete conversion is not achieved for any of the hydrocarbons in the reformer. Especially the conversion levels of methane and ammonia fall well below 100% at every set point.

To match this observation, the conversions have to be adjusted. This is done by estimating the appropriate conversion levels from experimental correlations, defined as a function of the reformer outlet temperature. These correlations, presented in Table 4, are used to calculate the fraction of each compound that doesn't react in the reformer, i.e. is handled as inert in the block.

The product stream of this block is the final product of the simulation and is labelled as 'Clean gas'.

2.5.1. *Shift*

Depending on the synthesis application, different values for the H_2/CO ratio are required. In typical reforming temperatures, the shift reaction is thermodynamically limited and can thus be used to adjust the H_2/CO ratio of the product gas to a desired value. This is normally performed in a separate shift conversion step over an appropriate shift catalysts.

For the purposes of the sensitivity study, a shift conversion step was added to the model to adjust the product gas H_2/CO ratio to 2. This is done in the block 10 (Rstoic) by setting the fractional conversion of the shift reaction to a level leading to the desired ratio.

2.5.2. *Model settings*

SOLIDS and RK-SOAVE were used as base and property methods in Aspen Plus. The selection was based on the instructions of Aspen Plus User Guide and VTT's in-house experiences about gasification modelling.

All components were considered as products in Aspen Plus and the fuel was described by its ultimate and proximate analyses. For enthalpy balance calculations, the higher heating value of the fuel was calculated from ultimate analysis according to the following equation proposed by Channiwala and Parikh [19]:

$$\mathrm{HHV} = 0.3491\,\mathrm{C} + 1.1783\,\mathrm{H} + 0.1005\,\mathrm{S} - 0.1034\,\mathrm{O} - 0.0151\,\mathrm{N} - 0.0211\,\mathrm{Ash}. \quad (9)$$

All the heat streams related to the calculation blocks are connected together and summed up (these are not shown in Fig. 2 for the sake of readability). This sum is interpreted as the heat losses from the system to the surroundings.

When gasifier and reformer temperature were fixed as an input, the energy balance was used to calculate heat losses and when heat losses were assumed, energy balance was used to predict the gasification and reforming temperatures. Inlet temperatures for steam, air and nitrogen were set to 200 °C and for biomass and limestone to 20 °C.

3. Results and discussion

3.1. *Validation*

Usable and publicly available experimental data about steam/O_2-blown gasification of biomass is not easy to find. This lack of independent data makes the proper validation of the model complicated.

However, previous validation experiences with a similar type of model for fluidised-bed air gasification of biomass [20] seem to suggest that if the model results agree reasonably well with the data that was used to fit some of the model parameters, the results can be expected to hold also for other fuels with similar type of reactivity.

Keeping in mind the restrictions caused by the lack of independent validation data, the values of biomass feed, equivalence ratio, steam to fuel ratio, outlet temperature of the gasifier and process pressure were set to correspond with the values of Table 1, and the model estimations were compared with the experimental data at every set point. The results are illustrated in Fig. 4 with lines demonstrating +10% and −10% deviations between measured and estimated values. Judging from the results, a fairly good agreement between experimental data and the model predictions has been achieved for the main gas components. The average relative error for the concentrations of H_2, CO, CO_2, and H_2O was 12%, while the magnitude of experimental error in the data is expected to be around 5%.

As enough information about reformer feedstreams is not included in Ref. [2], the validation was possible to be performed only for the gasification part of the model.

3.1.1. *Range of validity*

A semi-empirical model can be considered fully valid only within the range of the data that was used to fit the model parameters (Table 1). The gasifier type should also be considered when estimating the suitability of the model for process simulation purposes. It is emphasised that only gasifiers sharing a similar type of geometry with the PDU-gasifier (as described in Section 1.5) should be simulated with this model.

In addition to temperature, the gasifier's carbon conversion is also closely related with the gasification rate of the biomass, i.e. the reactivity of the fuel. As the carbon conversion predictor of this model depends only on the gasification temperature, and does not consider any fuel parameters, it is presumable that its prediction capability is restricted to fuels that share similar reactivity with the feedstocks used to fit the predictor itself.

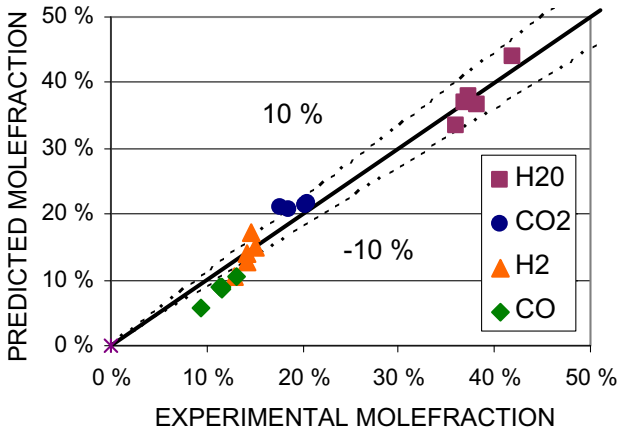

Fig. 4 – Comparison of measured values with values predicted by the model for the main product gas components in wet gas at the gasifier outlet.

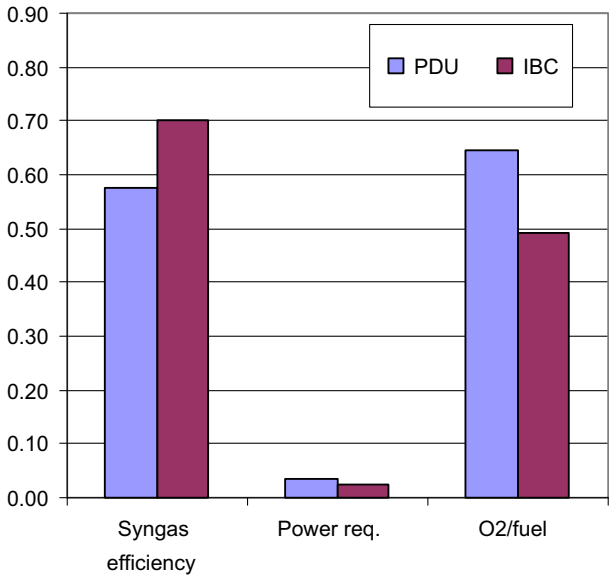

Fig. 5 – Comparison of PDU and IBC, where syngas efficiency and power requirement are given in percentages and O_2/fuel ratio in kg kg^{-1}.

3.2. *Parametric study*

The effects of main process parameters to the gasifier–reformer system are studied in this section. Three different cases were created for these purposes. The cases were:

1. Process development unit (PDU),
2. Industrial base case (IBC), and
3. Target concept (Target).

The PDU case corresponds with the VTT's process development unit, introduced in Section 1.5, and is characterized by large heat losses and steam/oxygen ratios as well as relatively moderate operating pressure.

The IBC is based on the PDU, but features significantly smaller heat losses, elevated operating pressure and smaller steam/oxygen ratios, thus reflecting the effects of an upscale to about 300 MW_{fuel} size.

The Target concept is in turn based on the IBC, but features elevated filtration temperature and higher conversion levels in the reforming unit.

Shift conversion block was used to adjust the H_2/CO ratio of the gas to 2 for all of the cases. As a final step, the product gas was compressed to 30 bar with three compressors incorporating intercoolers and an isentropic efficiency of 80%. Pressure losses were set to 200 mbar for the gasifier, filter and reformer and to 1 bar for oxygen and steam inlets. The main features are listed in Table 5. Set point 4 of Table 1 was chosen as the base for setting rest of the operating parameters. The performance of each case was calculated and the results are discussed in the following paragraphs.

Table 5 – Main process parameters related to the different cases.

	PDU	IBC	TARGET
Heat losses, %	7	1	1
Gasification pressure, MPa	0.25	1	1
Filtration temperature, °C	538	538	830
Steam/oxygen ratios, kg kg^{-1}	1.5	1	1
CH_4 and NH_3 conversions, %	*	*	80
Other hydrocarbon conversions, %	*	*	100
Final pressure, MPa	3	3	3
H_2/C_0 ratio after shift	2	2	2
Fuel moisture, wt%	10.4	10.4	10.4

* According to equations of Table 4.

3.2.1. *The influence of heat losses, gasification pressure and steam/oxygen ratios*

The influence of heat losses, gasification pressure and steam/oxygen ratios to the performance of a gasification-reformer

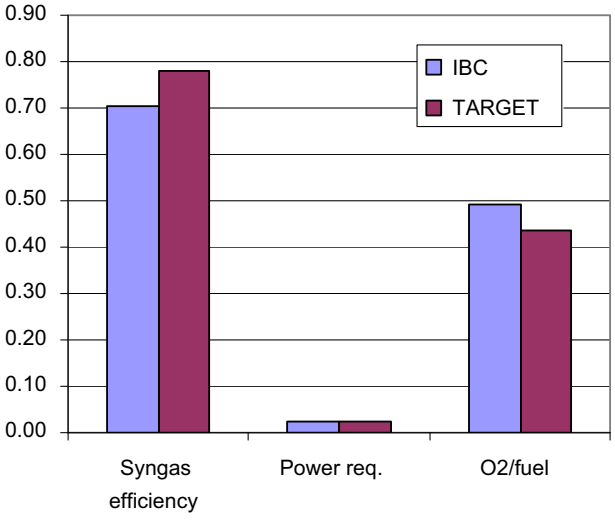

Fig. 6 – Comparison of IBC and Target concept, where syngas efficiency and power requirement are given in percentages and O_2/fuel ratio in kg kg^{-1}.

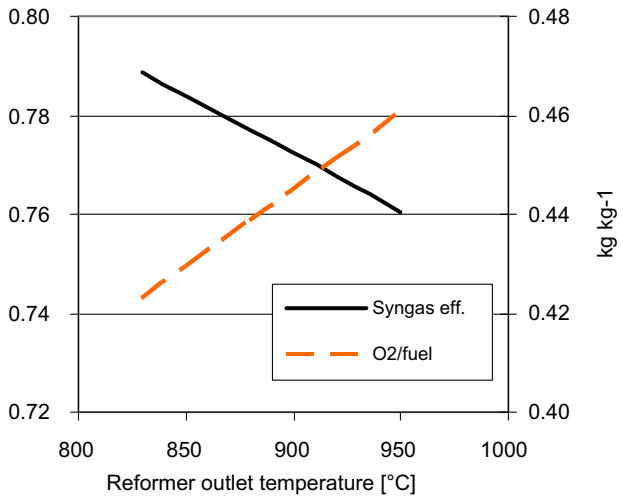

Fig. 7 – The effect of reforming temperature to the syngas efficiency and oxygen consumption.

system are studied first. These effects are of special interest for an engineer facing a task of process scale-up. For a PDU-scale gasifier the heat losses to surroundings are usually around 7–10%, whereas for commercial-scale gasifier these are only around 1%. Usually the gasification temperature is tried to be kept at the same level after the scale-up of reactor size. However, in larger reactors the same temperature can be achieved with smaller amount of oxygen as less heat is lost to the surroundings. This improves the gasifier's cold gas efficiency and also affects the product gas composition. In larger reactors the desired fluidisation properties are achieved with smaller steam/oxygen ratios which also improve the efficiency. The elevated gasification pressure reduces the need of product gas compression to the final synthesis pressure, resulting in a lower overall power consumption requirement.

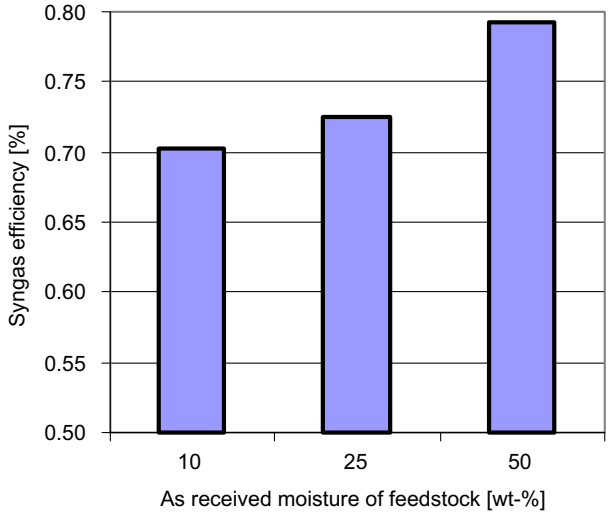

Fig. 8 – The effect of feedstock drying to the syngas efficiency when feedstock is dried to the moisture content of 10% with low level heat streams from the process.

The effects of these parameters are illustrated in Fig. 5, where the PDU case is compared with Industrial base case.

The syngas efficiency η_{syngas} is defined as:

$$\eta_{syngas} = \frac{\dot{m}_{sg} \times Q_{sg}}{\dot{m}_f \times Q_f}, \quad (10)$$

where $\dot{m}_{sg}$ denotes the combined mass flow of H_2 and CO in the product gas, Q_{sg} the combined heating value of H_2 and CO, $\dot{m}_f$ the fuel input flow and Q_f the heating value of the fuel on LHV basis.

The O_2/fuel ratio is reported in kilograms (kg kg^{-1}) where the fuel is considered dry and ash free. The power requirement η_{power} is defined as:

$$\eta_{power} = \frac{\text{Internal power consumption}}{\dot{m}_f \times Q_f} \quad (11)$$

where internal power consumption includes the compression of oxygen and steam (water) to gasification pressure and the compression of product gas to the final synthesis pressure (30 bar).

It can be observed that lower heat losses and steam/oxygen ratios cut down the oxygen need from 0.64 to 0.49 kg kg^{-1} and improve the syngas efficiency significantly from 58 to 70%. Rising the gasification pressure from 2.5 bar to 10 bar lowers the power requirement by 50% (from 4 to 2%).

3.2.2. *The effects of filtration temperature and reformer conversion levels*

When the filtration step has to be performed in a lower temperature than gasification, additional heat exchanger must be installed for cooling of the gas. After the filtration, the temperature needs to be elevated again for the reforming process by partial oxidation of the product gas, which leads to lower η_{syngas} and higher oxygen consumption. According to Fig. 6 the combined effects of elevated filtration temperature and higher reformer conversions amount to 8% points rise in the $\eta_{syngas.}$ More detailed calculations show that elevated filtration temperature contributes 5% points and higher reformer conversions 3% points share in this total improvement from 70 to 78%.

The change in oxygen consumption between the IBC and Target case is a result of two phenomena driving the oxygen consumption in opposite directions: For the Target case, oxygen consumption in the reformer must rise in order to maintain the same temperature, as more endothermic reforming reactions are taking place. However, the higher filtration temperature of the Target case leads to a reduced need for reheating before the reformer, contributing to lower oxygen needs. According to the calculations, an aggregate effect of these two phenomena lowers the oxygen consumption from 49 to 43 kg kg^{-1}. The differences between power requirements are small, because gasification pressure is same for both of the cases.

3.2.3. *The effect of reforming temperature*

It is also important to study the effects of reforming temperature to the process performance, as higher temperatures require higher oxygen consumption and thus lead to lower syngas efficiency. Fig. 7 illustrates the effects of reforming temperature to the process performance, while keeping the

conversion levels constant. It can be observed, that if the target conversions are achieved only after 950 °C instead of 850 °C, it will lower the η_{syngas} from 78 to 76%, and raise the oxygen consumption from 43 to 46 kg kg^{-1}.

3.2.4. *The effect of drying*

A commercial-scale gasification plant produces several kinds of heat streams as a by-product. Some of these streams can be used to generate process steam and electricity, whereas some streams are associated with such a low temperature levels that the production of electricity is not anymore technically possible. However, these low quality heat streams can be used for feedstock drying. If process performance calculations are performed on LHV basis, the incorporation of fuel drying can lead to a significant rise in the efficiency. This can be observed also in Fig. 8, where η_{syngas} is calculated for three different drying levels. The first column represents a case where drying is not applied (fuel moisture already at the targeted 10 wt-%). The second column indicates a rise in η_{syngas} from 70 to 73% when the fuel is dried from 25 to 10 wt-%, and the third column indicates a rise in syngas efficiency up to 79% when fuel is dried from 50 to 10 wt-%.

4. Conclusions

Experimental data from a PDU-scale reactor was used to fit a semi-empirical model for steam/O_2-blown fluidised-bed gasification of biomass with catalytic reformer. The model is capable of predicting product gas composition with an average relative error of 12% for fuels with a reactivity close to that of clean wood. A parametric analysis indicated that higher reformer conversions and filtration temperature have the potential to improve syngas efficiency from 70 to 78%. Achieving target conversions at 950 °C instead of 850 °C would decrease syngas efficiency by 2% points and drying the fuel from 50 to 10 wt-% moisture content would improve the efficiency by 9% points.

Acknowledgements

The work presented here was carried out in a research project "Fundamental studies of synthesis gas production based on fluidised-bed gasification of biomass" (UCGFunda). The project is funded by the Finnish Funding Agency for Technology and Innovation (Tekes) and Technical Research Centre of Finland (VTT).

REFERENCES

[1] Kurkela E. Formation and removal of biomass-derived contaminants in fluidized-bed gasification processes. In: VTT Publications, vol. 287. Technical Research Centre of Finland, VTT; 1996.

[2] Kurkela E, Simell P, McKeough P, Kurkela M. Production of synthesis gas and clean fuel gas [[synteesikaasun ja puhtaan polttokaasun valmistus]]. In: VTT Publications, vol. 682. Technical Research Centre of Finland, VTT; 2008.

[3] Rose L. Chemical reactor design in practise. Espoo, Finland: TKK; 1982.

[4] Buekens A, Schoeters J. Mathematical modelling in gasification. In: Bridgwater A, editor. Thermochemical processing of biomass. London, Boston: Buttherworths; 1984.

[5] Gururajan V, Agarwal P, Agnew J. Mathematical modelling of fluidized bed coal gasifiers. Chem Eng Res Des 1992;70:211–38.

[6] Konttinen J, Hupa M, Moilanen A, Kurkela E. Carbon conversion predictor for fluidized bed gasification of biomass fuels – model concept. In: Proceedings of the Science in Thermal and Chemical Biomass Conversion (STCBC) conference. 2004.

[7] Kovacik G, Oguztöreli M, Chambers A, Özüm B. Equilibrium calculations in coal gasification. Int J Hydrogen Energy 1990; 15(2):125–31.

[8] Kilpinen P, Hupa M, Leppälahti J. Nitrogen chemistry at gasification – a thermodynamic analysis. Åbo Akademi; 1991. Tech. Rep.

[9] Schuster G, Löffler G, Weigl K, Hofbauer H. Biomass steam gasification – an extensive parametric modeling study. Bioresour Technol 2001;77(1):71–9.

[10] Doherty W, Reynolds A, Kennedy D. The effect of air preheating in a biomass CFB gasifier using aspen plus simulation. Biomass and Bioenergy 2009;33(9):1158–67.

[11] Nikoo M, Mahinpey N. Simulation of biomass gasification in fluidized bed reactor using aspen plus. Biomass and Bioenergy 2008;32(12):1245–54.

[12] Kurkela E, Hepola J, Ståhlberg P, Lappi M. Sulphur removal by calcium-based sorbents in fluidized-bed gasification. In: International symposium on energy and environment. Espoo, Finland; 1991.

[13] Simell P. Catalytic hot gas cleaning of gasification gas. Ph.D. thesis; Helsinki University of Technology, TKK; 1997.

[14] Bruinsma O, Moulijn J. The pyrolytic formation of polycyclic aromatic hydrocarbons from benzene, toluene, ethylbenzene, styrene, phenylacetylene and n-decane in relation to fossil fuels utilization. Fuel Process Technol 1988; 18(3):213–36.

[15] Simell P, Leppälahti J, Bredenberg J. Catalytic purification of tarry fuel gas with carbonate rocks and ferrous materials. Fuel 1992;71(2):211–8.

[16] Kurkela E, Stahlberg P, Laatikainen J. Pressurized fluidized-bed gasification experiments with wood, peat, and coal at VTT [Espoo, Finland] in 1991–1992, Part 1. In: Test facilities and gasification experiments with sawdust. VTT Publications, vol. 161. Technical Research Centre of Finland, VTT; 1993.

[17] Anderson J, Boudart M, editors. Catalysis Science and Technology, vol. 5. Berlin, Heidelberg: Springer-Verlag, ISBN 3-540-12665-1; 1984.

[18] Tubular reforming and autothermal reforming of natural gas – an overview of available processes. Fuel Process Technol 1995;42(2–3):85–107. doi:10.1016/0378-3820(94)00099-F. Trends in Natural Gas Utilisation.

[19] Channiwala S, Parikh P. A unified correlation for estimating HHV of solid, liquid and gaseous fuels. Fuel 2002;81(8): 1051–63. Cited by (since 1996) 61.

[20] Hannula I, Kurkela E. A semi-empirical model for pressurised air-blown fluidised-bed gasification of biomass. Bioresour Technol 2010;101(12).

Paper III

Pekka Simell, Ilkka Hannula, Sanna Tuomi, Matti Nieminen,
Esa Kurkela, Ilkka Hiltunen, Noora Kaisalo, Johanna Kihlman

**Clean syngas from biomass –
process development and concept assessment**

Biomass Conversion and Biorefinery, 2014
Volume 4, Issue 4, pages 357-370.

Paper IV

Ilkka Hannula

Co-production of synthetic fuels and district heat from biomass residues, carbon dioxide and electricity: Performance and cost analysis

Biomass and Bioenergy, 2015
Volume 74, Pages 26-46.

Available online at www.sciencedirect.com

ScienceDirect

http://www.elsevier.com/locate/biombioe

Co-production of synthetic fuels and district heat from biomass residues, carbon dioxide and electricity: Performance and cost analysis

Ilkka Hannula *

Technical Research Centre of Finland, P.O. Box 1000, FI-02044 VTT, Finland

ARTICLE INFO

Article history:
Received 13 August 2014
Received in revised form
14 December 2014
Accepted 6 January 2015
Available online

Keywords:
Biomass residues
Gasification
Power-to-fuels
Carbon dioxide
Synthetic fuels
District heating

ABSTRACT

Large-scale systems suitable for the production of synthetic natural gas (SNG), methanol or gasoline (MTG) are examined using a self-consistent design, simulation and cost analysis framework. Three basic production routes are considered: (1) production from biomass via gasification; (2) from carbon dioxide and electricity via water electrolysis; (3) from biomass and electricity via hybrid process combining elements from routes (1) and (2). Process designs are developed based on technologies that are either commercially available or successfully demonstrated at precommercial scale. The prospective economics of future facilities coproducing fuels and district heat are evaluated from the perspective of a synthetic fuel producer. The levelised production costs range from 18–37 €/GJ for natural gas, 21–40 €/GJ for methanol and 23–48 €/GJ for gasoline, depending on the production route. For a given end-product, the lowest costs are associated with thermochemical plant configurations, followed by hybrid and electrochemical plants.

1. Background and scope

Deep reductions in anthropogenic emissions are required to stabilise the levels of atmospheric carbon dioxide (CO_2) [1]. As transportation and power generation are the two largest sources of global CO_2 emissions, they are also the most critical sectors of the economy where cuts need to take place [2].

In the power sector, near-term solutions for CO_2 management include photovoltaics, wind power, biopower, nuclear power and carbon capture and storage (CCS) technologies. Most of these options are ready for large-scale deployment and capable of inducing deep emissions cuts [3].

In the transportation sector, emissions can mainly be reduced by improvements in efficiency and change in vehicle fuel. However, most of the alternative fuel options (e.g. starch-based ethanol, biogas and electricity) require modifications to the current vehicle fleet and/or fuel distribution infrastructure, which severely limits the near-term potential for emissions cuts from the sector. For the medium-term, synthetically manufactured fuels (synfuels) are attracting attention as a way to produce alternative fuels that are compatible with the existing transportation infrastructure [4].

Technology for the production of synthetic fuels from fossil feedstocks, such as coal or shale, has existed for almost a century. However, when coal is used as feedstock, the resulting net greenhouse gas (GHG) emissions are about

* Tel.: +358 40 838 0960.
E-mail address: ilkka.hannula@vtt.fi.
http://dx.doi.org/10.1016/j.biombioe.2015.01.006
0961-9534/

double of those from petroleum fuels [5]. It is possible to cut down part of these emissions with capture and storage of the byproduct CO_2, but the net GHG emissions would still be reduced only to levels comparable to those from petroleum fuels [6].

Switching partly or completely from fossil feedstocks to biomass (plant matter) is a frequently proposed method for further decarbonisation of synthetic fuel production [6–9]. Unfortunately, all commercial scale synfuels plants to date have been operated with fossil feedstocks and redesign of some key parts of the process is required to make the switch to biomass possible. Currently, a lot of RD&D work is ongoing to commercialise such technology [10].

Another solution would be to produce synthetic fuels directly from carbon dioxide and renewable electricity with a process referred to here as 'power-to-fuels' (P2F). This process begins with splitting water (H_2O) into hydrogen (H_2) and oxygen (O_2) with electricity. The produced hydrogen is then synthesised with co-feed CO_2 to form hydrocarbons or alcohols. The hydrogen is thus stored chemically as conventional liquid or gaseous fuel that can be consumed at a chosen time and place within the existing infrastructure. In this sense, the power-to-fuels concept elegantly solves problems of distribution and storage that normally impede energy concepts based on hydrogen production. However, the present use of CO_2 as chemical feedstock is limited to few industrial processes, although commercial projects based on hydrogenation of CO_2 to synthetic fuels are already emerging[11].

Yet another solution would be to combine the above-described processes together into a hybrid process that exploits biomass gasification to produce CO but uses renewable electricity to make up for the hydrogen deficit in the produced syngas. This combination would not require any new equipment to be developed while it also provides a solution to the lack of large-scale catalyst systems capable of direct hydrogenation of carbon dioxide.

The objective of this paper is to investigate the production of synthetic[1] fuels from biomass residues, CO_2 and electricity and their potential role in decarbonisation of the transportation fuel pool. A unified analytical framework is employed to systematically analyse and compare different plant configurations based on their mass and energy balances calculated with ASPEN Plus® (Aspen) process simulation software. The overall economics are evaluated under alternative feedstock price assumptions in terms of euros (€) per gigajoule (GJ), based on an underlying component-level capital cost estimates.

2. Plant configurations

All the analysed plant configurations feature two basic parts: synthesis gas production (endothermic) and synthesis gas conversion (exothermic). Energy integration between these two parts is possible to a certain degree via steam. The configurations considered here illustrate three basic alternatives:

- Production from biomass via gasification;
- Production from carbon dioxide and electricity via electrolysis of water;
- Production from biomass and electricity via hybrid process.

In addition, following synthetic end-product options are evaluated:

- Natural gas (methane);
- Methanol;
- Gasoline.

The combination of these alternatives gives nine basic configurations, each characterised by distinctive plant designs. These configurations are summarised and named in Table 1.

2.1. *Thermochemical pathway*

Fischer-Tropsch (FT) synthesis is a well known method for producing liquid hydrocarbon fuels from synthesis gas. However, once synthesis gas is produced, other end-product alternatives are also available, including: natural gas (methane), methanol, dimethyl ether (DME) and gasoline [12–15].

Some of the attempts to produce these fuels from biomass-derived synthesis gas have ended in difficulties [16,17], although technical hurdles have since been overcome and synthetic biofuels technology can be currently considered successfully demonstrated at pre-commercial scale [18–20]. Nonetheless, commercial applications are still lacking. The slow commercialisation pace is often attributed to the technology's high specific investment cost, financing gaps on the path from pre-revenue stage to commercial operations, uncertainty about the stability of carbon policies and lack of knowhow in sourcing and processing lignocellulosic biomass.

2.2. *Electrochemical pathway*

The concept of producing synthetic fuels from carbon dioxide via electrochemical pathway was first proposed in the late 1970s and studied further in the early 80s [21–24]. The early concepts were based on nuclear energy sources and low temperature electrolysis, while more recently the focus has turned to solar and wind using high temperature electrolysis for hydrogen production [25]. The renewed interest in the topic has been fuelled by the improved availability and economics of electricity produced from renewable sources, especially from wind and solar. Synfuels are not currently

Table 1 – Summary of the basic plant configurations considered in this paper. The configurations are identified by a sequence of two letters: first letter identifies the production route and second letter the main product.

	Thermochemical	Hybrid	Electrochemical
Natural gas	TN	HN	EN
Methanol	TM	HM	EM
Gasoline	TG	HG	EG

[1] In this paper, synthetic fuels are defined as fuels manufactured from synthesis gas ($CO + H_2$) or a mixture of $CO_2 + H_2$.

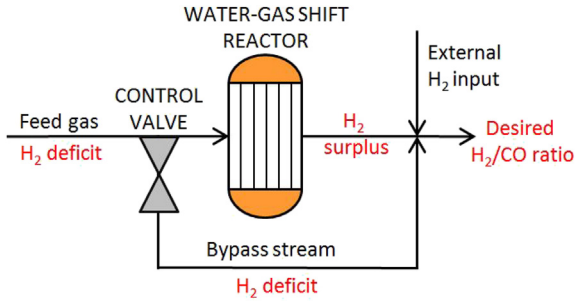

Fig. 1 – Schematic illustration of a configuration suitable for regulating the syngas stoichiometry with a combination of water–gas shift and external hydrogen input.

produced commercially from CO_2 as the main feed, although research is also ongoing to make it possible [26–28].

2.3. *Hybrid pathway*

Hydrogen and carbon needs to be fed to the synthesis in right proportions to achieve maximal conversion to fuels. Their ratios can be controlled upstream with a reactor that catalyses water-gas shift reaction (1). By controlling the amount of bypass around this reactor, almost any ratio[2] of H_2/CO can be achieved once the streams are again combined (see Fig. 1).

$$CO + H_2O = H_2 + CO_2 \quad \Delta H_{298\ K,\ 5\ MPa} = -49.8\ kJ/mol, \tag{1}$$

Another possibility for adjusting the syngas stoichiometry would be to remove the shift reactor completely and directly import the required amount of hydrogen from external sources [29–31]. This approach would also allow more of the syngas' CO to be converted into fuel as losses incurred during the WGS reaction could be avoided. However, such an arrangement requires constant flow of hydrogen leaving little space for flexibility.

The configuration examined in this paper combines the above-described approaches into a one hybrid system that features both a grid connected electrolyser and a WGS step. With such a hybrid approach, a time-variable control over the amount of external hydrogen addition becomes possible. The improved flexibility allows to operate the electrolyser only during times of excess supply of renewable electricity, making it possible to participate in levelling the peaks of time-variable renewable energy production. In principle, no additional technical barriers should be introduced as a result of the hybrid approach, making it possible to deploy such configurations in tandem with synthetic biofuels technology.

3. Technology review and design parameters

This section provides brief descriptions of technologies featured in this paper. The main design parameters are summarised in Table 2 and discussed in the text below. For a detailed list of modelling parameters and their sources please refer to the appendix. Gasoline is produced from methanol as a separate post-processing step and therefore shares upstream settings with the corresponding methanol plants.

3.1. *Biomass to synthesis gas*

A simplified block diagram of a plant suitable for the conversion of biomass residues to ultra-clean synthesis gas is shown in Fig. 2. The plant is operated with forest residue chips whose properties are given in Table 3. The wet biomass feedstock is first dried from its initial moisture of 50 wt% to 15 wt% in a belt dryer operated with hot water recovered from the gasification plant. The dried chips are pressurised with lock-hoppers to 0.4 MPa and fed to a circulating fluidised-bed gasification reactor operating at 850 °C. The gasifier is fluidised with equal amounts of steam and oxygen and used to convert wood chips into a raw product gas containing CO, H_2, CO_2, H_2O, CH_4 and small amount of higher hydrocarbons and tars [32].

Before filtration, the gas is cooled[3] down to 550 °C to condense alkali metals and to avoid blinding of the filter elements during dust removal [33]. The filtered gas is sent to a catalytic reformer where tars and hydrocarbons are converted to light gases. For plants that produce methanol the tar reformer is designed for maximal methane[4] conversion (95% at 957 °C), while for plants that produce synthetic natural gas (SNG) the methane conversion is minimised (35% at 850 °C) [33]. The model used to simulate this three-step (gasification, filtration, catalytic reforming) process is validated with experimental data derived from a 0.5 MW_{th} process development unit (PDU) that was run circa 4000 h in pressurised oxygen-blown mode using various wood residues as feedstock [34]. The model itself is described in detail in Refs. [35,36].

After reforming, the gas is cooled down to 260–80 °C, shifted in an adiabatic reactor and cooled further to 200 °C. The syngas is then fed to a two-stage water scrubber that cools the gas down to 60 °C while recovering the heat for feedstock drying and district heating, and then further to 30 °C to condense out the syngas moisture. The dried gas is compressed and fed to an acid gas (CO_2 and sulphur species) separation unit operated with chilled methanol as the washing solvent.

For plants that feature natural gas (SNG) production, syngas is compressed to 1.6 MPa at a one go (inlet pressure to methanation is 1.5 MPa), which allows for 0.1 MPa pressure drop in the AGR. For plants that feature methanol synthesis, syngas is compressed to 8.0 MPa (operating pressure of the methanol converter) in two steps: first to 3.1 MPa before acid gas removal followed by further compression[5] to 8.0 MPa.

[2] The minimum being that of the feed gas' and the maximum that of the shift reactor effluent's.

[3] In all plants heat is recovered to superheat steam, boil water or generate hot water, depending on the temperature window of cooling.

[4] This refers to methane that is unavoidably formed during biomass gasification.

[5] Dividing compression in two parts saves compression work due to the lack of CO_2 in the latter phase.

Table 2 – Main design parameters for the examined plant configurations. For sources and additional parameters, see appendix.

Configuration		TN	TM	HN	HM	EN	EM
Band conveyor dryer							
Specific heat consumption	kWh/tH_2O_{evap}	1300	1300	1300	1300		
Share of LT heat in belt dryer	%	20	20	20	20		
Moisture in	wt%	50	50	50	50		
Moisture out	wt%	15	15	15	15		
CO_2 capture from fluegas							
CO_2 purity	mol%					100	100
CO_2 pressure	MPa					0.1	0.1
Air separation unit (ASU)							
Oxygen purity	mol%	99.5	99.5	99.5	99.5		
Oxygen delivery pressure	MPa	0.105	0.105	0.105	0.105		
Steam/O_2 gasifier							
Pressure	MPa	0.4	0.4	0.4	0.4		
Temperature	°C	850	850	850	850		
Heat loss (HHV)	%	0.8	0.9	0.8	0.9		
Steam/O_2	kg/kg	1.0	1.0	1.0	1.0		
Carbon conversion	%	98.0	98.0	98.0	98.0		
O_2/air/steam mix inlet temp.	°C	203	215	203	215		
$CaCO_3$/Biomass (dry)	wt%	2.0%	2.0%	2.0%	2.0%		
Filter cooler							
Temperature before filtration	°C	550	550	550	550		
Reformer							
Outlet temperature	°C	850	957	850	957		
Heat loss (HHV)	%	1.0	1.0	1.0	1.0		
Steam/O_2	kg/kg	1.0	1.0	1.0	1.0		
Methane conversion	%	35	95	35	95		
O_2/air/steam mix inlet temp.	°C	206	218	206	218		
Sour shift reactor							
Steam/CO at inlet	mol/mol	2.0	2.0				
Reactor inlet temp.	°C	280	258				
Reactor outlet temp.	°C	404	405				
By-pass/syngas feed	mol/mol	0.43	0.68				
H_2/CO at exit	mol/mol	3.00	2.03				
Scrubber							
Temperature at inlet	°C	200	200	200	200		
Temp. at stage 1 outlet	°C	60	60	60	60		
Temp. at stage 2 outlet	°C	30	30	30	30		
Syngas compressor							
Syngas pressure at outlet	MPa	1.6	3.1	1.6	3.1		
Acid gas removal							
CO_2 removal extent	%	98	98	98	98		
Sulphur removal extent	%	99	99	99	99		
Alkaline electrolysis							
Pressure	MPa					0.1	0.1
H_2 purity	mol%					100	100
O_2 purity	mol%					100	100
System hydrogen efficiency	%			62	62	62	62
H_2/CO after H_2 addition	mol/mol			3	2.03		
H_2/CO_2 after H_2 addition	mol/mol					4	3
Syngas conversion							
Inlet pressure to synthesis	MPa	1.5	8.0	1.5	8.0	1.5	8.0
Syngas efficiency	%	>99.5	95	>99.5	95	>99.5	95
Auxiliary boiler							
Boiler fluegas oxygen	mol%	4	4	4	4		
Fluegas to stack	°C	150	150	150	150		

3.2. *Synthesis of methane*

Methane is synthesised by hydrogenation of carbon oxides over catalysts based on nickel and other metals (Ru, Rh, Pt, Fe and Co) [37], although in practise all commercially available modern catalyst systems are based on nickel due to its favourable combination of selectivity, activity and price [38].

Conversion of synthesis gas to methane can be described with the following reactions:

$$CO + 3H_2 = CH_4 + H_2O \quad \Delta H = -206\ \text{kJ/mol}, \tag{2}$$

$$CO_2 + 4H_2 = CH_4 + 2H_2O \quad \Delta H = -165\ \text{kJ/mol}. \tag{3}$$

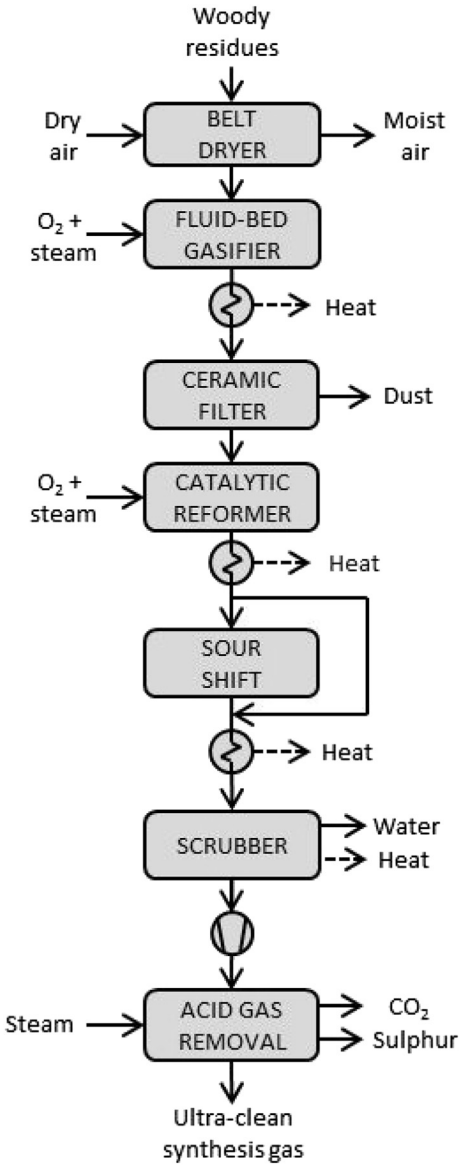

Fig. 2 – Schematic illustration of a thermochemical process capable of converting forest residue chips to ultra-clean synthesis gas.

The simulation model developed for this paper is inspired by the high temperature methanation process 'TREMP', developed and offered by Haldor Topsøe [38,39]. The design features six adiabatic fixed-bed reactors connected in series and equipped with intercoolers. The pressure at the inlet of the first reactor is 1.5 MPa. The inlet syngas is mixed with steam and preheated to 300 °C. The amount of steam addition is chosen to limit temperature increase in the first reactor to 700 °C.[6] The hot effluent exiting from the first four reactors is cooled to 300 °C before entering to the next reactor in series. Effluent from the fifth reactor is cooled down to condense and separate gas moisture before feeding to the last reactor. Overall conversion of syngas to methane is >99.5% and the effluent exits from the system at 1.1 MPa pressure. Equilibrium conversions in the reactors are calculated with Aspen using Soave-Redlich-Kwong (SRK) equation of state model. The recovered heat is used to produce high pressure superheated steam for the plant's steam cycle.

[6] An alternative design would employ a recycle around the first reactor to limit temperature rise. This design doesn't require steam, but calls for a compressor and electricity to run it.

3.3. *Synthesis of methanol*

Methanol is synthesised by hydrogenation of carbon oxides over catalysts composed of copper oxide and zinc oxide stabilised with alumina [13]. These catalysts allow the production of methanol at over 99.9% selectivity with higher alcohols as primary byproducts [40]. Synthesis of methanol can be described with the following reactions:

$$CO_2 + 3H_2 = CH_3OH + H_2O \quad \Delta H_{298\ K,\ 5\ MPa} = -40.9\ kJ/mol, \tag{4}$$

$$CO + 2H_2 = CH_3OH \quad \Delta H_{298\ K,\ 5\ MPa} = -90.7\ kJ/mol, \tag{5}$$

which both are exothermic and result in a decrease in volume [40].

The simulation model developed for this paper is based on the 'low-pressure methanol synthesis', a de facto industrial process for large scale methanol manufacture since the 1960's [41]. In the acid gas removal step, CO_2 is not removed completely, but about 1 mol-% of CO_2 is left to the syngas to improve kinetics of methanol formation. Before treated syngas (make-up gas) can be fed to the methanol process it needs to be compressed further to 8.0 MPa, which is the operating pressure of the methanol converter. The make-up gas is then admixed with the recompressed recycle stream and preheated to 260 °C in heat exchange with the hot reactor effluent. The methanol converter design is based on a tubular boiling-water reactor operated at 260 °C and 8.0 MPa. The equilibrium conversions are calculated with Aspen using Soave-Redlich-Kwong (SRK) equation of state model. Any unconverted synthesis gas is separated from the effluent at the reactor exit, recompressed and recycled back to the feed side of the reactor until 95% conversion of CO and H_2 to methanol is achieved. Small amount of unconverted gas needs to be continuously purged to control the build-up of inerts in the methanol loop, which is then transferred to combustion.

The produced raw methanol contains reaction water formed as byproduct of CO_2 conversion. This water (along with small amounts of higher alcohols) can be separated from methanol to achieve a desired product quality. Higher purities can be achieved simply by adding more distillation columns, thus contributing to additional capital and energy costs.

3.4. *Synthesis of gasoline*

Gasoline is synthesised by a two-step process that involves 1) production of oxygenates from synthesis gas and 2) subsequent conversion of oxygenates to higher hydrocarbons boiling in the gasoline range [42]. These processes may be carried out as separate steps using methanol as the intermediate oxygenate, or in integrated fashion by producing a methanol/DME mixture from syngas that is fed directly to a downstream gasoline converter [43].

Table 3 – Properties of forest residue chips used as feedstock for gasification [75].

Proximate analysis, wt% d.b.[a]	
Fixed carbon	18.3
Volatile matter	80.6
Ash	1.1
Ultimate analysis, wt% d.b.	
Ash	1.1
C	51.48
H	6.0
N	0.2
Cl	0.0
S	0.02
O (difference)	41.2
Other properties	
HHV, MJ/kg	20.67
LHV, MJ/kg	19.34
Bulk density, kg d.b./m^3[b]	293
Sintering temp. of ash, °C	>1000

[a] wt% d.b. = weight percent dry basis.
[b] 1 litre batch, not shaken.

Table 4 – MTG yield structure for a fixed-bed reactor given per kg of pure methanol input to DME reactor [49].

Component name	Formula	Molar mass	kmol/kgMeOH
Hydrogen	H_2	2.02	0.00001049
Water	H_2O	18.02	0.03137749
Carbon monoxide	CO	28.01	0.00000446
Carbon dioxide	CO_2	44.01	0.00001390
Methane	CH_4	16.04	0.00019586
Ethene	C_2H_4	28.05	0.00000473
Ethane	C_2H_6	30.07	0.00005067
Propene	C_3H_6	42.08	0.00002055
Propane	C_3H_8	44.10	0.00042752
1-Butene	C_4H_8	56.11	0.00008593
n-Butane	C_4H_{10}	58.12	0.00019381
i-Butane	C_4H_{10}	58.12	0.00062811
Cyclopentane	C_5H_{10}	70.13	0.00001514
1-Pentene	C_5H_{10}	70.13	0.00014015
N-pentane	C_5H_{12}	72.15	0.00008633
I-pentane	C_5H_{12}	72.15	0.00075797
Gasoline[a]	C_7H_{16}	100.2	0.00283472

[a] Gasoline is assumed to be represented as n-heptane (C_7H_{16}).

The conversion of methanol to gasoline proceeds essentially according to reaction

$$nCH_3OH \rightarrow (CH_2)_n + nH_2O, \quad (6)$$

where $(CH_2)_n$ represents a wide range of paraffinic and aromatic hydrocarbons produced in the gasoline synthesis step [44]. The process design developed for this paper is based on the conventional two-step methanol-to-gasoline (MTG) process, originally developed by Mobil in the 1970's [45–47]. The conversion of syngas to methanol is analogous to what has been described in section 3.3, although it is assumed that less distillation is required when preparing raw methanol for gasoline production. The MTG process begins by pumping methanol feed to 2.27 MPa followed by vaporisation and superheating to 297 °C in heat exchange with the hot reactor effluent. An adiabatic fixed-bed dehydration reactor is used to convert the feed to an equilibrium mixture of methanol, DME and water. The effluent exits the reactor at 409 °C and 2.17 MPa, is admixed with recycle gas and fed to a second reactor where it is converted to gasoline [47]. A large recycle stream is needed[7] to limit the outlet temperature of the adiabatic gasoline reactor to 400 °C. To control the build-up of inerts in the synthesis loop some gas needs to be continuously purged from the recycle flow, which is then transferred to combustion.

The equilibrium conversion of methanol to DME and water is simulated with Aspen using Soave-Redlich-Kwong (SRK) equation of state model. Due to the proprietary nature of the process, very little information has been published about the performance of the gasoline reactor, thus complicating the process simulation effort. However, a RYield block was chosen to simulate the gasoline synthesis (with SRK) using product yield structure (See Table 4) scrutinized by Larson et al. [49] based on the work of Barker et al. [50] and Schreiner [51].

The gasoline reactor effluent is condensed and separated into water, raw gasoline, purge and recycle gas streams. The raw gasoline is then fractionated by distillation to produce finished gasoline blendstock containing less than 2 wt% durene together with a byproduct stream resembling liquefied petroleum gas (LPG) [15,42]. It is assumed that the recovery of waste heat provides the needed utilities for the upgrading, leading to zero net parasitic utilities demand for the area.

3.5. *Carbon dioxide capture*

Carbon dioxide is available at almost inexhaustible quantities in the atmosphere where it can be captured either directly with an industrial process or indirectly via plant matter [52]. Capturing carbon dioxide from air is fairly easy in chemical sense, but as atmospheric CO_2 is very dilute[8] (0.04%), the development of a practical system for capturing commercially significant quantities has proved challenging [53].

In a direct air capture (DAC) plant diluted CO_2 is dissolved into a solution or solid sorbent from which a concentrated stream of CO_2 is produced in the regeneration phase. Currently proposed systems are often based on NaOH sorbent followed by regeneration with chemical caustic recovery [4]. The long term cost estimates[9] for such direct air capture systems are about 115 €/tCO_2 ± 40 €/tCO_2 [52,4]. Despite the high costs, it deserves to be noted that DAC has the unique ability to provide abatement across all economic sectors at a fixed marginal cost [52]. In other words, the cost of DAC represents the upper limit for any conceivable CO_2 abatement strategy.

[7] A molar recycle to fresh feed ratio of 7.5:1 is assumed, a design value for the New Zealand commercial unit [48].

[8] 402 parts per million by volume as of May 2014. Based on data collected by continuous atmospheric monitoring at the Mauna Loa Observatory in Hawaii, USA. See www.co2now.org.

[9] Based on US$150/t$CO_2$ ± $50/t$CO_2$.

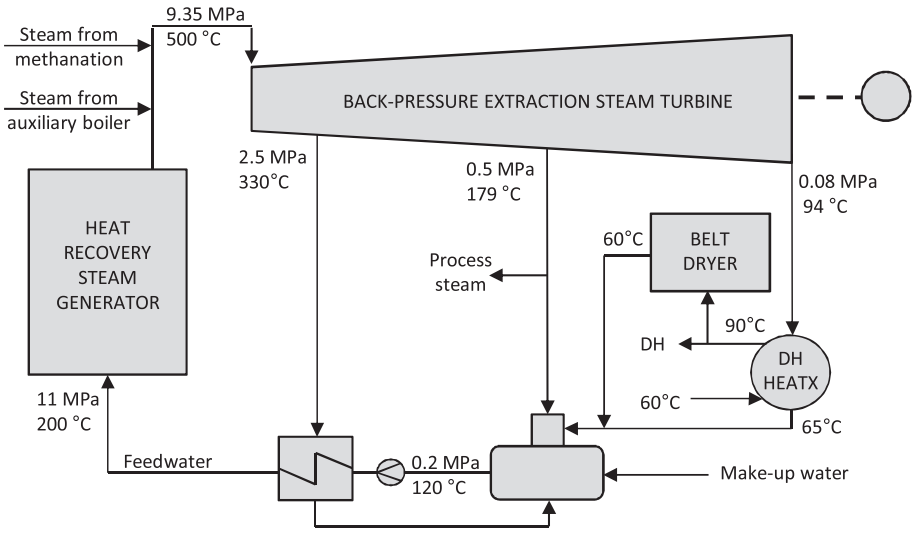

Fig. 3 – Simplified layout of the steam cycle design.

A third possible source for carbon dioxide, in addition to direct and indirect capture from air, is to utilise exhaust CO_2 from industrial plants [24] Today, carbon dioxide is routinely separated at some large industrial plants and also at several small power plants. The capture costs are estimated to be around 40 €/tCO_2 [54,55] for new supercritial pulverised coal boilers and around 50 €/tCO_2 for new natural gas combined cycle plants [55] both employing an amine-based system for post-combustion CO_2 capture, excluding the cost of transport and storage.[10] However, it is acknowledged that new or improved methods of CO_2 capture have the potential to significantly reduce the cost of capture and required energy use [56].

3.6. *Carbon dioxide hydrogenation*

Carbon dioxide can be used as a C_1 building block for making organic chemicals, materials and fuels [57]. However, it is considered less favourable feedstock for fuels production than carbon monoxide due to more intensive use of resources (energy, H_2, more reaction steps, etc.) [28]. Presently the use of CO_2 as chemical feedstock is limited to few industrial processes such as urea synthesis and its derivatives, salicylic acid and carbonates [28].

Production of methane from CO_2 via Sabatier reaction (3) is a well known route that can be realised using existing methanation catalysts. In addition, catalysts allowing direct hydrogenation of CO_2 to methanol via reaction (4) have been developed, and pilot-scale plants based on this technology demonstrated [58–62]. However, when methanol is synthesised from a mixture of CO_2 and H_2 instead of syngas, a greatly reduced yield is reported [31,26,63]. In addition, almost one third of the input H_2 is consumed to produce byproduct water.

Although in practise routes via CO are preferred, plant configurations developed for this paper assume that catalyst systems for CO_2 conversion are available and operate close to equilibrium conversion with the same catalyst productivity than commercial alternatives using carbon monoxide as the main feed.

3.7. *Electrolysis of water*

Hydrogen can be produced by passing an electric current through two electrodes immersed in water. In the process, water molecules are split to produce oxygen and hydrogen according to the following overall reaction:

$$2H_2O(l) \rightarrow 2H_2(g) + O_2(g). \quad (7)$$

Presently the production of hydrogen via electrolysis is mainly limited to small or special applications, while larger quantities are produced by steam reforming of natural gas or other fossil fuels. The most established and commercially available technology is based on alkaline electrolysers, while proton exchange membrane (PEM) electrolysis and solid oxide electrolysis cells (SOEC) are examples of more advanced and emerging systems [64]. SOEC electrolysers are most efficient but least developed. PEM electrolysers are more efficient than alkaline and do not have issues with corrosion or seals as the SOEC systems, but cost more than alkaline systems. Alkaline electrolysers have the lowest efficiency, but are the most developed and lowest in capital cost [65].

This paper examines hydrogen production via low temperature alkaline water electrolysis.[11] The system composes of electrodes, a microporous separator and an aqueous solution of water and 25–30 wt% of potassium hydroxide (KOH) as electrolyte [66]. The liquid electrolyte is not consumed in the reaction, but must be replenished over time to cover losses that occur during hydrogen recovery. Water is decomposed into hydrogen and OH^- in the cathode. The OH^- travels through the electrolytic material to the anode where O_2 is formed, while hydrogen is left in the alkaline solution and separated by a gas/liquid separator unit outside the electrolyser cell. Nickel with a catalytic coating, such as platinum, is

[10] Based on US$50/t$CO_2$ and US$60/t$CO_2$, respectively.

[11] Norsk Hydro's Atmospheric Type No. 5040 (5150 Amp DC).

Table 5 – Process simulation results for examined plant configurations.

Configuration		TN	TM	HN	HM	EN	EM
Carbonaceous inputs							
Biomass to dryer (moist. 50 wt-%)	MW (LHV)	100	100	100	100		
Biomass to gasifier (moist. 15 wt-%)	MW (LHV)	112	112	112	112		
Biomass dry feed	kg/s	5.9	5.9	5.9	5.9		
Captured and concentrated CO_2	kg/s					3.6	4.36
Oxygen balance							
On-site consumption, t/d		*280*	*324*	*280*	*324*		
Gasifier oxygen input	kg/s	2.3	2.3	2.3	2.3		
Reformer oxygen input	kg/s	0.9	1.4	0.9	1.4		
Air separation unit output, t/d		*280*	*324*	*280*	*324*		
Electricity balance							
On-site consumption, MW		−9.1	−12.4	−10.3	−13.9	−4.8	−7.3
Oxygen production	MW	−3.1	−3.6	−3.1	−3.6		
Oxygen compression	MW	−0.6	−0.7	−0.6	−0.7		
Feed screw and lock-hopper pres.	MW	−0.2	−0.2	−0.2	−0.2		
Feed drying	MW	−0.7	−0.7	−0.7	−0.7		
Syngas compression	MW	−3.0	−5.2	−2.5	−5.1		
Acid gas removal	MW	−1.0	−0.9	−0.8	−0.8		
Electrolytic H_2 compression	MW			−1.9	−1.6	−3.7	−5.4
CO_2 compression	MW					−0.9	−1.6
Synthesis	MW	0.0	−0.3	0.0	−0.4		
Power Island (all blowers + pumps)	MW	−0.2	−0.3	−0.2	−0.3		
Miscellaneous	MW	−0.4	−0.6	−0.4	−0.6	−0.2	−0.3
Turbine gross output, MW		*7.7*	*8.3*	*8.4*	*8.6*		
Steam balance							
On-site consumption (excl. synthesis), kg/s		*7.2*	*8.0*	*6.7*	*7.6*		
Gasifier	kg/s	2.4	2.4	2.4	2.4		
Reformer	kg/s	0.9	1.4	0.9	1.4		
AGR solvent regeneration	kg/s	1.2	1.1	0.9	0.9		
Deaerator	kg/s	1.2	1.4	1.1	1.3		
Economiser	kg/s	1.5	1.7	1.4	1.7		
Gross production, kg/s		*12.5*	*16.1*	*13.3*	*17.0*		
Gasification plant (9.35 MPa, 500 °C)	kg/s	9.3	10.6	8.6	10.2		
Auxiliary boiler (9.35 MPa, 500 °C)	kg/s	0.6	2.0	0.6	2.4		
Admission steam (4.3 MPa, 255 °C)	kg/s		3.5		4.4		2.2
Admission steam (9.35 MPa, 500 °C)	kg/s	2.7		4.1		2.9	
Turbine extractions, kg/s		*7.2*	*4.5*	*6.7*	*3.2*		
HP steam (2.5 MPa, 330 °C)	kg/s	1.5	1.7	1.4	1.7		
IP steam (0.5 MPa, 179 °C)	kg/s	5.7	2.8	5.3	1.5		
Turbine back pressure	MPa	0.08	0.08	0.08	0.08		
By-products							
Char							
Heating value (LHV)	MJ/kg	7.0	7.0	7.0	7.0		
Energy	MW (LHV)	2.1	2.1	2.1	2.1		
Purge gas							
Heating value (LHV)	MJ/kg		11.5		13.0		14.5
Energy	MW (LHV)		4.9		6.1		3.7
Alkaline electrolysis							
Electricity input	MW			65.8	35.4	129.6	116.1
Hydrogen output	kg/s			0.34	0.18	0.67	0.60
Oxygen output	kg/s			2.70	1.45	5.32	4.76
Energy outputs							
Methanol	MW (LHV)		60.0		78.3		60
SNG (methane)	MW (LHV)	66.7		100.3		66.7	
Net electricity output	MW_e	−1.4	−4.0	−67.7	−40.7	−134.4	−123.4
District heat (from steam cycle)	MW_{th}	3.1	12.3	8.0	16.6		
District heat (from methanation)	MW_{th}	7.4		13.3		12.1	

the most common cathode material, while for the anode nickel or copper metals coated with metal oxides, such as manganese, tungsten or ruthenium, are used [65].

Commercial systems are typically run with current densities in the range of 100–300 mA/cm^2. The product hydrogen and oxygen can be assumed to be of 100% purity due to the very low concentration of contaminants [67]. The system efficiency of an alkaline electrolyser, defined as hydrogen output (LHV) divided by electrical energy consumed by the electrolysis system, is set to 62% (74% HHV) [67].

3.8. Steam system

All thermochemical and hybrid plant configurations considered in this paper feature a back-pressure steam turbine design that co-generates electricity and district heat (DH) and has live steam parameters of 9.35 MPa and 500 °C. A simplified layout of the steam cycle is illustrated in Fig. 3. Steam is produced from syngas cooling and in the auxiliary boiler where unconverted carbon from gasifier (filter dust) and unconverted syngas from synthesis (if available) are combusted. Plant configurations that feature syngas methanation produce also superheated steam as a byproduct that is directly usable in the turbine as admission steam. The synthesis exotherm from the methanol plants is utilised to produce saturated admission steam at 4.3 MPa and 255 °C that is directly used to satisfy part of the plant's on-site steam consumption. The first steam extraction point from the turbine is fixed at 2.5 MPa and 330 °C and used to preheat the HRSG feedwater to 200 °C. The second extraction point is fixed at 0.5 MPa[12] and 179 °C and used to supply steam for the gasifier, reformer, deaerator and AGR solvent regeneration. Rest of the steam is extracted at the turbine's back-pressure (0.08 MPa), condensed and used to produce hot water at 90 °C. The hot water provides heat for drying the wet biomass feed and the rest is sold to a near-by district heating grid.

All the examined plant configurations are designed as self-sufficient in terms of heat and steam, while electricity is balanced with the electric grid. Design choices have notable impact to the electricity and steam outputs of the steam system. In this paper, the goal for the steam system design has been simplicity and low capital cost, even if at the cost of lower performance. Comparable results for synthetic biofuel plants equipped with a higher performance (and supposedly more expensive) steam system are available in Ref. [36].

4. Performance analysis

4.1. Mass and energy balances

Mass and energy balances have been simulated for all examined plant configurations. The thermochemical and hybrid plants are based on 100 MW (LHV) input of wet biomass, while fuel output for the electrochemical plants is set equal with the corresponding thermochemical plants.

The main simulation results are summarised in Table 5. With thermochemical plant configurations, 66.7 MW of natural gas or 60.0 MW of methanol can be produced from 100 MW of wet biomass. Producing the same fuel outputs with electrochemical configurations requires 129.6 MW of electricity and 3.6 kg/s of CO_2 (natural gas plants), or 116.1 MW of electricity and 4.36 kg/s of CO_2 (methanol plants). When syngas production is boosted with the maximum amount[13] of electrolytic hydrogen (hybrid configurations) natural gas output increases by 50 % to 100.3 MW and methanol output by 31 % to 78.3 MW. The greater increase in natural gas production is due to the larger stoichiometric hydrogen requirement in relation to methanol production.

The net electricity output is negative for all examined plant configurations. However, the on-site electricity consumption of thermochemical plants is fairly comparable with on-site generation and net electricity surplus could be achieved with a (more expensive) steam cycle designed for higher performance as discussed in section 3.8. For the electrochemical and hybrid plants, electricity consumption of the alkaline electrolysis clearly dominates electricity balance, leading to deeply negative net outputs. As already noticed, more electricity (i.e. hydrogen) is required to produce natural gas than methanol. However, the difference in net electricity requirement between methanol and natural gas production is smaller for the electrochemical than for hybrid configurations. This can be explained by the increased role of compression work in electrochemical plants (feed gases starting at atmospheric pressure, while gasifier operates at 0.4 MPa) that level down differences in electricity consumption during syngas conversion.[14]

In addition to synfuel, most plant designs co-produce district heat at 90 °C. The district heat outputs for methanol plants are 12.3 MW (TM) or 16.6 MW (HM) depending on the configuration. For natural gas configurations some DH can also be produced from the methanation area in addition to steam cycle. The combined DH output from such plants is 10.5 (TN), 21.3 (HN) or 12.1 MW (EN) depending on the configuration. As the electrochemical configurations omit steam cycle, district heat is available only from plants producing natural gas.

Differences in steam system designs are clearly visible from the simulation results: Less intermediate pressure extraction steam from turbine is required for methanol plants as part of the on-site consumption is satisfied directly with saturated steam produced from the methanol reaction's exotherm. In addition, auxiliary boiler's steam output is smaller for natural gas plants than for methanol plants because purge gas is not formed in methanation.

The gasifier's oxygen consumption is constant for all configurations, but the amount of oxygen required in reforming depends on the targeted methane conversion. For purely thermochemical plants, the combined oxygen requirement is 3.2 kg/s (natural gas) or 3.7 kg/s (methanol). Oxygen is also produced as a co-product with hydrogen in configurations that feature alkaline electrolysis. The net oxygen output for hybrid configurations is −2.3 kg/s (HM) or −0.5 kg/s (HN) and for the electrochemical plants, where oxygen is not consumed by the process, the net oxygen output is 4.8 kg/s (EM) and 5.3 kg/s (EN).

In this paper, gasoline production is treated as a post-processing step that may or may not take place at the same site with methanol production. Simulation results for the methanol-to-gasoline (MTG) conversion step are given in Table 6 together with the overall performance results for the total conversion path from feedstock to gasoline via methanol. Thermochemical and electrochemical configurations both produce 60.0 MW of methanol from which 51.8 MW of

[12] 0.1 MPa higher than gasification pressure to allow pressure drop for the inlet valves.

[13] Complete bypass of the water-gas shift reactor.

[14] Methanol production requires less hydrogen than methanation but takes place at much higher pressure.

gasoline and 6.1 MW of LPG can be further produced via MTG process. From the 78.3 MW of methanol produced by the hybrid process 67.6 MW of gasoline and 7.9 MW of LPG can be produced. Some high pressure saturated steam is also generated from the gasoline reaction's exotherm, which can be sold as process steam or utilised as an admission steam if a steam cycle is available nearby.

4.2. *Energy input breakdowns*

Fig. 4 illustrates energy input breakdowns for each of the examined plant configurations. The simulation results, presented in Tables 5 and 6, have now been rescaled to fit a situation where the fuel output is 200 MW (LHV) for all plants. For the thermochemical configurations, following amounts of wet biomass is required to produce 200 MW of synthetic fuel: 300 MW (TN), 333 MW (TM) or 386 MW (TG). A notable drop in biomass requirement is achieved with hybrid configurations where biomass is partly replaced with electricity. The feedstock requirements are: 199 and 131 MW (biomass and electricity) for natural gas, 255 and 90 MW for methanol, 296 and 105 MW for gasoline production. For pure electrochemical designs, where biomass is fully replaced with electricity and carbon dioxide, 200 MW of synthetic fuel can be produced from 389 MW (EN), 387 MW (EM) or 448 MW (EG) of electricity and 10.8 kg/s (EN), 14.5 kg/s (EM) or 16.8 kg/s (EG) of carbon dioxide.

5. Cost analysis

The capital cost and the cost of producing fuel are estimated for each of the modelled plant configurations using a set of simplified economic assumptions. The overall economics are evaluated under alternative feedstock price assumptions from the perspective of a synthetic fuel producer in terms of euros (€) per gigajoule (GJ). The value of the analysis lies not in the absolute accuracy of individual results, but in the fact that all plant designs have been consistently evaluated under the same set of technical and economic assumptions.

It is acknowledged that the use of 'unproven technologies' in a plant is likely to cause increased capital costs and decreased plant performance. In fact, conventional estimating techniques, like the one used here, have been found out to routinely understate the costs of innovative technologies [68]. Thus, it is highly likely for the first commercial scale installations of these plants to be more expensive than estimated here, although the probable level of misestimation is difficult to assess in advance. In any case, the aim of this paper is to evaluate and understand the long-term commercial viability of the examined plant designs, i.e. when all plant components have already reached commercial maturity. Methods suitable for the analysis of first-of-a-kind plant costs have been proposed, perhaps the most famous being that based on empirical formulae developed by RAND Corporation [68], but carrying out such analysis is out of the scope of this paper.

Table 6 – Simulation results for upgrading the methanol to synthetic gasoline with the MTG process.

Configuration		TG	HG	EG
Results for gasoline synthesis				
Methanol input	MW	60.0	78.3	60.0
Inlet pressure to synthesis	MPa	2.3	2.3	2.3
Outlet pressure from synthesis	MPa	1.7	1.7	1.7
DME reactor inlet temp.	°C	297	297	297
DME reactor outlet temp.	°C	407	407	407
Once-through MeOH conversion	%	82	82	82
MTG reactor outlet temp.	°C	400	400	400
Recycle/MeOH	mol/mol, wet	7.5	7.5	7.5
Purge gas energy flow	MW	3.0	3.9	3.0
Total MeOH conversion	%	100	100	100
Gasoline LHV	MJ/kg	44.7	44.7	44.7
LPG LHV	MJ/kg	45.9	45.9	45.9
Net electricity output	MW	−0.2	−0.2	−0.2
Net steam output	kg/s	2.2	2.8	2.2
Results for gasoline plant configuration				
Gasoline energy	MW	51.8	67.6	51.8
LPG energy	MW	6.1	7.9	6.1
Net electricity output	MW	−4.2	−40.9	−123.6
District heat (from steam cycle)	MW	12.3	16.6	
Net steam output	MW	2.2	2.8	2.2

5.1. *Scale of operations*

The overall costs of synthetic fuel production are subject to economies of scale, which creates an incentive to build large conversion plants. However, due to limitations in the availability of biomass feedstock, biofuel plants are confined to a much smaller scale than modern synfuel plants based on coal, shale or natural gas conversion. For example, the largest pulp and paper mills in Europe process annually about one million tons of dry biomass that relates to about 600 MW of constant energy flow,[15] which in this paper is considered as the maximum size of biomass conversion plants.

Another possible way of estimating proper scale for a biomass conversion plant would be to consider maximal byproduct utilisation. In northern Europe, a typical annual heat demand for district heating networks, situated at or close to wooded territories, range from 450 to 1700 GWh/a with peak loads between 150 and 650 MW.[16] However, a better indicator for scale would be the minimum continuous load (summer load), which ranges from 50 to 150 MW [69].

In observance of these limitations, fuel output for all examined plants is set to 200 MW (see Table 4), which is large enough to attain some economies of scale, while keeping feedstock requirements under practical limits and ensuring complete utilisation of byproduct heat.[17]

[15] Assuming 8000 annual operating hours and 8.6 MJ/kg lower heating value for forest residues at 50 wt% moisture.

[16] The data is based on municipal DH networks situated in eastern Finland sampled from Ref. [69].

[17] When fuel output is set to 200 MW, biomass feedstock requirements for the examined plant configurations vary from 199 to 386 MW (TG having the largest) and DH outputs from 0 to 43 MW (HN having the largest).

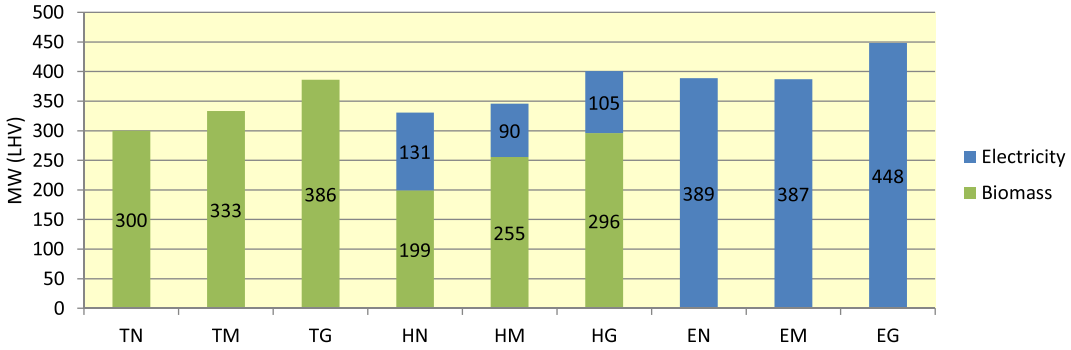

Fig. 4 – Feedstock requirements for all examined plant configurations producing 200 MW (LHV) of fuel. Only electricity used in the electrolyser is included.

5.2. *Reference equipment cost database*

Capital cost estimates provide the basis for evaluating prospective economics of synthetic fuel production. The estimates are based on a self-consistent set of component level capital cost data assembled using literature sources, vendor quotes and discussions with industry experts. When data for a given equipment has been unattainable, costs have been estimated based on similar equipment and engineering judgement. All reference costs in the database (see Table 9) have been escalated to correspond with 2010 euros using Chemical Engineering's Plant Cost index[18] (CEPCI) to account for inflation.

Total plant cost (TPC) is defined as the "overnight" capital investment required to construct a plant, and total capital investment (TCI) is TPC plus interest during construction. The TPC includes all main equipment (with initial catalyst loadings) plus installation (labour), indirect costs (engineering and fees), project contingency and unscheduled equipment. These cost items are estimated with cost factors that are reported as a fraction of the (installed) equipment costs. Two different cost factor sets have been employed: higher for bare equipment and lower for whole subprocesses delivered on turn-key basis. Costs for unscheculed equipment are added to represent pumps, blowers and other small equipment not included in the cost database. Following values for cost factors[19] are used in this paper:

- Installation costs: low 15%, high 50%;
- Indirect costs: low 10%, high 15%;
- Project contingency: low 10%, high 30%;
- Unscheduled equipment: 10%.[20]

The allocation of the above factors with reference equipment costs is shown in Table 9.

Table 7 – Financial parameters employed in the cost analysis.

Financial parameters	
Annuity factor (10%, 20 a)	0.12
Annual O&M cost factor	0.04[a]
Annual operating hours	8000
Interest during construction	5%[a]
Investment support, M€	0
Values of inputs/outputs	
Biomass residue chips, €/GJ	5
District heat, €/GJ	8
Fuel gas, €/GJ	10
LPG, €/GJ	12
Electricity, €/GJ	14
Water, €/t	0
Oxygen, €/t	27
Steam, €/t	30
Carbon dioxide, €/t	40

[a] Fraction of Total Capital Investment.

5.3. *Methodology and parameters*

Accurate information of absolute equipment costs are often unavailable in the open literature. In observance of this limitation, the aim is set rather to estimate how relative costs compare among alternative systems with a reasonably high degree of confidence. The analysis lends from methodologies put forth and discussed in Refs. [72,6,70].

The annual capital charges are calculated from the TCI using 0.12 annuity factor, which corresponds with 10% interest and 20 years lifetime. The yearly operating and maintenance (O&M) costs[21] are assumed to be 4% of the TCI [73] and the plants are expected to run 8000 h per year (91% on-stream factor). Biomass is valued at 5 €/GJ (18 €/MWh).[22] Costs

[18] For more information, see: www.che.com/pci.

[19] Cost factors, except uncscheduled equipment, are based on averaged values for selected equipment derived from "Exhibit 3-41" Case 2 of Ref. [70].

[20] Factor taken from Wan [71].

[21] Following breakdown is assumed for the O&M: Personnel costs 0.5%, Maintenance & insurances 2.5%, Catalysts & chemicals 1%.

[22] Price for forest residues (thinnings, stumps and slash) and industry byproduct (sawdust and bark) traded for energy or heat production purposes in Finland. Source: FOEX Indexes Ltd.

Table 8 – Breakdown of LCOFs under economic assumptions summarised in Table 7.

Configuration	TN	HN	EN	TM	HM	EM	TG	HG	EG	
Biomass	7.5	5.0		8.3	6.4		9.7	7.4		€/GJ
CO_2			2.2			2.9			3.4	€/GJ
Electricity	0.3	9.4	28.2	0.9	7.3	28.8	1.1	8.5	33.4	€/GJ
District heat	−1.3	−1.7	−1.5	−1.6	−1.7		−1.9	−2.0		€/GJ
Steam							−1.3	−1.2	−1.3	€/GJ
Oxygen		−0.7	−2.2		−0.5	−2.1				€/GJ
Fuel gas							−0.6	−0.6	−0.6	€/GJ
LPG							−1.4	−1.4	−1.4	€/GJ
O&M	2.8	2.7	2.5	3.2	3.2	2.6	4.2	4.2	3.6	€/GJ
Capital charges	8.3	8.0	7.6	9.7	9.7	7.9	12.7	12.7	10.9	€/GJ
Levelised production cost	17.7	22.7	36.8	20.6	24.4	40.0	22.6	27.6	48.0	€/GJ
	63.6	81.7	132.6	74.1	87.7	144.1	81.3	99.4	173.0	€/MWh

related to buying or selling other feedstocks, byproducts[23] and utilities are summarised with other financial assumptions in Table 7.

The maximum size S_{max} of a single gasification train, containing all equipment between dryer and acid gas removal unit, is set to 200 MW of biomass feedstock (as received, LHV). For plant configurations having size $S > S_{max}$, two gasification trains are installed in parallel, both the size of S/2. Since multiple trains typically share some auxiliary equipment and installation labour for two equal units is likely to be less than twice the cost for a single unit, it is assumed that the installed cost for additional train is somewhat less than for the first train [73]. This idea is captured in the analysis with the following equation:

$$C_{mult} = C \times n^{0.9}, \tag{8}$$

where C_{mult} is the joint cost of multiple trains, C the cost of first train and n the number of trains [73].

5.4. *Capital cost estimates*

Individual cost scaling exponents (k) have been used to scale the reference capital costs (C_o) to a capacity that corresponds with simulation results (S) using a following relation:

$$C = C_0 \times \left(\frac{S}{S_0}\right)^k, \tag{9}$$

where S_0 is the scale of reference equipment and C the cost of equipment at the size suggested by simulation. The aggregated Total Capital Investment estimates, based on an underlying component-level costing, are shown in Table 10. The results are based on a "feasibility study" level of design engineering, which usually carries an accuracy of −15%/+30% [70].

The TCIs range from 363 to 611 M€ among the cases analysed. The gasoline configurations (TG, HG and EG) are the most capital intensive as they include all the components of a methanol plant[24] plus equipment required for the conversion of methanol to gasoline. For all end-products, thermochemical configurations have the highest and electrochemical the lowest TCIs. The TCIs for hybrid plants are only slightly lower than those for corresponding thermochemical plants. Differences in TCIs are smaller among plants producing natural gas (TN, HN and EN) than other fuels. This can be explained by the higher hydrogen requirement in comparison to methanol production (3 instead of 2 in CO hydrogenation and 4 instead of 3 in CO_2 hydrogenation) that increases the size and cost of alkaline electrolysis and H_2 compression systems in natural gas configurations.

5.5. *Production cost estimates*

The levelised cost of fuel (LCOF) production is then evaluated according to the following equation:

$$LCOF(€/GJ) = \frac{F + E + C + O - R}{P}, \tag{10}$$

where

- F is the cost of feedstock (biomass residues and carbon dioxide),
- E the cost of electricity,
- C the capital charges,
- O the operating and maintenance costs and
- R the revenue from selling byproducts (district heat, steam, electrolytic oxygen, purge gas and LPG).[25]

The sum of these annual costs (€/a) is divided by P, which is the annual output of fuel (GJ/a) from the plants. When defined in this way, the LCOF (€/t) indicates the break-even price for the produced fuel under the technical and economic parameters assumed.

The contribution of different cost categories to the total LCOFs are shown in Table 8. Among the cases analysed, the LCOFs range from 18 to 48 €/GJ (64–173 €/MWh). For thermochemical configurations (TM, TN, TG) the capital charges and cost of biomass feedstock make about an equal contribution to the LCOF, whereas for hybrid plants (HM, HN, HG) the main contributions come from capital charges, biomass feedstock and electricity. Electricity clearly dominates the production costs in the electrochemical cases and revenue

[23] The value of byproduct oxygen from the electrolyser is based on a levelised cost of oxygen calculated for a cryogenic air separation unit featured in plant configuration TM.

[24] With the exception of methanol distillation, that is cheaper for gasoline configurations, because water does not have to be completely removed from the MTG unit's feed.

[25] Steam, purge gas and LPG are sold only from MTG plant, oxygen is sold only from plants that feature electrolysis.

Table 9 – Reference equipment costs and cost factors employed in estimating Total Plant Costs.

Cost component	Cost scaling parameter	S_0	*UEC*, M€	*IC*	C_0,M€	*IDC*	*PC*	*k*	Notes
Civil works (buildings and structures)	Feedstock, MW_{th} (LHV, AR)	300			12.8	10%	30%	0.85	a
ASU (stand alone) incl. compressor	Oxygen output, t/h	76.6			36.8	10%	10%	0.50	b
Feedstock handling	Feedstock, MW_{th} (LHV, AR)	157			5.3	10%	10%	0.31	c
Belt dryer	Water removal, kg/s	0.342			1.9	10%	10%	0.28	d
Pressurised fluidised-bed gasifier	Dry matter input, kg/s	17.8	25.1	50%	37.7	15%	30%	0.75	a
Ceramic hot-gas filter	Syngas input, kmol/s	1.466	5.9	15%	6.8	15%	30%	0.67	a
Catalytic POX reformer	Syngas input, kmol/s	2.037	14.5	50%	21.8	15%	30%	0.67	a
WGS reactor stage	Feed to gasifier, MW_{th} (LHV)	1377			12.6	15%	30%	0.67	e
Scrubber	Syngas input, kmol/s	1.446			5.2	15%	30%	0.67	a
Syngas compresssor	Compressor work, MW_e	10			5.0	15%	30%	0.67	f
CO_2 compressor	Compressor work, MW_e	10			5.0	15%	30%	0.67	f
O_2 compressor	Compressor work, MW_e	10			5.7	15%	30%	0.67	f
H_2 compressor	Compressor work, MW_e	10			5.7	15%	30%	0.67	g
Rectisol incidentals compression	Compressor work, MW_e	10			5.0	15%	30%	0.67	f
Rectisol, sep. capture of CO_2 and H_2S	Nm_3/hr (NTP) input sourgas	200000	49.3	15%	56.7	15%	30%	0.63	h
Alkaline electrolysis	Electricity input, MW_e	223.5			121.9	15%	10%	0.93	i
Heat recovery steam generation system	Heat transferred, MW_{th}	43.6	5.2	15%	6.0	15%	30%	0.80	b
Auxiliary boiler & fluegas treatment	Boiler input, MW_{th}	5.9	5.1	15%	5.9	10%	10%	0.65	j,k
Steam turbine unit	Power out, MW_e	15.2	6.8	15%	7.8	10%	10%	0.85	j,l
CHP equipment	Power out, MW_e	15.2	4.1	15%	4.7	10%	10%	0.85	j,m
Other steam cycle equipment	Power out, MW_e	15.2	6.3	15%	7.3	10%	10%	0.85	j,n
Guard beds	Syngas, MW_{th}	260	5.2	15%	6.0	10%	10%	0.85	o
Methanol loop	Methanol, MW (LHV)	210	28.3	15%	32.5	10%	10%	0.67	o
Methanol distillation (minimal)	Methanol, MW (LHV)	210	4.2	15%	4.8	10%	10%	0.88	o, p
Methanol distillation (chem-grade)	Methanol, MW (LHV)	210	12.6	15%	14.5	10%	10%	0.88	o, p
Methanation	Methane, MW (LHV)	210	28.3	15%	32.5	15%	30%	0.67	q
MTG DME reactor	Gasoline, bbl/day	16 667			45.3	15%	30%	0.67	r
MTG gasoline reactor	Gasoline, bbl/day	16 667			101.2	15%	30%	0.67	r
MTG gasoline finisher	Gasoline, bbl/day	5556			8.2	15%	30%	0.67	r

Note: C_0 is the cost of a installed reference equipment of size S_0 in 2010 euros and *k* is the cost scaling factor. *UEC* stands for uninstalled equipment cost, *IC* for installation costs, *IDC* for indirect costs and *PC* for project contingency.
a – Author's estimate.
b – Taken from Larson et al. [76].
c – Costs taken from Ref. [77]. Scaling exponent calculated from two different size handling systems using feedstock energy flow as scaling parameter.
d – Reference capacity and costs taken from Ref. [77]. Scaling exponent calculated based on information on two different size dryers using water removal rate as scaling parameter. Drying capacity is increased by extending the dryer, which results in unusually low scaling factor (middle parts are fairly affordable in comparison to the ends of the dryer).
e – Extracted from Kreutz et al. [72]. This cost is for two-stage equipment that includes balance of plant (15%) and indirect costs (15%). It is assumed that a single-stage adiabatic sour shift reactor is 40% of the cost of a two-stage system (see Ref. [73]). Balance of plant and indirect costs have been removed.
f – Taken from Kreutz et al. [72].
g – It is likely that H_2 compressor is more expensive than O_2 compressor of similar size (electricity usage), but in the lack of reliable cost data an equal cost is assumed.
h – This cost is for a Rectisol system that separates CO_2 and H_2S to separate streams (separate column for each compound). Taken from Liu et al. [73].
i – Cost is for an alkaline electrolysis installation containing 96 individual NorskHydro's No. 5040 atmospheric electrolysers each having a capacity of 2.3 MW. Cost taken and scaling exponent fitted with data from Floch et al. [78].
j – Costs based on Thermoflow PEACE equipment cost estimator and discussions with experts at ÅF-Consult.
k – Includes boiler and related systems such as air preheaters, fans, ducts, stack, fabric filter et cetera.
l – Includes turbine, generator and electrification related to the delivery.
m – Includes items such as water cooled condenser, district heaters, deaerator et cetera.
n – Includes items such as tanks, pumps, fans, makeup water system, fuel & ash handling systems et cetera.
o – Taken from Refs. [79], originally based on a quotation from Haldor Topsøe in September 2003. Recalculated.
p – Cost (down) scaling factor from Wan [71].
q – Methanation system is assumed to have same cost as methanol loop (i.e. distillation equipment excluded) with equal fuel output.
r – Taken from Larson et al. [49]. Approximately one third of the raw gasoline from MTG reactors is processed through finisher.

received from selling byproducts is small in comparison to the main cost items for all cases analysed. For each product, thermochemical plants have the lowest and electrochemical plants the highest LCOFs with hybrid configurations placing in between the two. For a given route, natural gas (SNG) is the cheapest and gasoline the most expensive to produce. It is interesting to note that for a given product, the configuration that has the highest investment has the lowest production

Table 10 – Total capital investment estimates for the examined plant configurations each producing 200 MW (LHV) of fuel.

Configuration	TN	HN	EN	TM	HM	EM	TG	HG	EG
Installed equipment cost									
Civil works	13	9		14	11		16	13	
Oxygen production	25	20		28	25		30	27	
Feedstock pretreatment	15	11		16	14		16	15	
Gasification	42	28		45	37		51	41	
Hot-gas cleaning	33	21		37	31		41	34	
CO shift	6	4		6	5		7	6	
Scrubber	7	5		8	7		9	8	
Syngas compression	7	4		10	8		11	9	
Acid gas removal	39	28		42	34		46	37	
Alkaline electrolysis		74	204		53	203		60	233
HRSG, boiler and steam cycle	45	33		54	44		60	49	
Additional syngas compression				3	3		3	3	
H_2 compression		3	6		3	8		3	9
CO_2 compression			2			3			4
Guard beds and methanol loop				37	37	37	41	41	41
Distillation (minimal)							5	5	5
Distillation (chemical-grade)				14	14	14			
Guard beds and methanation	37	37	37						
MTG synthesis							67	67	67
Sum of installed equipment cost	**269**	**278**	**249**	**314**	**326**	**266**	**403**	**418**	**359**
Indirect costs	34	25	37	40	34	37	53	46	52
Contingency	52	36	34	60	50	29	85	74	52
Unscheduled equipment	27	28	25	31	33	27	40	42	36
Total plant cost	**381**	**367**	**345**	**445**	**442**	**359**	**581**	**581**	**498**
Interest during construction	19	18	17	22	22	18	29	29	25
Total capital investment	**400**	**385**	**363**	**467**	**464**	**377**	**611**	**610**	**523**

cost and vice versa. This can be explained by the relative affordability of biomass residues in comparison to electricity under the assumptions made in this paper. The main results have been visualised in Fig. 5 that summarises TCIs and LCOFs for each of the examined plant configurations.

5.6. *Sensitivity analysis*

Cost implications of alternative feedstock prices are then investigated. Fig. 6 shows production costs for all examined plant configurations as a function of electricity price while keeping the cost of biomass and carbon dioxide constant at 5 €/GJ (18 €/MWh) and 40 €/t, respectively. All gasoline (MTG) plants are indicated with blue (in web version), methanol plants with red (in web version) and natural gas (SNG) plants with green (in web version) lines. In addition, the lines are continuous for thermochemical plants, dashed for hybrid plants and dotted for electrochemical plants. As expected, the LCOFs for the thermochemical plants are fairly unsensitive to changes in the cost of electricity due to their low net electricity consumption. When the price of electricity changes by 1 €/GJ, it causes a change in the LCOF that is, on average, 0.6 €/GJ for hybrid and 2.2 €/GJ for electrochemical plants. In addition, it can be seen that the costs for hybrid plants are lower in comparison to corresponding thermochemical plants producing the same fuel when the price of electricity is below 6 €/GJ (22 €/MWh). For electrochemical configurations this price threshold is 4 €/GJ (14 €/MWh). It should be noted that these required threshold values are markedly lower than the

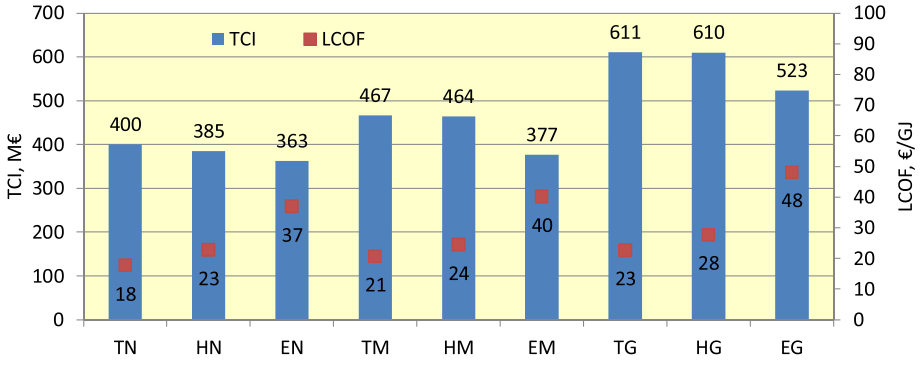

Fig. 5 – Summary of total capital investments (TCIs) and fuel production costs (LCOFs) for plants producing 200 MW (LHV) of fuel.

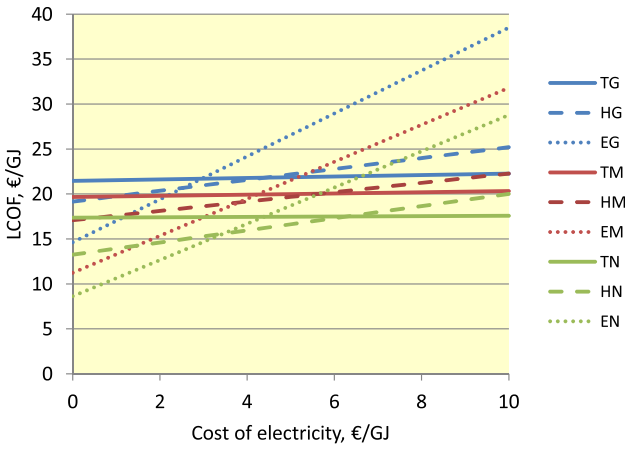

Fig. 6 – Levelised cost of fuel production (LCOF) for the examined plant configurations as a function of the electricity price.

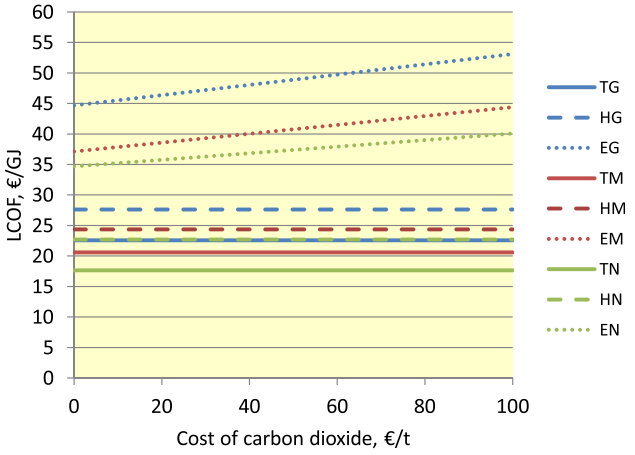

Fig. 7 – Levelised cost of fuel production (LCOF) for the examined plant configurations as a function of the carbon dioxide price.

current EU27 average prices 16–20 €/GJ (58–72 €/MWh) paid by the chemical industry.[26]

A similar analysis is performed as a function of carbon dioxide price while keeping the cost of biomass and electricity constant at 5 and 14 €/GJ, respectively (see Fig. 7). The costs of thermochemical and hybrid plants remain unchanged (because external CO_2 not used), but every 10 €/t change in the price of CO_2 causes, on average, a 0.7 €/GJ change in the LCOF for electrochemical plants. Somewhat surprisingly, even zero cost carbon dioxide would not be enough to make electrochemical plants more feasible in comparison to thermochemical configurations.

Cost implications of alternative biomass feedstock price are also investigated while keeping the cost of electricity and carbon dioxide constant at 14 €/GJ (50 €/MWh) and 40 €/t, respectively (see Fig. 8). The LCOFs of electrochemical plants

[26] Average prices for chlorine and ammonia sectors taken from Refs. [74], based on data from Centre for European Policy Studies.

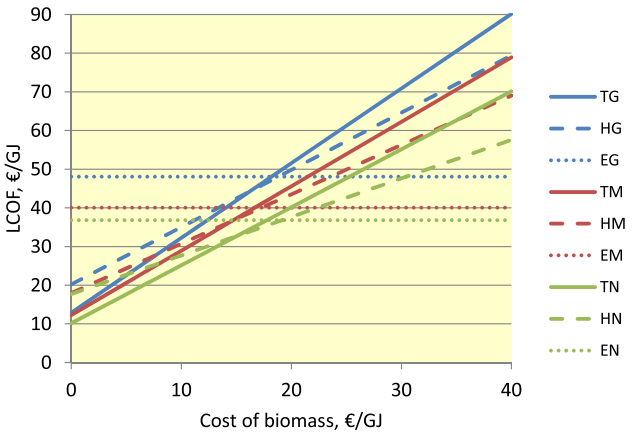

Fig. 8 – Levelised cost of fuel production (LCOF) for the examined plant configurations as a function of the biomass price.

are naturally unsensitive to changes in the cost of biomass feedstock. Hybrid and thermochemical plants are almost equally sensitive, although the slopes for thermochemical plants are steeper. When the price of biomass feedstock changes by 1 €/GJ, it causes a change in the LCOF that is, on average, 1.7 €/GJ for thermochemical and 1.3 €/GJ for hybrid plants. According to the results, purely thermochemical plants have lower production costs than corresponding hybrid plants producing the same fuel when the price of biomass stays under 14 €/GJ (50 €/MWh). For purely electrochemical configurations this threshold biomass feedstock price is about 17 €/GJ (61 €/MWh).

5.7. *Preconditions for electrolytic hydrogen*

The threshold electricity price that makes hybrid configurations more feasible than thermochemical plants was found to be 6 €/GJ. For purely electrochemical plants this value was found to be about 4 €/GJ. Using these electricity prices, the production cost of hydrogen is calculated to be 14 €/GJ for hybrid plants and 11 €/GJ for electrochemical plants. Therefore, when hydrogen is produced at a lower cost than these values, hybrid and electrochemical configurations become more feasible in comparison to thermochemical plants.

If the desire is to run the electrolysis only during times of excess renewable electricity, the impact of intermittant production to the levelised cost of hydrogen (LCOH) calls for additional analysis. This is carried out by calculating those electricity prices that maintain these threshold hydrogen prices (LCOH 14 and 11 €/GJ) at different annual operating hours, indicated by an on-stream factor (100% on-stream factor = 8766 h/a).

These results are illustrated in Fig. 9. It can be seen how the LCOHs gradually become more and more sensitive to the price of electricity as the on-stream factor becomes smaller. For both threshold values, there is a point on the axis where the average price of electrolyser feedstock (electricity) must go negative in order to maintain the fixed LCOHs as the annual operating hours continue to decrease: for the hybrid processes this happens at 40% (3530 h/a) and for electrochemical plants

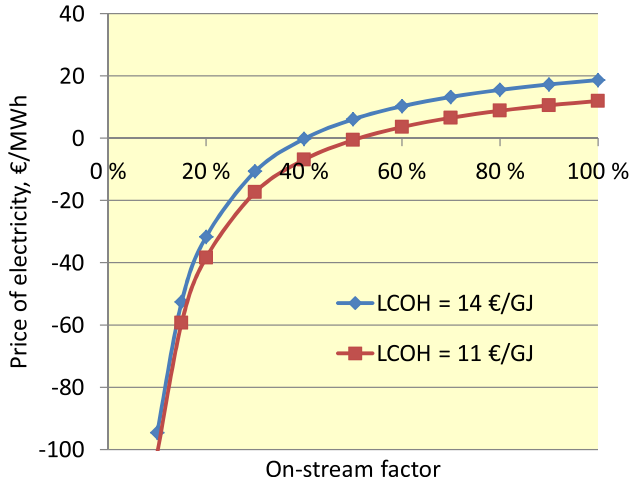

Fig. 9 – Electricity prices for an alkaline electrolysis system having a levelised cost of hydrogen (LCOH) of 14 or 11 €/GJ as a function of the on-stream factor.

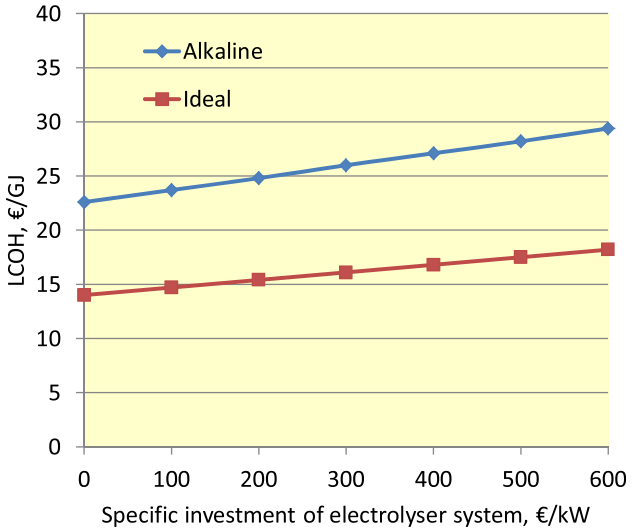

Fig. 10 – Levelised cost of hydrogen production (LCOF) for alkaline (system efficiency 62% (LHV)) and ideal (100%) electrolyser systems as a function of specific investment cost.

at 51% (4490 h/a). For on-stream factors smaller than 20%, the LCOHs become highly sensitive to the price of electricity. For example, if the electrolyser would operate only 10% of the year (877 h) the average price of electricity would need to be −91 €/MWh and −97 €/MWh to keep LCOHs at 14 €/GJ and 11 €/GJ, respectively.

Lastly, the impact of the electrolyser's investment cost is analysed. Fig. 10 shows LCOHs as a function of the specific investment cost while keeping the price of electricity and annual operating hours constant at 14 €/GJ and 8000 h, respectively.[27] The results are calculated for an alkaline electrolyser having a system efficiency of 62% (LHV) and also for an 100% efficient 'ideal' electrolyser.

When the specific investment cost changes by 100 €/, it causes a change in the LCOH that is 1.1 €/GJ for an alkaline electrolyser and 0.7 €/GJ for an 'ideal' electrolyser. Somewhat surprisingly, the target hydrogen prices (14 and 11 €/GJ) can not be reached even with an 100% efficient electrolyser system, running 8000 h annually and having zero investment cost.

6. Conclusions

A detailed and transparent analysis on the performance and costs of producing synthetic fuels from biomass, carbon dioxide and electricity has been presented, based on technologies that are either commercially available or at the very least successfully demonstrated at precommercial scale. The overall economics were evaluated from the perspective of a synthetic fuel producer in terms of euros (€) per gigajoule (GJ). The costs were:

- 18 €/GJ (natural gas), 21 €/GJ (methanol) and 23 €/GJ (gasoline) for purely thermochemical plants;
- 23 €/GJ (natural gas), 24 €/GJ (methanol) and 28 €/GJ (gasoline) for hybrid plants;
- 37 €/GJ (natural gas), 40 €/GJ (methanol) and 48 €/GJ (gasoline) for electrochemical plants.

For a given end-product, the lowest costs were associated with thermochemical production from forest residues, while the highest costs were associated with electrochemical production from carbon dioxide and electricity. The hybrid plants were found capable of producing fuels at a lower cost than purely electrochemical plants, but not lower than purely thermochemical plants. For all production routes, natural gas was the cheapest fuel to produce, followed by methanol and gasoline. However, out of the examined options, gasoline is the only fuel that can be readily consumed in the current transportation infrastructure without limitations, and costs related to the required modifications in vehicles and/or fuel distribution infrastructure were not included in the costs of natural gas and methanol.

It should be noted that the production costs for all the examined configurations are higher than the current price of fossil gasoline of about 15 €/GJ[28] and sustained subsidies either in the form of investment support, mandates or carbon price is required to make these processes economically feasible.

An analysis of the impact of feedstock prices to fuel production costs suggest that the above findings are generally robust. The following results were derived from sensitivity analysis:

- Electricity at the cost of 4 €/GJ (14 €/MWh) or lower is required to make electrochemical plants more feasible

[27] The value of byproduct oxygen is not considered as it was already included when the target LCOH values were calculated.

[28] Based on $100/bbl crude, $14/bbl refining margin and 1.3 €/$ exchange rate.

than corresponding thermochemical plants; for hybrid plants this threshold electricity price is 6 €/GJ (22 €/MWh).
- Zero cost CO_2 feedstock is not enough to make electrochemical plants more feasible than thermochemical or hybrid plants.
- Thermochemical plants are more feasible than corresponding hybrid plants when the cost of biomass feedstock is less than 14 €/GJ (50 €/MWh). For purely electrochemical plants this threshold biomass feedstock price is 17 €/GJ (61 €/MWh).

An analysis of the economic preconditions of using electrolytic hydrogen for synthetic biofuels production attests for the importance of long annual operating hours associated with continuous availability of low-cost renewable electricity:

- If electrochemical plants operate less than 4500 h annually, negative electricity prices are needed to make them more feasible than corresponding thermochemical plants. For hybrid plants this threshold value is 3500 h/a.
- Continuosly operating electrochemical plants using an electrolyser system having zero investment cost and 100% efficiency are less feasible than thermochemical plants under the assumed performance and cost parameters.

According to these findings, power-to-fuels concepts, despite their exciting technical potential, seem to be characterised by high overall costs under practical financial assumptions. From the perspective of a synthetic fuel producer, thermochemical route from biomass was found to be substantially more feasible than electrochemical route from carbon dioxide and electricity. However, additional analysis should be carried out to explore whether feasibility of the hybrid process could be further improved by deeper integration or more sophisticated operational strategies.

Acknowledgements

The research leading to these findings was funded by VTT Technical Research Centre of Finland and Tekes the Finnish Funding Agency for Innovation.

Appendix A

In order to enable the reader to reproduce the performance and cost analysis presented in this paper, detailed process design parameters are given in Table A.11

Table A.11: Process design parameters for the examined plant configurations.

Item	Design parameters	Notes
Air separation unit	Oxygen delivered from ASU at 1.05 bar pressure. Oxygen product (mol-%): $O_2 = 99.5\%$, $N_2 = 0.5\%$, Ar = 0%. Power consumption 263 kWh/tonO_2.	a
Feedstock preparation and handling	Feeding screw power consumption 7 kJ/kg biomass. Lock-hopper inert gas consumption: 0.07642 $Nm^3/kg_{BIOMASS}$ for a double lock-hopper system that uses purge gas from LH to partly pressurise another LH. For a single lock-hopper system inert gas consumption 50% higher.	b
Atmospheric band conveyor dryer	Biomass moisture: inlet 50 wt-%, outlet 15 wt-%, hot water: $T_{IN} = 90$ °C, $T_{OUT} = 60$ °C, steam: 1 bar, 100 °C heat consumption 1300 kWh/ton$H_2O_{EVAP.}$, power consumption 32 kWh/$ton_{DRYBIOMASS}$-	c
Pressurised circulating fluidised-bed steam/O_2 gasifier	Heat loss = 1% of biomass LHV. $\Delta p = -0.2$ bar. Carbon conversion: 98%. Modelled in two steps with RStoic and RGibbs using Redlich-Kwong-Soave equation of state with Boston-Mathias modification (RKS-BM). Hydrocarbon formation (kmol/kg of fuel volatiles): $CH_4 = 6.7826$, $C_2H_4 = 0.4743$, $C_2H = 0.2265$, $C_6H_6 = 0.2764$. Tars modelled as naphthalene: $C_{10}H_8 = 0.0671$, All fuel nitrogen converted to NH_3. All other components assumed to be in simultaneous phase and chemical equilibrium.	d, e
Ceramic hot-gas filter	$\Delta p = -0.2$ bar. Inlet temperature 550 °C.	e
Catalytic autothermal partial oxidation reformer	Modelled as RGibbs using Redlich-Kwong-Soave equation of state with Boston-Mathias modification (RKS-BM). Phase and chemical equilibrium conversion for C_2+ and tar. Ammonia conversion restricted to 50%. Outlet temperature and CH_4 conversion: 957 °C & 95% or 850 °C & 35% depending on the case investigated. $\Delta p = -0.2$ bar-	d, e
Sour shift	$T_{OUT} = 404$ °C, Steam/CO = 1.8 mol/mol, $\Delta p = -0.2$ bar. Modelled as REquil using Redlich-Kwong-Soave equation of state with Boston-Mathias modification (RKS-BM). Equilibrium reactions: $CO + H_2O = CO_2 + H_2$, $T_{APPR.} = 10$ K. $COS + H_2O = CO_2 + H_2S$, $T_{APPR.} = 0$ K. $HCN + H_2O = CO + NH_3$, $T_{APPR.} = 10$ K.	f, e
Scrubber	Scrubbing liquid: water. T_{INLET} 200 °C. Two-step cooling: $T^1_{OUT} = 60$ °C, $T^2_{OUT} = 30$ °C. Complete ammonia removal. Modelled as Flash using Soave-Redlich-Kwong (SRK) equation of state model.	e

– (continued)

Item	Design parameters	Notes
Rectisol acid gas removal	100% H_2S capture, for CO_2 capture level see case designs. Utilities: Electricity (other than for refrigeration) = 1900 kJ/kmol (CO_2+H_2S); Refrigeration 3× duty needed to cause −12 K temperature change in the syngas; 5 bar steam = 6.97 kg/kmol (H_2S + CO_2).	g
Low-pressure methanol	$T_{REACTION}$ = 260 °C, P_{MAKE}-UP = 80 bar, Δp = −5 bar, Boiling-water reactor modelled with REquil using Soave-Redlich- Kwong equation of state (SRK). Equilibrium reactions: CO + $2H_2$ = CH_4O, $T_{APPR.}$ = 10 K; CO_2 + $3H_2$ = CH_4O + H_2O, $T_{APPR.}$ = 10 K.	e
High temperature methanation	Six adiabatic fixed-bed reactors connected in series and equipped with intercoolers. Pressure at system inlet = 15 bar, pressure at system outlet 11 bar. T_{INPUT} to reactors 300 °C. T_{OUTPUT} from the first reactor resctricted to 700 °C with steam dilution. Gas dried before feeding to last reactor. Syngas conversion to methane ≥99.5%. Equilibrium reactions: CO + $3H_2$ = CH_4 + H_2O, $T_{APPR.}$ = 20 K; CO_2 + $4H_2$ = CH_4 + $2H_2O$, $T_{APPR.}$ = 20 K. Reactors modelled as REquils using Soave-Redlich-Kwong (SRK) equation of state model.	e
Methanol-to-Gasoline	DME reactor: T_{IN} = 297 °C, T_{OUT} = 407 °C, P_{IN} = 23 bar, Δp = −1 bar, Boiling-water reactor modelled with REquil using Soave-Redlich-Kwong equation of state (SRK). Equilibrium reaction: $2CH_4O$ = C_2H_6O + H_2O, $T_{APPR.}$ = 30 K. Gasoline reactor: $T_{REACTOR}$ = 400 °C, P_{IN} = 22 bar, Δp = −1 bar, Modelled as REquil using Soave-Redlich-Kwong equation of state (SRK). Relative mass yields from 1 ton of raw product in the refining area are 880 kg of gasoline blendstock, 100 kg of LPG and 20 kg of purge gas.	h
Alkaline electrolysis	H_2 and O_2 purity 100%. Both delivered at atmosperic pressure and 25 °C, Electrolyser system efficiency = 62% (LHV).	e, i
Auxiliary boiler	Modelled as RStoic, Δp = −0.1 bar, Lambda = 1.20, Air preheat to 250 °C with fluegas	e
Heat exchangers	Δp/p = 2%; ΔT_{MIN} = 15 °C (gas-liq), 30 °C (gas–gas). Heat loss = 1% of heat transferred.	g
Heat recovery & Steam system	Flue gas T_{OUT} = 150 °C, feed water pressure 110 bar, steam drum blowdowns: 2% of inlet flow, Deaerator T_{OUT} = 120 °C.	e
Steam turbine	Inlet steam parameters: 93.5 bar, 500 °C; Extraction steam parameters: HP = 25 bar, 330 °C; LP = 5 bar, 179 °C; $\eta_{ISENTROPIC}$ = 0.78, $\eta_{GENERATOR}$ = 0.97, $\eta_{mechanical}$ = 0.98.	c,e,j
Compressors	Stage pressure ratio <2$\eta_{POLYTROPIC}$ = 0.85, η_{DRIVER} = 0.92, $\eta_{MECHANICAL}$ = 0.98.	k
Multistage compressors (>4.5 kg/s)	Stage pressure ratio <2, $\eta_{POLYTROPIC}$ = 0.87, η_{DRIVER} = 0.92, $\eta_{MECHANICAL}$ = 0.98, $T_{INTERCOOLER}$ = 35°C, $\Delta p/p_{INTERCOOLER}$ = 1%.	l
Multistage compressors (<4.5 kg/s)[6]	Stage pressure ratio <2, $\eta_{POLYTROPIC}$ = 0.85, η_{DRIVER} = 0.90, $\eta_{MECHANICAL}$ = 0.98, $T_{INTERCOOLER}$ = 35°C, $\Delta p/p_{INTERCOOLER}$ = 1%	l
Pumps	$H_{HYDRAULIC}$ = 0.75, η_{DRIVER} = 0.90.	k

a – Taken from Smith et al. [80].
b – Taken from Swanson et al. [81]. The original value in the reference was given for bagasse (160 kg/m^3), which is here fitted for forest residues (293 kg/m^3) assuming that LH is filled with feedstock up to 90%.
c – Based on personal communication with Andras Horvath, Carbona-Andritz, May 15th 2012.
d – Modelling principles taken from Refs. [82] and [35].
e – Operating parameters chosen by author.
f – Outlet temperature and steam/CO ratio based on personal communication with Wolfgang Kaltner, Süd-Chemie AG, July 9th, 2012.
g – Taken from Liu et al. [73].
h – Taken from Larson et al. [49]. For MTG reactor yield structure, see section 3.4.
i – System efficiency calculated based on information taken from Ivy [67].
j – Based on personal communication with Reijo Kallio, ÅF-Consult, October 2012.
k – Taken from Chiesa et al. [83].
l – Taken from Glassman [84].

REFERENCES

[1] IPCC. Summary for policymakers. In: Pachauri R, Reisinger A, editors. Climate change 2007: synthesis report. Geneva: Switzerland; 2007.

[2] CO_2 emissions from fuel combustion – highlights. 9 rue de la Federation 75739 Paris Cedex 15, France: International Energy Agency; 2013.

[3] Breeze P. Coping with carbon: a near-term strategy to limit carbon dioxide emissions from power stations, Philosophical Transactions of the Royal Society A: mathematical. Phys Eng Sci 2008;366(1882):3891–900. http://dx.doi.org/10.1098/rsta.2008.0113.

[4] Zeman FS, Keith DW. Carbon neutral hydrocarbons, Philosophical Transactions of the Royal Society A: mathematical. Phys Eng Sci 2008;366(1882):3901–18.

[5] Kreutz T, Larson E, Williams R, Liu G. Fischer–Tropsch fuels from coal and biomass. Pittsburgh, PA, USA. In: Proceedings

of the 25th Annual International Pittsburgh Coal Conference; 2008.
[6] G. Liu, E. D. Larson, R. H. Williams, T. G. Kreutz, X. Guo. Making Fischer-Tropsch fuels and electricity from coal and biomass: performance and cost analysis, Energy Fuels;25(1). doi:10.1021/ef101184e.
[7] Van Bibber L, Shuster E, Haslbeck J, Rutkowski M, Olsen S, Kramer S. Baseline technical and economic assessment of a commercial scale Fischer–Tropsch liquids facility. Tech Rep DOE/NETL-2007/1260. National Energy Technology Laboratory; 2007.
[8] Hamelinck C, Faaij A, den Uil H, Boerrigter H. Production of FT transportation fuels from biomass; technical options, process analysis and optimisation, and development potential. Energy 2004;29(11):1743–71.
[9] McKeough P, Kurkela E. Process evaluations and design studies in the UCG project 2004–2007. VTT Research Notes 2434. Technical Research Centre of Finland, VTT; 2008.
[10] Landälv I. Demonstration plants for advanced biofuels production based on thermochemical pathways – status and reflections. In: Proceedings of the 21st European Biomass Conference and Exhibition, Copenhagen, Denmark; 2013.
[11] Audi unveils e-gas project, Green car congress. May 13, 2011. bit.ly/1qHXLke.
[12] Rath L. Cost and performance baseline for fossil energy plants volume 2: coal to synthetic natural gas and ammonia. Final Report, July 2011 DOE/NETL-2010/1402. U.S. National Energy Technology Laboratory; 2011.
[13] Appl M. In: More Alexander, editor. Ammonia, methanol, hydrogen, carbon monoxide – Modern production technologies, Nitrogen. 31 Mount Pleasant, London, WC1X 0AD England: CRU Publishing Ltd; 1997, ISBN 1 873387 26 1.
[14] Dybkjaer I, Hansen JB. Large-scale production of alternative synthetic fuels from natural gas. In: de Pontes M, Espinoza R, Nicolaides C, Scholtz J, Scurrell M, editors. Natural gas conversion IV. Studies in surface science and catalysis, 107. Elsevier; 1997. p. 99–116. http://dx.doi.org/10.1016/s0167-2991(97)80322-9.
[15] Penick J, Lee W, Maziuk J. Development of the methanol-to-gasoline process. Chemical reaction engineering – plenary lectures, ACS Symposium Series, 226; 1983. p. 19–48. Ch. 3.
[16] German biofuel firm Choren declares insolvency. Reuters; July 8, 2011. bit.ly/1nZYaus.
[17] Range fuels cellulosic ethanol plant fails, U.S. pulls plug. Bloomberg; December 3, 2011. bloom.bg/1lp8eJB.
[18] Oil Neste. Stora Enso shelve plans for renewable diesel plant. Biomass Magazine; August 22, 2012. bit.ly/1mUBfPz.
[19] Report from the bio-DME plant in Piteå. ChemrecNews; May, 2012. bit.ly/1u9aIlN.
[20] Haldor Topsøe and partners produce biobased gasoline. Biomass Magazine; June 26, 2013. bit.ly/1mUBv0U.
[21] M. Steinberg, Electrolytic synthesis of methanol from CO_2, U.S. patent 3959094, United States Energy Research and Development Administration (1976).
[22] J. Lewis, A. Martin, Method for obtaining carbon dioxide from the atmosphere and for production of fuels, U.S. patent 4140602, Texas Gas Transmission Corporation (1979).
[23] M. Steinberg, Synthetic carbonaceous fuels and feedstocks, U.S. patent 4197421, United States Energy Research and Development Administration (1980).
[24] M. Corbett, S. Salina, Production of synthetic hydrocarbons from air, water and low cost electrical power, U.S. patent 4282187, Grumman Aerospace Corporation (1981).
[25] Graves C, Ebbesen SD, Mogensen M, Lackner KS. Sustainable hydrocarbon fuels by recycling CO_2 and H_2O with renewable or nuclear energy. Renew Sustain Energy Rev 2011;15(1):1–23. http://dx.doi.org/10.1016/j.rser.2010.07.014.
[26] Inui T. Highly effective conversion of carbon dioxide to valuable compounds on composite catalysts. Catal Today 1996;29(14):329–37. http://dx.doi.org/10.1016/0920-5861(95)00300-2. Second Japan–EC Joint Workshop on the Frontiers of Catalytic Science and Technology for Energy, Environment and Risk Prevention.
[27] Kieffer R, Fujiwara M, Udron L, Souma Y. Hydrogenation of CO and CO_2 toward methanol, alcohols and hydrocarbons on promoted copper-rare earth oxides catalysts. Catal Today 1997;36(1):15–24. http://dx.doi.org/10.1016/S0920-5861(96)00191-5. Copper, Silver and Gold in Catalysis.
[28] Saeidi S, Amin NAS, Rahimpour MR. Hydrogenation of CO_2 to value-added products – a review and potential future developments. J CO_2 Util 2014;5(0):66–81. http://dx.doi.org/10.1016/j.jcou.2013.12.005.
[29] Ouellette N, Rogner H-H, Scott D. Hydrogen from remote excess hydroelectricity. part ii: hydrogen peroxide or biomethanol. Int J Hydrogen Energy 1995;20(11):873–80. http://dx.doi.org/10.1016/0360-3199(95)00018-9.
[30] Cifre PG, Badr O. Renewable hydrogen utilisation for the production of methanol. Energy Convers Manag 2007;48(2):519–27. http://dx.doi.org/10.1016/j.enconman.2006.06.011.
[31] Mignard D, Pritchard C. On the use of electrolytic hydrogen from variable renewable energies for the enhanced conversion of biomass to fuels. Chem Eng Res Des 2008;86(5):473–87. http://dx.doi.org/10.1016/j.cherd.2007.12.008.
[32] Kurkela E, Kurkela M, Hiltunen I. The effects of wood particle size and different process variables on the performance of steam-oxygen blown circulating fluidized-bed gasifier. Environ Prog Sustain Energy 2014;33(3):681–7. http://dx.doi.org/10.1002/ep.12003.
[33] Simell P, Hannula I, Tuomi S, Nieminen M, Kurkela E, Hiltunen I, et al. Clean syngas from biomass – process development and concept assessment. Biomass Convers Biorefinery 2014:1–14. http://dx.doi.org/10.1007/s13399-014-0121-y.
[34] Kurkela E, Simell P, McKeough P, Kurkela M. Production of synthesis gas and clean fuel gas [Synteesikaasun ja puhtaan polttokaasun valmistus]. VTT Publications 682, Technical Research Centre of Finland, VTT; 2008.
[35] Hannula I, Kurkela E. A parametric modelling study for pressurised steam/O_2-blown fluidised-bed gasification of wood with catalytic reforming. Biomass Bioenergy 2012;38(0):58–67. http://dx.doi.org/10.1016/j.biombioe.2011.02.045. Overcoming Barriers to Bioenergy: Outcomes of the Bioenergy Network of Excellence 2003-2009.
[36] Hannula I, Kurkela E. Liquid transportation fuels via large-scale fluidised-bed gasification of lignocellulosic biomass. VTT Technology 91, Technical Research Centre of Finland; 2013.
[37] Sabatier P, Senderens J. Nouvelles syntheses du methane. Acad Sci 1902;314:514–6.
[38] Kopyscinski J, Schildhauer TJ, Biollaz SM. Production of synthetic natural gas (SNG) from coal and dry biomass – a technology review from 1950 to 2009. Fuel 2010;89(8):1763–83.
[39] From solid fuels to substitute natural gas (SNG) using TREMP, Tech. rep. Haldor Topsøe; 2009.
[40] Hansen JB, Hojlund Nielsen PE. Methanol synthesis. In: Handbook of heterogeneous catalysis. Wiley-VCH Verlag GmbH & Co. KGaA; 2008. http://dx.doi.org/10.1002/9783527610044.hetcat0148.
[41] Tijm P, Waller F, Brown D. Methanol technology developments for the new millennium. Appl Catal A Gen 2001;221(1–2):275–82. http://dx.doi.org/10.1016/S0926-860X(01)00805-5. Hoelderich Special Issue.

[42] Yurchak S. Development of Mobil's fixed-bed methanol-to-gasoline (MTG) process. Stud Surf Sci Catal 1988;36:251–72.
[43] P. Nielsen, F. Joensen, J. Hansen, E. Sø rensen, J. Madsen, R. Mabrouk, Process for the preparation of hydrocarbons from oxygenates, Patent US 8067474 B2, Haldor Topsøe A/S (2011).
[44] E. Jorn, J. Rostrup-Nielsen, Process for the preparation of hydrocarbons, Patent US 4481305, Haldor Topsøe A/S (1984).
[45] Chang CD, Silvestri AJ. The conversion of methanol and other O-compounds to hydrocarbons over zeolite catalysts. J Catal 1977;47(2):249–59.
[46] Chang C. Hydrocarbons from methanol. Catal Rev 1983;25(1):1–118.
[47] Wiley critical content – petroleum technology, vol. 1–2, John Wiley & Sons, 2007.
[48] Kam A, Schreiner M, Yurchak S. Mobil methanol-to-gasoline process. In: Meyers RA, editor. Handbook of synfuels technology. McGraw-Hill.; 1984.
[49] Larson E, Williams R, Kreutz T, Hannula I, Lanzini A, Liu G. Energy, environmental, and economic analyses of design concepts for the co-production of fuels and chemicals with electricity via co-gasification of coal and biomass. Final report under contract DEFE0005373 to the National Energy Technology Laboratory, US Department of Energy, Princeton University. 2012.
[50] Barker E, Begovich J, Clinton J, Johnson P. Aspen modeling of the tri-state indirect liquefaction process. contract no. W-7405-eng-6. Oak Ridge National Laboratory; 1983.
[51] Schreiner M. Research guidance studies to assess gasoline from coal by methanol-to-gasoline and sasol-type Fischer–Tropsch technologies. Final report to doe under contract no. ef-77-c-01-2447. 1978.
[52] Keith D, Ha-Duong M, Stolaroff J. Climate strategy with CO_2 capture from the air. Clim Change 2006;74(1–3):17–45. http://dx.doi.org/10.1007/s10584-005-9026-x.
[53] Martin F, Kubic W. Green freedom – a concept for producing carbon-neutral synthetic fuels and chemicals, Overview. Los Alamos National Laboratory; 2007.
[54] Hamilton MR, Herzog HJ, Parsons JE. Cost and U.S. public policy for new coal power plants with carbon capture and sequestration. Energy Procedia 2009;1(1):4487–94. http://dx.doi.org/10.1016/j.egypro.2009.02.266. Proceedings of the 9th International Conference on Greenhouse Gas Control Technologies (GHGT-9), 1620 November 2008, Washington DC, USA.
[55] Rubin ES, Chen C, Rao AB. Cost and performance of fossil fuel power plants with CO_2 capture and storage. Energy Policy 2007;35(9):4444–54. http://dx.doi.org/10.1016/j.enpol.2007.03.009.
[56] Metz B, Davidson O, de Coninck H, Loos M, Meyer L, editors. IPCC special report on carbon dioxide capture and storage. Prepared by working Group III of the Intergovernmental Panel on Climate change. Cambridge, United Kingdom and New York, NY, USA: Cambridge University Press; 2005.
[57] Song C. Global challenges and strategies for control, conversion and utilization of CO_2 for sustainable development involving energy, catalysis, adsorption and chemical processing. Catal Today 2006;115(1–4):2–32.
[58] Inui T, Takeguchi T. Effective conversion of carbon dioxide and hydrogen to hydrocarbons. Catal Today 1991;10(1):95–106. http://dx.doi.org/10.1016/0920-5861(91)80077-M.
[59] Inui T, Kitagawa K, Takeguchi T, Hagiwara T, Makino Y. Hydrogenation of carbon dioxide to C_1–C_7 hydrocarbons via methanol on composite catalysts. Appl Catal A Gen 1993;94(1):31–44. http://dx.doi.org/10.1016/0926-860X(93)80043-P.
[60] Sahibzada M, Chadwick D, Metcalfe I. Hydrogenation of carbon dioxide to methanol over palladium-promoted Cu/ZnO/$A1_2O_3$ catalysts. Catal Today 1996;29(14):367–72. http://dx.doi.org/10.1016/0920-5861(95)00306-1. second Japan-EC Joint Workshop on the Frontiers of Catalytic Science and Technology for Energy, Environment and Risk Prevention.
[61] Ushikoshi K, Moria K, Watanabe T, Takeuchi M, Saito M. A 50 kg/day class test plant for methanol synthesis from CO_2 and H_2. In: Inui T, Anpo M, Izui K, Yanagida S, Yamaguchi T, editors. Advances in Chemical Conversions for Mitigating Carbon Dioxide Proceedings of the Fourth International Conference on Carbon Dioxide Utilization. Studies in Surface Science and Catalysis, vol. 114. Elsevier; 1998. p. 357–62. http://dx.doi.org/10.1016/S0167-2991(98)80770-2.
[62] Saito M. R&D activities in Japan on methanol synthesis from CO_2 and H_2. Catal Surv Jpn 1998;2(2):175–84.
[63] Amenomiya Y. Methanol synthesis from $CO_2 + H_2$ II. Copper-based binary and ternary catalysts. Appl Catal 1987;30(1):57–68. http://dx.doi.org/10.1016/S0166-9834(00)81011-8.
[64] Bertuccioli L, Chan A, Hart D, Lehner F, Madden B, Standen E. Study on development of water electrolysis in the EU, fuel cells and hydrogen joint undertaking. 2014.
[65] Holladay J, Hu J, King D, Wang Y. An overview of hydrogen production technologies. Catal Today 2009;139(4):244–60. http://dx.doi.org/10.1016/j.cattod.2008.08.039. Hydrogen Production – Selected papers from the Hydrogen Production Symposium at the American Chemical Society 234th National Meeting & Exposition, August 19-23, 2007, Boston, MA, USA.
[66] Turner J, Sverdrup G, Mann MK, Maness P-C, Kroposki B, Ghirardi M, et al. Renewable hydrogen production. Int J Energy Res 2008;32(5):379–407. http://dx.doi.org/10.1002/er.1372.
[67] Ivy J. Summary of electrolytic hydrogen production – milestone completion report. Tech. Rep. NREL/MP-560–36734. National Renewable Energy Laboratory; 2004.
[68] Merrow E, Phillips K, Myers C. Understanding cost growth and performance shortfalls in pioneer process plants. Tech. Rep. RAND/R-2569-DOE. Santa Monica, USA: RAND Corporation; 1981.
[69] Kaukolämpötilasto, statistics in Finnish. Energiateollisuus; 2012. bit.ly/1qjFidl.
[70] Black J. Cost and performance baseline for fossil energy plants volume 1: bituminous coal and natural gas to electricity. Revision 2a, September 2013 DOE/NETL-2010/1397. U.S. National Energy Technology Laboratory; 2007.
[71] Wan V. Methanol to olefins. Report no. 261. SRI Consulting; 2007.
[72] Kreutz T, Williams R, Consonni S, Chiesa P. Co-production of hydrogen, electricity and CO_2 from coal with commercially ready technology. Part B: economic analysis. Int J Hydrogen Energy 2005;30(7):769–84. http://dx.doi.org/10.1016/j.ijhydene.2004.08.001.
[73] G. Liu, E. D. Larson, R. H. Williams, T. G. Kreutz, X. Guo, Supporting information for making Fischer–Tropsch fuels and electricity from coal and biomass: performance and cost analysis, Energy Fuels 25(1). doi:10.1021/ef101184e.
[74] Energy prices and costs report, European Commission staff working document. 2014. bit.ly/1tANeta.
[75] Wilen C, Moilanen A, Kurkela E. Biomass feedstock analyses. VTT Publications 282, Technical Research Centre of Finland, VTT; 1996.
[76] Larson ED, Jin H, Celik FE. Large-scale gasification-based coproduction of fuels and electricity from switchgrass. Biofuels Bioprod Biorefining 2009;3(2):174–94. http://dx.doi.org/10.1002/bbb.137. 10.1002/bbb.137.

[77] Project co-funded by the European Commission within the Sixth Framework Programme project no. 019761 Bigpower deliverable 71: Finnish case study report. Carbona, Inc.; 2009.
[78] Floch P, Gabriel S, Mansilla C, Werkoff F. On the production of hydrogen via alkaline electrolysis during off-peak periods. Int J Hydrogen Energy 2007;32(18):4641–7. http://dx.doi.org/10.1016/j.ijhydene.2007.07.033.
[79] Ekbom T, Lindblom M, Berglin N, Ahlvik P. Technical and commercial feasibility study of black liquor gasification with methanol/DME production as motor fuels for automotive uses – BLGMF. Tech. Rep. Contract No. 4.1030/Z/01–087/2001. Nykomb Synergetics; 2003.
[80] Smith A, Klosek J. A review of air separation technologies and their integration with energy conversion processes. Fuel Process Technol 2001;70(2):115–34. http://dx.doi.org/10.1016/S0378-3820(01)00131-X.
[81] Swanson M, Musich M, Schmidt D, Schultz J. Feed system innovation for gasification of locally economical alternative fuels (FIGLEAF) final report, Tech. rep.. U.S. Department of Energy; 2002.
[82] Hannula I, Kurkela E. A semi-empirical model for pressurised air-blown fluidised-bed gasification of biomass. Bioresour Technol 2010;101(12).
[83] Chiesa P, Consonni S, Kreutz T, Williams R. Co-production of hydrogen, electricity and CO_2 from coal with commercially ready technology. Part A: performance and emissions. Int J Hydrogen Energy 2005;30(7):747–67. http://dx.doi.org/10.1016/j.ijhydene.2004.08.002.
[84] Glassman A. Users manual for updated computer code for axial-flow compressor conceptual design, Tech. rep.. Toledo, Ohio: University of Toledo; 1992.

Paper V

Ilkka Hannula, Vesa Arpiainen

Light olefins and transport fuels from biomass residues via synthetic methanol: performance and cost analysis

Biomass Conversion and Biorefinery, 2015
Volume 5, Issue 1, pages 63-74.

Series title and number

VTT Science 107

Title	**Synthetic fuels and light olefins from biomass residues, carbon dioxide and electricity** Performance and cost analysis
Author(s)	Ilkka Hannula
Abstract	The objective of this compilation dissertation is to examine and compare the technical and economic feasibility of selected large-scale plant configurations capable of producing synthetic fuels or chemicals from renewable feedstocks. The evaluation of technical performance is based on mass and energy flows calculated with ASPEN Plus® simulation software. The investment costs and the sensitivity of overall economics to different price assumptions are investigated with a spreadsheet based tool. The production of synthetic fuels from CO_2, water and electricity is an emerging process alternative, whose feasibility against gasification-based production is evaluated in detail. Three basic production routes are considered: (1) production from biomass residues via gasification; (2) from CO_2 and electricity via water electrolysis; (3) from biomass and electricity via a hybrid process combining elements from gasification and electrolysis. Process designs are developed based on technologies that are either commercially available or at least successfully demonstrated on a pre-commercial scale. The following gasoline equivalent production cost estimates were calculated for plants co-producing fuels and district heat: 0.6–1.2 €/L_{geq} (18-37 €/GJ) for synthetic natural gas, 0.7–1.3 €/ L_{geq} (21-40 €/GJ) for methanol and 0.7–1.5 €/L_{geq} (23-48 €/GJ) for gasoline. For a given end-product, the lowest costs are associated with thermochemical plant configurations, followed by hybrid and then by electrochemical plants. Production costs of gasification-based configurations can be further reduced by five per cent, if filtration temperature can be successfully elevated from its present 550 °C level to the target of 850 °C. The results of this thesis can be used to guide future process development work towards configurations identified as best candidates for near-term deployment at scale. The results can also be used by the industry and the government to make rational decisions about development projects and policy measures that will help renewable fuel technologies to reach a self-sustaining growth path.
ISBN, ISSN, URN	ISBN 978-951-38-8342-3 (Soft back ed.) ISBN 978-951-38-8343-0 (URL: http://www.vttresearch.com/impact/publications) ISSN-L 2242-119X ISSN 2242-119X (Print) ISSN 2242-1203 (Online) http://urn.fi/URN:ISBN:978-951-38-8343-0
Date	October 2015
Language	English, Finnish abstract
Pages	118 p. + app. 76 p.
Name of the project	
Commissioned by	
Keywords	forest residues, gasification, reforming, electrolysis, synthetic fuels, light olefins, district heat
Publisher	VTT Technical Research Centre of Finland Ltd P.O. Box 1000, FI-02044 VTT, Finland, Tel. 020 722 111

Julkaisun sarja ja numero

VTT Science 107

Nimeke	**Synteettisiä polttoaineita ja olefiineja metsätähteistä, hiilidioksidista ja sähköstä** Teknistaloudellinen tarkastelu
Tekijä(t)	Ilkka Hannula
Tiivistelmä	Tässä yhdistelmäväitöskirjassa tarkastellaan uusiutuvien polttoaineiden ja kemikaalien valmistamiseen soveltuvien tuotantoprosessien teknistaloudellista suorituskykyä. Tarkastelujen lähtökohtana on Suomessa viime vuosina kehitetty metsätähteiden paineistettuun leijukerroskaasutukseen, kaasun kuumasuodatukseen, katalyyttiseen tervojen ja hiilivetyjen reformointiin sekä konventionaaliseen synteesiteknologiaan perustuva prosessi. Teknologian toimivuus demonstroitiin VTT:llä vuosina 2007 – 2011 toteutetuissa pitkäkestoisissa prosessikehityskokoluokan koeajoissa sekä teollisella pilottilaitoksella. Hiilidioksidista ja vedestä sähköenergialla valmistetut polttoaineet ovat mielenkiintoinen uusi teknologiavaihtoehto, jonka suorituskykyä suhteessa kaasutukseen perustuvaan prosessiin arvioitiin nyt ensimmäistä kertaa. Tutkimuksessa vertaillaan kolmea eri tuotantoreittiä, joissa synteettisiä liikennepolttoaineita tuotetaan joko (1) metsätähteistä kaasutuksen kautta; (2) hiilidioksidista ja sähköstä veden elektrolyysin kautta; tai (3) metsätähteistä ja sähköstä kaasutusta ja elektrolyysiä yhdistelevän hybridiprosessin kautta. Tuotantoreittien teknistä suorituskykyä vertaillaan laskemalla laitosten aine- ja energiavirrat ASPEN Plus® -simulointiohjelmalla. Taloudellista suorituskykyä vertaillaan arvioimalla investointi- ja tuotantokustannukset taulukkolaskentaohjelmalla. Tuotantokustannusten riippuvuutta lähtöoletuksista tutkitaan lisäksi herkkyystarkastelujen avulla. Polttoaineille laskettiin seuraavat, tuotantoreitistä riippuvat, bensiinilitran energiasisältöä vastaavat tuotantokustannusarviot: metaani 0,6–1,2 €/$L_{b\text{-}ekv.}$ (18–37 €/GJ), metanoli 0,7–1,3 €/$L_{b\text{-}ekv.}$ (21–40 €/GJ) ja bensiini 0,7–1,5 €/$L_{b\text{-}ekv.}$ (23–48 €/GJ). Alhaisimmat kustannukset saavutetaan kaasutukseen perustuvalla prosessilla, toiseksi alimmat hybridiprosessilla ja korkeimmat elektrokemiallisella prosessilla. Metsätähteiden kaasutukseen perustuvan prosessin tuotantokustannukset alenevat viisi prosenttia, mikäli reformointia edeltävä suodatuslämpötila pystytään nostamaan nykyisestä 550 °C asteesta tavoiteltuun 850 °C asteeseen. Väitöskirjassa tarkasteltujen prosessien tuotantokustannukset ovat nykyisellään fossiilisia liikennepolttoaineita korkeammalla tasolla. Uusiutuvien polttoaineiden kehittäminen kilpailukykyisiksi edellyttääkin pitkäkestoisia edistämistoimia. Näihin lukeutuu merkittävä panostus tutkimukseen, mutta erityisesti toimet, jotka nopeuttavat demonstraatiolaitosten rakentamista.
ISBN, ISSN, URN	ISBN 978-951-38-8342-3 (nid.) ISBN 978-951-38-8343-0 (URL: http://www.vtt.fi/julkaisut) ISSN-L 2242-119X ISSN 2242-119X (Painettu) ISSN 2242-1203 (Verkkojulkaisu) http://urn.fi/URN:ISBN:978-951-38-8343-0
Julkaisuaika	lokakuu 2015
Kieli	Englanti, suomenkielinen tiivistelmä
Sivumäärä	118 s. + liitt. 76 s.
Projektin nimi	
Rahoittajat	
Avainsanat	
Julkaisija	Teknologian tutkimuskeskus VTT Oy PL 1000, 02044 VTT, puh. 020 722 111

Synthetic fuels and light olefins from biomass residues, carbon dioxide and electricity

Performance and cost analysis

The objective of this compilation dissertation is to examine and compare the technical and economic viability of selected large-scale plant configurations capable of producing synthetic fuels or chemicals from renewable feedstocks. The evaluation of technical performance is based on mass and energy flows calculated with ASPEN Plus® simulation software. The investment costs and the sensitivity of overall economics to different price assumptions are investigated with a spreadsheet based tool. The production of synthetic fuels from CO_2, water and electricity is an emerging process alternative whose feasibility against gasification-based production is evaluated in detail.

Three basic production routes are considered: (1) production from biomass residues via gasification; (2) from CO_2 and electricity via water electrolysis; (3) from biomass and electricity via a hybrid process combining elements from gasification and electrolysis. Process designs are developed based on technologies that are either commercially available or at least successfully demonstrated on a pre-commercial scale.

The results of this thesis can be used to guide future process development work towards configurations identified as best candidates for near-term deployment at scale. The results can also be used by the industry and the government to make rational decisions about development projects and policy measures that will help renewable fuel technologies to reach a self-sustaining growth path.

ISBN 978-951-38-8342-3 (Soft back ed.)
ISBN 978-951-38-8343-0 (URL: http://www.vttresearch.com/impact/publications)
ISSN-L 2242-119X
ISSN 2242-119X (Print)
ISSN 2242-1203 (Online)
http://urn.fi/URN:ISBN:978-951-38-8343-0